STRUCTURE AND SPECTRA OF IONIZED TIN ATOMS: Sn II - V

ABSTRACT
OF THE
THESIS
SUBMITTED FOR THE AWARD OF THE DEGREE OF
Doctor of Philosophy
IN
PHYSICS

BY
HARIS KUNARI

UNDER THE SUPERVISION OF
PROF. TAUHEED AHMAD

DEPARTMENT OF PHYSICS
ALIGARH MUSLIM UNIVERSITY
ALIGARH-202002 (INDIA)

2014

ABSTRACT

A comprehensive spectroscopic study of the tin ions has special interest from astrophysical, technological and fundamental physics point of views. The updating processes of new version of atomic databases require the highly precise data on energy levels, radiative transitions with intensities and transition rates etc. This enhanced spectral information is always a requisite for astrophysical object studies, for instance cosmic presence of tin is confirmed in various stellar objects [1-6]. The technological application is that tin plasma source is considered to be as source of future/new generation extreme ultraviolet lithography (EUVL) designed for its unresolved transition arrays (UTA) at 13.5 nm [7-11]. Many other application based researches are continuing for the development of micro-plasma which might be applicable to lithography and some metrology [12,13]. The experimental observations are always important to improve and/or include the lacking parameters or interactions in theoretical models of present atomic structure calculations.

The thesis entitled "**Structure and spectra of ionized tin atoms: Sn II–V**" contains extensive interpretations of the spectra of singly to quadruply ionized tin ions (Sn II–V) on the basis of spectrum of tin taken by us on a 3m normal incidence vacuum spectrograph (300–2080Å) of the Antigonish laboratory (Canada), Wu's [14] measurements (350–9000Å) and Troitsk's measurements in 200–650Å wavelength region [15]. The thesis comprised of an introduction, separate chapters for the theory and experimental details involved, and from chapters 3–6, the studies on Sn II–V were discussed in detail. The conclusion of the present work is given at the end.

The **chapter 1** contains the theoretical method of atomic structure calculations based on Hartree-Fock formulism with relativistic effects and superposition of configurations which incorporated in the Cowan's code [16].

Chapter 2 covers the details of the experiments involved and the strategy employed to the critical evaluation of the analyses was also given. The recording of

tin spectrum in 300–2080Å wavelength range, the tin ions/atoms were excited by ns of a vacuum triggered spark source, which consists of a 14.5 μF fast-charging -inductance capacitor, chargeable up to 20 kV, and a trigger module to initiate the harge in vacuum. A holographic osmium-coated grating with 2400 lines/mm was l to obtain the spectrum with reciprocal linear dispersion of about 1.385 Å/mm in first order of diffraction. At least four or five different tracks of spectra were tographed on Kodak SWR (short-wave radiation) plates with varied experimental ditions, such as electric current and charging voltage. Relative positions of ctral lines on the plates were measured using a Zeiss Abbe comparator. For their elength reductions, we used as internal standards the known impurity lines of –IV, N II, O II–IV, Al II–III and Si II–IV. The data were reduced with polynomial of second or third degrees to obtain corrections to the dispersion curve. The ertainties of the measurements were found to be varying from 0.003 Å to 0.008 Å sharp and unperturbed lines on different spectral regions and different plates. The 's original wavelengths are corrected with Ritz-type of internal standards derived n highly accurate lines of Sn I and Sn II. The shifts were varying smoothly with elength between +0.019 Å near 900 Å and −0.25 Å near 8300 Å. Thereafter the ertainties of lines have been estimated.

The observed energy levels, in each spectrum, were optimized with a least ares level optimization method (LOPT)[17] within a level of one standard iation and consequently, the corresponding Ritz wavelengths with uncertainties e generated. The relative intensities of lines are determined within the local modynamical equilibrium states of optically thin plasmas. The analyses are ported by the quasi–relativistic Hartree-Fock method with superposition of figurations to take interaction effect due to inter-configuration interactions (CI) plemented in Cowan's code. The extensive calculations with least squares fitted ametric variation was done to reduce the disagreement between observed and oretical values. Finally, the observed spectroscopic data were used for deriving the ization potentials.

In **Chapter 3**, the electronic structure of singly ionized tin (Sn II) is described. e structure of Sn II is partly a one-electron and partly a three-electron system with und configuration $5s^2 5p$. The excited configurations are of the type $5s^2 n\ell$ in the

one-electron part, and $5s5p^2$, $5p^3$ and $5s5pn\ell$ ($n\ell$=6s, 5d) in the three-electron part with quartet and doublet levels. The existing interpretation of the one-electron level system was confirmed, while all the levels of $5s5p^2$ have been confirmed except $^2S_{1/2}$ level which is revised. The analysis has been extended to include new configurations $5p^3$, 5s5p5d and 5s5p6s. The ionization potential obtained from the *n*g series was found to be 118023.7(7) cm^{-1} or 14.63307(8) eV. A complete set of critically evaluated data on energy levels, observed wavelengths and transition probabilities of Sn II in the wavelength range 888–10740 Å is presented in this chapter.

The **chapter 4**, contains the revised and extended analysis of Sn III, which includes the previous reported level values of $5p^2$, 5sns (n=6-9), 5snd (n=5-7) and 4f5s configurations with improved energy values. The missing $^1S_0$ level of $5p^2$ and 5sns (n=7, 9) configurations is established now. All the levels of 5s5g, except $^3G_5$ for which the value is revised, have been confirmed. In extension of the analysis, the levels of 5s8d, 5p (5d+6s), 5snf (n=5-10), 5sng (n=6-7), 5p6p configurations with a few levels of 5snd (n=10-12) Rydberg members have been established. These observed series have been used for the improved determination of the ionization potential to be 246059±9 cm^{-1}. A total of 115 levels (50 being new) based on more than 350 lines, have been observed.

In **chapter 5**, the spectroscopic interpretations of the trebly ionized tin (Sn IV) is given, in which all the levels of previously known single electron configurations have been confirmed. The 15 levels of $4d^9$5s5p configuration are known now. The optimization of levels values have been made with the help of 139 observed lines for this spectrum, out which more than 50 lines are newly identified. The outermost single electronic excitations results to establish the levels of $4d^{10}$np (n=7-8), $4d^{10}$5f, $4d^{10}$ng (8, 9), $4d^{10}$nh (n=6-9) and $4d^{10}$ni (7, 8) configurations. With help of non-penetrating high-lying series, the ionization limit of the Sn IV has been derived most accurately to 328909.3±2.5cm^{-1} or 40.77955(31) eV. This enabled us to determine of the energy values more precisely for unobserved levels of $4d^{10}n\ell$ ($n\geq5$, ℓ= g, h, i, k) Rydberg members. A total of 66 levels observed for this ion, out of which 25 are newly observed in this work.

The **chapter 6** is devoted to describe the fifth spectrum of tin (Sn V). The experimental data was mostly used from the measurements of Ryabtsev [15] and

higher wavelength data from our VUV list. It includes, the confirmation of all the earlier known levels of $4d^9n\ell$ ($n\ell$ = 5s, 5p, 5d, 6s, 6p, 6d, 7s), $4d^85s^2$ and $4d^85s5p$ configurations, except $^1S_0$ and $^1G_4$ of $4d^95d$ configuration and for them new values were obtained. More than 450 lines have been used in optimization of the energy levels, out of which 194 lines are from our VUV measurements and 10 lines from the Wu's measurements. We have observed fourteen new lines, in 1650-2010Å range, that are associated to the $4d^95d \rightarrow 4d^96p$ array. With the help of the longer-wavelength data observed by us, improved energy values with greater accuracies have been obtained for the earlier reported levels of $4d^95s$, $4d^95p$, $4d^95d$, $4d^96p$ and $4d^96d$ configurations. A total of 137 levels are observed in this spectrum. The transition probabilities (gA) for observed lines were also given. The reported value of ionization potential of this ion is substantially revised to 617620cm^{-1} against the previously reported value 621300 cm^{-1} which was derived from the perturbed series.

In the end, **conclusion** of the present investigation contains the final summary of the analyses of four different spectra of tin (Sn II–V). At last, an appendix on the thesis contains some portraits of sample tin spectra used for this work in VUV wavelength region along with a few marked prominent lines of Sn II–V and impurities present in them.

References:

[1] Hobbs L M, Welty D E, Morton D C, Spitzer L and York D G 1993 *Astrophys. J.* **411** 750

[2] Sofia U J, Meyer D M and Cardelli J A 1999 *Astrophys. J.* **522** L137

[3] Proffitt C R, Sansonetti C J and Reader J 2001 *Astrophys. J.* **557** 320

[4] O'Toole S J, 2004 *Astron. Astrophys.* **424** L25

[5] O'Toole S J and Heber U 2006 *Astron. Astrophys.* **452** 579

[6] Chayer P, Vennes S, Dupuis J and Kruk J W 2005 *Astrophys. J.* **630** L169

[7] Bakshi V 2009 *EUV Lithography* (SPIE and John Wiley & Sons, Inc.,Bellingham, WA/Hoboken, NJ)

[8] Kieft E R, van der Mullen J J A M, and Kroesen G M W 2005 *Phys. Rev.* E **71** 026409

[9] Ohashi H *et al* 2007 *J. Phys.: Conf. Ser.* **58** 235

[10] Katsunobu Nishihara *et al* 2008 *Phys. Plasmas* **15** 056708

[11] Fujioka S *et al* 2008 *J. Phys.: Conf. Ser.* **112** 042049

[12] Kambali I *et al 2013 J. Phys. D: Appl. Phys.* **46** 495104

[13] Roy A *et al* 2014 *Appl. Phys. Lett.* **105** 074103

[14] Wu C M 1967 *The Atomic Spark Spectra of Tin, Sn III, Sn IV, Sn V*, Master thesis, University of British Columbia, Canada

[15] Ryabtsev A N 2013 *The spectral data of tin ions*, private communication

[16] Cowan R D 1981 *The Theory of Atomic Structure and Spectra* (Berkeley, CA: University of California Press) and Cowan code package for Windows by A. Kramida, available from http://das101.isan.troitsk.ru/COWAN

[17] Kramida A E 2011 *Comput. Phys. Commun.* **182** 419

List of Publications

A. In refereed journals

1. **K. Haris,** Param Jeet Singh, Aparna Shastri, Sunanda K., Babita K. , S.V.N. Bhaskara Rao and A. Tauheed
   "Photostimulable phosphor based image plate detection system for the high resolution vacuum ultraviolet beamline at the Indus-1 synchrotron radiation source", *Nuclear Instruments and Methods in Physics Research Section A: Accelerators, Spectrometers, Detectors and Associated Equipment* 767,199 (2014). arXiv:1408.4015 [physics.ins-det]

2. **K. Haris,** A. Kramida and A. Tauheed
   "Extended and Revised analysis of singly ionized tin: Sn II", *Phys. Scr.* **89**, 115403 (2014). arXiv:1312.0261 [physics.atom-ph]

3. T. Nandi, **K. Haris,** Hala, Gurjeet Singh, Pankaj Kumar, Rajesh Kumar, S. K. Saini, S. A. Khan, Akhil Jhingan, P. Verma, A. Tauheed, D. Mehta, and H. G. Berry
   "Fast ion surface energy loss and straggling in the surface wake fields", *Phys. Rev. Lett.* **110** (16) 163203 (2013). arXiv:1312.0446 [physics.atom-ph]

4. **K. Haris** and A. Tauheed
   "Revised and extended analysis of doubly ionized tin: Sn III", *Phys. Scr.* **85** 055301 (2012).

B. In conference proceedings

1. T. Nandi, P. Sharma, D. Chandvani, Hala, G. Sharma, G. Singh, B. Kumar, **K. Haris**, Gurpreet, J. Gehlot, A. Jhingan, B. J. Roy, and A.P. Mishra "QED of Highly Charged Ions with Z>92", *SPARC India workshop, TIFR, Mumbai, India,* 28-29 Jan, 2014.

2. Gordon Berry, T. Nandi and **K. Haris** "SELF: Fast Ion Surface Energy Loss in Wake Fields of Solid Foils" *Division of Atomic, Molecular & Optical Physics (DAMOP-2013), Quebec,* Canada, June 3–7, 2013

3. T. Nandi, B. J. Roy, Biraja Mohanty, Mumtaz Oswal, V. Jha, D.C. Biswas, Akhil Jhingan, Sunil Kumar, V. Singh, B. Kumar and **K. Haris** "Study of reactions ^{56}Fe, ^{58}Ni (^{12}C, αα) and formation of fully stripped ions in multi-nucleon transfer reaction" *DAE Symposium on Nuclear Physics, held at University of Andra, Visakhapatnam, India,* Dec 26 – 30, 2011.

4. T. Nandi, **K. Haris** *et al* "Experimental evidence of wakefield effect on the energy loss of ions in the solids", 3rd International Conference on Current Development in Atomic, Molecular and Optical physic (CDAMOP-2011), held at University of Delhi, New Delhi, India, 14 – 16 Dec, 2011.

5. **K. Haris** and A. Tauheed "Theoretical and Experimental Investigation of Singly Ionized Tin: Sn II", DAE-BRNS Symposium on atomic, Molecular and Optical Physics (SAMOP 2011), held at Karnatak University, Dharward, India, during 22-25 Feb, 2011.

6. **K. Haris and A. Tauheed,** "The spectrum of trebly ionized tin: Sn IV", *Topical Conference on Atomic and Molecular Physics (TC2010), RRCAT, Indore, India* March 3-6, 2010.

STRUCTURE AND SPECTRA OF IONIZED TIN ATOMS: Sn II - V

THESIS

SUBMITTED FOR THE AWARD OF THE DEGREE OF

Doctor of Philosophy

IN

PHYSICS

BY

HARIS KUNARI

UNDER THE SUPERVISION OF

PROF. TAUHEED AHMAD

DEPARTMENT OF PHYSICS
ALIGARH MUSLIM UNIVERSITY
ALIGARH-202002 (INDIA)

2014

Fed in Computer

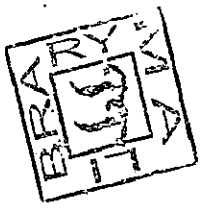

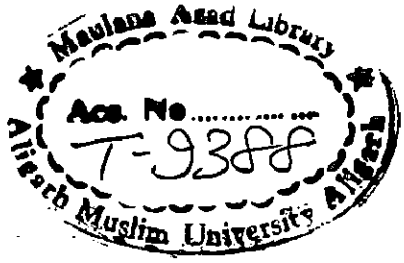

31 OCT 2015

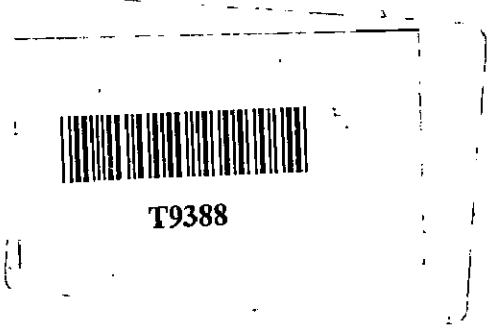

CANDIDATE'S DECLARATION

I, **Haris Kunari**, Department of Physics certify that the work embodied in the Ph.D. thesis entitled "**Structure and Spectra of Ionized Tin Atoms: Sn II–V**", is my own bonafide work carried out by me under the supervision of **Prof. Tauheed Ahmad** at Aligarh Muslim University, Aligarh. The matter embodied in this Ph.D. thesis has not been submitted for the award of any other degree.

I declare that I have faithfully acknowledged, given credit to and referred to the research workers wherever their works have been cited in the text and the body of the thesis. I further certify that I have not willfully lifted up some other's work, para, text, results, etc. reported in the journals, books, magazines, reports, dissertations, theses, etc., or available at web-sites and included them in this Ph.D. thesis and cited as my own work.

Aligarh

Date: 01-12-14

Haris Kunari

.....

CERTIFICATE FROM THE SUPERVISOR

This is to certify that the above statement made by the candidate is correct to the best of my/our knowledge.

Prof. Tauheed Ahmad

Department of Physics

01.12.14

(Signature of the Chairman of the Department with seal)

Chairman
Department of Physics
A.M.U., Aligarh

Dr. Tauheed Ahmad

Professor

DEPARTMENT OF PHYSICS
ALIGARH MUSLIM UNIVERSITY
ALIGARH – 202 002 (INDIA)
Phone : +91571 – 2701001 (O)
Mobile : +919837404077
Fax : +91571 – 2701001
E-mail : ahmadtauheed@rediffmail.com

Certificate

It gives me pleasure to certify that the work presented in the thesis entitled "**Structure and Spectra of Ionized Tin Atoms: Sn II-V**" is mainly carried out by **Mr. Haris Kunari** under my supervision. The work is original and sufficient for the award of degree of Doctor of Philosophy of The Aligarh Muslim University, Aligarh. I permit him to submit this thesis for the award of the degree.

Dr. Tauheed Ahmad
Professor of Physics
Dated: 1·12·2014

Prof. Rahimullah Khan

Chairman

DEPARTMENT OF PHYSICS
ALIGARH MUSLIM UNIVERSITY
ALIGARH – 202 002 (INDIA)
Phone : +91571 – 2701001 (O)
Mobile : +919319683858
Fax : +91571 – 2701001
E-mail : rahimullah@rediffmail.com

PRE-SUBMISSION SEMINAR COMPLETION CERTIFICATE

This is to certify that Mr. **Haris Kunari,** Department of Physics has satisfactorily completed the pre-submission seminar requirement, which is part of his Ph.D. programme.

Date: 01.12.2014

(Signature of the Chairman of the Department)

Chairman
Department of Physics
A.M.U., Aligarh

COPYRIGHT TRANSFER CERTIFICATE

Title of the Thesis: "Structure and Spectra of Ionized Tin Atoms: Sn II-V"

Candidate's Name: Haris Kunari

COPYRIGHT TRANSFER

The undersigned hereby assigns to the Aligarh Muslim University, Aligarh copyright that may exist in and for the above thesis submitted for the award of the Ph.D. degree.

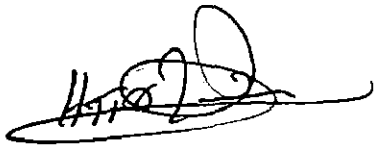

Signature of the candidate

Note: However, the author may reproduce or authorize others to reproduce material extracted verbatim from the thesis or derivative of the thesis for author's personal use provide that the University's copyright notice are indicated.

Acknowledgements

All praise is due to Almighty Allah who is the ultimate source of knowledge, a part of which he reveal to man and peace be up on all his messengers for guidance and success of mankind.

I express *my deep respect and profound sense of gratitude to* my supervisor, Prof. Tauheed Ahmad, for his able guidance, kind support and blessings. He pushed me up whenever needed, provided necessary facilities and boosted my confidence to carry out this work. I am very thankful to you sir.

Collaboration with Dr. Alexander Kramida of *National Institute of Standards and Technology* (NIST), USA was very fruitful and that made this thesis work into the realization. I express my deep sense of gratitude for his valuable collaboration. I should state that it was a great opportunity to follow his directions and words that boosted my knowledge in this subject and facilitated me to present the thesis in the current form.

I am deeply indebted to Prof. Rahimullah Khan, Chairman, *Dept. of Physics, AMU* for providing me necessary facilities to carry out this work and for being a mentor and motivator throughout my research work.

I am thankful to Dr. A. N. Ryabtsev, *Institute for Spectroscopy RAS*, Troitsk, Russia for providing the spectral data of tin in shorter wavelength region and other necessary help.

I thankfully remember Dr. Tapan Nandi, *Inter University Accelerator Centre (IUAC)*, New Delhi, Dr. A. P. Mishra, *Bhabha Atomic research Centre*, (BARC), Mumbai, Prof. Gordon Berry, *Notre Dame University*, USA for giving valuable guidance and training on accelerator based atomic physics studies.

I extend my warm thanks to Dr. Bhashkar Rao, Dr. Sunanda K, Dr. Aparna Shastri and Dr. Param Jeet Singh of BARC for giving me an opportunity involve with photoabsorption studies using synchrotron radiations.

I am grateful to Prof. A. K. Pradhan and Prof. S. N. Nahar, the distinguished visitors from The Ohio State University (OSU), USA for delivering lecture series in a condensed course on "Atomic and Molecular Radiation Physics: Astronomy to

Biomedicine", held at Dept. of Physics and giving some basis training in Superstructure and R-Matrix codes.

I also remember with thanks the other distinguished members of spectroscopy group, Prof. Shabbir Ahamd, Dr. S. M. Afzal, Dr. S. Jabeen and Dr. Anjum Naz for their kind cooperation and motivation throughout. My sincere thanks go to spectroscopy lab technicians Mr. Rahimuddin and Mr. Mohan Lal for their kind cooperation. My since gratitude to all other teachers and non-teaching staffs of the department of physics for their support, affection and encouragement.

I am highly grateful to my parents, uncle, brothers and sisters for their blessings and moral support in all thick and thin.

It was a pleasure to work with my colleagues, Swapnil, Hala, , Sumit Mishra, Jane Alam, Manoj Sharma, Riyaz, Adil, Basu Kumar and I am very thankful to them.

I enjoyed the sincere friendships of Salim, Salih, Aslam, Nisar, Shafeeq, Ullas, Subair, Khalid, Abin Sha, Sakeer and they made my stay at Aligarh memorable. I am grateful to them for being so kind towards me.

I duly acknowledge the Council of Scientific and Industrial Research (CSIR) for sanctioning financial support through the Senior Research Fellowship (SRF) Scheme to complete this research. I also acknowledge the prior financial aids procured from the University Grant Commission (UGC) and Dept. of Atomic Energy-Board of Research in Nuclear Sciences (DAE-BRNS) at various stages of Ph.D. tenure.

Finally, I thank to all those, respected teachers and other friends, who helped and boosted me up during scholarly life with their valuable knowledge and help.

Haris Kunari

List of Publications

A. In refereed journals

1. **K. Haris**, Param Jeet Singh, Aparna Shastri, Sunanda K., Babita K. , S.V.N. Bhaskara Rao and A. Tauheed
   "Photostimulable phosphor based image plate detection system for the high resolution vacuum ultraviolet beamline at the Indus-1 synchrotron radiation source", *Nuclear Instruments and Methods in Physics Research Section A: Accelerators, Spectrometers, Detectors and Associated Equipment* **767**,199 (2014). arXiv:1408.4015 [physics.ins-det]

2. **K. Haris**, A. Kramida and A. Tauheed
   "Extended and Revised analysis of singly ionized tin: Sn II", *Phys. Scr.* **89**, 115403 (2014). arXiv:1312.0261 [physics.atom-ph]

3. T. Nandi, **K. Haris**, Hala, Gurjeet Singh, Pankaj Kumar, Rajesh Kumar, S. K. Saini, S. A. Khan, Akhil Jhingan, P. Verma, A. Tauheed, D. Mehta, and H. G. Berry
   "Fast ion surface energy loss and straggling in the surface wake fields", *Phys. Rev. Lett.* **110** (16) 163203 (2013). arXiv:1312.0446 [physics.atom-ph]

4. **K. Haris** and A. Tauheed
   "Revised and extended analysis of doubly ionized tin: Sn III", *Phys. Scr.* **85** 055301 (2012).

B. In conference proceedings

1. T. Nandi, P. Sharma, D. Chandvani, Hala, G. Sharma, G. Singh, B. Kumar, **K. Haris**, Gurpreet, J. Gehlot, A. Jhingan, B. J. Roy, and A.P. Mishra "QED of Highly Charged Ions with Z>92", *SPARC India workshop, TIFR, Mumbai, India,* 28-29 Jan, 2014.

2. Gordon Berry, T. Nandi and **K. Haris** "SELF: Fast Ion Surface Energy Loss in Wake Fields of Solid Foils" *Division of Atomic, Molecular & Optical Physics (DAMOP-2013), Quebec,* Canada, June 3–7, 2013

3. T. Nandi, B. J. Roy, Biraja Mohanty, Mumtaz Oswal, V. Jha, D.C. Biswas, Akhil Jhingan, Sunil Kumar, V. Singh, B. Kumar and **K. Haris** "Study of reactions ^{56}Fe, ^{58}Ni (^{12}C, αα) and formation of fully stripped ions in multi-nucleon transfer reaction" *DAE Symposium on Nuclear Physics, held at University of Andra, Visakhapatnam, India,* Dec 26 – 30, 2011.

4. T. Nandi, **K. Haris** *et al* "Experimental evidence of wakefield effect on the energy loss of ions in the solids", 3rd International Conference on Current Development in Atomic, Molecular and Optical physic (CDAMOP-2011), held at University of Delhi, New Delhi, India, 14 – 16 Dec, 2011.

5. **K. Haris** and A. Tauheed "Theoretical and Experimental Investigation of Singly Ionized Tin: Sn II", DAE-BRNS Symposium on atomic, Molecular and Optical Physics (SAMOP 2011), held at Karnatak University, Dharward, India, during 22-25 Feb, 2011.

6. **K. Haris and A. Tauheed,** "The spectrum of trebly ionized tin: Sn IV", *Topical Conference on Atomic and Molecular Physics (TC2010), RRCAT, Indore, India* March 3-6, 2010.

CONTENTS

LIST OF FIGURES

LIST OF TABLES

Dedicated to:
My Loving Parents

INTRODUCTION

The spectroscopy is a branch of physics which deals with the interaction of electromagnetic radiations with matters. Etymologically, it is rooted to both Latin (*spectrum*: spectrum) and Greek (*skopein*: to examine). It was instituted by *Sir Isaac Newton* (1642-1727) at first, however, the elementary practical development of this field was enriched in the 19^{th} century;- many instrumental developments, analytical tools which led to the discovery of various elements in the periodic table, and the characteristic spectra (by G. Kirchhoff) of numerous elements etc. The followed century concretized the spectroscopy from both theoretical and experimental point of view. Precisely speaking, the subfield:- theoretical atomic physics is instigated on the basis of idea given by Niels Bohr in the past century only. The next advancement of spectroscopy was rapid, where the quantitative spectroscopic analysis being introduced into the field. In this regard, the contributions from William Meggers were outstanding [1]. When the language of quantum mechanics became more popular, as other areas of physics the atomic physics also started growing, and the later augmentations were uncountable and those are beyond the scope of the subject of this discussion.

It can be said that the observable appearance of the world made possible because of the structure of the atoms and their physical behavior. The fundamentals of the atomic properties can be investigated through the spectra of them. This has been exploited to the current advancement in the field of atomic physics, various subfields and interdisciplinary field [2, 3], for example, development of lasers, identification of elemental compositions and other parameters of various stars and interstellar sources, and many metrological devices like atomic clock. The space astrophysics could not have been better understood without the accurate and highly precise data from the laboratory. Besides, astrophysics, the data users were from many applied researches, like plasma diagnostics, fusion researches (tokomak, ITER), short-wave radiation source constructions and researches on efficient lighting devices, optical-clock

transition designs etc. In fusion devices, such as ITER, the atomic data on tungsten and molybdenum etc play an important role [4, 5]. The developments of the next generation of atomic frequency clocks, based on optical transitions in laser-cooled neutral atoms, are the center of attention for the time measurements in future [6, 7].

The interest of the theorists is always at pinnacle to produce the bunch of atomic accurate data at once [3, 8-10]; however, this needs the continuous testing with the observed values. The atomic data through semiempirical parametrizations and the linearity manifest by them are powerful tools, cannot be replaced by modern *ab initio* methods. The validity of an experimental observation is always being increased if it is supported by good theoretical predictions. However, in reverse process, the precise experimental values are more instrumental to ensure the consistency of the theoretical models and sometimes to improve them by means of inclusion of unknown/missing interaction based on the observed facts (e.g. Lamb Shift). The semiempirical results are still useful, as the wide use of them was presented by Prof. Bengt Edlén in *Handbuch de Physik* for the complex atomic structures [11].

The initial high-resolution measurements were made with giant classical grating spectrographs and are one of the most apposite techniques for wide wavelength coverage from intra-red (IR) to *extreme ultraviolet* (EUV). However, some accurate measurements taken using the interferometric method firstly employed by Michelson and later developed by C. Fabrt and A Perot. The current version of interferometer, *Fourier transform spectrometer* (FTS), has many advantages of wavelength calibration and intensity measurement over the grating instruments, but, its extension down to *vacuum ultraviolet* (VUV) region is restricted, as below 1400Å, the fluoride windows persist with the cut-off issues. In addition to this, the wavelengths measurements of higher ionization sources are unflavored in FTS as it needs continuous stable source [12-14]. If these hurdles are overcome, the next future would be for FTS. Therefore at present, the grating spectroscopy is the only accessible technique for wavelength measurements in VUV region.

A spectroscopic analysis essentially provides data on observed energy levels, wavelengths, intensities spectral lines etc. When theoretical advancements are achieved, the data on transition probabilities and oscillator strengths etc become available. When the interests and developments in various fields are considered, the

requirement of high accurate and more precise data is vastly increased, for instance the data in VUV region; there is an immense increased interest after the launching of spectrograph like Goddard High Resolution Spectrograph (GHRS) on board Hubble Space Telescope (HST) [15, 16]. In early days, the spectroscopic data were not subjected to the statistical examination; however in modern times the statistical tools are more developed and hence such technique must be employed to mass scale of atomic data too. Therefore, the energy levels with uncertainties, transition wavelengths with uncertainties and intensities, as well as transition probabilities are the present requirement to compete with the future.

The present work exemplifies the spectral information, energy levels, wavelengths, and intensities of lines of *tin ions* (Sn II–V). Some general information of tin atom is given here: the symbol Sn stands for: *stanuum* (Latin), its natural existence in ore cassiterite (SnO_2) and stannine (Cu_2FeSnS_4). The pure metal is produced by the reduction with coal. It was used as a component of bronze from antiquity (as early as 35,000 BC). The electronic configurations of the neutral tin (Z=50), can be written as [Kr] $4d^{10}5s^25p^2$. It has largest number of stable isotopes (ten), and most abundant are ^{120}Sn (32.59%), ^{118}Sn (24.23%) and ^{119}Sn (8.59%). It has important applications in environmental protection and food technology tramp [17, 18]. Spectroscopic investigation of the tin ions has drawn special attention from astrophysical, technological, and fundamental physics point of views. The tin plasma sources are considered to be a modern candidate for new generation *extreme ultra violet plasma lithography* (EUVL) [19-23], presently aimed at 13.5nm where the $4p^64d^x \rightarrow [4p^64d^{x+1} + 4d^{x-1}$ (5p+4f); $1 \leq x \leq 6]$ is named as *unresolved transition array* (UTA). There are tremendous interests of broadband EUV light source development at micro-levels for various metrological applications like photoelectron spectroscopy, nano-surface patterning, reflectometry, surface chemical analysis and microscopy etc [24, 25]. Several laser levels of tin (Sn II-IV) were reported for the improvement energy efficient intense plasma sources and in that regard, several stark width studies were made for tin plasmas [26-30].

The stellar importance of tin comes after the discovery of its abundances in various stellar objects, such as Sn II lines were used for gas-phase abundance determination in a few interstellar diffused clouds [31, 32], photospheric resonance

lines of Sn IV detected in B main-sequence star AV 304 of the small magellanic cloud (SMC) [33] and in dozens of sdB and sdOB stars at temperatures varying from 22,000K to 40,000K [34, 35], and recently its presence is discovered through the Sn IV lines in cool DO white dwarfs [36]. In erosion probing of vessel wall tiles of future fusion power plants, such as ITER, spectroscopic data on tin may play a major diagnostic role [37].

The early analyses on the spectra of tin ions (Sn II-V) were mainly focused to the finding of energy levels and the transition wavelengths with relative intensities. In this regard, the depending source is *Atomic Energy Level* (AEL) [38]. The data in AEL are poorly known in order to meet the requirements of the modern times. The spectral data taken by Chien M. Wu [39] is still helpful after the corrections to be applied. In the present work, the motivation is to give comprehensive spectral analyses of singly to quadruply ionized tin ions (Sn II–V) on the basis of the wavelength measurements taken on a 3m normal incidence vacuum ultraviolet spectrograph in 300–2080Å region and also spectral line list given by Wu [11]. The reported data on each individual ion is subjected to critical evaluation. A brief introduction the theoretical supported given for the present analyses is given in Chapter 2. The experimental procedure involved for the recording of tin spectra in VUV region and spectra obtained in longer wavelength (λ>2000 Å) are presented in Chapter 3. This chapter also includes the general description of the analysis and various statistical tools involved. The analyses of Sn II–V are portrayed in detail from Chapter 4–7. At last, the conclusion of the present investigation is depicted separately.

References:

[1] http://www.nist.gov/pml/div684/grp01/atomic-history.cfm

[2] Sneddon J 1998 *Advances In Atomic Spectroscopy* (Jai Press Inc, London)

[3] Pradhan A K and Nahar S N 2011 *Atomic Astrophysics and Spectroscopy* (Cambridge University Press)

[4] Horton L D 1996 *Phys. Scr.* **T65** 175

[5] Quinet P 2011 *J. Phys. B: At. Mol. Opt. Phys.* **44** 145005

[6] Diddams S A et al 2001 *Science* **293** 825

[7] Hollberg L *et al* 2005 *J. Phys. B: At. Mol. Opt. Phys.* **38** S469

[8] Hibbert A 1975 *Rep. Prog. Phy.* **38** 1217

[9] Safronova M S *et al* 2009 *Nucl. Phys. A* **827** 411c

[10] Safronova M S and Johnson W R 2008 *All-order methods for relativistic atomic structure calculations*, in "*Advances in Atomic, Molecular, and Optical Physics,*" **55** Eds. Arimondo E, Berman P R, and Lin C C (Academic Press, San Diego)

[11] Edlén B 1964 *Atomic spectra in Handbuch der physic*, vol.27 (Springer, Berlin); p.125.

[12] Throne A 1995 *Phys. Scr.* **T65** 31

[13] Pickering J C 2002 *Vib. Spectrosc.* **29** 27

[14] Kramida A E and Nave G 2006 *Eur. Phys. J. D* **37**, 1

[15] Soderblom D R and Sherbert L E 1997 *HST Calibration Workshop, Space Telescope Science Institute* 486

[16] Federman S R and Cardelli J A 1996 *Phys. Scr.* **T65** 158

[17] Detcheva A and Grobecker K H 2006 *Spectrochim. Acta Part B* **61** 454

[18] D'Ulivo A, Mester Z, Meija J and Sturgeon R E 2006 *Spectrochim. Acta Part B* **61** 778

[19] Bakshi V 2009 *EUV Lithography* (SPIE and John Wiley & Sons, Inc.,Bellingham, WA/Hoboken, NJ)

[20] Kieft E R, van der Mullen J J A M, and Kroesen G M W 2005 *Phys. Rev.* E **71** 026409

[21] Ohashi H *et al* 2007 *J. Phys.: Conf. Ser.* **58** 235

[22] Katsunobu Nishihara *et al* 2008 *Phys. Plasmas* **15** 056708

[23] Fujioka S *et al* 2008 *J. Phys.: Conf. Ser.* **112** 042049

[24] Kambali I *et al 2013 J. Phys. D: Appl. Phys.* **46** 495104

[25] Roy A *et al* 2014 *Appl. Phys. Lett.* **105** 074103

[26] Djeniže S 2007 *Spectrochim. Acta Part B* **62** 403

[27] Naeem T M, Matsuta H, and Wagatsuma K 2006 *Spectrochim. Acta Part B* 58 891

[28] Cal C, Macaluso R and Mosca M 2001 *Spectrochim. Acta Part B* **56** 743

[29] Djeniže S *et al* 2006 *J. Phys. B: At. Mol. Opt. Phys.* **39** 3037

[30] Alonso-Medina A and Colón C 2008 *ApJ* **672** 1286

[31] Hobbs L M, Welty D E, Morton D C, Spitzer L and York D G 1993 *Astrophys. J.* **411** 750
[32] Sofia U J, Meyer D M and Cardelli J A 1999 *Astrophys. J.* **522** L137
[33] Proffitt C R, Sansonetti C J and Reader J 2001 *Astrophys. J.* **557** 320
[34] O'Toole S J, 2004 *Astron. Astrophys.* **424** L25
[35] O'Toole S J and Heber U 2006 *Astron. Astrophys.* **452** 579
[36] Chayer P, Vennes S, Dupuis J and Kruk J W 2005 *Astrophys. J.* **630** L169
[37] Foster A R, Counsell G F and Summers H P 2007 *J. Nucl. Mater.* **363** 152
[38] Moore C E 1958 *Atomic Energy Levels, National Bureau of Standards Circular 467* vol. III (Washington, DC: US Govt. Printing Office)
[39] Wu C M 1967 *The Atomic Spark Spectra of Tin, Sn III, Sn IV, Sn V*, Master thesis, University of British Columbia, Canada

CHAPTER 1

Theoretical background

The theoretical atomic physics is interlinked with the developments of quantum mechanics itself. The idea to treat the multi-electron atomic system was given by Niels Bohr through the assumptions of each electron moving in stationary states around combined field produced by nucleus and other electrons [1]. In this conjecture approximate wavefunctions are obtained for the entire atom/ion with the initialization from presumed single electron wavefunctions. This is a primary requirement for a many-electron atom/ion since the exact analytical solution, when Schrödinger equation is solved, is possible only for hydrogen or H-like ions. Hence the approximations are only a way to solve the Schrödinger equations for an N electronic atom as their constructions express a "catch 22" state [2]. For a multi-electron atom/ion the Hamiltonian for the electronic part can be written as

$$\hat{H} = \sum_{i}^{N}\left(-\frac{\hbar^2}{2m_e}\nabla_i^2 - \frac{Ze^2}{r_i}\right) + \sum_{i>j=1}^{N}\frac{e^2}{r_{ij}} \qquad \text{---------- (1)}$$

where the first term is related to kinetic and potential parts of each electron involved, and the second stands for mutual electrostatic interactions for the N electrons. This restricts one from splitting them into N set equations and solving them. A method that was well suggested and successfully applied is the **central-field approximation**, in which it is assumed that a larger part of electrostatic repulsion contains a spherically symmetric component which is predominately central (1/r variation). This reinforces to re-write the above equation as

$$\hat{H} = \hat{H}_0 + \hat{H}_1$$

$$where\ \hat{H}_0 = \sum_{i=1}^{N}\left(\frac{-\hbar^2}{2m_e}\nabla_i^2 + U(r_i)\right) \qquad \text{---------- (2)}$$

$$and\ \hat{H}_1 = \sum_{i>j=1}^{N}\frac{e^2}{r_{ij}} - \sum_{i=1}^{N}\left(\frac{Ze^2}{r_i} - U(r_i)\right)$$

The $\hat{H}_0$ is an unperturbed Hamiltonian, solution can be obtained directly by solving the Schrödinger equation and $\hat{H}_1$ treated as a perturbation and solved later. The difficulty that aroused to guess the U (r) is resolved by treating the concept of screening as r $\rightarrow\infty$ only Z-1 electrons are in spherically symmetric cloud, potential becomes proportional to 1/r (called perfect screening), and no screening, i.e. U (r)=Z/r as r is small. This basically provides a 'limit switch', however, further course of action necessitated is that an iterative approach should be followed.

1.1. Self-consistent field method

The strategy to solve a multi-electron problem was firstly given by D. R. Hartree, for which he had chosen 'indistinguishable particle approximation' to procure a wavefunction for N-electron as it is written as product of one electron wavefunctions.

$$\psi_N = \phi_1(1)\phi_2(2).....\phi_N(N) \qquad \text{---------- (3)}$$

Then to solve Schrödinger equation

$$H\psi_N = E_N\psi_N \qquad \text{---------- (4)}$$

In Hartree's self-consistent field method (SCF), it looks for the best estimate of the potential (initially guessed) obtained after iteration. For this purpose, set of Schrödinger equations is solved with a priori known potential, and then the charge distribution of the electrons are determined with the obtained approximate wavefunctions. The above charge distribution facilitates to improve potential and converging property of it is assessed. If they do not lie within the numerical criterion set for the convergence, the initial functions are varied in each successive cycle or iteration till a self consistency is achieved. It was Fock who incorporated the Pauli's exclusion principle to the Hartree's wavefunction, and thus they become anti-symmetric as per the Fermi-Dirac statistics and eqn (3) can be written in the form of a determinantal function.

$$\psi_N = \frac{1}{\sqrt{(N!)}}\begin{vmatrix} \phi_\alpha(1) & \phi_\alpha(2) & \cdots & \phi_\alpha(N) \\ \phi_\beta(1) & \phi_\beta(2) & \cdots & \phi_\beta(N) \\ \cdot & \cdot & \cdots & \cdot \\ \cdot & \cdot & \cdots & \cdot \\ \phi_\pi(1) & \phi_\pi(2) & \cdots & \phi_\pi(N) \end{vmatrix} \qquad \text{---------- (5)}$$

The above determinant is often known as 'Slater determinant' of spin orbitals, named after John C Slater. The sign of above determinant changes at every time when odd permutation operations carried out for N identical electrons. The product states of each electron consist of both space and spin functions, can be written as

$$\phi_\alpha(j) = \frac{1}{r_j} P(n_\alpha l_\alpha, r_j) S(l_\alpha m_\alpha \theta_j, \varphi_j) \chi_j(s_j) \qquad \text{---------- (6)}$$

Where P, S, and χ are radial, spherical harmonic and spin wavefunctions, respectively. The (n_α, ℓ_α, m_α) are the quantum number of a function has α spin and whereas (r_j, θ_j, φ_j and s_j) are the radial, spherical, polar and spin coordinates of the j^{th} electron. The potential is considered to be the same for all the electrons and to achieve a minimum energy for the system, once will be obtained when potential varies accordingly. This is something same as the variational principle and has same effect as looking for a self-consistent field. Thus the self consistent solutions, attained through the expectation value of the Hamiltonian in Slater determinant wavefunctions to be 'extremum', are achieved by invoking the variational principle.

$$\delta\langle \psi_N | H | \psi_N \rangle = 0 \qquad \text{---------- (7)}$$

This method is most commonly applied to get the wavefunctions and energy levels of multi-electron atoms. Although the intrinsic property of electron the 'spin' comes from the consequences of the Dirac relativistic equations, the Hartree-Fock SCF approximation takes account of it. Details on HF SCF method can be found in ref. [2-11]. It is well known that the Hamiltonian of eqn (1) has the remaining terms such as spin-orbit interactions (H_{SO}), spin-spin interaction term (H_{SS}) and H_{hfs} for accounting the hyperfine interaction. The spin-orbit interaction mostly treated as H_2 in Hamiltonian splitting, when $H_2 < H_1$. However, when spin-orbit interaction exceeds the electronic gross energy, .i.e. $H_2 > H_1$, the treatment would be different. It can be summarized that the gross structure energy (n, ℓ) is achieved from unperturbed Hamiltonian due to the central field. These energies were splitted into term because of the left-over electrostatic part in Hamiltonian H_1. And their final fine-structure splitting is facilitated by the spin-orbit interaction.

The HF SCF gives reasonably good results for light atoms; however for heavy atoms/ions the relativistic corrections are needed. The solutions of HF SCF are

numerical, rather than analytical, as they involve many integro-differential equations known as "Slater Parameters" (discussed in given sections).

In the present study, the theoretical interpretation of the analysis, such as energy levels, wavelengths and their transition parameters etc., are carried out within the framework of pseudo-relativistic Hartree-Fock method implemented in Cowan code [11]. Some important aspects of Cowan code [11] will also be discussed in coming sections. It is worth mentioning here that a number of other atomic structure codes are also available nowadays as the rapid advancements in the field and demand from various other sub-fields [12]. A few of them are given here, like many-body perturbation theory (MBPT), multi configuration Dirac-Fock (MCDF) method in employed through A general purpose relativistic atomic structure program (GRASP) code, Relativistic configuration interaction code (RCI) and Superstructure code featured by Thomas-Fermi-Dirac-Amaldi potential model.

1.2. The Cowan code's description

As discussed in above section, the Hartree-Fock self-consistent field method yields to numerical solutions than the analytic, as it involves many integro-differential equations to solve it. The contributions of J. C. Slater were outstanding in this regard as the simplification in inclusion of exchange interactions. The following parameters are named after J. C. Slater, and often used in the Cowan code [11] calculations.

i. E_{av}: This symbolizes for the average energy of the configuration, and has the form:

$$E_{av} = \int_0^\infty \left[r^{2l+2} \frac{d}{dr}\left(\frac{R^*_{nl}}{r^l}\right)\frac{d}{dr}\left(\frac{R_{nl}}{r^l}\right) - 2ZrR^*_{nl}R_{nl} \right] dr \qquad \text{---------- (8)}$$

ii. F^k **integral:**

$$F^k = \int_0^\infty \int_0^\infty R^*_{n_i l_i}(r_1) R^*_{n_j l_j}(r_2) R_{n_i l_i}(r_1) \times R_{n_j l_j}(r_2) \frac{2r(a)^k}{r(b)^{k+1}} r_1^2 r_2^2 dr_1 dr_2 \qquad \text{---------- (9)}$$

This parameter describes a part of the coulomb electrostatic energy of a single configuration, which is relied on the ℓ vectors orientation and it decides separation of the terms with same S but different L values.

iii. **G^k parameter:**

$$G^k = \int_0^\infty \int_0^\infty R^*_{n_i l_i}(r_1) R^*_{n_j l_j}(r_2) R_{n_j l_j}(r_1) \times R_{n_i l_i}(r_2) \frac{2r(a)^k}{r(b)^{k+1}} r_1^2 r_2^2 dr_1 dr_2 \quad \text{--------- (10)}$$

This is often known as **exchange integral** is an extra term, appears when spin-orbitals of two electrons are interchanged. This energy is always positive, and causes the shifting of same terms with different multiplicity. It should be mentioned that this parameter is vanishing for equivalent electronic configurations i.e. for np^2,nd^2 etc, in accordance with the Pauli's exclusion principle

iv. **R^k integral:**

$$R^k = \int_0^\infty \int_0^\infty R^*_{n_i l_i}(r_1) R^*_{n_j l_j}(r_2) R_{n_r l_r}(r_1) \times R_{n_i l_i}(r_2) \frac{2r(a)^k}{r(b)^{k+1}} r_1^2 r_2^2 dr_1 dr_2 \quad \text{-------- (11)}$$

This involves when more than one configuration is presented in a given parity such that the electron-electron Coulomb operator of them leads to the configuration interaction (CI) radial integral. They have both direct and exchange part, viz. RD^k , RE^k. Unlike F^k and G^k, the R^k may also have the negative values. The configurations whose average energies are not too far away, the effect of CI is more significant [11].

v. **ζ_{nl} spin-orbit interaction:**

$$\zeta_{nl} = h^2 \int_0^\infty |R_{nl}|^2 \zeta(r) r^2 dr = \frac{e^2 h^2 Z^4}{2m^2 c^2 a_0^3 n_i^3 l_i (l_i + 1/2)(l_i + 1)} \quad \text{-------- (12)}$$

$$and \ \zeta(r) = \frac{\alpha^2}{2}\left[\frac{1}{r_i}\frac{dV^i(r_i)}{dr_i}\right]$$

The spin-orbit interaction energy is dealt by the parameter ζ_{nl} and it has always positive sign since $dV_i/dr>0$ everywhere. The fine structure splitting of terms are decided by this parameter.

The Cowan's code [11] consists of a group of computer codes, which calculate the energy levels, transition wavelengths and their transition parameters etc through the superposition-of-configuration method. The original program was written by Dr. R. D Cowan of Los Alamos National Laboratory, USA, in Fortran 77 with four sets of main programs (**RCN, RCN2, RCG** and **RCE**). The suite includes many additional sub-codes which may either be used by the main program or others are utility based. In this work the windows based version of Cowan code [11] is exploited. This version was developed by Dr. A Kramida (see ref [12]). Some explanations of the key-programs are as follows:

(i) The foremost code **RCN** calculates the one-electron radial wavefunctions P_{nl} (r) (either bound or free) for each electrons of any number of given configurations of a spherically symmetrized atom through any of the following method (i) Hartree, (ii) Hartree-plus-statistical-exchange (HX), (iii) Hartree-Fock-Slater (iv) true HF and (v) Hartree-Slater. To run this, the inputs (ASCII) named IN2 and IN36 are compulsory. The relativistic correction to radial wavefunction will be also taken into account, generally the relativistic energy correction significant to inner orbital if Z>20 or outer sub-shells only when Z>50. The IN2 contains one line universal control card to run the program and IN36 comprises of the electronic composition of each configuration to be studied. The main output of this program contains the values of all Slater parameters (except R^k) which are later, used to determine the energy structure of that configuration(s). It generates two type of output, one in ASCII (OUT36) and other in binary form (TAPE2N). This TAPE2N will be an input for the next successive program. Table 1 presents the input file IN36.

(ii) The second code **RCN2** calculates the CI parameter R^k integrals between the couple of interaction configurations, and radial integrals of transition parameters like E1, or E2. Two files named OUT2 and ING11 are being created as output.

(iii) The code **RCG** takes the inputs from ING11 and generates the energy matrices for each possible J-value of the configurations in both parity, and obtains the energy eigenvalues and eigenvectors by matrix diagonalization. It results to compute the transition parameters, such multipole transition rates, oscillator strengths and radiative lifetimes of the levels involved. The outputs are named

as OUGINE and OUTG11 which is ASCII and TAPE2E binary file to back the subsequent program **RCE**.

Table 1. Sample input file, **IN36**, of Sn V to run primary code RCN [#]

```
200-90 0 2 01. 0.2   5.E-08   1.E-11-2 00190 0 1.0  0.65  0.0 1.00  -6
  50      5sn 5     4d10          4s2 4p6 4d10
  50      5sn 5     4d95s         4s2 4p6 4d9 5s
  50      5sn 5     4d96s         4s2 4p6 4d9 6s
  50      5sn 5     4d95d         4s2 4p6 4d9 5d
  50      5sn 5     4d96d         4s2 4p6 4d9 6d
  50      5sn 5     4d95g         4s2 4p6 4d9 5g
  50      5sn 5     4d96g         4s2 4p6 4d9 6g
  50      5sn 5     4d8s2         4s2 4p6 4d8 5s2
  50      5sn 5     4d8p2         4s2 4p6 4d8 5p2
  50      5sn 5     4d8sd         4s2 4p6 4d8 5s1 5d
  50      5sn 5     4d8d2         4s2 4p6 4d8 5d2
  50      5sn 5     4d95p         4s2 4p6 4d9 5p
  50      5sn 5     4d96p         4s2 4p6 4d9 6p
  50      5sn 5     4d94f         4s2 4p6 4d9 4f
  50      5sn 5     4d95f         4s2 4p6 4d9 5f
  50      5sn 5     4d8s5p        4s2 4p6 4d8 5s1 5p
  50      5sn 5     4d8s6p        4s2 4p6 4d8 5s1 6p
  50      5sn 5     4d8s4f        4s2 4p6 4d8 5s1 4f1
  -1
```

[#] The description of the input can be found in ref. [11]

(iv) The Least-squares fitting (LSF) of parameters employed in the Cowan code [11] makes it more versatile in experimental sense of the atomic structure studies. This has been facilitated through a chief-routine called **RCE** which let the 'Salter parameters' to be varied and adjust them in accordance of least-squares fitted values of the experimental energy levels. This minimization procedure, between experimental and theoretical quantities, is seldom adopted in other atomic codes, and in that sense the Cowan code [11] results are more reliable for the spectroscopic analyses. The other advantage is that the fitted parameters can be fed back to input to main program and to re-calculate the wavefunctions accordingly. This enables to generate the energy scaled transition parameters .i.e. transition rates, oscillator strengths etc. The RCE is also helpful to find the unobserved levels in atoms/ions concerned to which semi-empirical approaches can be applied either from the known series extrapolation or the isoelectronic trend of the particular ion in the sequence. It has also been observed that when significant number of levels of a configuration was established and subjected to the LSF, then remaining levels, mostly the single transition based, can be predicted (from LSF) within a few

hundred cm^{-1}. Thus, from the analysis point of view, the Cowan code [11] is very handy and flexible.

1.3. Transition probability

Once the energy levels involved in each configuration is determined, the transition wavelengths along with various transition parameter like oscillator strengths, transition probabilities, lifetimes of levels are being computed. In this work the electric dipole (E1) transition are mainly studied.

The selection rules for E1 transitions states that $\Delta\ell=\pm1$, $\Delta J= 0, \pm1$ (J=J'=0, is not allowed). The primary calculated quantity for the transitions are the line strength **S**. Thus the transition probability for an electric-dipole (E1) transition involved between $\gamma'J'$ and γJ, the upper and lower state, respectively, is defined as

$$A=\frac{64\pi^2e^2a_0^2\sigma^3}{3h(2J'+1)}S \qquad \text{;where} \quad S\equiv\left|\left\langle\gamma J\left\|P^{(1)}\right\|\gamma'J'\right\rangle\right|^2 \qquad \text{-------- (13)}$$

is known as the electric dipole line strength. The weight transition probability gA (where g=statistical weight of the upper level) is easily expressed in

$$gA=(2J'+1)A=\frac{2.0261*10^{18}}{\lambda^3}S \qquad \text{---------- (14)}$$

Where λ is in Å ($\lambda=1/\sigma$), A in sec^{-1} and **S** in atomic units. The weight Oscillator strength (g_i=2J+1, statistical weight of lower level) can conveniently be expressed in the form

$$g_if=1.4992*10^{-16}\lambda^2g_kA \qquad \text{---------- (15)}$$

The further information can be found in ref. [11, 14].

References:

[1] Bohr N 1922 *The Theory of Spectra and Atomic Calculation*, Cambridge University Press, Cambridge

[2] Deshmukh P C, Banik A and Angom D 2011 'Hartree-Fock self-consistent field method for many-electron systems' in Srivastava R and Choubisa R (editors), *Atomic and molecular physics-introduction to advanced topics* (Narosa Publishing House, New Delhi)

[3] Condon E U and Shortley G H 1959 *The theory of atomic spectra* (Cambridge University Press)

[4] Hartree D R 1928 *Proc. Camb. Phil. Sco.* **24** 89

[5] Slater J C 1929 *Phys. Rev.* **34** 1293

[6] Hartree D R 1960 *The calculation of atomic structure* (John Wiley and Sons, Inc. New York)

[7] Slater J C 1960 *Quantum theory of atomic structure* vol. I chapter 8 & 9 (Mc. Graw-Hill Book Company, Inc. New York)

[8] Slater J C 1960 *Quantum theory of atomic structure* Vol. II chapter 17 (Mc. Graw-Hill Book Company, Inc. New York)

[9] Fischer C F 1977 *The Hartree-Fock Method for atoms* (J. Wiely and Sons)

[10] Bethe H A and Jackiew R W 1997 *Intermediate Quantum mechanics* (Addison Wesley)

[11] Cowan R D 1981 *The Theory of Atomic Structure and Spectra* (Berkeley, CA: University of California Press)

[12] Pradhan A K and Nahar S N 2011 Atomic Astrophysics and Spectroscopy (Cambridge University Press)

[13] Kramida A, PC *version of Cowan code package for Windows* available from http://das101.isan.troitsk.ru/COWAN

[14] Martin W C and Wiese W L 1996 'Atomic spectroscopy-A compendium of basis ideas, notations, data, and formulas' in Drake G W F Edited, *Atomic, Molecular, and Optical Physics Handbook*, (AIP Press, Woodbury, NY) http://www.nist.gov/pml/pubs/atspec/index.cfm

CHAPTER 2

Experimental details

This chapter exemplifies the experimental part that involved in the present investigation. The experimental spectroscopic study would be incomplete without the descriptions of the *spectrograph*-an instrument which disperses the light into its minimal components and later, allows measuring each, the *light source*-the source which emits/absorbs the radiations under investigation, and suitable *detectors* to perceive the radiation that falling on it and let it to be identified. There are two distinct classifications for the light sources (i) continuous light sources and (ii) discontinuous sources, based on their nature of emission. The radiations falling thoroughly in all wavelengths are defined by continuous sources (e.g. incandescent filaments and liquids). However, the latter source contains the sharp lines or bands of the wavelength for a region, e.g. individual atomic or molecular emissions.

The present study is mainly supported with spectrum of tin obtained from a 3m normal incidence vacuum spectrograph (NIVS) in wavelength 300-2000Å range (called vacuum ultraviolet (VUV) region) with the triggered spark light source. The details regarding the descriptions of the light source, the spectrograph and radiation detection technique used are discussed below in different sections of this chapter, followed by the method of wavelengths or data reductions, their ionization discrimination and uncertainty assessment. Later, the methodology of analysis involves the usage of wavelengths or wavenumbers measured and their further implications in light of present investigation are also shown in a separate section. The intensity of lines observed in spectrogram and their plasma modeling leading to the determination of the source temperature of spectrum under investigation is also given in this chapter. The analysis is supplemented from the measurements of others, in such cases, some criteria is fixed for accepting them. The systematic corrections and realistic estimate of their statistical uncertainty are also added in a separate section. At the end some salient features related to the spectroscopic data acquisition and their applications are also described briefly

2.1. The light source

It is one of the prerequisite for the spectroscopic studies an appropriate source, either emission/absorption, as desirable for the investigation under consideration. Other than this, the compatibility of the source within the instrumental conditions such as vacuum requirement may also be satisfied. As far the emission sources are concerned, there are a plenty of them, namely different type of discharges (arc, spark, gaseous discharges), laser produced plasma (LPP) sources, beam-foil-plasma, many other ion sources like electron beam ion trap (EBIT), electron cyclotron resonance (ECR) etc. were proficiently used in various studies [1-5].

The present work mainly focused on the spectral analyses of low charged (singly to four times ionized) tin atoms. i.e Sn II–V in VUV wavelength region, and hence a vacuum compatible triggered spark was used for this purpose [6]. This source is a modification of conventional spark source that contains a high voltage power unit (DC), an energy storage fast charging capacitor, an analytical spark gap (a pair of electrodes), and couple of resistors and/or inductors as components of the charging and discharging unit. The charging and discharging mechanism enable to charge the capacitor alternatively and so that it allows the capacitor to be discharge across the spark gap, i.e. between electrodes, to flash out the radiations which are to be analyzed. In vacuum spark source [7-9], the field distortion is necessitated for the discharge, have been attained in various ways;- electrical, gas, irradiation etc. [10]. In this work, a vacuum triggered spark source used, which has an extra-electrode, other than those for analytical spark gap, to initiate the discharge in the vacuum state. A triggering model, TM-11 A, which is capable to launch electrical pulses upto 30 kV in 0.3 ms rise time, was used in this regard. The charging potential may vary from 2–50 kV, largely relied on the ionic stages to be excited. Sometimes the multiple units of capacitors are used. The power supply used in this study was a 1-20 kV DC type, and a 14.5μF low inductance capacitor used was having a fast charging capacity to carry on the discharge and charging mechanism in successive spark shots. At high voltage discharge, the spectral density is dominated by lines from the higher ionization, hence segregation of the ions of various charge state was to be carried out. This has been achieved in two ways: (i) reducing the discharge voltage (ii) introducing the required amount of inductance coil into the spark circuit to reduce the ionization power of the source. In either method, the production of higher ionic stages can be trimmed down

and hence their spectral lines. The other type of spark source "sliding spark" is also widely used for the spectroscopic studies, and it is basically a low-voltage but high current source (V_o= 200V–2 kV & I_{peak}=200–4000 A). It has no triggering mechanism; instead the charging is made fast by rotating spark gap and hence the spark just slides around the spacer used. More descriptions about them can be found in ref. [11-18].

2.2. The spectrograph and detection plates

The choice of the spectrograph also depends on the requirements of study, the wavelength range of investigation, required resolution, region of coverage with the grating and their design etc. The spectrograph consists of primarily, an entrance slit, prism or diffraction grating, sometimes extra optics like lens or mirrors (depends on the geometry), and an exit part where the suitable detectors are placed. Depending upon the design and construction, the type of gratings and their mounting would be different. In the present study, the two type of spectrographs were used for covering the two sets of wavelengths region; for $300>\lambda<2080$ Å and $\lambda>2000$ Å. The VUV data is vital for the scope of this analysis as low resolution wavelengths of tin ions are available in the literature. The wavelengths above 2000 Å are taken on 1.5m Wadsworth spectrograph using two sets of gratings with an open air spark as a light source. It is important to mention that this data helped us at qualitative level only, as there can be more improvements especially for the detection and calibration etc (see section 2.5.3).

The wavelength measurements below 2000 Å will only be possible if vacuum conditions are persisted inside spectrograph. Thus, a vacuum of the order of 10^{-5} to 10^{-6} Torr is typically maintained inside the spectrograph tank where the grating is housed. The selection of grating is again related the above concerns that mentioned for the spectrographs and mostly the reflection gratings are used. The following parameters of the grating are very important (i) the focal length, surface design and type of ruling, they may either be mechanically ruled or holographicaly designed, the geometry namely plano, concave, spherical, toroidal etc. are very common, (ii) the grooves density, for example 1200 lines/mm, and (iii) blazing parameters like blazed angle and wavelength (the blazing is employed for improving the efficiency of grating at desired order). There are various types of mounting that have been readily used in

grating spectroscopy and they mainly depend on grating surface design, other conditions such as orientation of optics involved etc [12-15]. In case of concave grating, the most essential criteria to be satisfied are the Rowland conditions; such that the slit and detector or plate holder must be placed on point in a circle formed by the curved surface of the grating and the grating radius is equal to circle diameter. This would strictly be applied to normal incidence type of spectroscopic instruments and also to grazing incidence device with exemption that some disposing conditions permitted for entrance channel length [12-15].

For this work, the spectrograph used to record the spectrum of tin was a 3m normal incidence vacuum spectrograph (NIVS), of Antigonish laboratory, Canada. This spectrograph was equipped with a concave osmium coated holographic grating having 2400 lines/mm surface ruling, capable of producing 1.385 Å/mm linear inverse dispersion in first order. The grating was mounted in simple eagle type design such that it was facilitated to cover the full wavelength range 300–2080 Å at the two settings of fixed angle of incidence. The angle of incidence in first setting is 9°, and that covers the 300–1240 Å wavelength range. For covering the longer wavelength, an angle 17° is chosen which will cover the spectral region 1050–2080 Å.

The spectrograph is fully designed in a cylindrical pipe of internal diameter (ID) of 32 inches and total length of 3.5m. The grating was housed on a rigid support at one end on the axis of the cylindrical tank. The other end consists of (i) a slit adjustment unit which is fixed at outer surface of the main cylinder such that about 7° off geometry exists between their axes (ii) a 30x2 inches long plate holder unit which is inside the main chamber. The triggered spark source chamber is connected next to the slit. In order to preserve the vacuum environments the compatible components are used and hence the outgasing can be reduced. From either side, cylinder is closed by using big flanges with proper gasket for vacuum sealing and the vacuum was preserved to $1.2*10^{-5}$ mbar with the aid of a silicone oil diffusion pump (operated after rough vacuum obtained with a rotary pump).

The plate holder total length fits along the Rowland circle to accumulate such that either three plates of dimension 10"x2" each or two of 15"x2" could be placed. The slit width was variable from 10 to 50 micron and optimum slit width 15-25 micron was normally chosen for the recording the spectrum. The plate holder has a vertical movement system controlled from outside of the main tank without disturbing

the vacuum. This enables one to take multiple tracks of spectrum under varied experimental conditions. The full experimental set-up of spectrograph can be seen in figure 2.1. In the present study the spectrograms were taken on a specially made (gelatin-free) short-wave radiation (SWR) Kodak plates available in 10" and 15" (length) dimension.

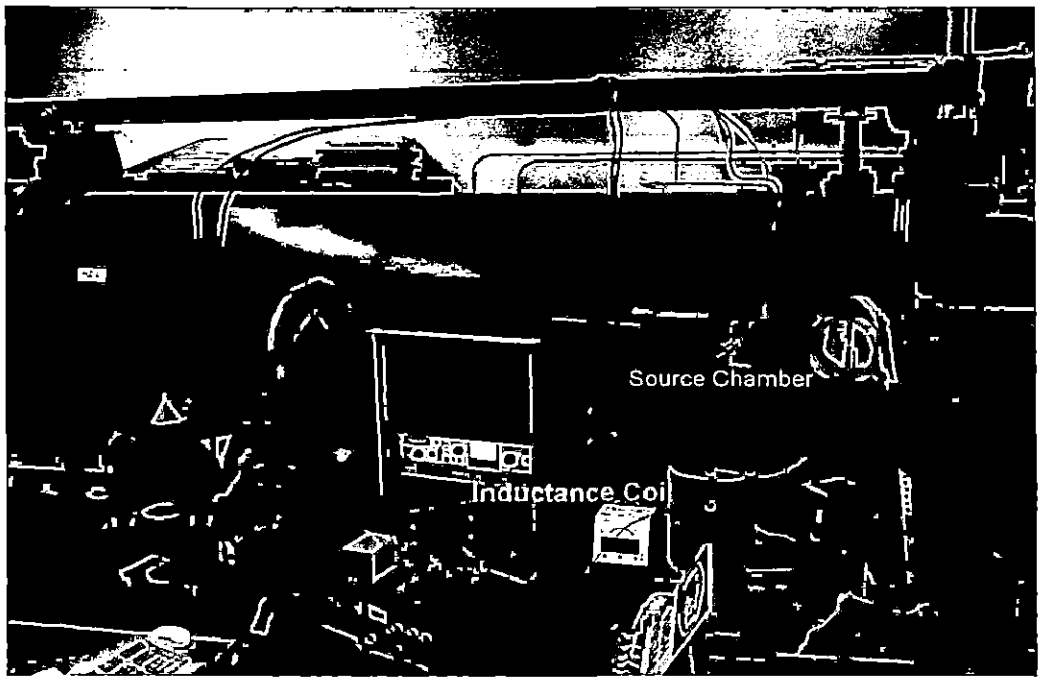

Figure 2.1. The experimental set-up of a 3m normal incidence vacuum spectrograph

2.3. The spectral recording of tin ions

The tin ions/atoms were excited by means of a vacuum triggered spark source of above specifications. Either pure electrodes made of tin, or tin samples inserted into a cavity in aluminum electrodes were used. The tin spectrum was recorded at St. Francis Xavier University, Antigonish (Canada) using a 3m normal incidence vacuum ultraviolet (VUV) spectrograph in the 300–2080 Å wavelength region by Prof. Tauheed Ahmad.

At least four or five different tracks of spectrum were photographed on Kodak SWR plates with varied experimental conditions, such as electric current and voltage. The exposure time for each track was set for getting 20-30 spark shots. The purpose of the different exposures was to distinguish the lines of particular ionic state from

other ionization species. This was achieved by inserting a low, medium, or high inductance in series with the spark circuit or by varying the charging potential within the limits of 2 kV and 6 kV. The inductances were made of copper wire, 2 mm in diameter, wounded on a cylinder of diameter 24 cm in turns separated by about 4 mm. A low inductance coil had 8 or 9 turns of wire, a medium one had 25 turns, and the high inductance one had 40 to 50 turns. The summary of analyzed ionization separation of different ions is given in section 2.6.

In 300 - 1240Å wavelength range, i.e. at first setting of the spectrograph, three 10" plates were used to cover the 30 inch spectral region. In the second setting, two 15" plates were used. After the exposure, the plates were preserved in dark conditions till they were subjected to photographic 'conventional' image processing. For this purpose, plates were developed in a Kodak D-19 developer (about 3 minutes) and then fixed at F-5 Kodak rapid fixer (for 5-10 minutes).

2.4. The wavelength calibration and assessment of uncertainty

Once the spectrum is obtained, then the relative positions of spectral lines on the plates were measured using a Zeiss Abbe comparator at the Aligarh Muslim University (India). By this time, the intensities of lines, i.e. a measure of the photographic emulsion blackening, with some line characteristics such as sharpness/broadness, polarity, asymmetry, length, haziness etc were also noted. This partially helps for the identification of their ionization origin. For their wavelength reduction, one has to use the highly accurate reference lines. In this regard the interferometrically measured lines and/or Ritz-type of standards are, generally used, as the accuracy of Ritz wavelength is often 2 to 3 orders of magnitude higher than that of the observed lines [20]. Thus, we used as internal standards the known impurity lines of C II [21, 22], C III [21, 23, 24], C IV [25], N II [18], O II [26], O III [27], O IV [28], Al II [21, 29], Al III [21, 25], Si II [21, 25], Si III [30], and Si IV [25]. The measured positions of the reference lines on the plates were fitted with second or third degree polynomials to obtain corrections to the dispersion curve. The standard deviation of the fits varied from 0.003 Å to 0.007 Å for different spectral regions and different plates. The mean value of 0.005 Å represents a rough estimate of the wavelength uncertainty of our measurements for sharp and unperturbed lines.

The rough estimate of uncertainty given in above, 0.005 Å for strong unperturbed lines is insufficient for deriving accurate energy level values from the observed wavelengths. For that purpose, it is necessary to estimate the uncertainty for each individual line. The two main factors determining our measurement uncertainty are the uncertainties of the reference wavelengths and statistical uncertainties in measuring the line positions on the plates [8]. The first of these two factors contributes to the systematic uncertainty. About 70% of the used reference wavelengths have uncertainties $\leq$ 0.003 Å. However, in order to provide a sufficiently uniform coverage of the studied wavelength range, in some regions we had to use a few less accurately known wavelengths with uncertainties up to 0.005 Å. The uncertainties of the reference lines were either taken from the original papers or estimated from deviations of the quoted reference wavelengths from the Ritz values given in the *Atomic Spectra Database* (ASD) [20]. Our statistical uncertainties greatly depend on the shape and width of the line profiles. The width (full width at half-maximum) of a selection of 23 lines on our plates in the region from 1190 Å to 1800 Å was roughly estimated from the comparator displacement readings and the known dispersion factor. For isolated symmetrical lines showing no visible broadening but their widths were between 0.02 Å to 0.04 Å, while several lines, appearing as hazy, showed a significant broadening of up to 0.15 Å. We attribute this clearly visible broadening to autoionization of the upper level. In addition to this, a number of lines with wider and stronger characteristics appeared on the plates, as they are mostly the first resonance lines and/or the transition involved between the low-lying excited states. These types of lines were also measured at less accuracy.

The statistical uncertainties of the measurement of line position on the plates, estimated by repeated measurements, were the greatest for the widest lines, which were those with longest wavelengths, those of low-lying state and those widened by autoionization. One of our plates had unusually large line widths in the long wavelength region, which was excluded from the measurements. Positions of sharp isolated lines could be measured on our comparator with uncertainties of about 2 μm for the shortest wavelengths and up to 5 μm for the longest ones. This corresponds to statistical uncertainties of about 0.003 Å at 900 Å and 0.007 Å at 1900 Å. For the widest lines broadened either by strong nature or by autoionization, we estimated the statistical uncertainty by extrapolation, i.e., by multiplying the uncertainty of narrow

lines in the same region by the ratio of the line widths, yielding uncertainties as large as 0.02 Å. For blended lines, the uncertainty was doubled. Most of the lines were measured on two to four plates, and some were also measured in the second order of diffraction. For such multiply measured lines the statistical uncertainty of the reported average wavelength was significantly reduced, leaving the uncertainty of the reference lines as the main contributing factor. They vary from 0.006 Å for sharp lines below 1050 Å to 0.02 Å for very wide and blended lines. All uncertainties reported in the present work are meant to be on the level of one standard deviation.

2.5. Supplementary data

The spectra of tin atoms/ions became a subject of interest by various researcher in the past (see the introduction of chapter 3 – 6). Most of the previous studies made, had reported only the spectral lines of individual ions. However, a few exceptions are there and given in sub-sections here. The details regarding the tin spectra recorded by us, at Aligarh for above 2000 Å will also be discussed.

2.5.1. Measurements by Chien-M. Wu

A master thesis on *The Atomic Spark Spectra of Tin, Sn III, Sn IV, Sn V* by Chien-Ming Wu [31], (available online) gave the spectral linelist of the tin. Wu photographed the tin spectra in the region between 350 Å and 9000 Å using an electrodeless discharge. A condensed spark in helium with a 3m normal incidence vacuum grating spectrograph and a prism spectrograph were used in the regions below and above 2400 Å, respectively. Wu reported a total of 3403 spectral lines, of which he assigned 110 to Sn I, 128 to Sn II, 321 to Sn III, 177 to Sn IV, and 118 to Sn V, leaving the remaining 2549 lines unassigned to any particular ionization stage. The Wu's reported wavelengths were affected to severe systematic errors by various reasons like his measurements were from low resolution instruments and availability of less accurate standards at that time etc. Although all wavelengths in Wu's line list were given with three digits after the decimal point (in angstroms), the wavelength uncertainty varied greatly depending on the wavelength region and on the spectrographs used. In the present work, the efforts were made to correct the reported wavelengths of Wu's [31] with the help of lines of tin observed by us and some highly

accurate interferometric lines of tin reported by Brill [32]. The entire procedure of this internal calibration is explained in chapter 3.

2.5.2. High resolution measurements of tin at Troitsk

Our wavelength data of tin were also supplemented by the high resolution measurements of tin made by Dr. Ryabtsev at Troitsk, Moscow [33]. A brief description of the experiment is presented here. The light source used was a three-electrode vacuum spark. A set of spectrum were taken in 200–350 Å, for which a 3m grazing incidence spectrograph was used with a holographic grating of grooves density 3600 lines/mm. The reciprocal linear dispersion was varying from 0.36–0.45 Å/mm for the given region. In the second set of experiment, for covering the wavelength 350–650 Å range, a 6.65m normal-incidence spectrograph with a grating of surface ruling 1200 lines/mm with first order linear dispersion of 1.25 Å/mm was used. Both Spectra were photographed on Q2 plates from Ilford. The ionization separation was made with lines intensity variation on different tracks with varying experimental conditions. The position measurements of spectrogram were made with the help of a UMAX Power-Look 3000 scanner with standard image processing. The wavelength reduction of normal incidence spectrum was made with the known lines of oxygen, carbon, and silicon impurity ions. The gazing data is calibrated with known lines of titanium and Sn VI ions. The quoted uncertainty of the measurements was 0.003 and 0.006 Å for shorter and longer wavelength region, respectively for sharp and unblended strong lines. More explanations can be found in ref. [34-36].

2.5.3. The measurements at Aligarh

The spectral data of tin ions are inadequate for above 2000Å, in modern spectroscopic times with higher resolution instruments available, with only a few exceptions in Sn I and Sn II where some interferometric lines are reported [32]. As mentioned above, the only available source for the above VUV region is Wu's linelist. However, the ionization identifications and the reliability of his observed values are not quite encouraging. We recorded spectrum of tin ions at spectroscopy laboratory of Aligarh on a 1.5m Wadsworth grating spectrograph using an open air spark source. Both the electrodes were made of pure tin metal (99.99%). Two sets of gratings were used for covering the wavelength range 2200–9000Å. A grating of 1200

lines/mm for covering 2200–4800Å region and another grating of surface ruling 600 lines/mm for longer wavelength 4300–9000Å. The spectrum was photographed on a commercially available film and for identification and calibration of the tin lines, the spectrum of Hg-vapor lamp was blended (at different slit length). Due to some instrumental limitations and detection methods etc., the estimated accuracy of lines was less estimated. Therefore, in level optimization the longer wavelengths (>2000Å) were taken from the Wu's corrected line list [31]. However, this spectrum was helpful in the identification of ionization character of various ions as evident from figure 2.2.

Figure 2.2. Spectrum of tin in 2800–3750Å, the short lines are of Hg I as marked, the value left to it is wavelength in Å, and others are Sn lines. Certain indentified lines are marked.

2.6. The spectroscopic analysis and tools involved

In atomic spectroscopy, the analysis principally means the establishing of the atomic energy levels, thereby reporting wavelengths and their transition probabilities. It basically elucidates the structure of the atom/ion under consideration. The atomic data have number of attractions from various fields of research and technology. It has become a growing trend in physical research that the importance of high resolution and more-precise measurements are increasing. It may not be right when the demands from space astrophysics were taken into consideration, where the collected data still were un-interpreted due to inadequate laboratory measurements.

As far as the atomic databases are concerned, the current existing, most update database is the *Atomic Spectra Database* (ASD) of National Institute of Standards and Technology (NIST), USA [20, 37]. Nowadays, the people at NIST are more focused to the critical assessments of existing atomic data of an ion/atom [38]. This involves reporting of (i) the transition wavelengths with their uncertainty and intensities, (ii) observed energy level values and uncertainties, and were optimized within one level standard deviation, (iii) generation of the Ritz wavelengths with their uncertainties,

and (iv) acquiring of radiative transition probabilities and/or the oscillator strengths of transitions involved and assessing uncertainty of the calculated values. Therefore, we have focused mainly on these issues.

Once the spectral line list is readied, the analysis of the ion of the interest can be started. However, it would always be good if the previously known lines of different ionic state, for example Sn II, Sn III, have to be discriminated before the analysis of any particular ion.

The **ionization separation** of various ionic stages is briefly described here The spectrum on first track was taken at 6kV potential. It comprises with dense appearance the spectra of Sn IV and higher ions, only some prominent lines of Sn I and Sn III appeared on this track as strong. The second track, was taken at 6 kV with low inductance, the intensity of Sn V lines decrease, showing polar character with a few exception from strong lines. The third tack of the spectrum was recorded at 4kV without any inductor coil; the Sn IV and Sn III lines are prominent on this track, but Sn V lines declined further. The next track again at 4kV with medium inductance in the circuit, showing enhancement of intensities of Sn II and Sn III lines. The last track at 2kVdischarging potential with higher number of spark shots reveals that the lines from Sn II ions get much stronger than Sn III, and Sn IV gets weaker, while Sn V disappears (see in appendix).

The above described ionization separation helped to confirm all the reported lines, and finding new lines for the ion under investigation. It should be mentioned that the complex structures of atom/ion always pose some complication, and such things were always a challenge for the analysis [39]. A schematic diagram of the analysis is demonstrated in figure 2.3, basically it is an illustration given by Kramida [38] for the critical evaluation of atomic reference data that presently implemented at NIST [20]. The strategy that applied in this work is that the main analysis was carried out with data which are most recent and reliable; viz. the measurement by us supplemented data of Ryabtsev, some interferometric lines reported by Brill [32] particularly for Sn II. When significant part of the main analysis is completed, i.e. multiple series are known and transitions between many nearby excited configurations connected from the longer wavelength (Wu's linelist), the extension of series or search for new levels were taken into consideration. In this approach, there were

number of fixed/fixable quality criteria for accepting the data either existing or new, such as wavelengths with their uncertainties and observed intensities (sometimes

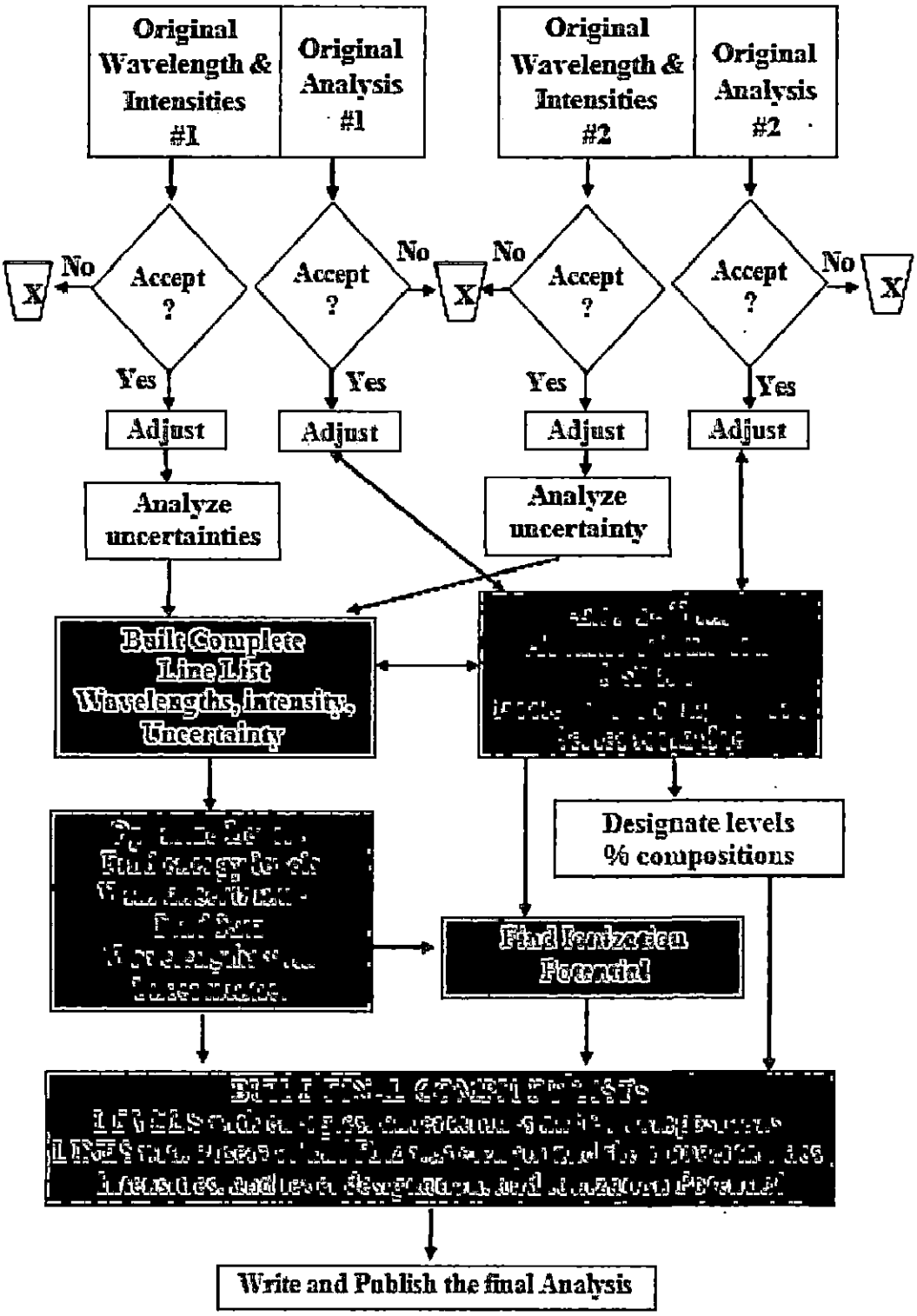

Figure 2.3. The schmatic diagram of the procedure invlolved in the analysis.

plasma modelling were applied to test the consistency in given intensities), for observed levels their agreements with ab-initio calculations and least-squares fitted values, if many series are known then their series regularities etc.

The other type of consistency check is carried out when the observed wavelengths subject to the level optimization (see section 2.6.3). It has been recently reported by Kramida [40] that these critical assessments sometimes lead to dismissal of the previous analysis. The levels searching are made easy by using two computer programs, FIND3 [41] and GENTRAN [42]. The development of latter, was encouraged by the methods that described by Reader [43].

2.6.1. Isoelectronic comparison

The term 'isoelectronic' is self-explanatory, as the number of extra-nuclear electrons is same for a atom/ion concerned then such atom/ion is called isoelectronic member of its sequence. For example, if we take a sequence of In, Sn^{+}, Sb^{2+}, Te^{3+}, I^{4+}, Xe^{5+}, ..., they all having same number of outer electrons around the nucleus with their spectroscopic representations In I, Sn II, Sb III, Te VI, I V ....., then it can be said that Sn II (second spectrum of Sn or singly ionized tin) is a member of In I isoelectronic sequence. The Sn II can also be classified as In-like Sn, (read as Indium like tin) is also very common; however this classification is very much used when atoms/ions were highly stripped. The important features of isoelectronic members are (i) they will have same structure (ii) their similarity or regularity can easily be tested along z (the spectrum number or core ionic charge Z_c, defined as z=Z-(N-1) where Z is atomic number and N is the total number of extra-nuclear electrons in atom/ion) provided no other circumstances exhorted.

The isoelectronic trend of levels or configuration along the sequence is a well applied tool in the past and even now to confirm the analyses or sometimes to hunt the new levels of atom/ion under investigation. The efforts of Prof. Bengt Edlén were excellent in this regard. In general, the E_x/z vs z, or $E_x/(z+c)$ vs z are used in this regard (x stands for either HF or observed energy), more details can be found ref. [44-45]. It has to be mentioned that isoelectronic regularity can be distorted by the presence of configuration interaction existing in a particular atom/ion.

2.6.2. Plasma modeling for the observed intensity

In early course of atomic spectroscopy, the central attention of the research was limited for finding energy levels and reporting of the transition wavelength with relative intensities. The relative intensities were mostly just a measure of photographic emulsion blackening or plate transmission, in limited cases the area under the peak/densitometric traces were given. Apart from these, if the analysis of a particular ion contained the observations from many, where each had used different type of light source, instruments and detectors, causes a lot of difficulty in scaling of their intensities into a common scale.

The ideal case of intensity measurement is possible if and only if a unique test source having uniform emission of radiation at all wavelengths and/or the special spectral instrument and detector should have equal quantum efficiency to all wavelengths. This is an unattainable task, thus, the relative intensities are somewhat reliable estimate for many application researches. In modern times, the challenges in reporting of relative intensities of lines are somewhat fulfilled with measurement from Fourier transform spectrometer (for λ>1400Å) and for shorter wavelengths, by applying a new detection mechanism, phosphor based screens (called image plates or IP) other than the conventional photographic technique [46, 47].

The different scaling of intensities always creates difficulties to many researchers, like the branching ratio data needed in space astrophysics. It has been shown that a method well applied and formulated in studies by Kramida [38, 40, 48], the local thermodynamical equilibrium (LTE) based thin plasma modeling would qualitatively describe the intensities of the transition wavelengths of a given spectrum. In this process the observed line intensities from various light sources are subjected to certain approximation by LTE states, and the source temperature of each is determined and then they are re-scaled to a uniform common excitation temperature of the source.

The actual intensities observed in any spectroscopic experiment would have the contributions from various sources such as (1) the light source excitation temperatures, (2) the instrumental sensitivity across the full wavelengths (for example grating efficiency), and (3) the wavelengths response of the photographic emulsion (or any registration equipment) other than the non-linearity appearing at some places due to the non-uniform emulsion coating. The effects due to latter two, i.e. in general

the wavelength dependence of the set-up (both from instrument and detector) should be removed before the determination of the source temperature.

The basic assumption applied in this method is Boltzmann distribution law for optically thin plasma at LTE such that collisional processes which are more local conditioned than the non-local radiative processes. The following equations can easily be written for an atom at z ionic state:

$$\frac{n_k}{n_i} = \frac{g_k}{P}\exp\left(\frac{-E_k}{k_B T}\right) \qquad \text{---------- (1)}$$

$$I_{ki} = \frac{hc}{4\pi\lambda_{ki}} * A_{ki} * n_k * L \qquad \text{---------- (2)}$$

Where n_k and n_i are for population of atoms in given k and i states, P is the partition function of the given ion, E_k the energy of upper level k, g_k stands for upper level degeneracy and T for the plasma temperature. In eqn (2), I_{ki} is the intensity for λ_{ki} transition whose transition rate is A_{ki} and L represents the characteristic length of the plasma. The other symbols have their common meaning. The above equations can often be combined and rewritten as

$$\ln\left(\frac{I_{ki}\lambda_{ki}}{g_k A_{ki}}\right) = \frac{-1}{k_B T}E_k + \ln\left(\frac{hcn_i L}{4\pi P}\right) \qquad \text{---------- (3)}$$

It can be inferred from eqn (3) that it leads to linear-plot (called the Boltzmann plot) as the last term reduced to a constant for an atom/ion at given ionic state z. Thus a general formula can be written in form

$$Iobs \propto (gA/\lambda) * \exp(-E_k / k\,T_{eff}) \qquad \text{---------- (4)}$$

The proportionality constant is replaced with derived wavelength response curve of the given spectrum. The eqn (4) quickly indicates to the validity of LTE-thin plasma model as it requires transition probability values, gA, for which the Cowan's code calculations are relied. The right side of the eqn (4) collectively represents to I_{cal} (calculated intensity) which has intrinsic quantities involved, however the observed intensity is extrinsic that can be affected by actual plasma conditions. Thus, the strength of this model is at qualitative only for taking the relative intensities of lines from a particular ion. It should be mentioned that the given model fails to account the real plasma conditions, such as decay from the plasma temperature, instabilities due to many plasma state processes and deviations of intensity due to similar or other

atoms/ions etc. Rather than the collisional processes the radiative processes are of non-local character, the latter deviate the LTE states present in the plasma.

This work also involves the wavelengths and intensities from many sources, VUV measurements from triggered spark (300-2080Å), Wu's measurements (350-9000Å) and Troitsk's measurements (200-650 Å). Thus a common scaling for intensities was necessitated to remove the source variation and the spectral response of different equipments etc. The results and their further discussions are given in each respective chapter (chapters 3-6).

2.6.3. The energy level optimization

Once the transitions are identified between the levels involved, the values of energy levels observed are to be optimized. For this purpose, earlier we used to do optimization with the aid of a computer program 'KLAS' [49], which finds the solution by matrix inversion method, but it does not account for uncertainty of each observed wavelength. Recently, a more efficient method was addressed and implemented in a program called least-squares level optimization LOPT by Kramida [50]. This is basically a combination of methods suggested by Radziemski *et al* [51] and formalism given by van het Hof [52]. In first stage, the levels were optimized by solving the matrix equation corresponding to a set of linear equations. In stage two, the obtained matrix equation is modified and the inverse of matrix is determined. This enables to estimate the uncertainty of Ritz values as linear combination of the components of this inverse matrix. The full description of method and program can be found in ref. [50].

In this work, levels of each observed spectrum of tin ions were optimized with LOPT code. Before the optimization of the levels it was ensured that no systematic errors/shifts exist for the observed wavelengths. The LOPT code takes the inverse square of uncertainty of each observed lines as weight in optimization procedure. Thus, the observed wavelengths and their uncertainties, associated with lower and upper level designations are required for each transitions involved. This is the main input file. The other input contains the level values of fixed levels; the mandatory entry is that ground most level must be fixed at zero energy with absolute zero uncertainty. To run the program, the parameters involved are fed into a file named as

".PAR". The output of LOPT contains two files, one for optimized energies and other for classified transitions.

The formatting of the transition input file was assisted at great extent by an excel application made by us called "INGEL" (stands for Input generator for LOPT) [53]. As pointed out in above sections, some consistency tests could be carried out with LOPT before the analysis to be approved. The foremost indicator is the residual sum of squares, RSS, of deviations of measured transition values from the differences of the corresponding optimized levels. It takes a statistical measure on how values obtained with the assigned uncertainties limits. For a normal statistical distribution, the RSS should be close to the number of degree of freedom (N_{dof} =difference between total number of observed transitions and total number of levels involved, excluding the ground level).

The second stage of consistency is checked by looking at the outliers (defined as fractional value of absolute difference between observed and calculated wavelengths with respect to the uncertainty). In a normal statistical distribution, the 1σ, 2σ, 3σ etc., the outliers must follow the **68–95–99.7** rule (called three sigma rule). Thus the number of lines within one level of absolute standard deviation (STD) must not be less than to 68.3% and fractions of lines deviating from one level of STD should not exceed by 31.7% and deviation from 2σ or more should be within 5%. The other type of statistical check, the wavelengths observed from particular measurement can often be tested with those of Ritz values. In this regard, a plot for $\Delta\lambda_{obs\text{-}Ritz}$(Å) vs λ_{obs} is used. The lines with multiple assignments are normally less accurate, sometimes an extra weight is given for such transitions (if their energy separation is large) in the form of intensities obtained with some plasma models (either calculated or observed). Once the satisfactory outputs are obtained the optimization process is complete.

2.6.4. Determination of ionization potential

The ionization potential (IP) of the atom or ion concerned is defined as the energy required ejecting the outermost electron to ionization continuum above the first series limit. The ionization energy can be determined both ways, theoretically and experimentally. There are some semi-empirical methods too, successfully applied when less experimental data are available [54]. However, once the levels are

established, the determination of IP is favored by two methods (1) the Ritz quantum defect series expansion for low ℓ states to infinity and (2) core-polarization parametrization of the levels with high n and ℓ values [38, 45, 55]. The complete formalism is described in ref. [38, 45]. As the approaches are different, two set of computer codes, RITZPL and POLAR, are developed, by Sansonetti of NIST [56]. Both the codes take account of inverse squares of observed uncertainty as a weight of the levels in the least square fitting procedure.

For RITZPL, the unperturbed series must be used for deriving IP. If more than 3 members of the series are known, the uncertainty can be estimated from their fitted standard deviations. The isoelectronic comparison (not too far Z_c) or homologous ionic trends are used in case where less than 3 members of a series or multiple-series are unknown.

The POLAR is based on the core-polarization parametric extension of high n and ℓ states observed i.e. levels with nonpenetrating external electron in series like ng, nh, ni etc. In this case centre of gravity of n,ℓ states must be taken in to account.

The series formulas can be used to interpolate and extrapolate energy levels along the series. By this method it is very promising for deriving the accurate values for unobserved levels and sometimes to detect the incorrect identifications if they are free from perturbations.

2.6.5. Critical evaluation of transition probabilities

The methods of critical evaluation of transition probabilities (TP) were given by Wiese [57] and Kramida [38]. It requires many criteria to be tested and to decide the final estimation of TP values and its error. A few are given here (i) making a correspondence of calculated transition probabilities with experimental observed levels (ii) comparisons of TP from various theoretical codes and experimental values. The calculated transition probabilities are often vary with the effects of configuration interactions, nearer coincidences of the energy levels, relativistic effects, cancellation effects in the line strength computations, convergence of results in length and velocity form. As far as the experimental values are concerned, departures were quickly noticed due to the plasma conditions and validity of applied model, intensity alteration and calibration issues, blending problem, cascading issues, etc. Some critically evaluated values are given for Sn II (chapter 3).

Thus once the analysis of a given ion is completed, the results are tabulated in different tables, one for classified lines, the other for optimized levels (along with LS compositions) and next for LSF parameters. Some utility programs in Cowan's code version by Kramida [58] and a subsequent compatible excel spreadsheet [59] prepared by us were used to prepare the final tables.

References:

[1] Berry H G 1977 *Rep. Prog. Phys.* **40** 155
[2] Kieft E R *et al* 2004 *Phys. Rev. E* **70** 066402
[3] Nozomu K *et al* 2008 *J. Phys. Con. Ser.* **112** 042063
[4] Fujioka S et al 2008 *J. Phys. Con. Ser.* **112** 042049
[5] Gillaspy J 2001 *J. Phys. B: At. Mol. Opt. Phys.* **34** R93
[6] Feldman U, Swartz M and Cohen L I 1976 *Rev. Sci. Instrum.* **38** 1372
[7] Bockasten K 1955 *Ark. Fys.* **9** 457
[8] Svensson L A and Ekberg J O 1969 *Ark. Fys.* **40** 145
[9] Romand J 1962 *J. Quant. Spectrosc. Radiat. Transfer.* **2** 691
[10] Wainfan N and Rudisill J E 1969 *App. Opt.* **8** 345
[11] Reader J, Epstine G L and Ekberg J O 1972 *J. Opt. Soc. Am.* **62** 273
[12] Sawyer R A 1951 *Experimental Spectroscopy* (Prentice- Hall Inc, New York)
[13] Harisson G R, Lord R C and Loofbourow J R 1948 *Practical Spectroscopy* (Prentice Hall Inc, New York)
[14] Samson J A R 1967 *Techniques of Vacuum Ultraviolet Spectroscopy* (John Wiely & Sons. Inc, New York)
[15] Samson J A R and Ederer D L 1999 *Vacuum Ultraviolet Spectroscopy II* (Academic Press, Elsevier, Inc London)
[16] Rana T 2002 *Spectral Studies of Multiply Ionized Antimony Atoms: Sb II-V* Ph.D. thesis, Aligarh Muslim University, India
[17] Anjum N 2008 *Spectral Studies Of Ionized Iodine* Atoms: I III – I VI Ph.D. thesis, Aligarh Muslim University, India
[18] Sharma M K 2013 *Spectroscopic Study of Ionized Barium Atoms* Ph.D. thesis, Aligarh Muslim University, India
[19] van het Hof G J 1994 *A computer program Mosfit for wavelength calibration using polynomial fit* (Zeeman Lab Amsterdam)
[20] Kramida A, Ralchenko Yu., Reader J and NIST ASD Team 2012 *NIST Atomic Spectra Database, v.5.0,* National Institute of Standards and Technology, Gaithersburg, MD, USA. Available from: http://physics.nist.gov/ASD.
[21] Kaufman V and Edlén B 1974 *J. Phys. Chem. Ref. Data* **3** 825
[22] Glad S 1954 *Ark. Fys.* **7** 7
[23] Edlén B 1963 *Rep. Prog. Phys.* **26** 181
[24] Bockasten K 1955 *Ark. Fys.* **9** 457
[25] Griesmann U and Kling R 2000 *Astrophys. J.* **536** L113
[26] Eriksson K B S 1987 *J. Opt. Soc. Am. B* **4** 1369
[27] Edlén B 1934 *Nova Acta Reg. Soc. Sci. Upsalien., Ser. IV* **9**(6) 153 pp
[28] Bromander J 1969 *Ark. Fys.* **40** 257
[29] Kaufman V and Hagan L 1979 *J. Opt. Soc. Am.* **69** 232
[30] Toresson Y G 1961 *Ark. Fys.* **18** 389
[31] Wu C M 1967 *The Atomic Spark Spectra of Tin, Sn III, Sn IV, Sn V,* Master thesis, University of British Columbia, Canada

[32] Brill W G 1964 *The Arc Spectrum of Tin*, Ph. D. thesis, Purdue University, Lafayette, IN, USA, 119 pp.
[33] Ryabtsev A N 2013 *The spectral data of tin ions*, private communication
[34] Ryabtsev A N, Churilov S S and Kononov É Ya 2006 *Opt. and Spectrosc.* **100** 652
[35] Ryabtsev A N, Churilov S S and Kononov É Ya 2007 *Opt. and Spectrosc.* **102** 354
[36] Ryabtsev A N, Churilov S S and Kononov E Ya 2005 *Phys. Scr.* **72** 377
[37] Reader J 1995 *Phys. Scr.* **T65** 15
[38] Kramida A 2013 *Fusion Sci. Technol.* **63** 313
[39] Azarov V I 1993 *Phys. Scr.* **48** 656
[40] Kramida A 2012 *J. Res. Natl. Inst. Stand. Technol.* **118** 168
[41] van het Hof G J 1994 *A computer program, FIND3, for searching the levels* (Zeeman Lab Amsterdam)
[42] Haris K 2014 *An excel spreadsheet application, GENTRAN, for finding new levels*; unpublished
[43] Reader J 1997 *Comp. Phys.* **11** 190
[44] Martin W C and Wiese W L 1996 *'Atomic spectroscopy-A compendium of basis ideas, notations, data, and formulas'* in Drake G W F Edited, *Atomic, Molecular, and Optical Physics Handbook*, (AIP Press, Woodbury, NY) http://www.nist.gov/pml/pubs/atspec/index.cfm
[45] Edlén B 1964 *Atomic Spectra handbuch der Physik Springer Verlag* **27** 80
[46] Nave G *et al* 2011 *Rev. Sci. Instrum.* **82** 013107
[47] Haris K *et al* 2014 *Nucl. Instrum. Meth. A* **767** 199
[48] Kramida A 2013 *J. Res. Natl. Inst. Stand. Technol.* **118** 52
[49] van het Hof G J 1994 *A computer program, KLAS, for Energy level optimization* (Zeeman Lab Amsterdam)
[50] Kramida A E 2011 *Comput. Phys. Commun.* **182** 419
[51] Radziemski Jr. L J, Fisher K J, Steinhaus D W, Goldman A S 1972 *Comput. Phys.Comun.* **3** 9
[52] van het Hof G J, 1990 *Orthogonal operators in atomic 3d systems* (Ph.D. thesis, Amsterdam University, The Netherlands)
[53] Haris K 2014 *An excel based application 'INGEL' for generating the input for LOPT code*; unpublished
[54] Kramida A E and Reader J 2006 *At. Data Nucl. Data Tables* **92** 457
[55] Martinson I 1989 *Contem. Phys.* **30** 173
[56] Sansonetti C J 2005 *Computer programs RITZPL and POLAR*, private communication
[57] Wiese W L 1996 *Phys. Scr.* **T65** 188
[58] Kramida A, PC *version of Cowan code package for Windows* available from http://das101.isan.troitsk.ru/COWAN
[59] Haris K 2014 *An excel spreadsheet application, 'PUBLIN' for publishing the results*; unpublished

CHAPTER 3

The spectrum of singly ionized tin: Sn II

Accurate data on the spectrum of singly ionized tin are needed in different fields of scientific research and industry. Such data are useful for astrophysical observations, development of various light sources, and for plasma diagnostics in fusion power plants. The astrophysical importance of tin has increased since gas-phase tin was first detected by Hobbs et al. [1] in the spectra acquired with the Goddard High Resolution Spectrograph on board the Hubble Space Telescope. They observed the absorption line of Sn II at 1400.45 Å from various interstellar sources. Later, the same line was observed in diffuse interstellar clouds by Sofia et al. [2]. They discovered that the gas-phase abundance of Sn in the interstellar medium (ISM) appears to be supersolar, which further substantiates the slow neutron capture (s-process) enrichment believed to be a major contributor to the nucleosynthesis of elements beyond the iron peak in the ISM. In erosion probing of vessel wall tiles of future fusion power plants, such as ITER, spectroscopic data on tin may play a major diagnostic role [3].

Singly ionized tin (Sn II) is the second member of the In I isoelectronic sequence with the ground configuration $4d^{10}5s^{2}5p$ consisting of the ground level $^{2}P^{o}_{1/2}$ and first excited level $^{2}P^{o}_{3/2}$. The currently available spectroscopic information on Sn II compiled in Moore's Atomic Energy Levels (AEL) compilation [4] and listed in the Atomic Spectra Database (ASD) [5] of the National Institute of Standards and Technology (NIST) is based on an unpublished work of Shenstone. Prior to AEL, extensive work in this spectrum was carried out by McCormick and Sawyer [6], who revised the earlier findings of Green and Loring [7], Narayan and Rao [8], and Lang [9]. Shenstone in his work quoted in AEL re-investigated this spectrum in the wavelength range of 600 Å to 2500 Å and extended the analysis to include the 5s5p5d and 5s5p6s configurations. Shenstone revised some energy levels of Sn II and improved the accuracy of the earlier reported energy level values on the basis of his

observations. Some spectral lines of Sn II were also reported by Brill [10] in his doctoral thesis and by Wu [11] in his master thesis. Apart from spectroscopy of valence-shell electrons, spectral studies of the 4d-core excitation of Sn II in the extreme ultraviolet (EUV) region with the dual laser plasma (DLP) method were made by Lysaght et al. [12] and by Duffy et al. [13].

Despite those extensive studies, the currently available data are still inadequate, since there are considerable anomalies in energy level values and line assignments. Many of the energy levels given in AEL [4] are not supported by any published line lists. The lines determining these energy levels have to be re-discovered.

There are many theoretical studies on radiative lifetimes, transition rates, and oscillator strengths of Sn II. Among them, the most accurate and reliable calculation of oscillator strengths was made by Oliver and Hibbert [14]. Schectman et al. [15] improved the earlier lifetime measurements of Andersen and Lindgård [16] and, by combining them with measured branching fractions, determined *f*-values for several transitions. Data from Ref. [16] were used by Sofia et al. [2] to derive the gas-phase interstellar abundance of tin in several diffuse clouds.

In the present work, our motivation is to provide a comprehensive spectroscopic analysis of singly ionized tin on the basis of tin spectra taken by us, the tin spectral line list given by Wu [11], the Sn II spectral classification by McCormick and Sawyer [6], and lines reported by Brill [10]. All previously reported energy levels of this spectrum are subjected to a critical investigation. One of our goals is to resolve the questions in Moore's assignments of the $5s5p^2\ ^2S_{1/2}$ and $^2P_{1/2}$ levels [4]. Excitation from the $5s5p^2$ configuration to 5s5p (5d+6s) and $5p^3$ is studied extensively in this work. Although some of the levels of these highly-excited configurations were tentatively identified by Shenstone and listed in AEL [4], Shenstone's analysis was incomplete in many respects. Some of the level values were given with question marks, and some had uncertain *J* values and/or designations. A very recent study carried out by Alonso-Medina et al. [17] using laser-produced plasma of a Sn/Pb target reproduced some of the levels reported in AEL [4], but the majority of their suggested 5s5p5d and $5p^3$ level assignments and line classifications are made on the basis of a physically inadequate theoretical atomic model. For example, the spin-orbit

coupling parameter ζ_{5p} should be approximately the same in all $n = 5$ configurations. However, the values reported in Ref. [17] vary from 745 cm^{-1} for 5s5p5d to 29667 cm^{-1} for $5p^3$. We attempt to resolve all these questions in the present analysis. Interestingly, many of the 5s5p5d and $5p^3$ levels are located above the first ionization limit. Therefore, only those levels that have autoionization rates comparable to or smaller than the radiative decay rate were observed via their corresponding photon decay channel.

Although, as noted above, some studies of the 4d core-excited spectrum of Sn II have been published [12, 13], we restrict the scope of this work to excitations of the $n = 5$ electrons.

3.1. Level structure of Sn II

The Ground configuration of Sn II is [Kr] $4d^{10}5s^25p$ with $2P_{1/2, 3/2}$ ground structure

Configuration[a]	Parent Term	Term[b]	J
$4d^{10}.5s^2.np$	(^1S)	$^2P^\circ$	1/2, 3/2
$4d^{10}.5s^2.ns$	(^1S)	^2S	1/2
$4d^{10}.5s^2.nd$	(^1S)	^2D	3/2, 5/2
$4d^{10}.5s^2.nf$	(^1S)	$^2F^\circ$	5/2, 7/2
$4d^{10}.5s^2.ng$	(^1S)	^2G	7/2, 9/2
$4d^{10}.5s.5p^2$	(^3P)	^4P	1/2, 3/2, 5/2
	(^1D)	^2D	3/2, 5/2
	(^1S)	^2S	1/2
	(^3P)	^2P	1/2, 3/2
$4d^{10}.5s.5p.6s$	($^3P^\circ$)	$^4P^\circ$	1/2, 3/2, 5/2
		$^2P^\circ$	1/2, 3/2
	($^1P^\circ$)	$^2P^\circ$	1/2, 3/2
$4d^{10}.5p^3$	($^4S^\circ$)	$^4S^\circ$	3/2
	($^2D^\circ$)	$^2D^\circ$	3/2, 5/2
	($^2P^\circ$)	$^2P^\circ$	1/2, 3/2
$4d^{10}.5s.5p.5d$	($^3P^\circ$)	$^4F^\circ$	3/2, 5/2, 7/2, 9/2
		$^4D^\circ$	1/2, 3/2, 5/2, 7/2
		$^4P^\circ$	1/2, 3/2, 5/2
		$^2F^\circ$	5/2, 7/2
		$^2D^\circ$	3/2, 5/2
		$^2P^\circ$	1/2, 3/2
	($^1P^\circ$)	$^2F^\circ$	5/2, 7/2
		$^2D^\circ$	3/2, 5/2
		$^2P^\circ$	1/2, 3/2

[a] To the given configurations, the Kernel structure '[Kr]' must be added before each of it for the completeness of electronic structure. The principal quantum number, $n \geq 5$ for all ℓ except for f sub-shell ($n \geq 4$).

[b] The strict ordering of levels are governed by Hund's rule for the fine structures.

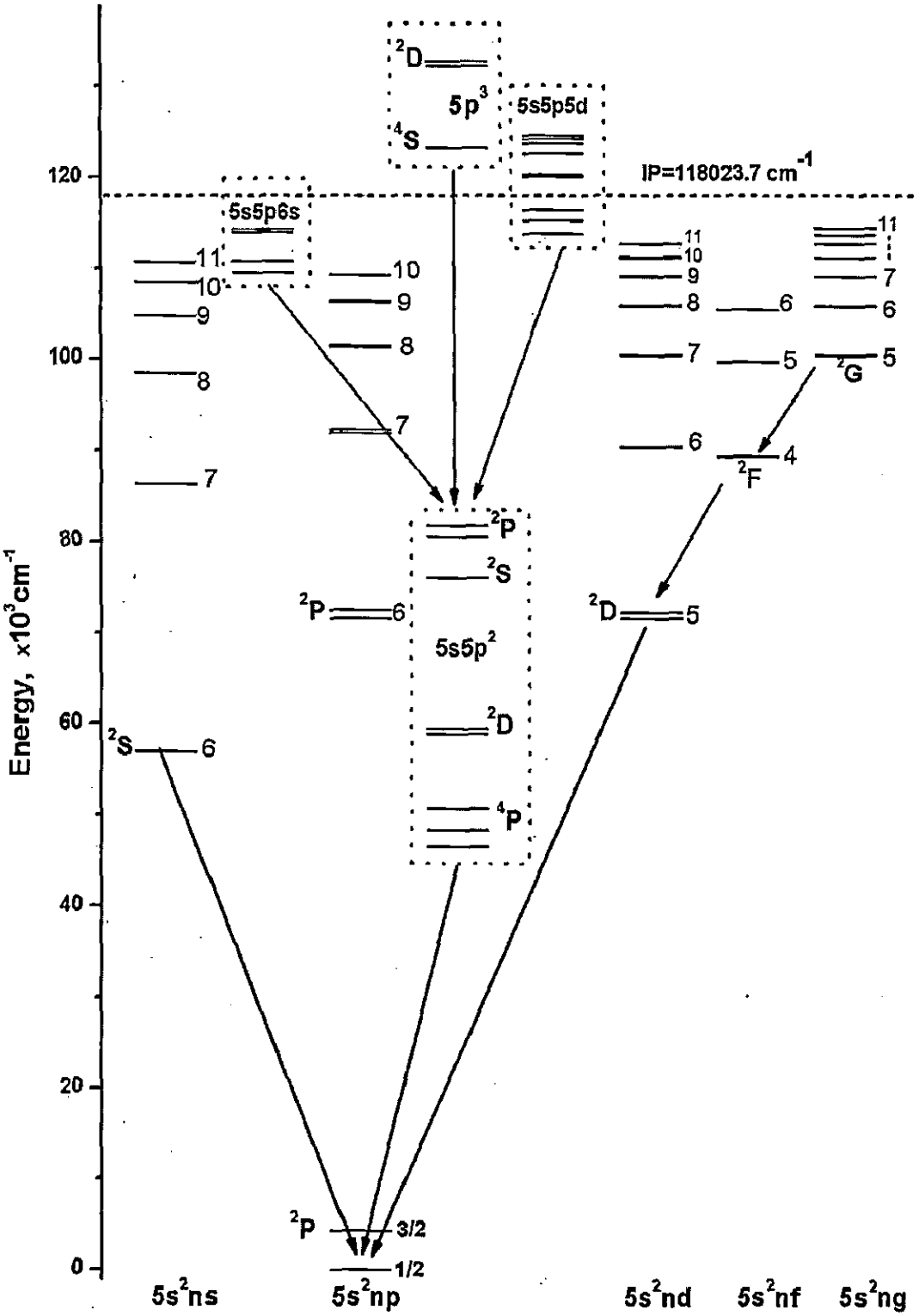

Figure 3.1. Energy level diagram of observed mutiplets in Sn II

3.2. Measuremental correction of the Wu's line list

The VUV data of tin measured by us has the values of uncertainty 0.006 Å for sharp lines below 1050 Å to 0.02 Å for very wide and blended lines. All uncertainties reported in the present work are meant to be on the level of one standard deviation.

Many of the known classified lines of Sn II were observed by other researchers [6, 10, 11] outside the wavelength range studied in the present work. Thus, to obtain optimized level values, wavelength values and uncertainties reported by other observers have to be evaluated.

The most valuable of the previously reported measurements are those of Brill [10] made with an electrodeless discharge tube as a light source. He reported 42 wavelengths of Sn II between 2150 Å and 10740 Å, with uncertainties estimated individually for each line. For 39 of these lines, the measurements were made with a Fabry-Perot interferometer, and their uncertainties vary between 0.0006 Å and 0.006 Å. Three weak lines were measured with a 9.14 m, 590 lines/mm grating spectrograph having inverse linear dispersion of 1.7 Å/mm. Uncertainties of these three lines are between 0.06 Å and 0.09 Å, as reported by Brill [10].

Two other large sets of wavelengths were taken from Wu's thesis [11] and from McCormick and Sawyer [6]. Wu photographed the tin spectra in the region between 350 Å and 9000 Å using an electrodeless discharge. A condensed spark in helium with a 3 m normal incidence vacuum grating spectrograph and a prism spectrograph were used in the regions below and above 2400 Å, respectively. Wu reported a total of 3403 spectral lines, of which he assigned 110 to Sn I, 128 to Sn II, 321 to Sn III, 177 to Sn IV, and 118 to Sn V, leaving the remaining 2549 lines unassigned to a particular ionization stage. Although all wavelengths in Wu's line list were given with three digits after the decimal point (in angstroms), the wavelength uncertainty varied greatly depending on the wavelength region and on the spectrographs used.

To assess the uncertainties of Wu's wavelength measurements, we compared his reported wavelengths with more accurate Sn I measurements and with Sn II Ritz wavelengths. The reference wavelengths of Sn I were taken mainly from Brill's thesis [10] for wavelengths above 2064 Å and from absorption measurements of Brown et al. [18] below that. Both sets have uncertainties less than 0.002 Å. The Sn II Ritz

wavelengths (see section 3.3.3) were determined mainly by our measurements in the VUV and by Brill's measurements [10] in the air region.

The comparison shown in figures 3.2(a)–(c) revealed significant systematic shifts in Wu's measurements. These shifts vary smoothly with wavelength between +0.019 Å near 900 Å and −0.25 Å near 8300 Å. The presence of systematic shifts in the earlier measurements is not surprising, since the spectrometers used therein had poorer resolution. For example, the grating spectrograph used by Wu [11] was equipped with a 1200 lines/mm grating, in contrast to our 2400 lines/mm (although Wu did not specify what grating he used, we assume it was the same as described in Bhatia's thesis [19] made at the same institution two years later). Thus, our spectrometer had a twice greater resolving power. The grating used by McCormick and Sawyer [6] had only 567 lines per mm, and its radius of curvature was 1 m, three times less than in our spectrometer. Thus, in their work the reciprocal linear dispersion was 17 Å, more than an order of magnitude worse than in our work. The quality and number of available wavelength standards has also greatly improved since the work of Wu [11] and especially McCormick and Sawyer [6]. In particular, the high-precision measurements of Brill [10] in Sn I and Sn II were not available to those authors. Nevertheless, as often happens with old measurements, they can be re-calibrated using improved internal standards of the same spectrum. This re-calibration is done here by subtracting the systematic shifts shown in figure 3.2. After this subtraction, the measurement uncertainties of the corrected wavelengths were estimated from their average deviations from reference values. In the region below 2400 Å, where the grating spectrograph was used, the estimated wavelength uncertainty is almost constant, about 0.019 Å. In the region 2400 Å to 3050 Å, where the quartz prism spectrograph was used, the uncertainties are about 0.024 Å on average. However, uncertainties of Wu's prism spectra are better described by a constant uncertainty in wavenumber, about 0.3 cm^{-1} for this wavelength region. This implies a gradual increase of uncertainties from 0.019 Å at 2400 Å to 0.03 Å at 3050 Å. Above this wavelength, as figure 3.2(c) shows, uncertainties increase abruptly to 1.7 cm^{-1}, corresponding to 0.16 Å at 3100 Å and 1.2 Å at 8300 Å. We note that the plots in figure 3.2 use different scales on the vertical axes in order to make the random scatter of the data points nearly constant in magnitude throughout

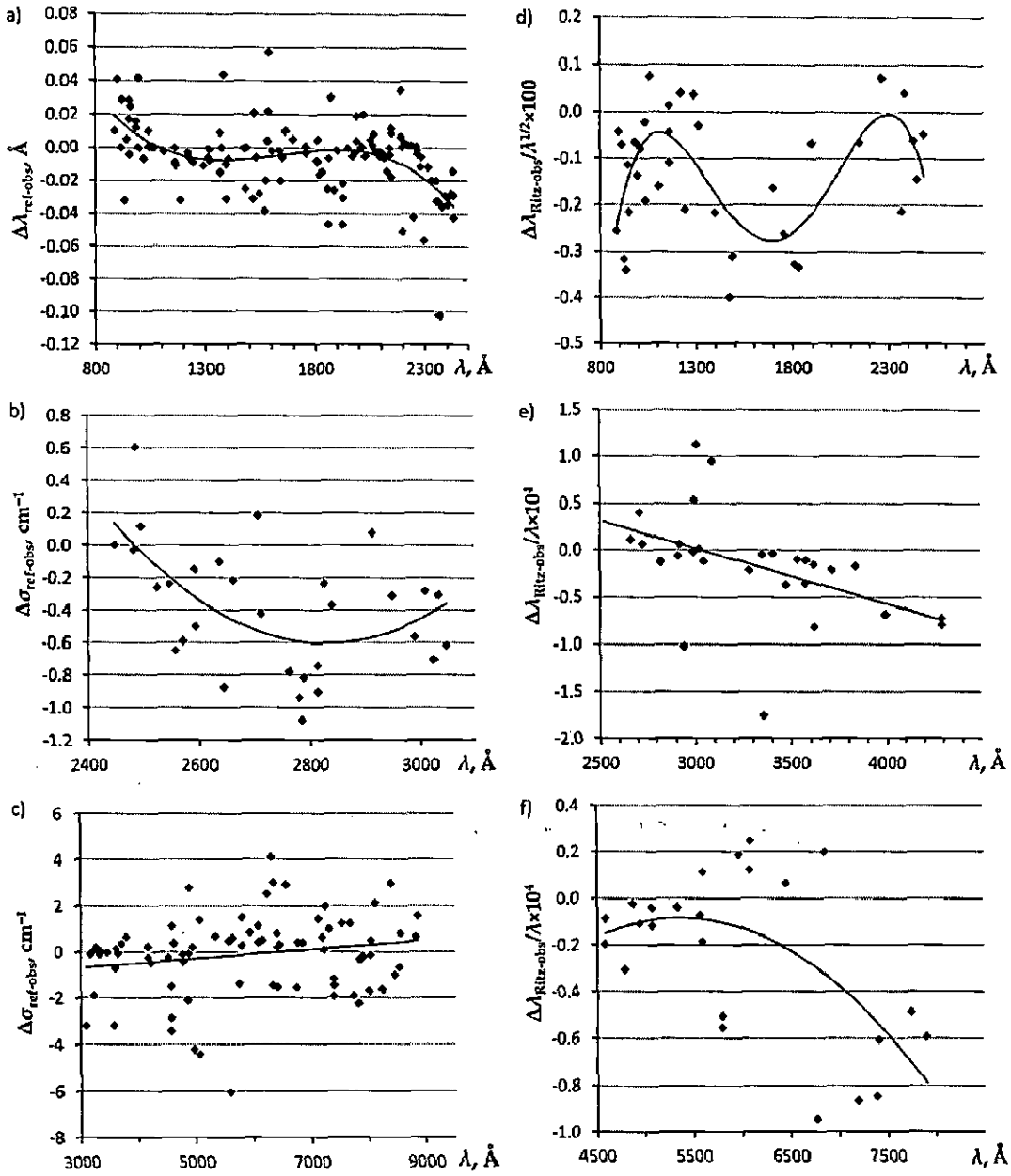

Figure 3.2. Differences between observed and reference wavelengths λ or wave numbers σ for the measurements of Wu [11] (a b c) and McCormick and Sawyer [6] (d e f). The solid lines are linear or polynomial fits determining the systematic corrections to the original measurements.

the wavelength ranges covered by the panels. Then the correction polynomial curves can be easily found by unweighted interpolation.

McCormick and Sawyer [6] excited the Sn II spectrum in a hollow cathode discharge in helium and photographed it in a similarly wide wavelength range from 800 Å to 10 000 Å. In the region below 2200 Å, they used a 1 m vacuum grating spectrograph. The region from 2200 Å to 2700 Å was photographed with a quartz

prism spectrograph. Above 2700 Å, two other prism spectrographs were used. Since these authors reported only the Sn II wavelengths, the only means of assessment of their uncertainties was a comparison with more accurate Ritz wavelengths. For this comparison, we used the Ritz wavelengths from our preliminary level optimization (see section 3.3.3) that were mainly determined by our VUV measurements and those of Brill [10] in the region above 2150 Å. Figure 3.2(d) shows these deviations, scaled in such a way that their scatter has similar magnitudes throughout the wavelength range covered by the figure.

As with the work of Wu, measurements of McCormick and Sawyer [6] appear to have significant systematic shifts smoothly varying with wavelength, from −0.11 Å at 1700 Å to zero at 2300 Å. At longer wavelengths, as figures 3.2(e) and (f) show, statistical uncertainties appear to be almost constant, if they are scaled by dividing them by wavelength. Systematic shifts are significant in these regions as well, varying from +0.08 Å at about 3000 Å to −0.6 Å at 8000 Å.

3.3. Results and discussion

The energy Structure of Sn II is given in figure 3.1. All identified lines of Sn II are collected in table 3.4 with the adopted wavelengths and their uncertainties. In total, there are about 200 lines, of which 70 were measured in the present work, 42 are from Brill [10], 27 are from McCormick and Sawyer [6], and 63 are from Wu [11]. Among Wu's lines [11], 12 were classified as Sn II transitions by us.

3.3.1. Theoretical calculations

The theoretical calculation for energy levels, wavelengths, and transition probabilities of Sn II was made with Cowan's codes [20], which implement the Hartree–Fock (HF) method with perturbative account for relativistic and configuration-interaction (CI) effects. For the even parity system, the configurations included were $5s5p^2$, $5s^2ns$ ($n = 6$–12), $5s^2nd$ ($n = 5$–12), $5s^2ng$ ($n = 5$–12), 4f5s5p, and $5s5d^2$; the odd parity set included $5s^2np$ ($n = 6$–20), $5s^2nf$ ($n = 4$–20), $5p^3$, 5s5p5d, 5s5p6s, 4f5s5d, $4f5p^2$, and $5p5d^2$ configurations. The initial scaling of the Slater parameters was 100 % of the HF values for E_{av} and ζ_{nl}, while the F^k, G^k, and the CI parameters were scaled to 80 % of the HF values. Then the Slater parameters were

varied in the least-squares fitting (LSF) procedure minimizing discrepancies between calculated and observed level values.

In the parametric fitting, the energy level calculations for even parity converged with a standard deviation of 77 cm^{-1}, while the odd-parity configurations were fitted with a standard deviation of 156 cm^{-1}. Transition probabilities and autoionization rates were calculated with wavefunctions modified according to the fitted parameters.

3.3.2. Analysis of the spectrum

Once the ionization separation, the search of energy level on basis of *ab-initio* calculations is conducted. The concordance between the observed and predicted values is tested at every stage of analysis.

3.3.2.1. The $5s^25p - [5s^2(ns+nd) + 5s5p^2]$ transition array

Excitation of the outer electron from the $5s^25p\ ^2P^\circ$ ground term leads to the $5s^2ns\ ^2S_{1/2}$ and $5s^2nd\ ^2D_{3/2,5/2}$ level series showing a simple doublet structure. The transitions from $5s^2ns\ ^2S_{1/2}$ (n = 6–8) to both levels of the ground term and those from $5s^29s$ to $5s^25p\ ^2P^\circ_{3/2}$ were already reported by McCormick and Sawyer [6]. The energy levels derived from their wavelengths were later improved by Shenstone and reported in AEL [4]. All these transitions are confirmed in our measurements with improved accuracy. McCormick and Sawyer [6] established the levels of $5s^210s$ and 11s by observing transitions to the $5s^26p$ levels in the air wavelength region. We were able to observe both transitions from $5s^29s$ to the levels of $5s^25p$ at 955.299 Å ($^2S_{1/2} \rightarrow {}^2P^\circ_{1/2}$) and 995.742 Å ($^2S_{1/2} \rightarrow {}^2P^\circ_{3/2}$). Wu [11] observed both transitions from $5s^210s$ to the ground-term levels. Other transitions from $5s^2ns$ (n = 7–11) to the $5s^2np$ (n = 6–7) levels have also been observed by us and by other researchers [6, 10, 11]. Thus, the levels of the $5s^2ns$ (n = 6–11) configurations are well established. They are almost unperturbed, showing the leading *LS* percentages of their composition above 99 %. Consistent trends of our LSF parameter values along both *ns* and *nd* series and good agreement of observed and predicted relative line intensities confirm all their identifications.

The $5s^2nd$ configurations were also listed in AEL [4]. We confirmed the levels of $5s^2nd$ (n = 5–9) with lines observed on our plates. Wu's identifications of

transitions from the $5s^2 10d$ and 11d configurations [11] are also confirmed. Some additional transitions between the $5s^2 np$ ($n = 6$–8) and $5s^2 nd$ levels have also been observed (see table 3.4). It is important to mention here that there is a strong interaction between the $5s^2 5d$ and $5s5p^2$ configurations. For this reason, the $^2D_{3/2,5/2}$ levels of these configurations are strongly mixed with each other. This strong mixing was indicated by relativistic CI calculations of Oliver and Hibbert [14], which, however, favored the old AEL designations. Percentage compositions of eigenvectors resulting from our calculations suggest that the configuration labels given in AEL for these two pairs of levels should be interchanged (see table 3.5). Nevertheless, to avoid confusion in line identifications we retained the AEL labels adopted also by Sansonetti and Martin [21].

Another type of excitation is represented by excitation of the inner 5s electron to the 5p shell, leading to the $5s5p^2$ configuration with seven levels containing a quartet and three doublet terms. All three quartet levels were firmly established by Brill [10], who observed four intercombination lines from these levels to the ground term $5s^2 5p\ ^2P^\circ_{1/2,3/2}$. In the present work, we confirm two of the doublet levels including $^2P_{1/2}$ at 80455.8 cm^{-1} reported in AEL [4] as questionable. We observed both transitions from this level to the ground term. However, we could not confirm the $^2S_{1/2}$ level reported at 80206.1 cm^{-1}. This level value was questionable for two reasons. Firstly, it strongly deviated from the LSF calculations. Secondly, its strongest predicted transition to the ground level was missing in our spectra. In Wu's line list this level value is supported by two observed lines classified as transitions to the ground term, However, Wu's observed intensity for the line he interpreted as the $5s^2 5p\ ^2P^\circ_{1/2} - 5s5p^2\ ^2S_{1/2}$ transition with $\Delta J = 0$ is four times smaller than for his classification of the $\Delta J = -1$ transition, while our calculation predicts it to be greater by a factor of 3×10^4. Therefore, this level value was rejected. We further disagree with the recent "verification" of this level value by Alonso-Medina et al. [17] based on one $5s5p^2\ ^2S_{1/2} - 5s5p(^3P^\circ)6s\ ^4P^\circ_{1/2}$ transition they presumably observed at 3418.9 Å (as shown in their figure 3.3).

According to our calculations, this intercombination transition should be too weak to be observable. Its radiative rate is at least four orders of magnitude smaller than that of the two *LS*-allowed transitions from the same upper level to $5s5p^2\ ^4P_{1/2,3/2}$. Connerade and Baig [22] revised the identification of the $5s5p^2\ ^2P_{1/2}$ and $^2P_{3/2}$ levels

by analyzing level separations along the In I isoelectronic sequence. Their suggested values for these two levels were 80206 cm^{-1} and 81718 cm^{-1}, respectively (i.e., they changed the term assignment of the value 80206 cm^{-1} from $^2S_{1/2}$ to $^2P_{1/2}$ and retained Moore's questionable assignment of the $5s5p^2$ $^2P_{3/2}$ level). We confirmed the identification of the second level and refined its position. However, the first one, as noted above, was found to be spurious. Calculations of Connerade and Baig [22] yielded a predicted value for the $5s5p^2$ $^2S_{1/2}$ level at 60024 cm^{-1}. We located this level at a much higher position, at 75954.3 cm^{-1}, by identifying transitions from it to both levels of the ground term. The strongest of these transitions (to $^2P_{1/2}$) was observed in our spectra at 1316.572 Å. A line near this wavelength was previously interpreted by Wu [11] as the $5s^25p$ $^2P^o_{3/2}$ – $5s5p^2$ $^2S_{1/2}$ transition. That $\Delta J = -1$ transition, predicted to be much weaker than $\Delta J = 0$, was not observed on our plates. However, it was observed by Wu [11] at 1394.667 Å as a relatively weak line in two exposures. The newly revised $5s5p^2$ $^2S_{1/2}$ level value fits well in our parametric LSF calculations with reasonable values of the fitted parameters. This identification is further validated by an isoelectronic comparison presented in figure 3.3 for the sequence In I to Xe VI. The $^2S_{1/2}$ and $^2P_{1/2}$ levels of $5s5p^2$ are strongly mixed in these spectra. In In I, the leading terms are ^2S and ^2P for the lower and upper of these two levels, respectively, while in Xe VI they are reversed. The previously adopted position of $5s5p^2$ $^2S_{1/2}$ level in Sn II, indicated by dashed lines in figure 3.3, is strikingly inconsistent with the smooth isoelectronic trend of other data points. Our new LSF calculations for this sequence result in interchange of the term labels $^2S_{1/2}$ and $^2P_{1/2}$ in Te IV and predict a much lower position for the $^2S_{1/2}$ level in Sn II. This prediction is in qualitative agreement with findings of Connerade and Baig [22]. As indicated by the solid lines in figure 3.3, our revised identification produces a smooth isoelectronic trend for the lower $J = 1/2$ level, similar to the behavior of the upper level. The revised level values and term labels, along with the calculated percentage compositions, are given in table 3.1. Additional support for our new identification of the $5s5p^2$ $^2S_{1/2}$ level in Sn II is provided by a recent theoretical calculation by Oliver and Hibbert [14]. They predicted $^2S_{1/2}$ in Sn II to be at 76215 cm^{-1}, which is in close agreement with our newly found level value. Colón and Alonso-Medina [23] suggested an explanation of the anomaly in the $5s5p^2$ $^2S_{1/2}$ and $^2P_{1/2}$ levels of Sn II by the presence of some mysterious interacting configuration(s). As this anomaly is now resolved, their

suggestion can be dismissed. It should be noted that these two levels are strongly mixed (see tables 3.1 and 3.3). Thus, their *LS* labels have little physical meaning and are used in our tables for bookkeeping purpose only.

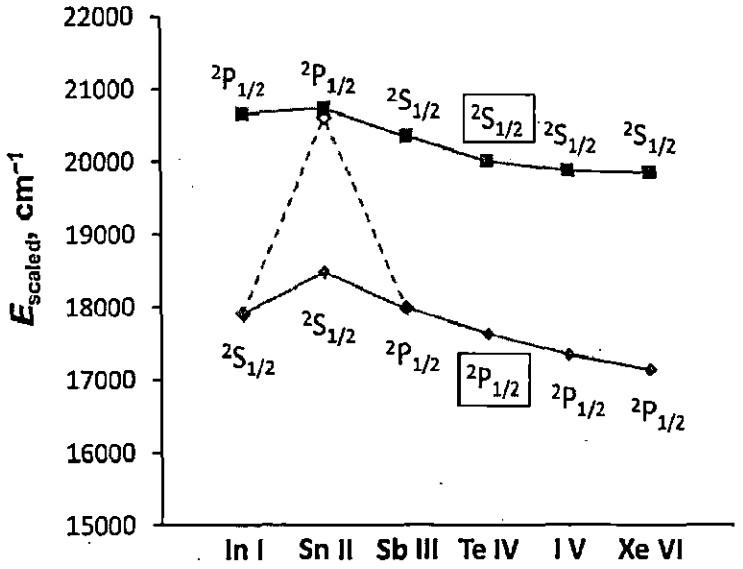

Figure 3.3. Isoelectronic comparison of scaled energies $E_{scaled} = (E - 39000)/Z_c$ of the strongly mixed $5s5p^2\ ^2S_{1/2}$ and $^2P_{1/2}$ levels. The dominant term labels of the lower and upper levels interchange at ionic core charge $Z_c = 3$ (Sb III). The open circle just below the $^2P_{1/2}$ data point for Sn II indicates the previously adopted position of the $^2S_{1/2}$ level in Sn II at 80206 cm^{-1} [4]. Dashed lines connecting this data point with the other ones of the lower level show how this graph would look if that incorrect value were used instead of our revised value (solid rhombs and lines). Solid boxes indicate the revised term labels for Te IV. See table 3.1 for details.

Table 3.1. The two $J = 1/2$ doublet levels of the $5s5p^2$ configuration in the In I isoelectronic sequence. All percentage compositions and the Sn II energies are from the present work; for the rest of the data the references are given in the first column.

Isoelectronic member	Lower level				Upper level			
	Energy, cm^{-1}	Percentages		Term label	Energy, cm^{-1}	Percentage		Term label
		^2S	^2P			^2S	^2P	
In I [24]	56906	74	24	^2S	59657	23	76	^2P
Sn II	75954.3 [a]	51	46	^2S	80455.1	45	53	^2P
Sb III [4]	92948.9	31	37	^2P [b]	100010	57	41	^2S
Te IV [4]	109536	40	57	^2P [c]	119009	56	42	^2S [c]
I V [25]	125703.5	36	61	^2P	138328.3	60	38	^2S
Xe VI [26]	141837.2	32	64	^2P	157995.6	62	36	^2S

[a] Our revised value replaces the previously reported 80206 cm^{-1} [4].

[b] Third leading component: 31 % of $5s^26s\ ^2S$ (at 93417.8 cm^{-1} [4]).

[c] The level designations for Te IV are interchanged according to our LSF calculations.

3.3.2.2. The $5p^3$ and 5s5p(5d+6s) configurations

These configurations arise from excitation of the $5s5p^2$ configuration. In the sequence Sb III – I V [27–29], transitions from these configurations have been observed in the Antigonish laboratory with moderate intensity. Therefore, we expected them to occur in Sn II as well. Our preliminary calculations for Sn II show that these configurations strongly interact with each other and also with other configurations, e.g., ^{4}F5s5d and $5p5d^2$, which are completely unknown at present. The $5p^3$ and 5s5p (5d+6s) configurations are predicted to extend past the ionization limit. Thus, many of their levels should be autoionizing, making the analysis more difficult. Additional complication stems from the fact that some of the levels of these configurations are embedded within highly excited levels of the $5s^2np$ and nf series, with which they strongly interact. A few levels of these configurations were listed in AEL [4] with incomplete designations; some were marked as doubtful. We attempted to improve interpretation of these levels. The level at 109223.4 cm^{-1} in AEL [4] is supported by two transitions terminating on the $5s5p^2\ ^4P_{1/2,3/2}$ levels, observed in our spectra, and one transition to $5s^25d\ ^2D_{3/2}$ observed by Wu [11]. We now identified this level as $5s^210p\ ^2P_{1/2}$ on the basis of our LSF calculation. Observed relative intensities of the lines are in satisfactory agreement with calculations. We were able to confirm the quartet levels of 5s5p6s configuration listed in AEL [4], as they give rise to strong transitions to the lowest quartet levels of the $5s5p^2$ configuration. The level at 113819.0 cm^{-1} is also confirmed. In AEL [4], the J value of this level was given as 3/2 with a question mark, and no configuration label was attributed to it. Our present calculation with extensive configuration interaction shows that this level should be assigned to $^2D_{5/2}$ of the 5s5p5d configuration.

As noted above, identification of autoionizing levels presented considerable difficulties. We could not confirm the level at 124627.7 cm^{-1} in AEL [4]. Wu [11] assigned three observed lines at 1520.153 Å, 2907.33 Å, and 7412.5 Å to this level. However, no satisfactory match could be found for this level in our calculations. All other autoionizing levels given in AEL [4] have been identified in our spectra. In particular, three levels previously reported at 123156, 132168 and 132708 cm^{-1} with uncertain designations are found to be associated with the $5p^3$ configuration. The first of them is identified as $5p^3\ ^4S^o_{3/2}$, while the other two have dominant contributions of $5s5p(^1P^o)5d\ ^2D^o_{3/2}$ and $^2D^o_{5/2}$, respectively. Since the 5s5p5d configuration strongly

interacts with $5p^3$, these levels have large admixtures of $5p^3\ ^2D°$ in their wavefunctions. A few of the other autoionizing levels that were based on just one or two observed transitions remain questionable. In all such cases, the observed lines attributed to these levels are the strongest predicted ones.

3.3.2.3 The $5s^2np$ and $5s^2nf$ configurations

After the successful establishment of the $5s^2ns$ and nd levels, a further analysis of the $5s^2np$ and nf configurations was undertaken. The $5s^2np$ ($n = 6$–9) and $5s^2nf$ ($n = 4$–6) configurations were already reported in AEL [4]. Some transitions from $5s^26p$ and 7p to levels of the $5s^26s$, $5s^25d$, and $5s5p^2$ configurations were measured interferometrically by Brill [10]. Lines arising from the $5s^2np$ ($n = 6$–9) configurations were classified by McCormick and Sawyer [6], and some additional lines were also observed by Wu [11]. We confirm all these identifications, as the observed level energies and relative line intensities are in satisfactory agreement with our calculations.

The $5s^26f\ ^2F°_{7/2}$ level was given by Moore [4] at 105367 cm^{-1}, while the $J = 5/2$ level of this configuration was previously unknown. On our plates, we did not observe any transitions from the $J = 7/2$ level. In Wu's line list [11], the only line placing this level near the AEL value is at 6661.1 Å, which we tentatively interpreted as the $5s^26d\ ^2D_{5/2} - 5s^26f\ ^2F°_{7/2}$ transition. This interpretation yields the position of the $J = 7/2$ level at 105360.3 cm^{-1}, slightly lower than the AEL value. However, this transition is by far not the strongest predicted from this level. The $5s^25d\ ^2D_{5/2} - 5s^26f\ ^2F°_{7/2}$ transition, predicted to occur at 2178.12 Å, should be about ten times stronger, but there is no line near this wavelength in Wu's list [11]. Another possible transition to the $5s5p^2\ ^4P_{5/2}$ level should occur at 1830.49 Å with approximately the same intensity as $5s^26d\ ^2D_{5/2} - 5s^26f\ ^2F°_{7/2}$. Neither our plates nor Wu's line list show a line near this wavelength. Thus, we retained the above tentative identification with a question mark. In the search for the missing $5s^26f\ ^2F°_{5/2}$ level, we relied on the expectation that the $J = 5/2$–7/2 fine-structure interval should be slightly greater than the value predicted by our LSF, 3 cm^{-1}. This expectation was grounded on the observation that experimental values for this interval in the $5s^{24}F$ and $5s^25f$ configurations, 5.800(5) cm^{-1} and 5.349(8) cm^{-1}, are close to the LSF values, 3.7 cm^{-1} and 3.4 cm^{-1}, respectively. The only suitable pair of observed lines was

found at 2148.61 Å (from McCormick and Sawyer [6]) and 2943.30 Å (from Wu [11]). We tentatively classified these lines as transitions from $5s^26f\ ^2F°_{5/2}$ to the $5s^25d\ ^2D_{3/2}$ and $5s5p^2\ ^2D_{3/2}$ levels, respectively. Wu has a line 2148.85 Å identified as a Sn III transition, which could possibly mask the first of these two lines. However, the second line at 2943.30 Å, as observed by Wu [11], is a factor of ten stronger than expected from our predicted intensities (see section 3.3.4), while several other transitions from the same level, predicted to be stronger or of comparable intensities, were not observed. Furthermore, the $J = 5/2–7/2$ fine-structure interval 11.4(18) cm^{-1} resulting from the above classifications appears to be greater than expected. Thus, both our values for the $5s^26f\ ^2F°_{5/2}$ and $5s^26f\ ^2F°_{7/2}$ levels are questionable and need further confirmation.

3.3.2.4. Levels of $5s^2ng$ configurations

The $5s^2ng$ ($n = 6–11$) ^2G energy levels were established by transitions from the levels of $5s^{24}F$ configuration, identified primarily by McCormick and Sawyer [6]. Some of the transitions observed by McCormick and Sawyer were more accurately measured by Wu [11]. Brill [10] re-measured the $^4F–6g$ transitions with much better accuracy. No discernible fine-structure splitting was detected in any of the observed $5s^2ng\ ^2G$ multiplets. The lowest member of this series, $5s^25g\ ^2G$, was unknown so far. Brill [10] observed a pair of lines at 9058.880 Å and 9063.658 Å with a separation 5.818(6) cm^{-1} closely matching his measured $5s^{24}F\ ^2F°$ $J = 5/2–7/2$ interval, 5.804(9) cm^{-1}. He recognized that these lines must correspond to transitions combining the $5s^{24}F\ ^2F°_{5/2,7/2}$ levels with some unknown level, but he was unable to decide whether this level is located above or below $5s^{24}F\ ^2F°$. Thus, he gave two possible energy values for this unknown level, 78258.194(6) cm^{-1} or 100324.103(6) cm^{-1}. By extrapolating the known energies of the $5s^2ng\ ^2G$ terms with $n \geq 6$ to $n = 5$ with the core-polarization formula (see section 3.3.5), we found that the upper of these two suggested values almost exactly coincides with the predicted position of the $5s^25g\ ^2G$ term. Our LSF calculations ruled out the existence of a level at the lower of the two positions suggested by Brill that could possibly combine with $5s^{24}F\ ^2F°$. Thus, we identified the level at 100324.111(7) cm^{-1} as $5s^25g\ ^2G$. Observed level energies and relative line intensities of all transitions from $5s^2ng$ levels agree well with our calculations.

3.3.3. Optimization of energy levels

To derive the energy level values that best fit all observed transition wavelengths, we used the least-squares level optimization program LOPT [30]. The crucial factors for the level optimization procedure are the correct identification of the spectral lines, estimation of their uncertainties, and absence of systematic shifts. Correctness of identifications was ensured by the analysis described above. Estimation of the statistical and systematic uncertainties of wavelengths was described in section 3.2. This estimation partially relies on the level optimization procedure, since some of the reference wavelengths used in this procedure are the Sn II Ritz wavelengths. Therefore, the level optimization was made in several iterations. In the initial stage, only the accurate measurements of Brill [10], as well as our measurements in the VUV, for which independent estimates of uncertainties are available, were included in the optimization. This resulted in initial estimates of the energy levels and Ritz wavelengths derived from them. Deviations of wavelengths observed by Wu [11] and by McCormick and Sawyer [6] from these Ritz wavelengths revealed systematic shifts smoothly varying with wavelength. After these systematic shifts were removed, residual deviations of corrected wavelengths from Ritz values provided a sufficient statistical basis to assign uncertainties to all the measurements. Then the corrected wavelengths from Wu [11] and McCormick and Sawyer [6] were also included in the level optimization, leading to an extended and more accurate set of energy levels and Ritz wavelengths. This process was repeated until the estimated systematic shifts stopped changing.

The final list of optimized energy levels is given in table 3.5. In this table, the level uncertainties are given for separations from the $5s^2 6p\ ^2P^o_{3/2}$ level. This level was chosen as the base, because it has the largest number of accurately measured transitions. To infer the uncertainty of an excitation energy from the ground level, one should combine the given uncertainty value in quadrature with the uncertainty of the ground level, 0.05 cm^{-1}. It can be seen that the level uncertainties vary greatly, from 0.003 cm^{-1} to 4 cm^{-1}, depending on the number and measurement accuracy of the lines determining the level. With a few exceptions, the level values are rounded using the "rule of 24," i.e., the uncertainty of the value does not exceed 24 units of the least significant digit of the value. In a few cases, an additional significant figure was required in order to reproduce the precisely measured transition wavelengths.

Twelve levels listed in table 3.5 have only one observed connecting line, as indicated in the last column. Four of them, $5s^2 6f\ ^2F^o_{7/2}$ and three autoionizing levels, were already discussed in sections 3.3.2.2 and 3.3.2.3. The $5s^2 1\ ^1S\ ^2S_{1/2}$ level, although it is based on only one transition to $5s^2 6p\ ^2P^o_{3/2}$ observed by McCormick and Sawyer [6] at 2608.74 Å, is supported by the regular behavior of energies along the $5s^2 ns$ series, as well as by good agreement of the observed intensity with our prediction. The remaining eight single-line levels are the members of the $5s^2 ng$ series. As discussed in section 3.3.2.4, all these levels are actually unresolved terms with negligibly small $J = 7/2–9/2$ fine-structure intervals. Thus, to consider reliability of their identification, one should take into account all the lines observed from each ^2G term. Each of these terms, except $5s^2 11g$, is based on two distinct observed lines. These lines are the strongest predicted from these terms. Similar to the $5s^2 ns$ series, all these identifications are confirmed by the regular behavior of energies and observed intensities along the series.

Some of the results of our LSF calculations, such as percentage compositions and differences of observed energies from those calculated in the parametric fitting are also given in table 3.5. The fitted parameter values obtained in the LSF are given in table 3.6.

Natural tin consists of ten stable isotopes with abundances ranging from 0.3 % to 33 %. Three of these isotopes have nuclear spin 1/2 and a rather large nuclear magnetic moment about $-1.0\ \mu_N$. Thus, lines observed from samples of natural tin (which were used in all experimental works quoted in the present work) must be broadened by isotope shifts and hyperfine structure. Since there is no such entity as an atom of natural tin, the energy levels derived by our level optimization do not correspond to any physical object but are empirical values that best describe the observed spectral lines. This should be kept in mind when using the high-precision values from tables 3.2 and 3.3. Asymmetry of line profiles caused by isotope shifts and hyperfine structure may result in deviations of observed peak wavelengths from the Ritz values given in table 3.4. Observed isotope shifts between adjacent even isotopes are typically (0.005–0.02) cm^{-1}, while the hyperfine structure in less abundant odd isotopes is an order of magnitude larger. References to studies of isotope shifts and hyperfine structure of Sn II can be obtained from the NIST Atomic Energy Levels and Spectra Bibliographic Database at http://physics.nist.gov/Elevbib.

For completeness, we note that there is only one reported measurement of the Landé *g*-factor for Sn II. Namely, David et al. [31] accurately measured the Landé *g*-factor for the $5s5p^2\ ^4P_{3/2}$ level to be 2.6609(7).

3.3.4. Intensities of observed lines

In the history of atomic spectroscopy, it has been an unfortunate long-standing tradition to give very rough estimates of relative intensities of observed lines. Although line intensities were always recognized to be important in correct identification of transitions causing them, the arguments had to be qualitative because the sensitivity of registration strongly varies with wavelength and depends on rarely quantified properties of detectors, spectrographs, and optics used. Also, different excitation conditions in light sources lead to large variations in line intensities. A method suggested and successfully used in a recent series of papers [32–34] overcomes these problems and allows one to reduce line intensities observed by different authors using different equipment to a common uniform scale. The method is based on using the Boltzmann equation to approximate populations of energy levels together with theoretically estimated radiative rates. It was shown in the papers quoted above that this approximation in most cases allows one to describe the observed intensities by a simple formula with weighted transition rate (gA) multiplied by a Boltzmann factor with a suitable effective excitation temperature. Then spectral response functions of the registration equipment can easily be derived by comparing observed and modeled intensities, and intensities observed with different setups can be reduced to a uniform scale with a common excitation temperature. Deviations of plasma conditions from the local thermodynamic equilibrium (LTE) and inaccuracies in estimated transition rates and derived response functions of registration equipment typically lead to errors of about a factor of three in such modeled intensities. Nevertheless, thus derived intensities provide a robust quantitative criterion for line identification and can even be used to estimate transition rates, when such estimates cannot be obtained from theory. Of course, the above-mentioned factor-of-three uncertainty is a restriction for many applications, but there are many cases where such estimates can be useful. This method was applied to obtain the reduced relative intensities given in table 3.4. Below, we explain reduction of intensities for each set of observations.

The Boltzmann plot for our observed line intensities, shown in figure 3.4(a), indicates an effective excitation temperature of 2.0 eV in our triggered spark source. This plot was built with intensities corrected for the variation of response function of our equipment with wavelength, denoted as I_{corr}. The logarithmic intensity-correction function $F(\lambda)$ used for this correction is shown in figure 3.4(b). Correction is made by multiplying the observed intensities by exponent of $F(\lambda)$. Transition rates gA used in the Boltzmann plots were calculated with Cowan's codes using our fitted parameters from the LSF.

Similarly, figures 3.4(c) and 3.4(d) present the Boltzmann plot and intensity-correction function for exposure 1 in Wu's line list [11]. It should be noted that the quantity given by Wu in the intensity columns is actually transparency (not the commonly used darkening) of the photographic plate on the scale 0 to 1000. To obtain the intensities, we subtracted his transparency values from 1000. Effective temperature in the source used for exposure 1 turned out to be 4.2 eV, which is the highest for all light sources used in the published literature. Apparently, this high temperature allowed Wu to observe lines from very highly excited levels not observed in other experiments. Reduction of intensities observed in the other three exposures reported by Wu [11] was made in a similar way. Effective temperatures for his exposures 2, 3, and 4 turned out to be about 3.6 eV, 3.7 eV, and 3.8 eV, respectively. Response functions derived from exposures 2 and 3, which cover the same wavelength range as exposure 1, are similar to the one shown in figure 3.4(d). For the final reduction of Wu's intensity values, we used the correction function averaged over these three exposures.

It should be noted that, despite the non-linear properties of photographic plates, the original observed intensities in both our and Wu's work did not show any significant non-linearity with exposure. This can easily be verified by plotting the ratio of calculated and observed intensities versus the observed intensity. Non-linearity would result in a trend on such plots, which was not detected.

Intensities observed by Brill [10] and by McCormick and Sawyer [6] were reduced by the same method as described above. The effective excitation temperature in the light source used by Brill was found to be 1.9 eV, which is close to our triggered-spark value of 2.0 eV.

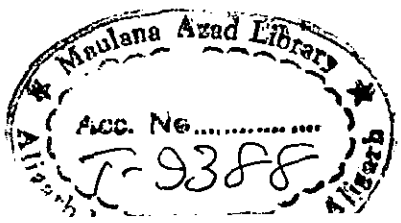

For the light source used by McCormick and Sawyer [6], the effective temperature was found to be somewhat lower, about 1.4 eV.

The values of effective excitation temperature given above are determined from Boltzmann plots which, as illustrated by figure 3.4, have a large scatter of data points. Thus, their accuracy is estimated as 20–40 %. Effective excitation temperatures may differ from electron temperatures in the plasma. Rather than that, they approximately describe excitation conditions leading to the observed line intensities and can be used to reduce intensities from different light sources to a uniform scale that better represents relative intensities expected to occur in a single experiment.

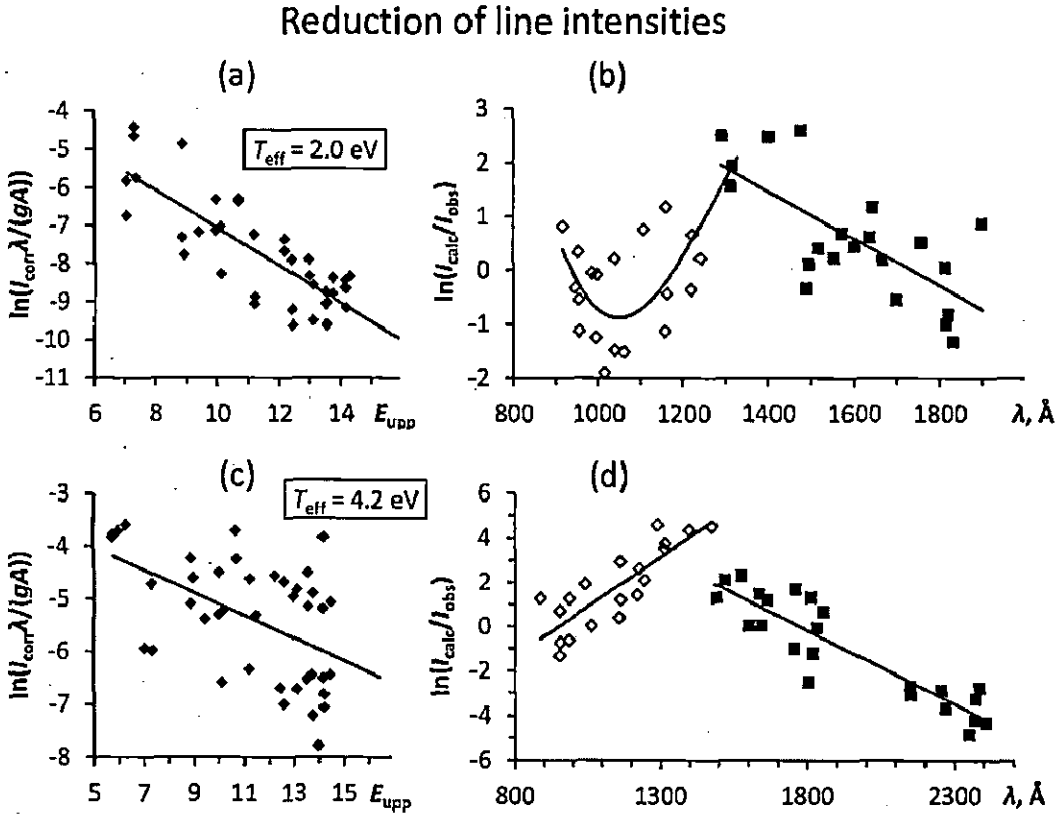

Figure 3.4. Boltzmann plots (a, c) and logarithmic intensity correction functions (b, d) for our observations and those of Wu [11]. The upper level energies E_{upp} in the Boltzmann plots are given in eV. The effective temperatures derived from the negative slope of the Boltzmann plots are shown in boxes. The calculated intensities I_{calc} in panels b and d are obtained from weighted transition rates gA calculated in the present work with a formula $I_{calc} = (gA/\lambda)\exp(-E_{upp}/T_{eff})$. Open diamonds and solid squares denote data points for separate wavelength ranges used to derive the linear or quadratic fits shown by solid lines.

After the variations of response functions of registration equipment were removed from the observed intensities, and the effective temperatures were determined for each set of observations, it was easy to scale the corrected observed intensities to the same effective temperature. We chose the highest temperature in all

sets of measurements, 4.2 eV, as the basis for the unified scale. This choice is motivated by the need to have the smallest range of final intensity values, which is convenient for presentation purposes.

3.3.5. Ionization potential

The ionization potential (IP) given in AEL [4] is the value obtained by McCormick and Sawyer [6] using the $5s^2ng$ ($n = 6–11$) series. As the 5g level was established in the present work, and the measurements of McCormick and Sawyer contained significant systematic shifts, the IP has to be revised. We obtained the new value of IP using both the Ritz-type quantum-defect series extrapolation and core-polarization formula fitting for the $5s^2ng\ ^2G$ ($n = 5–11$) series using computer codes RITZPL and POLAR [35]; both leading to almost the same value. The formulas used in these series-fitting computer codes and explanation of their application can be found, for example, in reference [32]. The IP obtained from RITZPL using the two-parameter extended Ritz formula was 118023.6(7) cm^{-1} and that from POLAR was 118023.8(7) cm^{-1}. Fitting of the three-parameter extended Ritz formula for the $5s^2ns$ ($n = 6–11$) series yields 118036.3(2) cm^{-1} for the ionization energy. It is known that the ns series is slightly perturbed by an interaction with $5s5p^2\ ^2S_{1/2}$. The ng series is free from such perturbations. Therefore, we adopted the average IP value obtained from the two fits of the $5s^2ng$ series, 118023.7(7) cm^{-1}, which is equivalent to 14.63307(8) eV. All fits were made using weights inversely proportional to squared uncertainties of the level values from table 3.5 combined in quadrature with the uncertainty of the ground level, 0.05 cm^{-1}. Our value is 6.7 cm^{-1} higher than the previously recommended value from McCormick and Sawyer [6].

3.4. Comparison with observed Auger electron spectrum

The Auger electron spectrum of Sn I and Sn II in the low-energy region 0–20 eV was observed by Forrest et al. [36] in a crossed atomic and electron beams experiment. They assigned several observed peaks to autoionization decay of the $^4D^9 5s^2 5p^2$ configuration of Sn II, not considered in this work. In addition, they tentatively assigned a strong peak observed at 2.529 eV to the autoionization decay of the $5p^3\ ^2P°$ term of Sn II. This assignment does not agree with our identifications. According to our parametric fitting, the $5p^3$ configuration is highly mixed with

5s5p5d, and the largest contribution of $5p^3\ ^2P°$ is predicted for the levels with large contributions from $5s5p(^3P°)5d\ ^2P°$ at about 128000 cm^{-1} and $5s5p(^1P°)5d\ ^2P°$ at about 152000 cm^{-1}. Autoionization decay of these levels to the $5s^2$ ground state of Sn III would produce Auger peaks at about 1.2 eV and 4.3 eV, respectively. Forrest et al. [36] observed a weak peak at 1.023 eV and medium-strength peaks at 4.117 eV and 4.277 eV, which may be associated with these predicted levels. However, for the peak at 1.023 eV our calculations yield a higher autoionization rate from a close predicted $5s5p(^3P°)5d\ ^2F°_{5/2}$ level at about 127000 cm^{-1}.

A few of the peaks observed by Forrest et al. [36] closely match the experimental energies of autoionizing Sn II levels we derived from our observed optical spectrum. In particular, the peaks observed at 1.761 eV and 1.829 eV closely match the predicted Auger energies for the $5s5p(^1P°)5d\ ^2D°$ $J = 3/2$ and 5/2 levels (observed at 132168.83 cm^{-1} and 132707.7 cm^{-1}), respectively.

The peak observed at 0.657 eV can be a blend of Auger decays of the $5p^3\ ^4S°_{3/2}$ and $5s5p(^3P°)5d\ ^4P°_{5/2}$ levels (which we observed at 123156.6 cm^{-1} and 123688.2 cm^{-1}, respectively). These decays are predicted to be of comparable strengths, due to small admixtures of doublet terms in the composition of these levels.

The peak at 0.285 eV was assigned by Forrest et al. [36] to the decay of the Sn I $5s5p^3\ ^3P°_1$ level to the $5s^25p\ ^2P°_{1/2}$ ground level of Sn II. However, this assignment was later rejected by Dembczynski and Wilson [37]. This peak closely matches our observed energy for the Sn II $5s5p(^3P°)5d\ ^4D°_{5/2}$ level (120253.6 cm^{-1}, corresponding to the Auger electron energy of 0.2773 eV), while the observed peak at 0.523 eV matches the decay of the $5s5p(^3P°)5d\ ^4D°_{7/2}$ level (122491.5 cm^{-1}, corresponding to the Auger electron energy of 0.5548 eV).

Finally, our calculations predict the metastable $5s5p(^3P°)5d\ ^4F°_{9/2}$ level at 118700 cm^{-1}. Autoionization of this level should produce an Auger peak at ejected electron energy of 0.088 eV. The strongest peak observed by Forrest et al. [36] is at 0.053 eV. This peak may be due to the decay of this metastable level.

We note that autoionization rates calculated for the Sn II levels discussed in this section are unreliable, because they strongly depend on very small mixing between doublet and quartet levels and on poorly known interaction between the $5p^3$ and 5s5p5d configurations. This, as well as the low resolution of the observed Auger electron spectrum [36], precludes definite identification of the observed Auger

features. More sophisticated calculations, as well as higher-resolution experiments, are needed to elucidate the structure of autoionizing Sn II levels in the region just above the first ionization limit.

3.5. Transition probabilities

Oliver and Hibbert [14] made a large-scale Breit-Pauli configuration-interaction (CI) calculation of transition probabilities of Sn II using the CIV3 code of Hibbert and co-workers (see references in [14]). They presented three sets of results: one for their *ab initio* calculation (in the length gauge) and two for the fine-tuned calculation (one in the length gauge and the other in the velocity gauge). The fine tuning consisted of semiempirical adjustment of the diagonal matrix elements of the Hamiltonian minimizing the differences between the calculated and experimental eigenvalues. The line strengths S_L obtained in the length gauge in the fine-tuned calculation are considered to be the most accurate ones from the three sets. Their accuracy can be assessed by comparing them with the other two data sets, S_v (fine-tuned, velocity gauge) and S_{ab} (*ab initio*, length gauge). This comparison, illustrated in figure 3.5, shows that for strong lines with $S_L > 0.28$ the length and velocity forms of line strength agree within 6 % on average, while for weaker lines with $S_L = (0.03–0.28)$ the agreement is somewhat worse, about 12 % on average. We adopted these standard deviations as conservative estimates of uncertainties of S_L in the corresponding ranges of line strength.

For the ten weakest lines with $S_L < 0.03$, the length and velocity forms strongly disagree with each other. Most of these transitions are intercombination ones between doublet and quartet levels. As pointed out by Oliver and Hibbert [14], for such transitions, calculation of the line strength in velocity gauge requires additional terms not accounted for in the CIV3 code. This makes the comparison meaningless for intercombination transitions. Instead, the comparison of the *ab initio* and fine-tuned calculations in the length gauge can be used for estimating their uncertainties. Except for one large deviation for the $5s^25p\ ^2P^\circ_{3/2} - 5s5p^2\ ^2S_{1/2}$ transition at 1394.667 Å, S_{ab} agrees with S_L within 12 %. However, because of low statistics, we adopt a conservative estimate of 35 % for the uncertainty of transitions with $S_L = (0.001–0.03)$ and omit the three weakest transitions, for which the transition rate given by Oliver and Hibbert [14] strongly contradicts the observed line intensities.

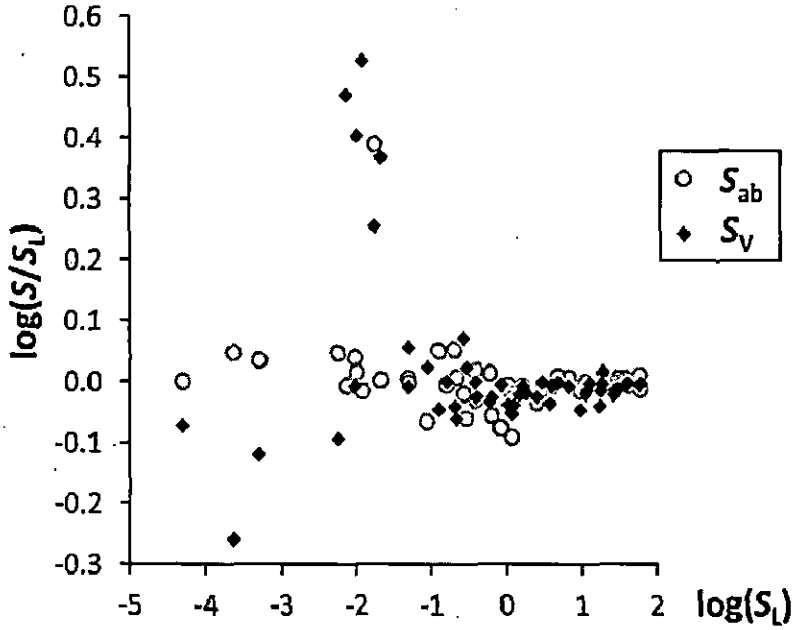

Figure 3.5. Comparison of line strengths S calculated by Oliver and Hibbert [14] in different approximations and gauges: S_L – fine tuned calculation in length gauge; S_V – fine tuned calculation in velocity gauge; S_{ab} – *ab initio* calculation in length gauge.

The high accuracy of calculations of Oliver and Hibbert [14] for strong lines is further confirmed by comparison of calculated and observed radiative lifetimes presented in table 3.2. David et al. [31], employing the direct magnetic resonance method, measured the lifetime of the $5s5p^2\ ^4P_{1/2}$ level in Sn II to be 325(40) ns. They supported this result by two additional less accurate measurements with two independent methods.

Schectman et al. [15] measured the lifetimes of three levels, $5s^25d\ ^2D_{3/2,5/2}$ and $5s^24F\ ^2F°_{5/2}$, with a beam-foil method. Using a similar method, Andersen and Lindgård [16] measured the lifetime of the $5s^26s\ ^2S_{1/2}$ and $5s^25d\ ^2D_{3/2}$ levels. Both these studies carefully accounted for effects of cascades on the measured decay curves. Gorshkov and Verolainen [41] determined the lifetimes of the two $5s^24F\ ^2F°_{5/2,7/2}$ levels by using intersecting atomic and electron beams and a multichannel method of retarded coincidences. Although they reported very small uncertainties of ±0.5 ns, their description of the experiment lacks any mention of an account for cascading effects. Therefore, in table 3.2 we have doubled their uncertainty estimate.

Table 3.2. Comparison of observed and calculated lifetimes in Sn II

Level		Energy cm^{-1}	τ_{obs} ns	Ref.[a]	τ_{th} ns	Ref.[a]
$5s5p^2$	$^4P_{1/2}$	46464.3	**325(40)**	D80	**375**	OH10
			1500[b]	AM00	215	TW
					237	AM05
$5s^26s$	$^2S_{1/2}$	56886.4	**1.10(10)**	AL77	**1.16**	OH10
					1.2	TW
					1.13	AM05
$5s^25d$	$^2D_{3/2}$	71406.1	**0.44(2)**	S00	**0.45**	OH10
			0.50(5)	AL77	0.37	TW
					0.41	AM05
$5s^25d$	$^2D_{5/2}$	72048.3	**0.46(4)**	S00	**0.51**	OH10
					0.45	TW
					0.5	AM05
$5s^24F$	$^2F°_{7/2}$	89288.3	**5.0(10)**[c]	GV85	**3.82**	OH10
			6.9[b]	AM00	3.28	TW
					3.21	AM05
$5s^24F$	$^2F°_{5/2}$	89294.1	**4.6(10)**	S00	**3.78**	OH10
			5.2(10)[c]	GV85	3.24	TW
			4.8[b]	AM00	3.04	AM05

[a] References: AL77 – Andersen and Lindgård [16]; AM00 – Alonso-Medina and Colón [38]; AM05 – Alonso-Medina et al. [40] (Cowan code); D80 – David et al. [31]; GV85 – Gorshkov and Verolainen [41]; OH10 – Oliver and Hibbert [14]; S00 – Schectman et al. [15]; TW – this work (Cowan code).

[b] Determined from the sum of measured radiative rates.

[c] Original estimate of uncertainty doubled (see text).

As can be seen from table 3.2, lifetimes calculated by Oliver and Hibbert [14] agree with all the best measurements within the uncertainties. Our own calculations made with the Cowan codes (using the LSF parameters) are compared with the calculations of Oliver and Hibbert [14] in figure 3.6.

For strong transitions with line strength $S > 0.5$, our calculations agree with those of Oliver and Hibbert [14] to 28 % on average. For weaker transitions, the results of Cowan's codes deviate from Oliver and Hibbert [14] by more than a factor of two on average. Calculations of Alonso-Medina et al. [40], also using a parametric fitting with Cowan's codes, are of similar quality, although they display somewhat larger deviations from Oliver and Hibbert [14] (about 30 % on average for $S > 1$, and 70 % for weaker transitions). We note that the *f*- and *A*-values given by Alonso-

Medina et al. [40] in their table V for the $5s^2nf$–$5s^2n'g$ transitions are not consistent with each other and strongly disagree with our calculations.

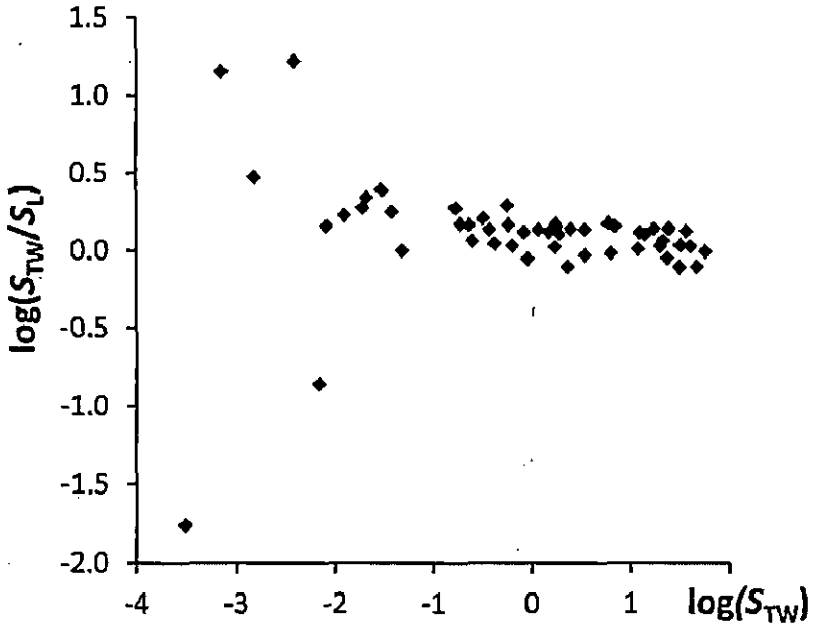

Figure 3.6. Comparison of line strengths calculated in the present work with Cowan's codes (S_{TW}) with those from fine tuned calculations of Oliver and Hibbert [14] in the length gauge (S_L).

Results of Oliver and Hibbert [14] also compare well with the relativistic all-order calculations of Safronova et al. [42]. These authors presented their results only for a few $5s^2ns$–$5s^2n'p$ and $5s^2np$–$5s^2n's$ transitions. They agree with Oliver and Hibbert [14] with an average deviation of 12 %, except for one $5s^25p\ ^2P^o_{3/2} - 5s^27s\ ^2S_{1/2}$ transition (1219.088 Å), for which their S value is lower by a factor of 2.5.

Aside from a few discrepancies mentioned above, theoretical calculations of line strengths agree with each other, at least for strong transitions, and they agree reasonably well with the few available lifetime measurements. However, comparison with experimentally measured radiative rates (A-values) presents problems. The A-values were measured for several tens of transitions by Alonso-Medina and Colón [38], Schectman et al. [15], Miller et al. [43], Wujec and Weniger [44], and Wujec and Musielok [45]. Experimental line strengths reported in these papers are compared with the critically evaluated theoretical data in figure 3.7. Only a few measured values agree with theory within the claimed measurement uncertainties. The greatest discrepancies are observed for the weakest lines measured by Alonso-Medina and

Colón [38]. It is difficult to identify the causes of the discrepancies. However, from the above analysis of the theoretical data, we conclude that the discrepancies originate in some flaws in the measurements. For this reason, we retained in table 3.4 only four experimental A-values, three from Alonso-Medina and Colón [38] and one from Miller et al. [43], and assigned greatly increased uncertainties to them.

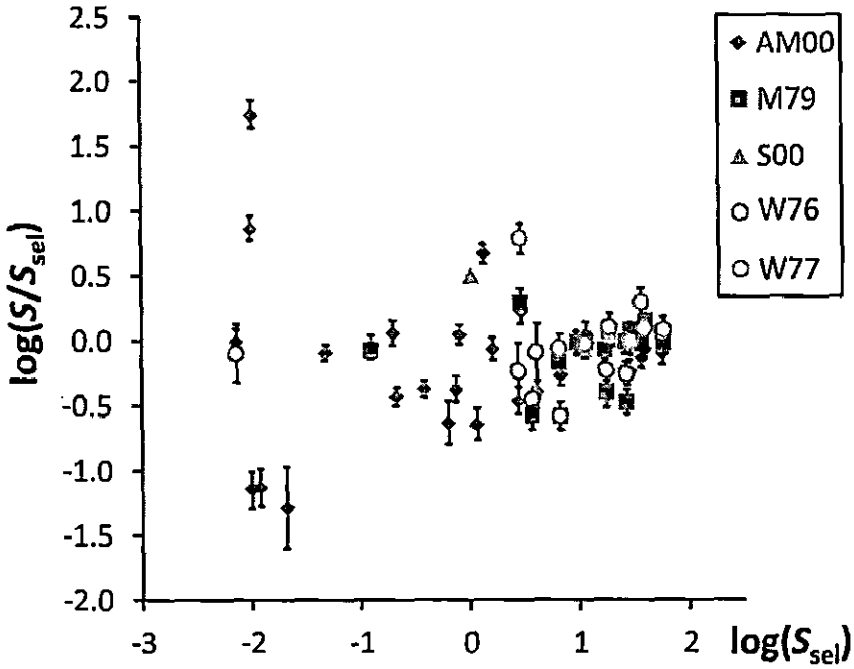

Figure 3.7. Comparison of experimental line strengths S with selected theoretical data. The selected line strengths S_{sel} were taken from Oliver and Hibbert [14] and from our calculations and have estimated uncertainties between 6 % and 35 %. The error bars correspond to claimed measurement uncertainties (one standard deviation). Key to experimental work: AM00 – Alonso Medina and Colón [38]; M79 – Miller et al. [43]; S00 – Schectman et al. [15]; W76 – Wujec and Musielok [45]; W77 – Wujec and Weniger [44].

We included in table 3.4 four lines at 2442.7 Å, 2486.6 Å, 2592.3 Å, and 3351.3 Å, for which Alonso-Medina and Colón [38] reported measured A-values. Since these authors did not attempt to accurately measure the wavelengths, and these lines were not reported by other authors, the wavelengths given in the column λ_{obs} are actually the rounded Ritz wavelengths. We note that the last two of these lines, as well as two other lines reported by Alonso-Medina and Colón [38] at 2592.6 Å and 3351.9 Å, were incorrectly identified by these authors.

We also included in table 3.4 one unobserved parity-forbidden line corresponding to the transition between the levels of the ground term. Our predicted wavelength for this far-infrared line is 23521.14(24) Å. According to calculations of Biémont et al. [39], Warner [46], and Garstang [47], this line is dominated by the magnetic dipole (M1) transition. The *A*-values calculated for this M1 transition in these works agree with each other within 1 %. The *A*-value for the electric quadrupole transition, 2.893 s^{-1} [39], amounts to only 0.4 % of the M1 decay rate and can be neglected in most applications.

Since the statistical distribution of both measured and calculated *A*-values is far from normal, uncertainties of the adopted *A*-values are specified in table 3.4 with a letter code instead of numerical values. The letter code is explained in table 3.3.

Table 3.3. Transition probability uncertainty code

Letter	Uncertainty in *A*-value	Uncertainty in log(*gf*)
AAA	≤ 0.3 %	≤ 0.0013
AA	≤ 1 %	≤ 0.004
A+	≤ 2 %	≤ 0.009
A	≤ 3 %	≤ 0.013
B+	≤ 7 %	≤ 0.03
C+	≤ 18 %	≤ 0.08
C	≤ 25 %	≤ 0.11
D+	≤ 40 %	≤ 0.18
D	≤ 50 %	≤ 0.24
E	> 50 %	> 0.24

References:

[1] Hobbs L M, Welty D E, Morton D C, Spitzer L and York D G 1993 *Astrophys. J.* **411** 750

[2] Sofia U J, Meyer D M and Cardelli J A 1999 *Astrophys. J.* **522** L137

[3] Foster A R, Counsell G F and Summers H P 2007 *J. Nucl. Mater.* 363 152

[4] Moore C E 1958 *Atomic Energy Levels, National Bureau of Standards Circular 467* vol. III (Washington, DC: US Govt. Printing Office)

[5] Kramida A, Ralchenko Yu., Reader J and NIST ASD Team 2012 *NIST Atomic Spectra Database, v.5.0,* National Institute of Standards and Technology, Gaithersburg, MD, USA. Available from: http://physics.nist.gov/ASD.

[6] McCormick W W and Sawyer R A 1938 *Phys. Rev.* **54** 71

[7] Green J B and Loring R A 1927 *Phys. Rev.* **30** 574

[8] Narayan A L and Rao K R 1927 *Nature Comm.* **120** 120

[9] Lang R J 1930 *Phys. Rev.* **35** 445

[10] Brill W G 1964 *The Arc Spectrum of Tin,* Ph. D. thesis, Purdue University, Lafayette, IN, USA, 119 pp.

[11] Wu C M 1967 *The Atomic Spark Spectra of Tin, Sn III, Sn IV, Sn V,* Master thesis, University of British Columbia, Canada

[12] Lysaght M A, Kilbane D, Cummings A, Murphy N, Dunne P, O'Sullivan G, Kampen P van, Costello J T and Kennedy E T 2005 *J. Phys. B* **38** 4247

[13] Duffy G, van Kampen P and Dunne P 2001 *J. Phys. B: At. Mol. Opt. Phys.* **34** 3171

[14] Oliver P and Hibbert A 2010 *J. Phys. B: At. Mol. Opt. Phys.* **43** 074013

[15] Schectman R M, Cheng S, Curtis L J, Federman S R, Fritts M C and Irving R E 2000 *Astrophys. J.* **542** 400

[16] Andersen T and Lindgård A 1977 *J. Phys. B: At. Mol. Opt. Phys.* **10** 2359

[17] Alonso-Medina A, Colón C and Martínez H C 2003 *Astrophys. J.* **595** 550

[18] Brown C M, Tilford S G, and Ginter M L 1977 *J. Opt. Soc. Am.* **67** 607

[19] Bhatia K S 1969 *Analysis of Doubly and Triply Ionised Indium,* Ph.D. Thesis, University of British Columbia, Canada

[20] Cowan R D 1981 *The Theory of Atomic Structure and Spectra* (Berkeley, CA: University of California Press) and Cowan code package for Windows by A. Kramida, available from http://das101.isan.troitsk.ru/COWAN

[21] Sansonetti J E and Martin W C 2005 *J. Phys. Chem. Ref. Data* **34** 1559

[22] Connerade J P and Baig M A 1981 *J. Phys. B: At. Mol. Opt. Phys.* **14** 29

[23] Colón C and Alonso-Medina A 2004 *Astron. Astrophys.***422** 1109

[24] Garton W R S, Parkinson W H and Reeves E M 1966 *Can. J. Phys.* **44** 1745

[25] Kaufman V, Sugar J and Joshi Y 1988 *J. Opt. Soc. Am. B* **5** 619

[26] Kaufman V and Sugar J 1987 *J. Opt. Soc. Am. B* **4** 1924

[27] Tauheed A, Joshi Y N and Rana T 2000 *Physica Scripta* **61** 696

[28] Tauheed A, Zafaran A F and Joshi Y N 1999 *J. Phys. B: At. Mol. Opt. Phys.* **32** 2917
[29] Tauheed A, Joshi Y N and Pinnington E H 1998 *J. Phys. B: At. Mol. Opt. Phys.* **31** 393
[30] Kramida A E 2011 *Comput. Phys. Commun.* **182** 419
[31] David D, Hamel J and Barrat J-P 1980 *Opt. Commun.* **32** 241
[32] Kramida A 2013 *Fusion Sci. Technol.* **63** 313
[33] Kramida A 2013 *J. Res. Natl. Inst. Stand. Technol.* **118** 52
[34] Kramida A 2013 *J. Res. Natl. Inst. Stand. Technol.* **118** 168
[35] Sansonetti C J 2005 *Computer programs RITZPL and POLAR*, private communication
[36] Forrest L F, James G K, Ross K J, Wilson M and Pantinakis A 1985 *J. Phys. B: At. Mol. Opt. Phys.* **18** 3123
[37] Dembczynski J and Wilson M 1988 *Z. Phys. D* **8** 329
[38] Alonso-Medina A and Colón C 2000 *Physica Scripta* **61** 646
[39] Biémont E, Hansen J E, Quinet P and Zeippen C J 1995 *Astron. Astrophys., Suppl. Ser.* **111** 333
[40] Alonso-Medina A, Colón C and Rivero C 2005 *Physica Scripta* **71** 154
[41] Gorshkov V N and Verolainen Ya F 1985 *Opt. Spectrosc.* **59** 694
[42] Safronova U I, Safronova M S and Kozlov M G 2007 *Phys. Rev. A* **76** 022501
[43] Miller M H, Roig R A and Bengtson R D 1979 *Phys. Rev. A* **20** 499
[44] Wujec T and Weniger S 1977 *J. Quant. Spectrosc. Radiat. Transfer* **18** 509
[45] Wujec T and Musielok J 1976 *Astron. Astrophys.* **50** 405
[46] Warner B 1968 *Z. Astrophys.* **69** 399
[47] Garstang R H 1964 *J. Res. Nat. Bur. Stand., Sect. A* **68**(1) 61

ed lines in Sn II

λ_{obs} [c] Å	σ_{obs} cm^{-1}	λ_{Ritz} [d] Å	$\delta\lambda_{O-Ritz}$ [e] Å	Classification				E_{low} cm^{-1}	E_{upp} cm^{-1}	A [f] s^{-1}	Acc. [g]	Line Ref. [h]	TP Ref. [h]
88.313(19)	112572.9	888.304(4)	0.009	$5s^25p$	$^2P^o_{1/2}$	$5s^211d$	$^2D_{3/2}$	0.00	112574.1			Wu	
99.884(19)	111125.4	899.907(10)	−0.023	$5s^25p$	$^2P^o_{1/2}$	$5s^210d$	$^2D_{3/2}$	0.00	111122.6			Wu	
17.378(6)	109006.3	917.380(4)	−0.002	$5s^25p$	$^2P^o_{1/2}$	$5s^29d$	$^2D_{3/2}$	0.00	109006.1	9.+7	E	TW	TW
22.856(19)	108359.3	922.870(3)	−0.014	$5s^25p$	$^2P^o_{1/2}$	$5s^210s$	$^2S_{1/2}$	0.00	108357.6	2.4+7	E	Wu	TW
23.01(4)	108341	922.974(10)	0.04	$5s^25p$	$^2P^o_{3/2}$	$5s^211d$	$^2D_{5/2}$	4251.494	112596.9			MS	
35.571(19)	106886.6	935.525(10)	0.046	$5s^25p$	$^2P^o_{3/2}$	$5s^210d$	$^2D_{5/2}$	4251.494	111143.3			Wu	
35.802(6)	105730.4	945.794(3)	0.008	$5s^25p$	$^2P^o_{1/2}$	$5s^28d$	$^2D_{3/2}$	0.00	105731.3	1.5+8	E	TW	TW
44.440(6)	104773.5	954.4332(14)	0.007	$5s^25p$	$^2P^o_{3/2}$	$5s^29d$	$^2D_{5/2}$	4251.494	109025.72	9.+7	E	TW	TW
44.614(6)	104754.4	954.612(4)	0.002	$5s^25p$	$^2P^o_{3/2}$	$5s^29d$	$^2D_{3/2}$	4251.494	109006.1	1.8+7	E	TW	TW
45.299(6)	104679.3	955.3068(10)	−0.008	$5s^25p$	$^2P^o_{1/2}$	$5s^29s$	$^2S_{1/2}$	0.00	104678.41	3.9+7	E	TW	TW
50.545(19)	104107.6	960.558(4)	−0.013	$5s^25p$	$^2P^o_{3/2}$	$5s^210s$	$^2S_{1/2}$	4251.494	108357.6	4.+7	E	Wu	TW
55.110(6)	101511.5	985.1117(23)	−0.002	$5s^25p$	$^2P^o_{3/2}$	$5s^28d$	$^2D_{5/2}$	4251.494	105762.82	1.6+8	E	TW	TW
55.411(19)	101480.5	985.418(3)	−0.007	$5s^25p$	$^2P^o_{3/2}$	$5s^28d$	$^2D_{3/2}$	4251.494	105731.3	3.0+7	E	Wu	TW
65.742(6)	100427.6	995.7490(10)	−0.007	$5s^25p$	$^2P^o_{3/2}$	$5s^29s$	$^2S_{1/2}$	4251.494	104678.41	7.+7	E	TW	TW
77.168(6)	100284.0	997.1669(5)	0.001	$5s^25p$	$^2P^o_{1/2}$	$5s^27d$	$^2D_{3/2}$	0.00	100284.111	2.8+8	D+	TW	TW
16.238(6)	98402.1	1016.2353(5)	0.003	$5s^25p$	$^2P^o_{1/2}$	$5s^28s$	$^2S_{1/2}$	0.00	98402.412	7.+7	E	TW	TW
40.720(6)	96087.3	1040.71860(19)	0.001	$5s^25p$	$^2P^o_{3/2}$	$5s^27d$	$^2D_{5/2}$	4251.494	100338.947	3.0+8	D+	TW	TW
41.313(6)	96032.6	1041.31287(19)	0.000	$5s^25p$	$^2P^o_{3/2}$	$5s^27d$	$^2D_{3/2}$	4251.494	100284.111	6.+7	E	TW	TW
62.123(7)	94151.1	1062.12453(17)	−0.002	$5s^25p$	$^2P^o_{3/2}$	$5s^28s$	$^2S_{1/2}$	4251.494	98402.412	1.3+8	E	TW	TW
08.138(10)	90241.5	1108.1369(6)	0.001	$5s^25p$	$^2P^o_{1/2}$	$5s^26d$	$^2D_{3/2}$	0.00	90241.554	4.7+8	B+	TW	OH10
59.014(10)	86280.2	1159.0129(6)	0.001	$5s^25p$	$^2P^o_{1/2}$	$5s^27s$	$^2S_{1/2}$	0.00	86280.318	1.01+8	C+	TW	OH10
61.434(10)	86100.5	1161.43479(20)	−0.001	$5s^25p$	$^2P^o_{3/2}$	$5s^26d$	$^2D_{5/2}$	4251.494	90351.894	5.5+8	B+	TW	OH10
62.926(10)	85990.0	1162.92511(20)	0.001	$5s^25p$	$^2P^o_{3/2}$	$5s^26d$	$^2D_{3/2}$	4251.494	90241.554	1.28+8	B+	TW	OH10
85.675(14)	84340.1	1185.684(5)	−0.009	$5s5p^2$	$^4P_{3/2}$	$5s5p(^1P^o)5d$	$^2D^o_{5/2}$	48368.185	132707.7			TW	
93.299(14)	83801.3	1193.308(3)	−0.009	$5s5p^2$	$^4P_{3/2}$	$5s5p(^1P^o)5d$	$^2D^o_{3/2}$	48368.185	132168.83			TW	
19.088(10)	82028.3	1219.08367(22)	0.004	$5s^25p$	$^2P^o_{3/2}$	$5s^27s$	$^2S_{1/2}$	4251.494	86280.318	3.35+8	B+	TW	OH10
23.715(10)	81718.4	1223.716(5)	−0.001	$5s^25p$	$^2P^o_{1/2}$	$5s5p^2$	$^2P_{3/2}$	0.00	81718.3	4.08+8	B+	TW	OH10
42.928(10)	80455.2	1242.929(7)	−0.001	$5s^25p$	$^2P^o_{1/2}$	$5s5p^2$	$^2P_{1/2}$	0.00	80455.1	4.5+8	B+	TW	OH10

λ_{obs} [c] Å	σ_{obs} cm^{-1}	$\lambda_{Ritz.}$ [d] Å	$\delta\lambda_{O-Ritz}$ [e] Å	Classification				E_{low} cm^{-1}	E_{upp} cm^{-1}	A [f] s^{-1}	Acc. [g]	Line Ref. [h]	TP Ref. [h]
85.659(7)	77781.1	1285.655(3)	0.004	$5s5p^2$	$^4P_{1/2}$	$5s5p(^3P^o)5d$	$^4P^o_{3/2}$	46464.290	124245.66			TW	
90.871(10)	77467.1	1290.875(5)	−0.004	$5s^25p$	$^2P^o_{3/2}$	$5s5p^2$	$^2P_{3/2}$	4251.494	81718.3	2.95+9	B+	TW	OH10
93.902(14)	76692.9	1303.912(7)	−0.010	$5s5p^2$	$^4P_{1/2}$	5p3	$^4S^o_{3/2}$	46464.290	123156.6	9.+8	D+	TW	TW
12.275(10)	76203.5	1312.274(7)	0.001	$5s^25p$	$^2P^o_{3/2}$	$5s5p^2$	$^2P_{1/2}$	4251.494	80455.1	1.77+9	B+	TW	OH10
13.087(14)	76156.4	1313.087(14)		$5s5p^2$	$^4P_{3/2}$	$5s5p(^3P^o)5d$	$^4P^o_{1/2}$	48368.185	124524.6	2.0+9	D+	TW	TW
16.572(10)	75954.8	1316.581(6)	−0.009	$5s^25p$	$^2P^o_{1/2}$	$5s5p^2$	$^2S_{1/2}$	0.00	75954.3	2.14+9	B+	TW	OH10
17.907(7)	75877.9	1317.914(3)	−0.007	$5s5p^2$	$^4P_{3/2}$	$5s5p(^3P^o)5d$	$^4P^o_{3/2}$	48368.185	124245.66	1.3+9	D+	TW	TW
27.669(14)	75320.0	1327.668(10)	0.001	$5s5p^2$	$^4P_{3/2}$	$5s5p(^3P^o)5d$	$^4P^o_{3/2}$	48368.185	123688.2			TW	
37.103(14)	74788.6	1337.105(7)	−0.002	$5s5p^2$	$^4P_{3/2}$	5p3	$^4S^o_{3/2}$	48368.185	123156.6	1.3+9	D+	TW	TW
53.843(14)	73863.8	1353.848(6)	−0.005	$5s5p^2$	$^2D_{3/2}$	$5s5p(^1P^o)5d$	$^2D^o_{5/2}$	58844.181	132707.7	3.6+8	D+	TW	TW
58.707(14)	73599.4	1358.695(10)	0.012	$5s5p^2$	$^4P_{1/2}$	$5s5p(^3P^o)5d$	$^4D^o_{3/2}$	46464.290	120064.3	1.9+9	D+	TW	TW
60.226(20)	73517.2	1360.259(4)	−0.033	$5s5p^2$	$^4P_{5/2}$	$5s5p(^3P^o)5d$	$^4P^o_{3/2}$	50730.224	124245.66	7.5+8	D+	TW	TW
60.226(20)	73517.2	1360.233(12)	−0.007	$5s5p^2$	$^4P_{1/2}$	$5s5p(^3P^o)5d$	$^4D^o_{1/2}$	46464.290	119981.1	3.3+9	D+	TW	TW
63.799(7)	73324.6	1363.798(4)	0.001	$5s5p^2$	$^2D_{3/2}$	$5s5p(^1P^o)5d$	$^2D^o_{3/2}$	58844.181	132168.83	3.6+9	D+	TW	TW
65.282(14)	73244.9	1365.295(6)	−0.013	$5s5p^2$	$^2D_{5/2}$	$5s5p(^1P^o)5d$	$^2D^o_{5/2}$	59463.481	132707.7	3.4+9	D+	TW	TW
70.651(14)	72958.0	1370.652(10)	−0.001	$5s5p^2$	$^4P_{3/2}$	$5s5p(^3P^o)5d$	$^4P^o_{5/2}$	50730.224	123688.2	2.1+9	D+	TW	TW
75.416(7)	72705.3	1375.415(5)	0.001	$5s5p^2$	$^2D_{5/2}$	$5s5p(^1P^o)5d$	$^2D^o_{3/2}$	59463.481	132168.83	1.8+8	D+	TW	TW
80.704(14)	72426.8	1380.712(7)	−0.008	$5s5p^2$	$^4P_{5/2}$	5p3	$^4S^o_{3/2}$	50730.224	123156.6	2.3+9	D+	TW	TW
91.100(7)	71885.6	1391.103(5)	−0.003	$5s5p^2$	$^4P_{3/2}$	$5s5p(^3P^o)5d$	$^4D^o_{5/2}$	48368.185	120253.6	2.3+9	D+	TW	TW
93.510(20)	71761.2	1393.510(20)		$5s5p^2$	$^4P_{5/2}$	$5s5p(^3P^o)5d$	$^4D^o_{7/2}$	50730.224	122491.5	3.1+9	D+	TW	TW
94.667(19)	71701.7	1394.646(7)	0.021	$5s^25p$	$^2P^o_{3/2}$	$5s5p^2$	$^2S_{1/2}$	4251.494	75954.3	7.+6	E	Wu*	OH10
94.764(14)	71696.7	1394.776(10)	−0.012	$5s5p^2$	$^4P_{3/2}$	$5s5p(^3P^o)5d$	$^4D^o_{3/2}$	48368.185	120064.3	1.0+9	D+	TW	TW
96.399(14)	71612.8	1396.396(13)	0.003	$5s5p^2$	$^4P_{3/2}$	$5s5p(^3P^o)5d$	$^4D^o_{1/2}$	48368.185	119981.1	2.4+8	D+	TW	TW
00.454(20)	71405.4	1400.4398(9)	0.014	$5s^25p$	$^2P^o_{1/2}$	$5s^25d$	$^2D_{3/2}$	0.00	71406.142	2.05+9	B+	TW	OH10
38.365(14)	69523.4	1438.365(6)	0.000	$5s5p^2$	$^4P_{5/2}$	$5s5p(^3P^o)5d$	$^4D^o_{5/2}$	50730.224	120253.6			TW	
74.995(20)	67796.8	1474.9966(3)	−0.002	$5s^25p$	$^2P^o_{3/2}$	$5s^25d$	$^2D_{5/2}$	4251.494	72048.260	1.95+9	B+	TW	OH10
81.747(7)	67487.9	1481.742(5)	0.005	$5s5p^2$	$^4P_{1/2}$	$5s5p(^3P^o)6s$	$^2P^o_{1/2}$	46464.290	113952.44			TW	

λ_{obs} [c] Å	σ_{obs} cm^{-1}	λ_{Ritz} [d] Å	$\delta\lambda_{O-Ritz}$ [e] Å	Classification				E_{low} cm^{-1}	E_{upp} cm^{-1}	A [f] s^{-1}	Acc. [g]	Line Ref. [h]	TP Ref. [h]
1489.091(10)	67155.1	1489.1002(4)	−0.009	$5s^25p$	$^2P^o_{3/2}$	$5s^25d$	$^2D_{3/2}$	4251.494	71406.142	1.59+8	B+	TW	OH10
1495.037(7)	66888.0	1495.037(7)		$5s5p^2$	$^4P_{3/2}$	$5s5p(^3P^o)5d$	$^4F^o_{5/2}$	48368.185	115256.2	1.1+8	D+	TW	TW
1517.961(7)	65877.8	1517.967(5)	−0.006	$5s5p^2$	$^4P_{3/2}$	$5s5p(^3P^o)6s$	$^4P^o_{5/2}$	48368.185	114245.75	4.4+8	D+	TW	TW
1522.206(20)	65694.1	1522.235(7)	−0.029	$5s5p^2$	$^4P_{5/2}$	$5s5p(^3P^o)5d$	$^4F^o_{7/2}$	50730.224	116423.1	8.3+7	D+	TW	TW
1527.856(14)	65451.2	1527.873(5)	−0.017	$5s5p^2$	$^4P_{3/2}$	$5s5p(^3P^o)5d$	$^2D^o_{5/2}$	48368.185	113818.65			TW	
1543.653(19)	64781.4	1543.634(5)	0.019	$5s5p^2$	$^2D_{5/2}$	$5s5p(^3P^o)5d$	$^4P^o_{3/2}$	59463.481	124245.66			Wu*	
1554.881(14)	64313.6	1554.896(5)	−0.015	$5s5p^2$	$^4P_{1/2}$	$5s5p(^3P^o)6s$	$^4P^o_{3/2}$	46464.290	110777.28	4.0+8	D+	TW	TW
1570.056(19)	63692.0	1570.028(10)	0.028	$5s5p^2$	$^2D_{3/2}$	5p3	$^4S^o_{3/2}$	59463.481	123156.6			Wu*	
1574.426(8)	63515.2	1574.418(5)	0.008	$5s5p^2$	$^4P_{5/2}$	$5s5p(^1P^o)6s$	$^4P^o_{5/2}$	50730.224	114245.75	7.2+8	D+	TW	TW
1585.071(16)	63088.7	1585.077(5)	−0.006	$5s5p^2$	$^4P_{5/2}$	$5s5p(^3P^o)5d$	$^2D^o_{3/2}$	50730.224	113818.65	6.2+7	D+	TW	TW
1587.532(19)	62990.9	1587.571(7)	−0.039	$5s5p^2$	$^4P_{1/2}$	$5s5p(^3P^o)6s$	$^4P^o_{1/2}$	46464.290	109453.6	1.5+8	D+	Wu	TW
1593.418(16)	62758.2	1593.414(7)	0.004	$5s5p^2$	$^4P_{1/2}$	$5s^210p$	$^2P^o_{1/2}$	46464.290	109222.6			TW	
1602.325(12)	62409.3	1602.331(5)	−0.006	$5s5p^2$	$^4P_{3/2}$	$5s5p(^3P^o)6s$	$^4P^o_{3/2}$	48368.185	110777.28	1.1+8	D+	TW	TW
1628.422(16)	61409.1	1628.415(7)	0.007	$5s5p^2$	$^2D_{3/2}$	$5s5p(^3P^o)5d$	$^4D^o_{5/2}$	58844.181	120253.6			TW	
1637.059(8)	61085.2	1637.052(7)	0.007	$5s5p^2$	$^4P_{3/2}$	$5s5p(^3P^o)6s$	$^4P^o_{1/2}$	48368.185	109453.6	6.6+8	D+	TW	TW
1643.262(12)	60854.6	1643.266(7)	−0.004	$5s5p^2$	$^4P_{3/2}$	$5s^210p$	$^2P^o_{1/2}$	48368.185	109222.6	1.4+8	D+	TW	TW
1648.562(12)	60658.9	1648.548(9)	0.014	$5s^25d$	$^2D_{5/2}$	$5s5p(^1P^o)5d$	$^2D^o_{5/2}$	72048.260	132707.7			TW	
1665.364(8)	60046.9	1665.361(6)	0.003	$5s5p^2$	$^4P_{5/2}$	$5s5p(^3P^o)6s$	$^4P^o_{3/2}$	50730.224	110777.28	3.8+8	D+	TW	TW
1699.418(16)	58843.7	1699.4034(13)	0.015	$5s^25p$	$^2P^o_{1/2}$	$5s5p^2$	$^2D_{3/2}$	0.00	58844.181	2.99+7	B+	TW	OH10
1755.621(19)	56959.9	1755.630(9)	−0.009	$5s5p^2$	$^2D_{5/2}$	$5s5p(^3P^o)5d$	$^4F^o_{7/2}$	59463.481	116423.1			Wu*	
1757.893(16)	56886.3	1757.8905(14)	0.002	$5s^25p$	$^2P^o_{1/2}$	$5s^26s$	$^2S_{1/2}$	0.00	56886.363	3.04+8	B+	TW	OH10
1778.898(16)	56214.6	1778.900(12)	−0.002	$5s5p^2$	$^2S_{1/2}$	$5s5p(^1P^o)5d$	$^2D^o_{3/2}$	75954.3	132168.83			TW	
1805.002(19)	55401.6	1805.003(7)	−0.001	$5s5p^2$	$^2D_{3/2}$	$5s5p(^3P^o)6s$	$^4P^o_{5/2}$	58844.181	114245.75			Wu	
1811.197(16)	55212.1	1811.2009(5)	−0.004	$5s^25p$	$^2P^o_{3/2}$	$5s5p^2$	$^2D_{5/2}$	4251.494	59463.481	6.4+7	B+	TW	OH10
1814.602(12)	55108.5	1814.610(8)	−0.008	$5s5p^2$	$^2D_{3/2}$	$5s5p(^3P^o)6s$	$^2P^o_{1/2}$	58844.181	113952.44			TW	
1819.039(12)	54974.1	1819.026(7)	0.013	$5s5p^2$	$^2D_{3/2}$	$5s5p(^3P^o)5d$	$^2D^o_{5/2}$	58844.181	113818.65			TW	
1831.757(16)	54592.4	1831.7472(5)	0.010	$5s^25p$	$^2P^o_{3/2}$	$5s5p^2$	$^2D_{3/2}$	4251.494	58844.181	2.2+7	C+	TW	OH10
1855.604(19)	53890.8	1855.600(7)	0.004	$5s^26s$	$^2S_{1/2}$	$5s5p(^3P^o)6s$	$^4P^o_{3/2}$	56886.363	110777.28			Wu	
1886.107(8)	53019.26	1886.110(6)	−0.003	$5s5p^2$	$^4P_{3/2}$	$5s^28p$	$^2P^o_{3/2}$	48368.185	101387.37			TW	
1899.901(16)	52634.3	1899.8812(5)	0.020	$5s^25p$	$^2P^o_{3/2}$	$5s^26s$	$^2S_{1/2}$	4251.494	56886.363	5.6+8	B+	TW	OH10

Char.[b]	λ_{obs}[c] Å	σ_{obs} cm^{-1}	λ_{Ritz}[d] Å	$\delta\lambda_{O-Ritz}$[e] Å	Classification				E_{low} cm^{-1}	E_{upp} cm^{-1}	A[f] s^{-1}	Acc.[g]	Line Ref.[h]	TP Ref.[h]
	2108.475(19)	47412.6	2108.493(12)	−0.018	$5s5p^2$	$^2D_{3/2}$	$5s^26p$	$^2P^o_{1/2}$	58844.181	106256.4			Wu	
	2131.208(19)	46906.9	2131.218(18)	−0.010	$5s5p^2$	$^2D_{5/2}$	$5s^26p$	$^2P^o_{3/2}$	59463.481	106370.2			Wu	
(Sn III)	2148.61(8)	46527.1	2148.589(16)	0.02	$5s5p^2$	$^2D_{3/2}$	$5s^26f$	$^2F^o_{5/2}$	58844.181	105371.7			MS	
	2150.8442(9)	46478.749	2150.8451(7)	−0.0009	$5s^25p$	$^2P^o_{3/2}$	$5s5p^2$	$^4P_{5/2}$	4251.494	50730.224	4.0+5	D+	Brill	OH10
	2151.5135(20)	46464.29	2151.5136(20)	−0.0001	$5s^25p$	$^2P^o_{1/2}$	$5s5p^2$	$^4P_{1/2}$	0.00	46464.290	2.1+6	C+	Brill	OH10
	2200.075(19)	45438.8	2200.0341(11)	0.041	$5s5p^2$	$^4P_{1/2}$	$5s^27p$	$^2P^o_{1/2}$	46464.290	91903.945			Wu	
(Sn I)			2246.443(8)		$5s^26s$	$^2S_{1/2}$	$5s^28p$	$^2P^o_{3/2}$	56886.363	101387.37			MS	
	2252.845(19)	44374.6	2252.831(15)	0.014	$5s^25d$	$^2D_{5/2}$	$5s5p(^3P^o)5d$	$^4F^o_{7/2}$	72048.260	116423.1			Wu*	
	2255.726(19)	44317.9	2255.729(19)	−0.003	$5s^26s$	$^2S_{1/2}$	$5s^28p$	$^2P^o_{1/2}$	56886.363	101204.2			Wu	
	2266.0156(10)	44116.677	2266.0149(7)	0.0007	$5s^25p$	$^2P^o_{3/2}$	$5s5p^2$	$^4P_{3/2}$	4251.494	48368.185	4.3+5	D+	Brill	OH10
	2296.293(19)	43535.0	2296.2548(9)	0.038	$5s5p^2$	$^4P_{3/2}$	$5s^27p$	$^2P^o_{1/2}$	48368.185	91903.945			Wu	
	2333.43(14)	42842	2333.573(11)	−0.14	$5s^25d$	$^2D_{3/2}$	$5s5p(^3P^o)6s$	$^4P^o_{5/2}$	71406.142	114245.75			Wu	
	2349.825(19)	42543.3	2349.833(9)	−0.008	$5s5p^2$	$^2D_{3/2}$	$5s^28p$	$^2P^o_{3/2}$	58844.181	101387.37			Wu	
	2350.698(19)	42527.5	2350.708(16)	−0.010	$5s5p^2$	$^2P_{3/2}$	$5s5p(^3P^o)5d$	$^4P^o_{3/2}$	81718.3	124245.66			Wu	
			2357.074(12)		$5s^25d$	$^2D_{3/2}$	$5s5p(^3P^o)5d$	$^2D^o_{5/2}$	71406.142	113818.65			Wu	
			2359.995(21)		$5s5p^2$	$^2D_{3/2}$	$5s^28p$	$^2P^o_{1/2}$	58844.181	101204.2			Wu	
	2360.28(10)	42355	2360.230(18)	0.05x	$5s^26d$	$^2D_{5/2}$	$5s5p(^1P^o)5d$	$^2D^o_{5/2}$	90351.894	132707.7			Wu*	
	2368.2265(6)	42212.795	2368.2265(6)	0.0000	$5s^25p$	$^2P^o_{3/2}$	$5s5p^2$	$^4P_{1/2}$	4251.494	46464.290	5.6+5	C+	Brill	OH10
	2369.15(10)	42196.4	2369.086(11)	0.06	$5s^25d$	$^2D_{5/2}$	$5s5p(^3P^o)6s$	$^4P^o_{5/2}$	72048.260	114245.75			Wu	
	2384.565(19)	41923.6	2384.548(9)	0.017	$5s5p^2$	$^2D_{5/2}$	$5s^28p$	$^2P^o_{3/2}$	59463.481	101387.37			Wu	
	2393.309(19)	41770.4	2393.311(12)	−0.002	$5s^25d$	$^2D_{5/2}$	$5s5p(^3P^o)5d$	$^2D^o_{5/2}$	72048.260	113818.65			Wu*	
	2406.712(19)	41537.8	2406.7088(6)	0.003	$5s5p^2$	$^4P_{5/2}$	$5s^27p$	$^2P^o_{3/2}$	50730.224	92268.106	3.4+5	D+	Wu	OH10
(Sn I)	2433.48(3)	41080.9	2433.49(3)	−0.01	$5s^26p$	$^2P^o_{1/2}$	$5s^211d$	$^2D_{3/2}$	71493.273	112574.1			Wu	
	2442.7	40926	2442.7019(6)		$5s5p^2$	$^4P_{3/2}$	$5s^24f$	$^2F^o_{5/2}$	48368.185	89294.055	2.4+5	D+	AM	OH10
	2448.9079(7)	40822.163	2448.9089(4)	−0.0010	$5s5p^2$	$^2D_{3/2}$	$5s^25f$	$^2F^o_{5/2}$	58844.181	99666.327	6.4+7	D+	Brill	TW
	2486.6	40203	2486.6356(5)		$5s5p^2$	$^2D_{5/2}$	$5s^25f$	$^2F^o_{5/2}$	59463.481	99666.327	1.0+7	D	AM	AM
	2486.9666(8)	40197.495	2486.9665(4)	0.0001	$5s5p^2$	$^2D_{5/2}$	$5s^25f$	$^2F^o_{7/2}$	59463.481	99660.978	6.8+7	D+	Brill	TW
	2522.69(9)	39628.3	2522.62(8)	0.07	$5s^26p$	$^2P^o_{1/2}$	$5s^210d$	$^2D_{3/2}$	71493.273	111122.6			MS	
	2538.95(10)	39374.5	2539.169(13)	−0.22x	$5s^25d$	$^2D_{3/2}$	$5s5p(^3P^o)6s$	$^4P^o_{3/2}$	71406.142	110777.28			Wu	
	2579.15(23)	38761	2578.82(7)	0.33	$5s^26p$	$^2P^o_{3/2}$	$5s^210d$	$^2D_{5/2}$	72377.4484	111143.3	1.0+7	D+	MS	TW

I_{obs}[a] arb. u.	Char.[b]	λ_{obs}[c] Å	σ_{obs} cm^{-1}	λ_{Ritz}[d] Å	$\delta\lambda_{O-Ritz}$[e] Å	Classification	E_{low} cm^{-1}	E_{upp} cm^{-1}	A[f] s^{-1}	Acc.[g]	Line Ref.[b]	TP Ref.[h]
550	:	2592.3	38564	2592.3281(5)		$5s5p^2$ $^4P_{5/2}$ $5s^24f$ $^2F^o_{5/2}$	50730.224	89294.055	1.9+5	D+	AM	OH10
1200		2592.7198(17)	38558.01	2592.7181(5)	0.0017	$5s5p^2$ $^4P_{5/2}$ $5s^24f$ $^2F^o_{7/2}$	50730.224	89288.255	2.9+6	C+	Brill	OH10
200		2608.74(24)	38321	2608.74(24)		$5s^26p$ $^2P^o_{3/2}$ $5s^211s$ $^2S_{1/2}$	72377.4484	110699			MS	
880	bl(Sn III)	2643.56(3)	37816.5	2643.564(19)	0.0	$5s^25d$ $^2D_{3/2}$ $5s^210p$ $^2P^o_{1/2}$	71406.142	109222.6			Wu	
860		2664.99(10)	37512.4	2664.96(3)	0.03	$5s^26p$ $^2P^o_{1/2}$ $5s^29d$ $^2D_{3/2}$	71493.273	109006.1	1.4+7	D+	MS	TW
220		2711.86(3)	36864.2	2711.85(3)	0.01	$5s^26p$ $^2P^o_{1/2}$ $5s^210s$ $^2S_{1/2}$	71493.273	108357.6			Wu	
400		2727.76(3)	36649.3	2727.834(11)	−0.07	$5s^26p$ $^2P^o_{3/2}$ $5s^29d$ $^2D_{5/2}$	72377.4484	109025.72	1.6+7	D+	Wu	TW
180		2778.4(3)	35982	2778.49(3)	−0.1	$5s^26p$ $^2P^o_{3/2}$ $5s^210s$ $^2S_{1/2}$	72377.4484	108357.6			MS	
240		2825.51(3)	35381.4	2825.4849(7)	0.03	$5s^26s$ $^2S_{1/2}$ $5s^27p$ $^2P^o_{3/2}$	56886.363	92268.106	1.11+6	C+	Wu	OH10
210		2868.61(3)	34849.9	2868.577(23)	0.03	$5s^25d$ $^2D_{3/2}$ $5s^29p$ $^2P^o_{1/2}$	71406.142	106256.4			Wu	
220		2912.82(10)	34320.9	2912.74(3)	0.08	$5s^25d$ $^2D_{5/2}$ $5s^29p$ $^2P^o_{3/2}$	72048.260	106370.2			MS	
610		2919.86(3)	34238.2	2919.87(3)	−0.01	$5s^26p$ $^2P^o_{1/2}$ $5s^28d$ $^2D_{3/2}$	71493.273	105731.3	2.4+7	D+	Wu	TW
190		2943.30(3)	33965.5	2943.30(3)	0.00	$5s^25d$ $^2D_{3/2}$ $5s^26f$ $^2F^o_{5/2}$	71406.142	105371.7			Wu	
400		2949.54(3)	33893.7	2949.533(17)	0.01	$5s^26d$ $^2D_{5/2}$ $5s5p(^3P^o)5d$ $^4P^o_{3/2}$	90351.894	124245.66			Wu	
220		2990.99(3)	33424.0	2990.9965(8)	−0.01	$5s5p^2$ $^2D_{3/2}$ $5s^27p$ $^2P^o_{3/2}$	58844.181	92268.106	9.1+5	C+	Wu	OH10
790		2994.46(3)	33385.3	2994.451(21)	0.01	$5s^26p$ $^2P^o_{3/2}$ $5s^28d$ $^2D_{5/2}$	72377.4484	105762.82	2.7+7	D+	Wu	TW
110		2997.1(3)	33355	2997.28(3)	−0.2	$5s^26p$ $^2P^o_{1/2}$ $5s^28d$ $^2D_{1/2}$	72377.4484	105731.3			MS	
260		3012.41(5)	33186.3	3012.519(9)	−0.11	$5s^26p$ $^2P^o_{1/2}$ $5s^29s$ $^2S_{1/2}$	71493.273	104678.41			Wu	
450		3023.92(3)	33060.1	3023.9444(14)	−0.03	$5s5p^2$ $^2D_{3/2}$ $5s^27p$ $^2P^o_{1/2}$	58844.181	91903.945	7.8+6	C+	Wu	OH10
680		3047.44(3)	32804.9	3047.4642(9)	−0.02	$5s5p^2$ $^2D_{5/2}$ $5s^27p$ $^2P^o_{3/2}$	59463.481	92268.106	6.8+6	B+	Wu	OH10
930		3094.68(11)	32304.1	3094.985(9)	−0.30	$5s^26p$ $^2P^o_{3/2}$ $5s^29s$ $^2S_{1/2}$	72377.4484	104678.41			MS	
480		3101.25(16)	32235.7	3101.40(4)	−0.15x	$5s5p^2$ $^2P_{3/2}$ $5s5p(^3P^o)6s$ $^2P^o_{1/2}$	81718.3	113952.44			Wu*	
15000		3283.1399(9)	30449.874	3283.1399(7)	0.0000	$5s5p^2$ $^2D_{3/2}$ $5s^24f$ $^2F^o_{5/2}$	58844.181	89294.055	1.70+8	B+	Brill	OH10
13000	:	3351.3	29830.6	3351.3021(8)		$5s5p^2$ $^2D_{5/2}$ $5s^24f$ $^2F^o_{5/2}$	59463.481	89294.055	1.21+7	B+	AM	OH10
13000		3351.9523(12)	29824.788	3351.9538(8)	−0.0015	$5s5p^2$ $^2D_{5/2}$ $5s^24f$ $^2F^o_{7/2}$	59463.481	89288.255	1.82+8	B+	Brill	OH10
87		3355.5(3)	29793	3354.96(4)	0.5	$5s^25d$ $^2D_{3/2}$ $5s^28p$ $^2P^o_{1/2}$	71406.142	101204.2			MS	
350		3407.41(12)	29339.4	3407.442(19)	−0.03	$5s^25d$ $^2D_{5/2}$ $5s^28p$ $^2P^o_{3/2}$	72048.260	101387.37			MS	
1700		3472.333(3)	28790.837	3472.3329(12)	0.000	$5s^26p$ $^2P^o_{1/2}$ $5s^27d$ $^2D_{3/2}$	71493.273	100284.111	4.5+7	D+	Brill	TW
660		3537.47(13)	28260.7	3537.5363(12)	−0.07	$5s^25d$ $^2D_{3/2}$ $5s^25f$ $^2F^o_{5/2}$	71406.142	99666.327	3.6+6	D	MS	AM
2100		3575.3255(12)	27961.499	3575.3255(12)	0.0000	$5s^26p$ $^2P^o_{3/2}$ $5s^27d$ $^2D_{5/2}$	72377.4484	100338.947	5.0+7	D+	Brill	TW

I_{obs}[a] arb. u.	Char.[b]	λ_{obs}[c] Å	σ_{obs} cm^{-1}	λ_{Ritz}[d] Å	$\delta\lambda_{O-Ritz}$[e] Å	Classification				E_{low} cm^{-1}	E_{upp} cm^{-1}	A[f] s^{-1}	Acc.[g]	Line Ref.[h]	TP Ref.[h]
440		3582.3511(14)	27906.663	3582.3511(13)	0.0000	$5s^2 6p$	$^2P^o_{1/2}$	$5s^2 7d$	$^2D_{3/2}$	72377.4484	100284.111	8.3+6	D+	Brill	TW
110		3612.68(22)	27672.4	3612.71(3)	−0.03	$5s^2 7s$	$^2S_{1/2}$	$5s5p(^3P^o)6s$	$^2P^o_{1/2}$	86280.318	113952.44			Wu*	
240		3619.96(13)	27616.7	3619.7860(12)	0.17	$5s^2 5d$	$^2D_{5/2}$	$5s^2 5f$	$^2F^o_{5/2}$	72048.260	99666.327	6.2+6	D	MS	AM
530		3620.4854(15)	27612.732	3620.4872(10)	−0.0018	$5s^2 5d$	$^2D_{5/2}$	$5s^2 5f$	$^2F^o_{7/2}$	72048.260	99660.978	2.0+6	E	Brill	M79
500		3715.1524(11)	26909.141	3715.1527(9)	−0.0003	$5s^2 6p$	$^2P^o_{1/2}$	$5s^2 8s$	$^2S_{1/2}$	71493.273	98402.412	1.6+7	D+	Brill	TW
440		3841.3756(14)	26024.959	3841.3749(9)	0.0007	$5s^2 6p$	$^2P^o_{3/2}$	$5s^2 8s$	$^2S_{1/2}$	72377.4484	98402.412	2.9+7	D+	Brill	TW
190	*	3984.6(4)	25089.8	3984.5(4)		$5s^2 4f$	$^2F^o_{7/2}$	$5s^2 11g$	$^2G_{9/2}$	89288.255	114378.1	2.4+6	D+	MS	TW
190	*	3984.6(4)	25089.8	3984.5(4)		$5s^2 4f$	$^2F^o_{7/2}$	$5s^2 11g$	$^2G_{7/2}$	89288.255	114378.1	8.+4	E	MS	TW
17		3994.3(4)	25028.7	3994.239(3)	0.0	$5s5p^2$	$^4P_{1/2}$	$5s^2 6p$	$^2P^o_{1/2}$	46464.290	71493.273			MS	
180	*	4110.3(4)	24322.6	4110.3(3)	0.0	$5s^2 4f$	$^2F^o_{7/2}$	$5s^2 10g$	$^2G_{9/2}$	89288.255	113610.5	3.4+6	D+	MS	TW
180	*	4110.3(4)	24322.6	4110.3(3)	0.0	$5s^2 4f$	$^2F^o_{7/2}$	$5s^2 10g$	$^2G_{7/2}$	89288.255	113610.5	1.2+5	E	MS	TW
180		4111.3(4)	24316.2	4111.3(3)	0.0	$5s^2 4f$	$^2F^o_{5/2}$	$5s^2 10g$	$^2G_{7/2}$	89294.055	113610.5	3.3+6	D+	MS	TW
28		4164.8(3)	24004.0	4164.76(4)	0.0	$5s^2 6d$	$^2D_{3/2}$	$5s5p(^3P^o)6s$	$^4P^o_{5/2}$	90241.554	114245.75			Wu	
31		4172.2(3)	23961.4	4172.18(3)	0.0	$5s^2 7d$	$^2D_{3/2}$	$5s5p(^3P^o)5d$	$^4P^o_{3/2}$	100284.111	124245.66			Wu	
36	bl(Sn IV)	4216.2(6)	23711	4216.28(4)	−0.1	$5s^2 6d$	$^2D_{3/2}$	$5s5p(^3P^o)6s$	$^2P^o_{1/2}$	90241.554	113952.44			Wu*	
170	*	4293.3(4)	23285.6	4293.27(14)	0.0	$5s^2 4f$	$^2F^o_{7/2}$	$5s^2 9g$	$^2G_{9/2}$	89288.255	112574.0	5.1+6	D+	MS	TW
170	*	4293.3(4)	23285.6	4293.27(14)	0.0	$5s^2 4f$	$^2F^o_{7/2}$	$5s^2 9g$	$^2G_{7/2}$	89288.255	112574.0	1.8+5	E	MS	TW
340		4294.33(15)	23280.0	4294.33(14)	−0.00	$5s^2 4f$	$^2F^o_{5/2}$	$5s^2 9g$	$^2G_{7/2}$	89294.055	112574.0	4.9+6	D+	MS	TW
6		4323.0925(13)	23125.086	4323.0922(13)	0.0003	$5s5p^2$	$^4P_{3/2}$	$5s^2 6p$	$^2P^o_{1/2}$	48368.185	71493.273	7.0+4	D+	Brill	OH10
120		4573.7(4)	21858.0	4574.32(23)	−0.6	$5s^2 4f$	$^2F^o_{7/2}$	$5s^2 10d$	$^2D_{5/2}$	89288.255	111143.3			Wu	
91		4575.0(4)	21851.8	4575.53(23)	−0.5	$5s^2 4f$	$^2F^o_{5/2}$	$5s^2 10d$	$^2D_{5/2}$	89294.055	111143.3			Wu	
	m			4579.9(3)		$5s^2 4f$	$^2F^o_{5/2}$	$5s^2 10d$	$^2D_{3/2}$	89294.055	111122.6			Wu	
150	*	4579.06(13)	21832.4	4579.03(9)	0.03	$5s^2 4f$	$^2F^o_{7/2}$	$5s^2 8g$	$^2G_{9/2}$	89288.255	111120.8	8.0+6	D+	MS	TW
150	*	4579.06(13)	21832.4	4579.03(9)	0.03	$5s^2 4f$	$^2F^o_{7/2}$	$5s^2 8g$	$^2G_{7/2}$	89288.255	111120.8	2.9+5	E	MS	TW
140		4580.22(13)	21826.9	4580.25(9)	−0.03	$5s^2 4f$	$^2F^o_{5/2}$	$5s^2 8g$	$^2G_{7/2}$	89294.055	111120.8	7.7+6	D+	MS	TW
90		4618.2359(10)	21647.226	4618.2363(10)	−0.0004	$5s5p^2$	$^4P_{5/2}$	$5s^2 6p$	$^2P^o_{3/2}$	50730.224	72377.4484	6.4+5	C+	Brill	OH10
48		4776.1(4)	20931.7	4775.98(10)	0.1	$5s5p^2$	$^2P_{1/2}$	$5s^2 8p$	$^2P^o_{3/2}$	80455.1	101387.37			Wu	
62	h	4792.0732(19)	20861.963	4792.0730(15)	0.0002	$5s^2 5d$	$^2D_{3/2}$	$5s^2 7p$	$^2P^o_{3/2}$	71406.142	92268.106	4.0+5	C+	Brill	OH10
100		4877.209(3)	20497.805	4877.209(3)	0.000	$5s^2 5d$	$^2D_{3/2}$	$5s^2 7p$	$^2P^o_{1/2}$	71406.142	91903.945	5.6+6	B+	Brill	OH10
66		4895.1(4)	20422.9	4894.50(5)	0.6	$5s^2 6d$	$^2D_{5/2}$	$5s5p(^3P^o)6s$	$^4P^o_{3/2}$	90351.894	110777.28			Wu	

I_{obs} [a] arb. u.	Char. [b]	λ_{obs} [c] Å	σ_{obs} cm^{-1}	λ_{Ritz} [d] Å	$\delta\lambda_{O-Ritz}$ [e] Å	Classification	E_{low} cm^{-1}	E_{upp} cm^{-1}	A [f] s^{-1}	Acc. [g]	Line Ref. [h]	TP Ref. [h]
83		4917.1(4)	20331.5	4917.8(3)	−0.7	$5s^2 7p\ {}^2P^o_{3/2}$ — $5s^2 11d\ {}^2D_{5/2}$	92268.106	112596.9	3.4+6	D+	Wu	TW
150		4944.2562(20)	20219.846	4944.2561(16)	0.0001	$5s^2 5d\ {}^2D_{5/2}$ — $5s^2 7p\ {}^2P^o_{3/2}$	72048.260	92268.106	4.9+6	B+	Brill	OH10
360	*	5071.09(15)	19714.1	5071.11(11)	−0.02	$5s^2 4f\ {}^2F^o_{7/2}$ — $5s^2 7g\ {}^2G_{9/2}$	89288.255	109002.3	1.4+7	D+	MS	TW
360	*	5071.09(15)	19714.1	5071.11(11)	−0.02	$5s^2 4f\ {}^2F^o_{7/2}$ — $5s^2 7g\ {}^2G_{7/2}$	89288.255	109002.3	5.+5	E	MS	TW
	m			5071.63(11)		$5s^2 4f\ {}^2F^o_{5/2}$ — $5s^2 9d\ {}^2D_{3/2}$	89294.055	109006.1			Wu	
360		5072.62(15)	19708.2	5072.60(11)	0.02	$5s^2 4f\ {}^2F^o_{5/2}$ — $5s^2 7g\ {}^2G_{7/2}$	89294.055	109002.3	1.3+7	D+	MS	TW
1600		5332.3391(16)	18748.281	5332.3391(11)	0.0000	$5s^2 6p\ {}^2P^o_{1/2}$ — $5s^2 6d\ {}^2D_{3/2}$	71493.273	90241.554	9.9+7	B+	Brill	OH10
2700		5561.9101(16)	17974.443	5561.9094(15)	0.0007	$5s^2 6p\ {}^2P^o_{3/2}$ — $5s^2 6d\ {}^2D_{5/2}$	72377.4484	90351.894	1.13+8	B+	Brill	OH10
2600		5588.8152(18)	17887.913	5588.8153(16)	−0.0001	$5s^2 5d\ {}^2D_{3/2}$ — $5s^2 4f\ {}^2F^o_{5/2}$	71406.142	89294.055	7.8+7	B+	Brill	OH10
530	h	5596.2644(15)	17864.103	5596.2636(12)	0.0008	$5s^2 6p\ {}^2P^o_{3/2}$ — $5s^2 6d\ {}^2D_{3/2}$	72377.4484	90241.554	1.91+7	B+	Brill	OH10
490		5796.9078(15)	17245.794	5796.9075(13)	0.0003	$5s^2 5d\ {}^2D_{5/2}$ — $5s^2 4f\ {}^2F^o_{5/2}$	72048.260	89294.055	5.1+6	B+	Brill	OH10
2700		5798.860(3)	17239.988	5798.8578(18)	0.002	$5s^2 5d\ {}^2D_{5/2}$ — $5s^2 4f\ {}^2F^o_{7/2}$	72048.260	89288.255	7.7+7	B+	Brill	OH10
470	H	5965.84(6)	16757.46	5965.78(5)	0.06	$5s^2 7p\ {}^2P^o_{3/2}$ — $5s^2 9d\ {}^2D_{5/2}$	92268.106	109025.72	7.6+6	D+	Brill	TW
1500	*	6077.6331(19)	16449.220	6077.6304(16)	0.0027	$5s^2 4f\ {}^2F^o_{7/2}$ — $5s^2 6g\ {}^2G_{9/2}$	89288.255	105737.482	2.7+7	D+	Brill	TW
1500	*	6077.6331(19)	16449.220	6077.6304(16)	0.0027	$5s^2 4f\ {}^2F^o_{7/2}$ — $5s^2 6g\ {}^2G_{7/2}$	89288.255	105737.482	1.0+6	D+	Brill	TW
1400		6079.7696(24)	16443.439	6079.7742(18)	−0.0046	$5s^2 4f\ {}^2F^o_{5/2}$ — $5s^2 6g\ {}^2G_{7/2}$	89294.055	105737.482	2.6+7	D+	Brill	TW
380		6242.1(7)	16015.8	6241.13(15)	1.0	$5s^2 6d\ {}^2D_{5/2}$ — $5s^2 9p\ {}^2P^o_{3/2}$	90351.894	106370.2			Wu	
760		6428.4(7)	15551.7	6429.08(10)	−0.7	$5s^2 8s\ {}^2S_{1/2}$ — $5s5p({}^3P^o)6s\ {}^2P^o_{1/2}$	98402.412	113952.44			Wu*	
2500		6453.5422(12)	15491.085	6453.5421(11)	0.0001	$5s^2 6s\ {}^2S_{1/2}$ — $5s^2 6p\ {}^2P^o_{3/2}$	56886.363	72377.4484	7.0+7	B+	Brill	OH10
830		6569.7(7)	15217.2	6568.51(11)	1.2	$5s^2 9d\ {}^2D_{5/2}$ — $5s5p({}^3P^o)5d\ {}^4P^o_{3/2}$	109025.72	124245.66			Wu	
1000		6661.1(8)	15008.4	6661.1(8)		$5s^2 6d\ {}^2D_{5/2}$ — $5s^2 6f\ {}^2F^o_{7/2}$	90351.894	105360.3	1.6+7	D+	Wu	TW
840		6760.812(3)	14787.041	6760.8103(22)	0.002	$5s^2 6p\ {}^2P^o_{1/2}$ — $5s^2 7s\ {}^2S_{1/2}$	71493.273	86280.318	3.82+7	B+	Brill	OH10
1300		6844.1859(20)	14606.911	6844.1864(15)	−0.0005	$5s^2 6s\ {}^2S_{1/2}$ — $5s^2 6p\ {}^2P^o_{1/2}$	56886.363	71493.273	6.0+7	B+	Brill	OH10
1100		7190.776(3)	13902.873	7190.7778(24)	−0.002	$5s^2 6p\ {}^2P^o_{3/2}$ — $5s^2 7s\ {}^2S_{1/2}$	72377.4484	86280.318	7.2+7	B+	Brill	OH10
670		7230.1(9)	13827.3	7230.05(16)	0.1	$5s^2 7p\ {}^2P^o_{1/2}$ — $5s^2 8d\ {}^2D_{1/2}$	91903.945	105731.3	1.2+7	D+	Wu	TW
500		7314.5(9)	13667.7	7314.17(12)	0.3	$5s^2 7d\ {}^2D_{3/2}$ — $5s5p({}^3P^o)6s\ {}^2P^o_{1/2}$	100284.111	113952.44			Wu*	
480		7387.1651(24)	13533.265	7387.1637(19)	0.0014	$5s5p^2\ {}^2D_{3/2}$ — $5s^2 6p\ {}^2P^o_{3/2}$	58844.181	72377.4484	2.27+6	B+	Brill	OH10
380		7408.22(21)	13494.8	7408.27(13)	−0.05	$5s^2 7p\ {}^2P^o_{3/2}$ — $5s^2 8d\ {}^2D_{5/2}$	92268.106	105762.82	1.3+7	D+	MS	TW
450		7729.6(10)	12933.7	7728.3(7)	1.3	$5s^2 5f\ {}^2F^o_{7/2}$ — $5s^2 11d\ {}^2D_{5/2}$	99660.978	112596.9			Wu	
500		7741.425(3)	12913.965	7741.423(3)	0.002	$5s5p^2\ {}^2D_{5/2}$ — $5s^2 6p\ {}^2P^o_{3/2}$	59463.481	72377.4484	1.89+7	B+	Brill	OH10

I_{obs} [a] arb. u.	Char.[b]	λ_{obs} [c] Å	σ_{obs} cm^{-1}	λ_{Ritz} [d] Å	$\delta\lambda_{O-Ritz}$ [e] Å	Classification	E_{low} cm^{-1}	E_{upp} cm^{-1}	A [f] s^{-1}	Acc.[g]	Line Ref.[h]	TP Ref.[h]
	m			7745.1(3)		$5s^25f\ ^2F°_{5/2}$ – $5s^211d\ ^2D_{3/2}$	99666.327	112574.1			Wu	
190		7825.97(9)	12774.45	7825.96(6)	0.01	$5s^27p\ ^2P°_{1/2}$ – $5s^29s\ ^2S_{1/2}$	91903.945	104678.41	4.7+6	D+	Brill	TW
280		7903.532(4)	12649.091	7903.532(3)	0.000	$5s5p^2\ ^2D_{3/2}$ – $5s^26p\ ^2P°_{1/2}$	58844.181	71493.273	1.96+7	B+	Brill	OH10
53		8055.72(9)	12410.13	8055.61(6)	0.11	$5s^27p\ ^2P°_{3/2}$ – $5s^29s\ ^2S_{1/2}$	92268.106	104678.41	8.6+6	D+	Brill	TW
2600	*	9058.880(4)	11035.863	9058.886(3)	−0.006	$5s^24f\ ^2F°_{7/2}$ – $5s^25g\ ^2G_{9/2}$	89288.255	100324.111	6.8+7	D+	Brill	TW
2600	*	9058.880(4)	11035.863	9058.886(3)	−0.006	$5s^24f\ ^2F°_{7/2}$ – $5s^25g\ ^2G_{7/2}$	89288.255	100324.111	2.4+6	D+	Brill	TW
2200		9063.658(5)	11030.045	9063.649(4)	0.009	$5s^24f\ ^2F°_{5/2}$ – $5s^25g\ ^2G_{7/2}$	89294.055	100324.111	6.5+7	D+	Brill	TW
1300		10607.434(6)	9424.768	10607.429(6)	0.005	$5s^26d\ ^2D_{3/2}$ – $5s^25f\ ^2F°_{5/2}$	90241.554	99666.327	4.9+7	D+	Brill	TW
1200		10739.257(6)	9309.081	10739.254(5)	0.003	$5s^26d\ ^2D_{5/2}$ – $5s^25f\ ^2F°_{7/2}$	90351.894	99660.978	5.1+7	D+	Brill	TW
	M1			23521.14(24)		$5s^25p\ ^2P°_{1/2}$ – $5s^25p\ ^2P°_{3/2}$	0.00	4251.494	6.94−1	A+		B95

[a] Observed relative intensities, in terms of total energy flux under the line profile, are reduced to a common arbitrary scale corresponding to a plasma in local thermodynamic equilibrium with an effective excitation temperature of 4.2 eV. These conditions correspond to exposure 1 of the experiment of Wu [11] (see section 3.3.4).

[b] Character of observed line: bl – blended by a close line (the blending spectrum is indicated in parentheses); h – hazy line; H – very hazy line; s – asymmetric line extending towards shorter wavelengths; * – intensity shared by two or more transitions; m – masked by a stronger neighboring line (no wavelength measured); : – the wavelength was not measured (the value in λ_{obs} is a rounded Ritz wavelength).

[c] Observed and Ritz wavelengths are given in standard air for wavenumbers σ between 5000 cm^{-1} and 50000 cm^{-1} and in vacuum outside of this range. The uncertainty (standard deviation) in the last digit is given in parentheses.

[d] Ritz wavelengths and their uncertainties were determined in the least-squares level optimization procedure (see section 3.3.3).

[e] Difference between observed and Ritz wavelength. If this column is blank, and λ_{obs} is not blank, this line alone determines one of the levels involved in the assigned transition. An "x" after the value indicates that this line was excluded from the level optimization.

[f] In the transition probability values, the number after the "+" or "−" symbol means the power of 10.

[g] Transition probability accuracy code is explained in table 3.3.

[h] References to observed wavelengths and transition probabilities: AM – Alonso-Medina and Colón 2000 [38]; B95 – Biémont et al. 1995 [39]; Brill – Brill 1964 [11]; M79 – Miller et al. 1979 [43]; MS – McCormick and Sawyer 1938 [6]; OH10 – Oliver and Hibbert 2010 [14]; Wu – Wu 1967 [11]; Wu* – line measured by Wu [11] with our new or revised classification; TW – this work.

Table 3.5. Optimized energy levels of Sn II

Configuration	Term	J	Energy[a] cm^{-1}		Unc.[b] cm^{-1}	Leading percentages[c]				E_{o-c}[d] cm^{-1}	No. of lin.[e]
$5s^25p$	$^2P^o$	1/2	0.00		0.05	97	2	$5p^3$	$^2P^o$	81	17
$5s^25p$	$^2P^o$	3/2	4251.494		0.014	97	2	$5p^3$	$^2P^o$	-81	25
$5s5p^2$	^4P	1/2	46464.290		0.018	98				-63	12
$5s5p^2$	^4P	3/2	48368.185		0.007	99				-20	17
$5s5p^2$	^4P	5/2	50730.224		0.005	97	3	$5s5p^2$	^2D	80	12
$5s^26s$	^2S	1/2	56886.363		0.003	100				0	7
$5s5p^2$	^2D	3/2	58844.181		0.004	41	58	$5s^25d$	^2D	-128	17
$5s5p^2$	^2D	5/2	59463.481		0.005	38	59	$5s^25d$	^2D	128	12
$5s^25d$	^2D	3/2	71406.142		0.008	41	54	$5s5p^2$	^2D	-120	11
$5s^26p$	$^2P^o$	1/2	71493.273		0.003	99				3	14
$5s^25d$	^2D	5/2	72048.260		0.007	40	56	$5s5p^2$	^2D	119	12
$5s^26p$	$^2P^o$	3/2	72377.4484			99				-3	16
$5s5p^2$	^2S	1/2	75954.3	R	0.4	51	46	$5s5p^2$	^2P	105	3
$5s5p^2$	^2P	1/2	80455.1	C	0.4	53	45	$5s5p^2$	^2S	-120	3
$5s5p^2$	^2P	3/2	81718.3		0.3	97	2	$5s5p^2$	^2D	18	3
$5s^27s$	^2S	1/2	86280.318		0.005	99				0	5
$5s^24f$	$^2F^o$	7/2	89288.255		0.007	96	3	$4f5p^2$	$^2F^o$	-1	10
$5s^24f$	$^2F^o$	5/2	89294.055		0.006	96	3	$4f5p^2$	$^2F^o$	1	11
$5s^26d$	^2D	3/2	90241.554		0.004	97	2	$5s5p^2$	^2D	-27	7
$5s^26d$	^2D	5/2	90351.894		0.005	97	2	$5s5p^2$	^2D	26	6
$5s^27p$	$^2P^o$	1/2	91903.945		0.015	99				-2	6
$5s^27p$	$^2P^o$	3/2	92268.106		0.009	99				2	10
$5s^28s$	^2S	1/2	98402.412		0.006	100				0	5
$5s^25f$	$^2F^o$	7/2	99660.978		0.006	99				-1	4
$5s^25f$	$^2F^o$	5/2	99666.327		0.006	99				1	4
$5s^27d$	^2D	3/2	100284.111		0.010	99				-11	6
$5s^25g$	^2G	7/2	100324.111	C	0.007	100				0	2
$5s^25g$	^2G	9/2	100324.111	C	0.007	100				0	1
$5s^27d$	^2D	5/2	100338.947		0.009	99				11	2

Configuration	Term	J	Energy[a] cm^{-1}		Unc.[b] cm^{-1}	Leading percentages[c]				E_{o-c}[d] cm^{-1}	No. of lin.[e]
$5s^2 8p$	$^2P^o$	1/2	101204.2		0.4	99				4	2
$5s^2 8p$	$^2P^o$	3/2	101387.37		0.16	99				1	5
$5s^2 9s$	^2S	1/2	104678.41		0.10	100				0	6
$5s^2 6f$	$^2F^o$	7/2	105360.3	?	1.8	99				9	1
$5s^2 6f$	$^2F^o$	5/2	105371.7	N?	0.3	99				17	2
$5s^2 8d$	^2D	3/2	105731.3		0.3	100				-6	5
$5s^2 6g$	^2G	7/2	105737.482		0.007	100				0	2
$5s^2 6g$	^2G	9/2	105737.482		0.007	100				0	1
$5s^2 8d$	^2D	5/2	105762.82		0.23	100				6	3
$5s^2 9p$	$^2P^o$	1/2	106256.4	N	0.3	99				-28	2
$5s^2 9p$	$^2P^o$	3/2	106370.2		0.4	99				-26	3
$5s^2 10s$	^2S	1/2	108357.6		0.4	100				0	4
$5s^2 7g$	^2G	7/2	109002.3		0.4	100				0	2
$5s^2 7g$	^2G	9/2	109002.3		0.4	100				0	1
$5s^2 9d$	^2D	3/2	109006.1		0.4	100				-4	3
$5s^2 9d$	^2D	5/2	109025.72		0.15	100				4	4
$5s^2 10p$	$^2P^o$	1/2	109222.6	R	0.3	81	16	$5s5p(^3P^o)6s$	$^4P^o$	61	3
$5s5p(^3P^o)6s$	$^4P^o$	1/2	109453.6		0.3	81	18	$5s^2 10p$	$^2P^o$	-13	2
$5s^2 11s$	^2S	1/2	110699		4	100				1	1
$5s5p(^3P^o)6s$	$^4P^o$	3/2	110777.28		0.21	79	12	$5s^2 11p$	$^2P^o$	-11	5
$5s^2 8g$	^2G	7/2	111120.8		0.4	100				0	2
$5s^2 8g$	^2G	9/2	111120.8		0.4	100				0	1
$5s^2 10d$	^2D	3/2	111122.6		1.2	100				-7	2
$5s^2 10d$	^2D	5/2	111143.3		1.1	100				5	4
$5s^2 9g$	^2G	7/2	112574.0		0.8	100				0	2
$5s^2 9g$	^2G	9/2	112574.0		0.8	100				0	1
$5s^2 11d$	^2D	3/2	112574.1	N	0.5	100				-8	2
$5s^2 11d$	^2D	5/2	112596.9		1.1	100				9	3
$5s^2 10g$	^2G	7/2	113610.5		1.5	100				0	2
$5s^2 10g$	^2G	9/2	113610.5		1.5	100				0	1

Configuration	Term	J	Energy[a] cm^{-1}		Unc.[b] cm^{-1}	Leading percentages[c]				E_{o-c}[d] cm^{-1}	No. of lin.[e]
$5s5p(^3P^o)5d$	$^2D^o$	5/2	113818.65	R	0.21	62	18	$5p^3$	$^2D^o$	44	4
$5s5p(^3P^o)6s$	$^2P^o$	1/2	113952.44	N	0.23	30	50	$5s^24p$	$^2P^o$	9	6
$5s5p(^3P^o)6s$	$^4P^o$	5/2	114245.75		0.20	95	2	$5s5p(^3P^o)5d$	$^2D^o$	9	6
$5s^211g$	^2G	7/2,9/2	114378.1		2.2	100				0	1
$5s5p(^3P^o)5d$	$^4F^o$	5/2	115256.2	N?	0.3	76	8	$5s5p(^3P^o)5d$	$^2D^o$	-31	1
$5s5p(^3P^o)5d$	$^4F^o$	7/2	116423.1	N	0.3	50	41	$5s^219f$	$^2F^o$	-49	3
Sn III $5s^2\,^1S_0$	Limit		**118023.7**	R	0.7						
$5s5p(^3P^o)5d$	$^4D^o$	1/2	119981.1	R?	0.6	93	4	$5s5p(^3P^o)5d$	$^4P^o$	-116	2
$5s5p(^3P^o)5d$	$^4D^o$	3/2	120064.3	R?	0.5	76	16	$5s5p(^3P^o)5d$	$^4P^o$	-73	2
$5s5p(^3P^o)5d$	$^4D^o$	5/2	120253.6	R	0.3	52	39	$5s5p(^3P^o)5d$	$^4P^o$	54	3
$5s5p(^3P^o)5d$	$^4D^o$	7/2	122491.5	R?	1.0	92	7	$5s5p(^3P^o)5d$	$^4F^o$	102	1
$5p^3$	$^4S^o$	3/2	123156.6	R	0.4	88	5	$5p^3$	$^2P^o$	-2	4
$5s5p(^3P^o)5d$	$^4P^o$	5/2	123688.2	N	0.5	55	41	$5s5p(^3P^o)5d$	$^4D^o$	60	2
$5s5p(^3P^o)5d$	$^4P^o$	3/2	124245.66	R	0.20	80	18	$5s5p(^3P^o)5d$	$^4D^o$	15	8
$5s5p(^3P^o)5d$	$^4P^o$	1/2	124524.6	N?	0.8	94	5	$5s5p(^3P^o)5d$	$^4D^o$	-13	1
$5s5p(^1P^o)5d$	$^2D^o$	3/2	132168.83	R	0.24	51	32	$5p^3$	$^2D^o$	-382	4
$5s5p(^1P^o)5d$	$^2D^o$	5/2	132707.7	R	0.3	54	32	$5p^3$	$^2D^o$	365	4

[a] Symbols next to the energy value have the following meaning: C – previous tentative identification has been confirmed here; N – new identification; R – previous value and/or interpretation has been revised here; ? – questionable identification.

[b] Uncertainties resulting from the level optimization procedure are given on the level of one standard deviation. They correspond to uncertainties of level separations from $5s^26p\ ^2P^o_{3/2}$. To determine uncertainties of excitation energies from the ground level, the given values should be combined in quadrature with the uncertainty of the ground level, 0.05 cm^{-1}.

[c] The first percentage value refers to the configuration and term given in the first two columns of the table. The second percentage value refers to the configuration and term given next to it. The percentage compositions were determined in this work by a parametric least-squares fitting with Cowan's codes [30] (see text).

[d] Differences between observed energies and those calculated in the parametric least squares fitting.

[e] Number of observed lines determining the level in the optimization procedure.

Table 3.6. LSF parameters (cm^{-1}) for Sn II

Configuration	Parameter	LSF	Group [a]	STD	HFR	LSF/HFR
Odd Parity [b]						
$5s^25p$	E_{av}	6860.3		116	0.0	
	$\zeta(5p)$	3016.3	1	83	2665.8	1.1315
$5s^26p$	E_{av}	72666.4		111	70522.8	1.0304
	$\zeta(6p)$	610.5	1	17	539.6	1.1314
$5s^27p$	E_{av}	92361.0		111	90536.8	1.0201
	$\zeta(7p)$	246.7	1	7	218.0	1.132
$5s^28p$	E_{av}	101458.0		111	99608.5	1.0186
	$\zeta(8p)$	127.0	1	3	112.2	1.132
$5s^29p$	E_{av}	106459.7	4	99	104563.0	1.0181
	$\zeta(9p)$	74.2	1	2	65.6	1.132
$5s^210p$	E_{av}	109339.8	4	101	107572.2	1.0164
	$\zeta(10p)$	47.2	1	1	41.7	1.132
$5s^211p$	E_{av}	111223.6	4	103	109540.5	1.0154
	$\zeta(11p)$	31.8	1	1	28.1	1.132
$5s^212p$	E_{av}	112521.2	4	104	110896.3	1.0147
	$\zeta(12p)$	22.5	1	1	19.9	1.131
$5s^213p$	E_{av}	113454.3	4	105	111871.2	1.0142
	$\zeta(13p)$	16.4	1	0	14.5	1.131
$5s^214p$	E_{av}	114151.8	4	106	112600.0	1.0138
	$\zeta(14p)$	12.4	1	0	11.0	1.13
$5s^215p$	E_{av}	114680.1	4	106	113152.0	1.0135
	$\zeta(15p)$	9.6	1	0	8.5	1.13
$5s^216p$	E_{av}	115095.4	4	107	113585.9	1.0133
	$\zeta(16p)$	7.6	1	0	6.7	1.13
$5s^217p$	E_{av}	115427.6	4	107	113933.0	1.0131
	$\zeta(17p)$	6.0	1	0	5.3	1.13
$5s^218p$	E_{av}	115694.7	4	107	114212.1	1.0130
	$\zeta(18p)$	4.9	1	0	4.3	1.14
$5s^219p$	E_{av}	115910.3	4	108	114437.3	1.0129
	$\zeta(19p)$	4.1	1	0	3.6	1.14
$5s^220p$	E_{av}	116095.8	4	108	114631.2	1.0128
	$\zeta(20p)$	3.4	1	0	3.0	1.13
$4f5s^2$	E_{av}	93783.8		114	87380.8	1.0733
	$\zeta(4f)$	0.4		fixed	0.4	1.0000
$5s^25f$	E_{av}	99981.2		112	97859.7	1.0217
	$\zeta(5f)$	0.2		fixed	0.2	1.0000

Configuration	Parameter	LSF	Group[a]	STD	HFR	LSF/HFR
$5s^2 6f$	E_{av}	105538.7	5	107	103503.1	1.0197
	$\zeta(6f)$	0.1		fixed	0.1	1.0000
$5s^2 7f$	E_{av}	108779.9	5	110	106886.6	1.0177
	$\zeta(7f)$	0.1		fixed	0.1	1.0000
$5s^2 8f$	E_{av}	110873.6	5	112	109072.3	1.0165
	$\zeta(8f)$	0.1		fixed	0.1	1.0000
$5s^2 9f$	E_{av}	112303.7	5	114	110565.2	1.0157
$5s^2 10f$	E_{av}	113325.1	5	115	111631.4	1.0152
$5s^2 11f$	E_{av}	114076.2	5	116	112415.5	1.0148
$5s^2 12f$	E_{av}	114646.3	5	116	113010.6	1.0145
$5s^2 13f$	E_{av}	115090.9	5	117	113474.8	1.0142
$5s^2 14f$	E_{av}	115440.1	5	117	113839.3	1.0141
$5s^2 15f$	E_{av}	115719.7	5	117	114131.2	1.0139
$5s^2 16f$	E_{av}	115953.9	5	118	114375.6	1.0138
$5s^2 17f$	E_{av}	116144.1	5	118	114574.2	1.0137
$5s^2 18f$	E_{av}	116301.7	5	118	114738.7	1.0136
$5s^2 19f$	E_{av}	116444.8	5	118	114888.1	1.0135
$5s^2 20f$	E_{av}	116564.1	5	118	115012.6	1.0135
5s5p6s	E_{av}	118905.2		211	109900.0	1.0819
	$\zeta(5p)$	3492.9	1	96	3087.0	1.1315
	$G^1(5s5p)$	29907.8	6	454	51164.2	0.5845
	$G^0(5s6s)$	1745.8	9	246	2522.8	0.6920
	$G^1(5p6s)$	2925.9	9	413	4228.1	0.6920
5s5p5d	E_{av}	128129.4		152	117237.6	1.0929
	$\zeta(5p)$	3415.7	1	94	3018.8	1.1315
	$\zeta(5d)$	77.2		fixed	77.2	1.0000
	$F^2(5p5d)$	20634.2		865	20388.4	1.0121
	$G^1(5s5p)$	29712.1	6	451	50829.4	0.5845
	$G^2(5s5d)$	10985.9		1189	9761.6	1.1254
	$G^1(5p5d)$	18655.8	7	663	20189.5	0.9240
	$G^3(5p5d)$	11538.5	7	410	12487.0	0.9240
$5p^3$	E_{av}	136589.5		179	127058.9	1.0750
	$F^2(5p5p)$	32281.3		fixed	37046.5	0.8714
	$\zeta(5p)$	3064.7	1	84	2708.6	1.1315
$5p5d^{2}$ [c]	E_{av}	262609.7		fixed	255939.8	1.0261 [c]
	$\zeta(5p)$	3732.4	1	103	3298.7	1.1315
$4f5p^{2}$ [c]	E_{av}	220238.9		fixed	213569.0	1.0312 [c]
	$\zeta(5p)$	3621.3	1	100	3200.5	1.1315

Configuration	Parameter	LSF	Group [a]	STD	HFR	LSF/HFR
4f5s5d [c]	E_{av}	223939.3		fixed	217269.4	1.0307 [c]
Even Parity						
$5s5p^2$	E_{av}	63956.0		36	55474.7	1.1529
	$F^2(5p5p)$	32090.9		286	36826.8	0.8714
	$\zeta(5p)$	3040.9		57	2681.9	1.1339
	$G^1(5s5p)$	30953.3		109	48632.5	0.6365
$5s^26s$	E_{av}	56981.0		77	55518.4	1.0263
$5s^27s$	E_{av}	86243.4		77	84679.3	1.0185
$5s^28s$	E_{av}	98398.8		77	96666.1	1.0179
$5s^29s$	E_{av}	104677.5		77	102872.0	1.0176
$5s^210s$	E_{av}	108357.2		77	106511.0	1.0173
$5s^211s$	E_{av}	110698.2	2	77	108830.1	1.0172
$5s^212s$	E_{av}	112202.1	2	78	110399.3	1.0163
$5s^25d$	E_{av}	64921.4		100	64114.7	1.0126
	$\zeta(5d)$	66.7		fixed	66.7	1.0000
$5s^26d$	E_{av}	89806.5		56	88201.0	1.0182
	$\zeta(6d)$	26.7		fixed	26.7	1.0000
$5s^27d$	E_{av}	100165.1		55	98423.5	1.0177
	$\zeta(7d)$	13.7		fixed	13.7	1.0000
$5s^28d$	E_{av}	105680.4		54	103874.8	1.0174
	$\zeta(8d)$	7.9		fixed	7.9	1.0000
$5s^29d$	E_{av}	108979.1		54	107136.5	1.0172
	$\zeta(9d)$	5.0		fixed	5.0	1.0000
$5s^210d$	E_{av}	111111.2		54	109247.0	1.0171
	$\zeta(10d)$	3.3		fixed	3.3	1.0000
$5s^211d$	E_{av}	112569.7	3	54	110689.9	1.0170
	$\zeta(11d)$	2.3		fixed	2.3	1.0000
$5s^212d$	E_{av}	113560.6	3	55	111722.9	1.0164
	$\zeta(12d)$	1.7		fixed	1.7	1.0000
$5s^25g$	E_{av}	100389.8		54	98428.2	1.0199
	$\zeta(5g)$	0.1		fixed	0.1	1.0000
$5s^26g$	E_{av}	105776.4		54	103823.2	1.0188
	$\zeta(6g)$	0.1		fixed	0.1	1.0000
$5s^27g$	E_{av}	109026.5		54	107087.6	1.0181
	$\zeta(7g)$	0.0		fixed	0.0	
$5s^28g$	E_{av}	111136.7		54	109207.1	1.0177
	$\zeta(8g)$	0.0		fixed	0.0	

Configuration	Parameter	LSF	Group [a]	STD	HFR	LSF/HFR
$5s^2 9g$	E_{av}	112585.0		54	110660.2	1.0174
	$\zeta(9g)$	0.0		fixed	0.0	
$5s^2 10g$	E_{av}	113618.4		54	111699.7	1.0172
	$\zeta(10g)$	0.0		fixed	0.0	
$5s^2 11g$	E_{av}	114383.9	4	54	112466.0	1.0171
	$\zeta(11g)$	0.0		fixed	0.0	
$5s^2 12g$	E_{av}	114944.3	4	55	113049.7	1.0168
	$\zeta(12g)$	0.0		fixed	0.0	
$4f5s5p$ [c]	E_{av}	148823.6		fixed	142153.7	1.0469 [c]
$5s5d^2$ [c]	E_{av}	196200.2		fixed	189530.3	1.0352 [c]
Configuration interaction [d]						
$5s5p^2$-$5s^25d$	R^1(5p5p,5s5d)	18161.1	1	124	27501.0	0.6604
$5s5p^2$-$5s^26d$	R^1(5p5p,5s6d)	9433.0	1	64	14284.3	0.6604
$5s5p^2$-$5s^27d$	R^1(5p5p,5s7d)	6265.9	1	43	9488.4	0.6604
$5s5p^2$-$5s^28d$	R^1(5p,5p,5s,8d)	4595.3	1	31	6958.6	0.6604
$5s5p^2$-$5s^29d$	R^1(5p5p,5s9d)	3570.9	1	24	5407.4	0.6604
$5s5p^2$-$5s^210d$	R^1(5p5p,5s10d)	2884.5	1	20	4368.0	0.6604
$5s5p^2$-$5s^211d$	R^1(5p5p,5s11d)	2396.1	1	16	3628.4	0.6604
$5s5p^2$-$5s^212d$	R^1(5p5p,5s12d)	2033.2	1	14	3078.9	0.6604

[a] Parameters in each numbered group were linked together with their ratio fixed at the Hartree-Fock level.

[b] All configuration-interaction parameters R^k for the odd configurations were fixed at 80 % of the Hartree-Fock value.

[c] These highly excited configurations are unknown experimentally. They were included in the calculations in order to account for their interaction with other configurations studied in this work. Except for the average energies E_{av} given here and $\zeta(5p)$ for $5p5d^2$ and $4f5p^2$, all other parameters of these configurations were fixed at the 80 % of the Hartree-Fock values (F^k, G^k, R^k) or 100 % of the Hartree-Fock values (ζ).

[d] Other R^k parameters of the even configurations were fixed at 80 % of the Hartree-Fock value.

CHAPTER 4

The spectrum of doubly ionized tin: Sn III

The third spectrum of tin (Sn III) is a Cd–like ion with ground configuration $4d^{10}5s^2$. The outer electron excitation gives the excited configurations of the type $4d^{10}5sn\ell$ and the two electron excitations leads to the $4d^{10}5p^2$, $4d^{10}5p$ (6s, 5d, 6p, and 4f) [1] configurations. The closed core excitations lead to $4d^95s^25p$ and $4d^95s^24f$ configurations. This is generally a two–electron system with singlet and triplet levels. The previous analysis was mainly made by Shenstone, which is included in Atomic Energy Levels (AEL) compilation [1], as well as also listed in ASD of the NIST [2]. This work had revised and extended the earlier works of Rao [3], Green and Loring [4] and Gibbs and Vieweg [5]. Shenstone added new configurations to include the 5s7d, 5sns (n = 8, 9) and a few levels of 5p5d. Moreover, Wu [6] has also included these configurations listed in AEL [1] and added a few additional configurations such as 5p6s, 5s5f, 5p6p, 5s7p and 5p4f. As far the spectral lines of Sn III are concerned, it was known since 1924, as thirty one prominent lines of Sn III were reported by Kirmura and his group [7–9] in 2200–5400Å range. Some lines of Sn III in vacuum ultraviolet (VUV) region were firstly exposed by Gibbs *et al* [10]. Other than this, the core excitation in Sn III was firstly reported by Dunne *et al* [11] using the dual–laser plasma (DLP) technique. Duffy *et al* [12] have identified a few transitions between 5s5p and $4d^95s5p^2$ using the same method. The radiative lifetimes of a few levels in Sn III have been experimentally measured by Andersen *et al* [13], followed by Kernahan *et al* [14] and Pinnington *et al* [15, 16] using beam–foil techniques. Besides these experimental works on Sn III, a number of papers have appeared on theoretical calculations [17–20]. The most extensive, covering almost all earlier works on oscillator strengths, transition probabilities and radiative lifetimes of the excited states, were published by Colón and Alonso–Medina [21].

[1] In the configuration naming the closed-core $4d^{10}$ is omitted when only n=5 electrons are excited.

In Cd I isoelectronic sequence the critical evaluation of In II was carried out by Kramida [22] and the analyses of two odd parity configurations, viz. 5p5d and 5p6s, in isoelectronic members Sb IV–I VI [23–25] have recently been reported from our laboratory and on Xe VII–Nd XIII [26–32] by others. Consequently, the missing information in the beginning of the sequence was highly desirable. Since we have a good understanding of these configurations, this project was undertaken to bridge the gap between Sn III and its higher isoelectronic members as well as to remove the ambiguities (some energy values/designations with question mark, unclear J values etc.) in the literature [1] and to extend the analysis with the help of spectrum of tin recorded by us and Wu's [6] line list.

4.1. Level structure of Sn III

Configuration[a]	Parent Term	Term[b]	J
$4d^{10}.5s^2$	(^{1}S)	^{1}S	0
$4d^{10}.5p^2$	(^{3}P)	^{3}P	0, 1, 2
	(^{1}D)	^{1}D	2
	(^{1}S)	^{1}S	0
$4d^{10}.5s.ns$	(^{2}S)	^{3}S	1
		^{1}S	0
$4d^{10}.5s.np$	(^{2}S)	^{3}P°	0, 1, 2
		^{1}P°	1
$4d^{10}.5s.nd$	(^{2}S)	^{3}D	1, 2, 3
		^{1}D	2
$4d^{10}.5s.nf$	n=4, (^{2}F°); n≥5, (^{2}S)	^{3}F°	2, 3, 4
		^{1}F°	3
$4d^{10}.5s.ng$	(^{2}S)	^{3}G	3, 4, 5
		^{1}G	4
$4d^{10}.5s.nh$	(^{2}S)	^{3}H°	4, 5, 6
		^{1}H°	5
$4d^{10}.5p.6s$	(^{2}P°)	^{3}P°	0, 1, 2
		^{1}P°	1
$4d^{10}.5p.5d$		^{3}F°	2, 3, 4
		^{3}D°	1, 2, 3
		^{3}P°	0, 1, 2
		^{1}F°	3
		^{1}D°	2
		^{1}P°	1
$4d^{10}.5p.6p$	(^{2}P°)	^{3}D	1, 2, 3
		^{3}P	0, 1, 2

Configuration[a]	Parent Term	Term[b]	J
		^3S	1
		^1D	2
		^1P	1
		^1S	0
$4d^9.5s^2.5p$	(^2D)	$^3F^\circ$	4, 3, 2
		$^3D^\circ$	3, 2, 1
		$^3P^\circ$	2, 1, 0
		$^1F^\circ$	3
		$^1D^\circ$	2
		$^1P^\circ$	1

[a] To the given configurations, the Kernel structure '[Kr]' must be added before each of it for the completeness of electronic structure. The principal quantum number, $n \geq 5$ for all ℓ except for f sub-shell ($n \geq 4$).

[b] The strict ordering of levels are governed by Hund's rule for the fine structures.

4.2. Results and discussion

The energy level structure of Sn III is shown in Figure 4.1. The list of classified lines for this spectrum is given in table 4.1. The observed energy levels and their LS compositions obtained with least squared fitting (LSF) procedure are assembled in table 4.2 and the least squares fitted parameters are listed in table 4.3.

4.2.1. Theoretical calculations

The energy structure, associated wavelengths and transition rates of Sn III were predicted using Cowan's code [33] with the scaled Slater parameters. For *ab initio* calculations, the parameters scaling were 100% of HF values for E_{av} and ζ_{nl}, 85% for F^k, 80% for G^k and R^k integrals. An extensive calculation includes $5s^2$, $5p^2$, 5sns (n = 6–18), 5snd (n = 5–18), 5sng (n = 5–12), 5p6p, 5p4f, $4f^2$, $5d^2$, $6s^2$, $6p^2$ and $4d^95s5p^2$ configurations in even parity system and 5snp (n = 5–15), 5snf (n = 4–15), 5snh (n = 6–10), 5pnd(n=5, 6), 5pns(n=6, 7), 4f5d, $4d^95s^2np$ (n=5, 6) and $4d^95s^24f$ configurations for the odd parity matrix. In the least squared parametric fitting, the standard deviation obtained for 53 known levels of even configuration set was 75cm^{-1}, however the odd parity systems (62 levels) were converged to 200 cm^{-1}. The fitted parameters were utilized to modify initial wavefunctions and hence to recalculate the transition rates that are given in table 4.1.

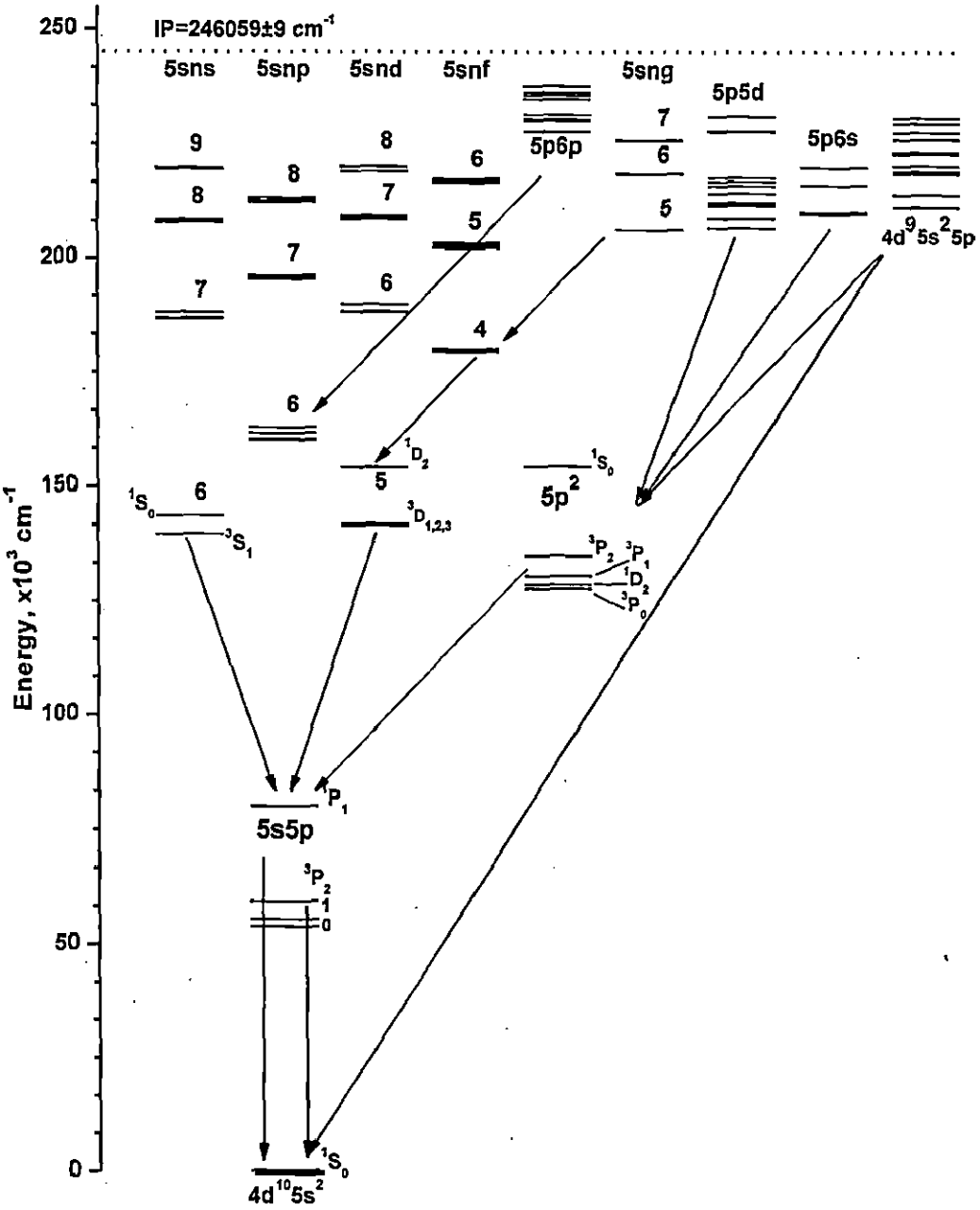

Figure 4.1. Energy level structure of Sn III

4.2.2. Analysis of the spectrum

The lines of Sn III are showing clear ionization separation on our plates as their intensities are gradually increased from track 1–4 , so it was easier to select the lines belonging to Sn III which indeed was very helpful in the investigation of earlier reported levels as well as in finding the additional transitions below 2080Å wavelength region. The following subsections describe various transition arrays studied in this spectrum.

4.2.2.1. The $5s^2$ – 5snp transitions array

The outermost electronic excitation from the ground $5s^2$; $^1S_0$ is possible through the 5snp configuration with $^3P^o_{0,\ 1,\ 2}$ and $^1P^o_1$ fine structures. Both J=1 transitions of 5snp (n=5, 6) to the ground level ($^1S_0$) were already reported by Green and Loring [4] and later improved by Shenstone and that are compiled in AEL [1]. We also have observed these transitions with better accuracies and therefore confirmed these levels However, the other two J=1 transitions from 5s7p configuration to the ground level were reported by Wu [6], could not be confirmed in the present work. We observe two lines at 511.836Å and 510.066Å, for $^3P^o_1$ and $^1P^o_1$ transitions, respectively on our plate. These lines were also present in Wu's [6] line list with proper intensity and character as predicted by Cowan's code [33]. The detailed analysis of the 5snp (n=8–10) configurations will be described in section 4.2.2.3, as these configurations are having significant interactions with the levels of 5p (5d+ 6s) and $4d^95s^25p$ configurations.

4.2.2.2. The 5s5p – [5s (ns+nd) + $5p^2$] transitions array

The 5p electron excitation to 5sns and 5snd series, are the strongest transitions from the lowest excited configuration 5s5p. We have confirmed the earlier reported [1] level values of $^3S_1$ of 5sns (n=6–9) configurations with improved wavelengths. However, we could confirm only the $^1S_0$ level of 5s6s configuration. We rejected the reported level value 187399.5 cm^{-1} of 5s7s $^1S_0$ listed in AEL [1] because of the several reasons:-firstly, it deviates from the parametric fit despite of its 99% LS purity, secondly we did not find its strongest transition to $^1P^o_1$ of 5s6p configuration. We established this level at 187994.8 cm^{-1} based on two transitions 925.217Å and 3956.0Å from $^1P^o_1$ levels of 5s5p and 5s6p configurations respectively. Further, we also established the $^1S_0$ level of 5s8s configuration with four observed transitions as

predicted. The 5s9s $^1S_0$ was also found at 219821.6 cm^{-1} with the observed transitions from 5snp (n=6–7) satisfactorily.

The other series of excited configurations is 5snd with ^3D and ^1D structure. We have confirmed all reported levels of 5snd (n=5–7) as repotted in AEL [1] with improved accuracies. In addition, we found all the levels of 5s8d configuration from Wu's [6] line list except $^3D_1$. A few more transitions were also observed between 5snd (n=5–8) and 5snp (n=6–7) configurations from Wu's [6] line list.

The $5p^2$ configuration is formed from 5s5p configuration by excitation of 5s electron to partially filled sub–shell of 5p. All the levels of $5p^2$ configuration are already reported in AEL [1] except $^1S_0$. We confirmed these levels in the present analysis and have established the missing $^1S_0$ level at 154203.39 cm^{-1} with the help of both transitions 1010.031Å and 1346.045Å lines from J=1 levels of 5s5p configuration as predicted. It is worth mentioning here that $^1D_2$ level (at 128205.82 cm^{-1}) of $5p^2$ configuration is highly interacting with the $^1D_2$ levels of 5s5d configuration. This interaction was seen very probable all along the sequence up to Xe VII [22–25]. We also noticed in our LSF, a slight perturbation of 5s6d $^1D_2$ by $5p^2$ $^1D_2$ (see table 4.2).

4.2.2.3. The levels of 5s[nf + np (n=8-10)], 5p (5d+6s) and $4d^9 5s^2 5p$ configurations

The levels of 4f5s configuration are established from 5s5d levels, and they were already reported in AEL [1]. We confirmed these previous assignments. However, it is important to note here that due to the configuration interaction between the levels of 5s5d and $5p^2$ configurations (see section 4.2.2.2. and table 4.2), some extra–transitions from the levels (namely, $^{3,\ 1}F_3$) of 4f5s are also observed to J=2 levels of $5p^2$ configuration (see table 4.1). Both Gibbs [5] and Wu [6] had shown some transitions and corresponding term values or energy levels of 5s5f configuration, however neither their energy values nor the reported transitions are satisfactory, as the predicted transitions are missing in linelist of Wu[6] and the given transitions are not showing the signature of Sn III lines. We established all four levels of 5s5f configuration based on the observed transitions from levels of both 5s5d and $5p^2$ configurations in the 330–2066Å range. Their further confirmation was more manifested when these levels gave transitions from the levels of 5s6d configuration (see table 4.1). The fine structure separations of the levels of 5s5f configuration are perturbed due to the presence of 5p5d configurations (see table 4.2).

We further extended the analysis to include 5p5d, 5p6s, 5snp (n=8–10) and 5snf (n=6–10) and $4d^9 5s^2 5p$ configurations. It must be pointed out that only six levels belonging to 5p5d were reported in AEL [1], although some of them without level designation. However, Wu's [6] analysis contains all the levels of 5p5d configurations. Both the above findings are limiting with theoretical predictions. From figure 4.2, it is evident that all above-mentioned configurations are significantly interacting with each other. Therefore, we incorporated all these interaction configurations in our extended calculations for reliable predictions. For example, for odd parity system, the 5p (5d, 6d, 6s, 7s), 5snp (n=8-18), 5snf (n=5-17) and $4d^9 5s^2 5p$ configurations were considered together. We confirmed four level values from AEL [1], namely 1° as 5p5d $^1D^\circ_2$, 4° as 5p6s $^3P^\circ_2$ and $^3P^\circ_1$ and $^3P^\circ_2$ with the same designation. Two doubtful levels (213840.7 and 215613.0 cm^{-1}) could not be confirmed and hence, rejected them. From Wu's [6] given energy values for the levels of 5p5d configuration, only three new energy level values are matching with our findings other than values given for $^3P^\circ_1$ and $^3P^\circ_2$ of 5p5d, and $^3P^\circ_2$ of 5p6s configurations. It should be mentioned that Wu's [6] observed configuration average energy (E_{av}^{obs}) for the 5p6s configuration is ~11000 cm^{-1} lower than our calculations, however this seems to be contradictory with the observations in other members of the sequence [21–32] where they were showing opposite effect (see E_{av}(LSF)-E_{av}(HFR) from table 4.3). All the levels of 5p (5d+6s) configurations have now been established.

We have observed all levels of 5s (8p+6f) configurations based on the lines on our plate from levels of $5p^2$ and 5s5d configurations. The excitation temperature of Wu's electrodeless discharge source was larger than the same for our triggered spark source (see section 4.2.4), the transitions from the ground level ($^1S_0$) should also be expected. We found two lines at 469.096Å and 471.115Å from Wu's [6] list for both J=1 levels of 5s8p configuration. However, due to the adverse configuration interaction among the odd configurations, their level assignment is a bit complicated (see table 4.2). Since Wu's [6] source favors higher excitation conditions, hence three levels (except J=0) of 5s9p have now been established. The $^1P^\circ_1$ of 5s10p is established at 228590.6 cm^{-1} with help of two strong predicted transitions (see table 4.1) from singlet levels of both $5p^2$ and 5s5d configurations; this was vindicated when this level is having 16% ^1P component of 5p5d configuration (cf. table 4.2). Apart from this, all levels of 5s6f configurations are established, the $^1F^\circ_3$ level is observed at 216519.87cm^{-1} with five strong observed transitions (cf. table 4.1, however, Wu [6]

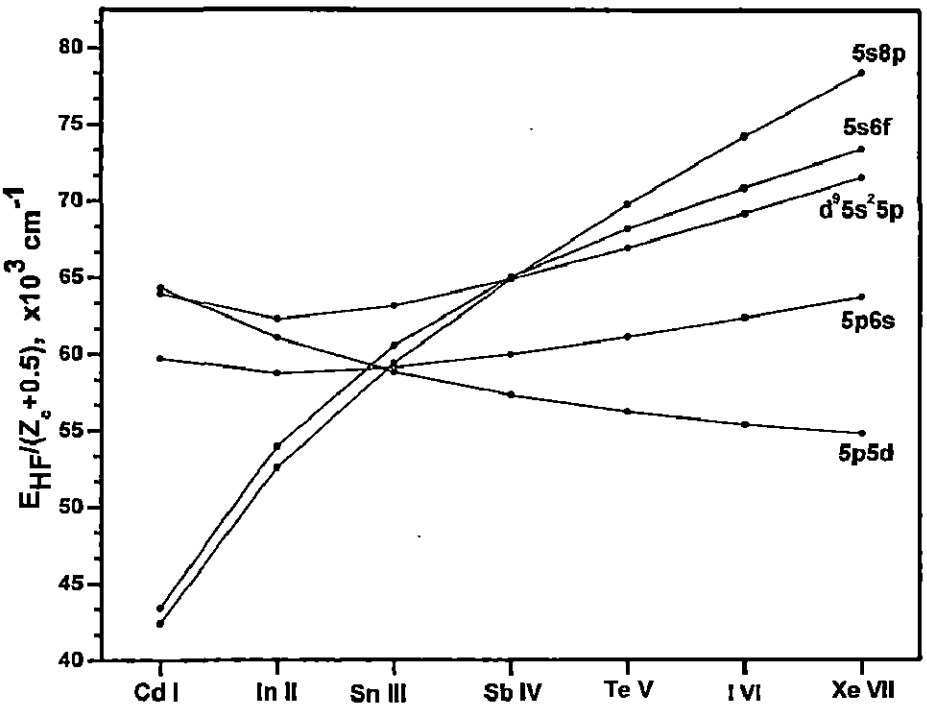

Figure 4.2. The reduced average energy $E_{HF}/(Z_c + 0.5)$ vs Z_c, where E_{HF} is the HF average energy and Z_c is the net charge of the core, in the Cd–I isoelectronic sequence.

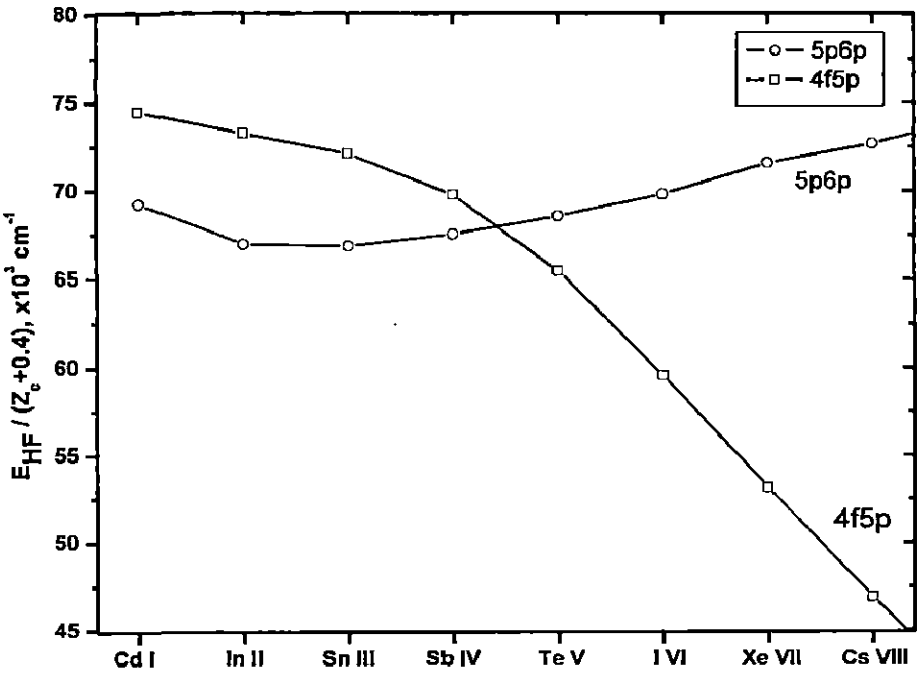

Figure 4.3. Isoelectronic plot for the 5p (4f+6p) configurations in Cd–I sequence, where E_{HF} is the HF average energy of the configuration.

also had assigned this level as 5p5d $^3D°_3$. We observed the 5p5d $^3D°_3$ at 215779.28 cm^{-1} with five supporting transitions, and hence the new assignments are validated. The only $^1F°_3$ level of 5snf (n=7-10) series have been established from the 5s5d $^1D_2$ level in accordance with the Cowan's code calculations.

The 4d electron excitation was facilitated to form the $4d^95s^25p$ configuration with 12 levels, and this was firstly reported by Dunne *et al* [11] through the photoabsorption spectra taken with dual-plasma laser (DPL) technique. They had observed all three J=1 (viz., $^3P°$, $^1P°$ & $^3D°$) transitions from the ground level of Sn III at 26.72, 27.58 and 28.03 eV with 0.04 eV uncertainty. There are enough reasons to less rely on the observation of Dunne *et al* [11] as their calculations do not include all those interacting configurations and as well the accuracy of their measurement significant upto four figures in electron volts (eV). In light of our extended calculations, levels of $4d^95s^25p$ are giving a number of transitions to the levels of $5p^2$ and 5s5d configurations. We have established all levels, except $^3F°_4$ and $^1S°_0$, of $4d^95s^25p$ configuration based on transitions observed from ours and Wu's [6] list.

4.2.2.4. Interpretation of 5sng (n=5-7) and 5p6p configurations

The AEL [1] also contains 5s5g levels as $^3G_{3,\,4}$ at 206110.3 cm^{-1}, $^1G_4$ at 206125.7 cm^{-1} and 206133.3 cm^{-1} for $^3G_5$. Since these transitions are λ>2000Å, therefore, Wu's [6] linelist is the only available data source to confirm these lines. It has been noticed that unlike to other member of Cd I isoelectronic sequence $^1G_4$ and $^3G_5$ of 5s5g in Sn III showing unusual energy splitting (7.6 cm^{-1}). This strongly indicates an erroneous assignment of transition for $^3G_5$ from 4f5s $^3F°_4$. This fact is substantiated from the assignment of Wu [6] as the line at 3745.33Å was attributed to this particular transition, however this line should belong to a very strong 5s6p $^3P°_2$ to 5s6d $^3D_3$ transition. We found that transitions for both J=4 and 5 are unresolved (at 3746.5Å) and hereafter the level value of $^3G_5$ would be 206125.5 cm^{-1}. The levels of 5s6g and 5s7g are also established on the basis of transitions from the levels of both 4f5s and 5s5f configurations (see table 4.1). This also confirms the identifications of 5s5f levels.

The lowest two electron excited configuration among the even parity configuration of Sn III is 5p6p with 10 levels. It is evident from figure 4.3 that this configuration is unique in Sn III such that its position is below the first series limit.

The other such configuration is 4f5p, whose most of the levels (>70%) are above the ionization limit in Sn III, but their E_{av} collapses down quickly as Z_c increases in the sequence. For this reason 5p6p configuration remain less investigated in the lower member of the isoelectronic sequence however, 5p4f configuration was studied from Xe VII-Nd XIII [26-31] in the sequence. With the help of the extended calculations, we established 8 levels of 5p6p configuration (except ^{1}D and ^{1}S) from the levels of 5s6p. A few levels of high-lying 5snd (n=11, 12) were also found due to the strong interactions of 5snd (n=10-15) series with 5p6p configuration. It should be mentioned that Wu [6] had also established the levels of both 5p (4f + 6p) configurations, however, none of them matching/fitting with our new calculations, hence they are rejected.

4.2.3. Optimization of energy levels

The levels of Sn III are optimized with least-squares level optimization code LOPT [34].

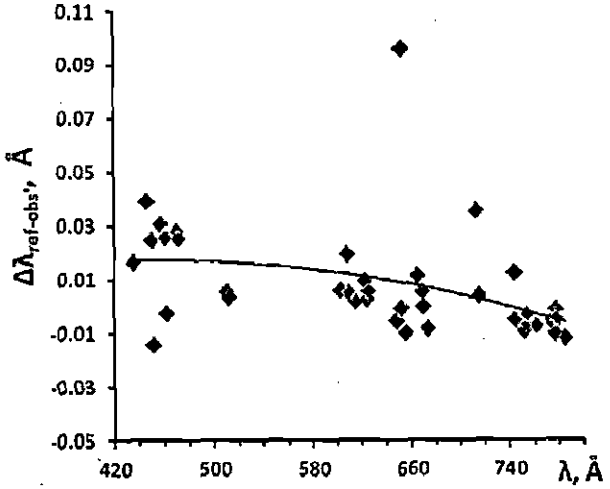

Figure 4.4. Difference between reference and observed wavelength. The solid line is polynomial fit determining the systematic corrections to the original measurements of Wu [6].

However, before the optimization, the corrections and afterward the accuracy assessment for Wu's [6] linelist λ<890Å was necessitated, since above this wavelength the corrections were already made with Sn I and Sn II internal standards (see chapter 3, section 3.2). We applied the similar procedure, as of Sn II, for the correction of lines below 890Å; on the basis of lines measured by us (TW= This Work) and Wu's [6] corrected wavelengths (between 890-8300Å) the Ritz

wavelengths are produced and used as references for correcting Wu's [6] wavelengths (λ<890Å). The correction curve is shown in figure 4.4.

About sixteen lines of Sn III are observed in second order wavelength of grating spectrum by us (marked as '2x' in table 4.1) and those are most accurate lines (0.004Å) in this analysis. A total 115 levels are observed for this spectrum and are listed in table 4.2. In this table, the uncertainty of observed energy values for each level is estimated with respect to separations from $5p^2\ ^1D_2$ level, since this level was connected by most number of accurate transitions observed for this spectrum. To determine the absolute error in excitation energy with respect to the ground, the given value should be added in quadrature with uncertainty of the ground 0.4 cm^{-1}.

There are 19 levels connecting with only one transition each; however, such levels have been established at final stage of the analysis when LSF parameters were optimized in accordance of other levels (more than one line). Among them, five transitions, all from $^1F^o_3$ level of 5snf (n=8-10), 5p5d and $4d^95s^25p$ configurations strongly connected to 5s5d $^1D_2$. The three are for $^3D_3$ of strong transition array 5s6p $^3P^o_2 \rightarrow$ {5p6p+5snd (n= 11, 12)} and another three for 5sng (n=6, 7).

4.2.4. Intensities of observed lines

This spectrum is significantly relied on Wu's [6] observed lines other than measurements by us in VUV region. Thus, bringing the intensity of lines observed by many others to a common uniform scale was essential. A method, Boltzmann LTE approach for thin plasma states, which described in chapter 2 and 3 applied for this purpose.

We have calculated the temperatures of Wu's all exposures for Sn III ions. The source first exposure shows the largest excitation temperature of ED lamp, and found to be 9.1 eV. The derived wavelength correction functions from Sn II intensity scaling were applied for the final determination of source temperature. However, the correction lower to 900Å was necessitated for both Wu's and our spectrographs. The obtained correction curves for < 800 Å is given in figure 4.5 (b, d) and they are in agreement with the response of the grating to the lower region in normal incidence geometry. As of the Sn II, the Wu's excitation temperatures for Sn III ions in exposures 2–4 are found to be 7.7, 8.4 and 8.8 eV. The triggered spark source of us shows the effective temperature at 3.8 eV for populating the levels of Sn III ions.

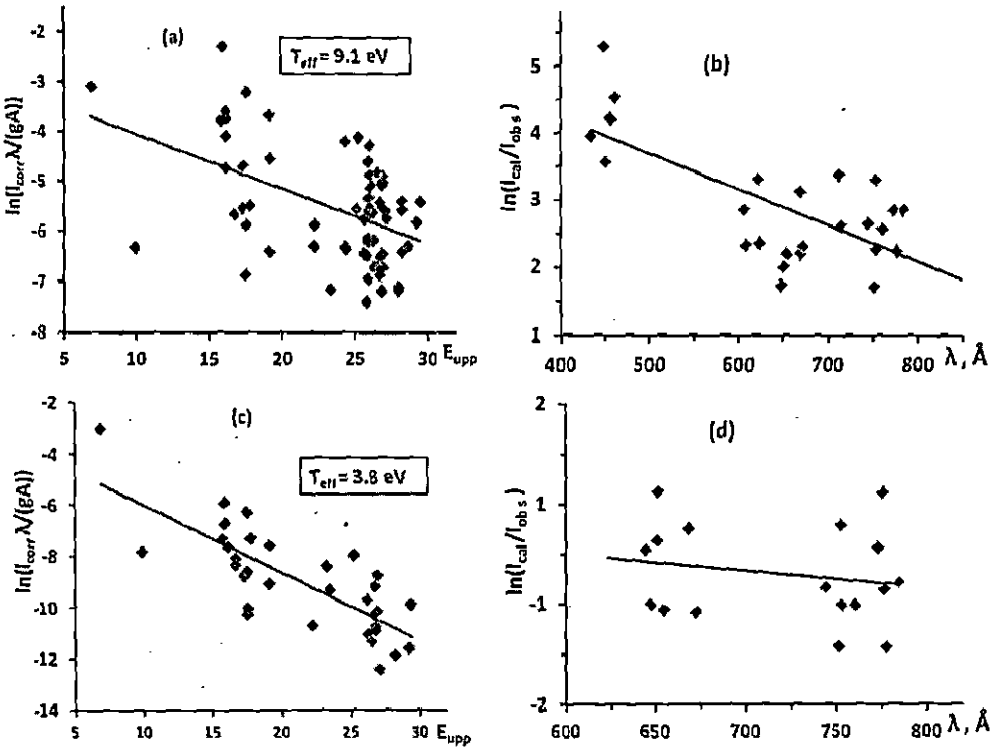

Figure 4.5. Boltzmann plots (a, c) and logarithmic intensity correction functions (b, d) for Wu [11] and those of triggered spark source. The upper level energies E_{upp} in the Boltzmann plots are given in eV. The effective temperatures derived from the negative slope of the Boltzmann plots are shown in boxes. The calculated intensities I_{calc} in panels b and d are obtained from weighted transition rates gA calculated in the present work with a formula $I_{calc} = (gA/\lambda)\exp(-E_{upp}/T_{eff})$.

The line intensities of Sn III ions were scaled to the highest excitation conditions obtained at Wu's exposure 1. The determined intensity of each line is given table 4.1.

4.2.5. Ionization potential

As low ℓ and n are concerned, 5sns $^3S_1$ (n=6–9) is known, hence Ritz series calculation can be applied to determine the ionization potential. Due to the perturbation 5s6s $^3S_1$, the limits obtained is differed by 33.5 cm^{-1} when the same is obtained from 5sns $^3S_1$ (n=7–9). However, the 5sng (n=5-7) are known now, hence the limit is calculated with both Ritz and polarization method by using computer code RITZPL and POLAR of Sansonetti [35]. We adopt an averaged value obtained from four different calculations of 5sns $^3S_1$ (n=7–9), $^3G_3$ and $^3G_5$ 5sng (n=5-7) and 5sng (n=5-7) to be the limit of Sn III at 246059 cm^{-1} within a standard deviation of 9 cm^{-1} (30.5074±0.0011 eV).

References:

[1] Moore C E 1958 *Atomic Energy Levels, National Bureau of Standards Circular* 467 vol III (Washington, DC: US Govt Printing Office)
[2] Kramida A, Ralchenko Yu., Reader J and NIST ASD Team 2012 *NIST Atomic Spectra Database, v.5.0*, National Institute of Standards and Technology, Gaithersburg, MD, USA. Available from: http://physics.nist.gov/ASD
[3] Rao K R 1926 *Proc. Phys. Soc.* **39** 161
[4] Green J B and Loring R A 1927 *Phys. Rev.* **30** 574
[5] Gibbs R C and Vieweg A M 1929 *Phys. Rev.* **34** 400
[6] Wu C M 1967 *The Atomic Spark Spectra of Tin, Sn III, Sn IV, Sn V* Master thesis University of British Columbia, Canada
[7] Kimura M and Nakamura 1924 *Jap. J. Phys.* **3** 29
[8] Kimura M and Nakamura 1924 *Jap. J. Phys.* **3** 197
[9] Kimura M 1924 *Jap. J. Phys.* **3** 217
[10] Gibbs R C, Vieweg A M and Gartlein C W 1929 Phys. Rev. **34** 406
[11] Dunne P, O'Reilly F, O'Sullivan G and Murphy N 1999 *J. Phys. B: At. Mol. Opt. Phys.* **32** L597
[12] Duffy G, van Kampen P and Dunne P 2001 *J. Phys. B: At. Mol. Opt. Phys.* **34** 3171
[13] Andersen T, Kirkegård Nielsen A and Sørensen G 1972 *Phys. Scr.* **6** 122
[14] Kernahan J A, Pinnington E H, Ansbacher W and Bahr J L 1985 *Nucl. Instrum. Methods Phys. Res. B* **9** 616
[15] Pinnington E H, Ansbacher W, Kernahan J A and Inamdar A S 1985 *J. Opt. Soc. Am. B* **2** 331
[16] Pinnington E H, Kernahan J A and Ansbacher W 1987 *Can. J. Phys.* **65** 7
[17] Migdalek J and BaylisWE 1986 *J. Phys. B: At. Mol. Phys.* **19** 1
[18] Migdalek J and Bojara A 1988 *J. Phys. B: At. Mol. Opt. Phys.* **21** 2221
[19] Chou H-S and Huang K-N 1992 *Phys. Rev. A* **46** 3725
[20] Bi'emont E, Froese Fischer C, Godefroid M R, Palmeri P and Quinet P 2000 *Phys. Rev. A* **62** 032512
[21] Colo´ n C and Alonso-Medina A 2010 *J. Phys. B: At. Mol. Opt. Phys.* **43** 165001
[22] Kramida A 2013 *J. Res. Natl. Inst. Stand. Technol.* **118** 52
[23] Tazeen R, Tauheed A and Joshi Y N 2001 *Phys. Scr.* **63** 108
[24] Tauheed A, Joshi Y N and Zafaran A F 2000 *Phys. Scr.* **62** 316
[25] Tauheed A, Joshi Y N and Pinnington E H 1997 *Phys. Scr.* **56** 289
[26] Churilov S S and Joshi Y N 2002 *Phys. Scr.* **65** 35
[27] Gayasov R and Joshi Y N 1999 *J. Opt. Soc. Am. B* **16** 1280
[28] Churilov S S and Joshi Y N 2000 *Phys. Scr.* **62** 282
[29] Ryabtsev A N, Churilov S S and Joshi Y N 2002 *Phys. Scr.* **65** 227
[30] Joshi Y N, Ryabtsev A N and Churilov S S 2001 *J. Opt. Soc. Am. B* **18** 1935
[31] Churilov S S and Joshi Y N 2003 *Phys. Scr.* **68** 128
[32] Churilov S S, Joshi Y N and Ryabtsev A N 2005 *Phys. Scr.* **71** 43
[33] Cowan R D 1981 *The Theory of Atomic Structure and Spectra* (Berkeley, CA: University of California Press) and Cowan code package for Windows by A. Kramida, available from http://das101.isan.troitsk.ru/COWAN
[34] Kramida A E 2011 *Comput. Phys. Commun.* **182** 419
[35] Sansonetti C J 2005 *Computer programs RITZPL and POLAR*, private communication

lines in Sn III spectrum.

λ_{obs} [c] Å	σ_{obs} cm^{-1}	λ_{Ritz} [d] Å	$\Delta\lambda_{O-Ritz}$ [e] Å	Classification		E_{low} cm^{-1}	E_{upp} cm^{-1}	gA [f] S^{-1}	Lin. Ref [h]
435.056(19)	229855	435.0563(14)	0.000	$5s^2\,{}^1S_0$	$4d^95s^25p\ {}^3D^*_1$	0.0	229855.3	1.8+9	Wu*
445.621(19)	224406	445.6437(17)	-0.023	$5s^2\,{}^1S_0$	$4d^95s^25p\ {}^1P^*_1$	0.0	224394.5	2.6+10	Wu*
449.481(19)	222479	449.489(3)	-0.008	$5s^2\,{}^1S_0$	$5s9p\ {}^1P^*_1$	0.0	222475.0	3.8+9	Wu*
450.730(19)	221862	450.699(3)	0.031	$5s^2\,{}^1S_0$	$5s9p\ {}^3P^*_1$	0.0	221877.4	5.9+8	Wu*
456.373(19)	219119	456.3866(10)	-0.014	$5s^2\,{}^1S_0$	$4d^95s^25p\ {}^3P^*_1$	0.0	219112.5	1.6+9	Wu*
460.559(19)	217127	460.5682(10)	-0.009	$5s^2\,{}^1S_0$	$5p6s\ {}^1P^*_1$	0.0	217123.1	1.1+9	Wu*
461.373(19)	216744	461.3538(10)	0.019	$5s^2\,{}^1S_0$	$5p5d\ {}^3P^*_1$	0.0	216753.37	1.3+9	Wu*
469.096(19)	213176	469.1071(11)	-0.011	$5s^2\,{}^1S_0$	$5s8p\ {}^1P^*_1$	0.0	213170.94	1.7+8 [CF]	Wu*
471.115(19)	212262	471.1237(10)	-0.009	$5s^2\,{}^1S_0$	$5s8p\ {}^3P^*_1$	0.0	212258.5	1.4+7 [CF]	Wu*
510.066(6)	196053.1	510.0630(12)	0.003	$5s^2\,{}^1S_0$	$5s7p\ {}^1P^*_1$	0.0	196054.2	1.5+8 [CF]	TW
511.836(6)	195375.1	511.8354(13)	0.001	$5s^2\,{}^1S_0$	$5s7p\ {}^3P^*_1$	0.0	195375.3	4.8+7 [CF]	TW
602.555(19)	165960	602.5479(20)	0.007	$5s5p\ {}^3P^*_0$	$5s9s\ {}^3S_1$	53547.9	219509.8	7.9+7	Wu
607.030(19)	164737	607.0373(14)	-0.007	$5s5p\ {}^3P^*_1$	$5s8d\ {}^3D_2$	55196.47	219931.0	3.3+8	Wu
608.600(19)	164312	608.5934(18)	0.007	$5s5p\ {}^3P^*_1$	$5s9s\ {}^3S_1$	55196.47	219509.8	2.3+8	Wu
614.531(4)	162725.7	614.5330(17)	-0.002	$5s^2\,{}^1S_0$	$5s6p\ {}^1P^*_1$	0.0	162725.20	4.2+7 [CF]	TW
622.043(4)	160760.6	622.0437(23)	-0.001	$5s5p\ {}^3P^*_2$	$5s8d\ {}^3D_3$	59228.50	219988.9	6.0+8	TW
623.905(4)	160280.8	623.9031(18)	0.002	$5s5p\ {}^3P^*_2$	$5s9s\ {}^3S_1$	59228.50	219509.8	3.6+8	TW
624.153(4)	160217.1	624.1576(18)	-0.005	$5s^2\,{}^1S_0$	$5s6p\ {}^3P^*_1$	0.0	160215.95	2.3+6 [CF]	TW
644.713(4)	155107.8	644.7150(16)	-0.002	$5s5p\ {}^3P^*_0$	$5s7d\ {}^3D_1$	53547.9	208655.2	3.5+8	TW
647.613(6)	154413.2	647.6144(16)	-0.001	$5s5p\ {}^3P^*_0$	$5s8s\ {}^3S_1$	53547.9	207960.78	1.5+8	TW
651.441(6)	153505.8	651.4411(14)	0.000	$5s5p\ {}^3P^*_1$	$5s7d\ {}^3D_2$	55196.47	208702.3	7.8+8	TW
651.638(6)	153459.4	651.6410(13)	-0.003	$5s5p\ {}^3P^*_1$	$5s7d\ {}^3D_1$	55196.47	208655.2	2.5+8	TW
654.605(4)	152763.9	654.6032(13)	0.002	$5s5p\ {}^3P^*_1$	$5s8s\ {}^3S_1$	55196.47	207960.78	4.3+8	TW
664.273(19)	150541	664.2765(14)	-0.003	$5s5p\ {}^1P^*_1$	$5p6p\ {}^1P_1$	79911.87	230451.6	1.1+9	Wu*
668.671(6)	149550.4	668.6718(21)	-0.001	$5s5p\ {}^3P^*_2$	$5s7d\ {}^3D_3$	59228.50	208778.7	1.4+9	TW
669.020(19)	149472	669.0136(15)	0.006	$5s5p\ {}^3P^*_2$	$5s7d\ {}^3D_2$	59228.50	208702.3	2.4+8	Wu
672.353(4)	148731.4	672.3490(14)	0.004	$5s5p\ {}^3P^*_2$	$5s8s\ {}^3S_1$	59228.50	207960.78	6.8+8	TW
713.021(6)	140248.3	713.0362(17)	-0.015	$5s5p\ {}^1P^*_1$	$5s8d\ {}^1D_2$	79911.87	220157.2	8.7+8	TW

λ_{obs} [c] Å	σ_{obs} cm^{-1}	λ_{Ritz} [d] Å	$\Delta\lambda_{O-Ritz}$ [e] Å	Classification		E_{low} cm^{-1}	E_{upp} cm^{-1}	gA [f] s^{-1}	Lin. Ref [h]
714.746(19)	139910	714.747(8)	-0.001	5s5p ^{1}P*$_1$	5s9s ^{1}S$_0$	79911.87	219821.6	2.7+8 [CF]	Wu
743.531(6)	134493.4	743.5330(24)	-0.002	5s5p ^{3}P*$_1$	5s6d ^{1}D$_2$	55196.47	189689.5	3.0+7 [CF]	TW
744.207(4)	134371.2	744.207(3)	0.000	5s5p ^{3}P*$_0$	5s6d ^{3}D$_1$	53547.9	187919.1	9.1+8	TW
751.176(4)	133124.6	751.1765(24)	-0.001	5s5p ^{3}P*$_0$	5s7s ^{3}S$_1$	53547.9	186672.4	3.0+8	TW
752.995(4)	132803.0	752.996(3)	-0.001	5s5p ^{3}P*$_1$	5s6d ^{3}D$_2$	55196.47	187999.3	2.0+9	TW
753.448(4)	132723.2	753.4510(24)	-0.003	5s5p ^{3}P*$_1$	5s6d ^{3}D$_1$	55196.47	187919.1	6.6+8	TW
760.598(4)	131475.5	760.5955(23)	0.003	5s5p ^{3}P*$_1$	5s7s ^{3}S$_1$	55196.47	186672.4	8.7+8	TW
773.099(6)	129349.5	773.1098(20)	-0.011	5s5p ^{1}P*$_1$	5s7d ^{1}D$_2$	79911.87	209259.6	1.6+9	TW
775.775(4)	128903.4	775.771(3)	0.004	5s5p ^{3}P*$_2$	5s6d ^{3}D$_3$	59228.50	188132.5	3.4+9	TW
776.564(6)	128772.4	776.574(3)	-0.010	5s5p ^{3}P*$_2$	5s6d ^{3}D$_2$	59228.50	187999.3	6.2+8	TW
777.054(6)	128691.2	777.058(3)	-0.004	5s5p ^{3}P*$_2$	5s6d ^{3}D$_1$	59228.50	187919.1	4.1+7	TW
777.407(6)	128632.7	777.4156(20)	-0.009	5s5p ^{1}P*$_1$	5s8s ^{1}S$_0$	79911.87	208543.2	3.6+8	TW
784.655(4)	127444.5	784.6590(24)	-0.004	5s5p ^{3}P*$_2$	5s7s ^{3}S$_1$	59228.50	186672.4	1.3+9	TW
910.932(4)	109777.7	910.932(3)	0.000	5s5p ^{1}P*$_1$	5s6d ^{1}D$_2$	79911.87	189689.5	4.2+9	TW
925.217(6)	108082.8	925.215(6)	0.002	5s5p ^{1}P*$_1$	5s7s ^{1}S$_0$	79911.87	187994.8	6.8+8	TW
936.665(19)	106761.8	936.676(3)	-0.011	5s5p ^{1}P*$_1$	5s7s ^{3}S$_1$	79911.87	186672.4	5.1+6	Wu
1010.031(6)	99006.9	1010.030(3)	0.001	5s5p ^{3}P*$_1$	5p^2 ^{1}S$_0$	55196.47	154203.39	4.0+7 [CF]	TW
1010.925(4)	98919.3	1010.9265(19)	-0.001	5s5p ^{3}P*$_1$	5s5d ^{1}D$_2$	55196.47	154115.63	2.0+8	TW
1046.311(7)	95573.9	1046.318(3)	-0.007	5p^2 ^{1}D$_2$	5s7f ^{1}F*$_3$	128205.82	223779.1	6.4+8 [CF]	TW
1053.882(10)	94887.3	1053.8837(24)	-0.002	5s5p ^{3}P*$_2$	5s5d ^{1}D$_2$	59228.50	154115.63	9.6+7	TW
1074.903(7)	93031.7	1074.904(6)	-0.001	5p^2 ^{3}P$_1$	4d^{9}5s^{2}5p ^{3}P*$_0$	130120.80	223152.4	1.1+8	TW
1100.033(7)	90906.4	1100.029(3)	0.004	5p^2 ^{1}D$_2$	4d^{9}5s^{2}5p ^{3}P*$_1$	128205.82	219112.5	8.7+8	TW
1118.363(7)	89416.4	1118.3736(25)	-0.011	5p^2 ^{1}D$_2$	5p5d ^{3}P*$_2$	128205.82	217621.38	4.6+8 [CF]	TW
1120.916(14)	89212.8	1120.936(4)	-0.020	5p^2 ^{3}P$_2$	5s7f ^{1}F*$_3$	134567.92	223779.1	5.5+8	TW
1122.874(7)	89057.2	1122.880(3)	-0.006	5p^2 ^{1}D$_2$	5s6f ^{3}F*$_3$	128205.82	217262.5	6.4+8	TW
1123.690(7)	88992.5	1123.700(3)	-0.010	5p^2 ^{3}P$_1$	4d^{9}5s^{2}5p ^{3}P*$_1$	130120.80	219112.5	1.6+9	TW
1124.634(7)	88917.8	1124.641(3)	-0.007	5p^2 ^{1}D$_2$	5p6s ^{1}P*$_1$	128205.82	217123.1	1.7+9	TW
1126.531(19)	88768.1	1126.536(7)	-0.005	5p^2 ^{1}D$_2$	5s6f ^{3}F*$_2$	128205.82	216973.5	9.8+7	Wu*
1129.339(7)	88547.4	1129.337(3)	0.002	5p^2 ^{1}D$_2$	5p5d ^{3}P*$_1$	128205.82	216753.37	3.2+6 [CF]	TW
1131.277(7)	88395.7	1131.280(3)	-0.003	5s5p ^{3}P*$_1$	5s6s ^{1}S$_0$	55196.47	143591.94	4.9+7	TW

λ_{obs} [c] Å	σ_{obs} cm^{-1}	λ_{Ritz} [d] Å	$\Delta\lambda_{O-Ritz}$ [e] Å	Classification		E_{low} cm^{-1}	E_{upp} cm^{-1}	gA [f] S^{-1}	Lin. Ref [h]
1131.697(19)	88362.9	1131.697(19)		$5p^2\,^3P_2$	$4d^9 5s^2 5p\ ^1D'_2$	134567.92	222930.8	2.4+8	Wu*
1132.318(7)	88314.4	1132.323(3)	-0.005	$5p^2\,^1D_2$	$5s6f\ ^1F'_3$	128205.82	216519.87	5.7+8 [CF]	TW
1137.882(19)	87882.6	1137.844(5)	0.038	$5p^2\,^3P_2$	$4d^9 5s^2 5p\ ^3D'_3$	134567.92	222453.4	1.8+8 [CF]	Wu*
1139.288(10)	87774.1	1139.294(4)	-0.006	$5s5p\ ^3P'_0$	$5s5d\ ^3D_1$	53547.9	141321.54	5.8+9	TW
1140.859(7)	87653.3	1140.863(3)	-0.004	$5p^2\,^1D_2$	$5p6s\ ^3P'_2$	128205.82	215858.8	2.4+9	TW
1141.894(7)	87573.8	1141.898(3)	-0.004	$5p^2\,^1D_2$	$5p5d\ ^3D'_3$	128205.82	215779.28	4.8+9	TW
1142.840(7)	87501.3	1142.850(3)	-0.010	$5p^2\,^3P_1$	$5p5d\ ^3P'_2$	130120.80	217621.38	2.0+9 [CF]	TW
1143.380(7)	87460.0	1143.385(5)	-0.005	$5p^2\,^3P_1$	$5p5d\ ^3P'_0$	130120.80	217580.4	2.5+9	TW
1154.292(7)	86633.2	1154.300(3)	-0.008	$5p^2\,^3P_1$	$5p5d\ ^3P'_1$	130120.80	216753.37	4.3+9	TW
1158.347(10)	86329.9	1158.3451(25)	0.002	$5s5p\ ^3P'_1$	$5s5d\ ^3D_2$	55196.47	141526.53	1.2+10	TW
1161.100(10)	86125.2	1161.102(3)	-0.002	$5s5p\ ^3P'_1$	$5s5d\ ^3D_1$	55196.47	141321.54	4.1+9	TW
1161.560(10)	86091.1	1161.559(4)	0.001	$5s5p\ ^3P'_0$	$5s6s\ ^3S_1$	53547.9	139639.13	8.7+8	TW
1163.495(7)	85947.9	1163.5025(24)	-0.007	$5p^2\,^1D_2$	$5p5d\ ^3D'_2$	128205.82	214153.21	5.1+8 [CF]	TW
1164.664(7)	85861.7	1164.667(4)	-0.003	$5p^2\,^3P_0$	$5s8p\ ^1P'_1$	127309.52	213170.94	5.1+8	TW
1171.442(7)	85364.9	1171.449(6)	-0.007	$5p^2\,^3P_2$	$4d^9 5s^2 5p\ ^3F'_2$	134567.92	219932.3	5.6+8	TW
1177.176(7)	84949.1	1177.177(4)	-0.001	$5p^2\,^3P_0$	$5s8p\ ^3P'_1$	127309.52	212258.5	7.0+9	TW
1180.614(7)	84701.7	1180.613(4)	0.001	$5p^2\,^3P_0$	$5p5d\ ^3D'_1$	127309.52	212011.3	4.4+9	TW
1182.819(7)	84543.8	1182.808(3)	0.011	$5p^2\,^3P_2$	$4d^9 5s^2 5p\ ^3P'_1$	134567.92	219112.5	7.1+8	TW
1184.243(10)	84442.1	1184.235(3)	0.008	$5s5p\ ^3P'_1$	$5s6s\ ^3S_1$	55196.47	139639.13	2.5+9	TW
1184.944(7)	84392.2	1184.938(3)	0.006	$5p^2\,^1D_2$	$5s8p\ ^3P'_2$	128205.82	212598.4	3.1+8	TW
1189.734(7)	84052.4	1189.730(3)	0.004	$5p^2\,^1D_2$	$5s8p\ ^3P'_1$	128205.82	212258.5	2.0+7 [CF]	TW
1190.024(7)	84031.9	1190.017(3)	0.007	$5p^2\,^3P_1$	$5p5d\ ^3D'_2$	130120.80	214153.21	1.7+10	TW
1204.053(14)	83052.8	1204.044(3)	0.009	$5p^2\,^3P_2$	$5p5d\ ^3P'_2$	134567.92	217621.38	6.9+9	TW
	83052.8	1204.092(3)		$5p^2\,^3P_1$	$5s8p\ ^1P'_1$	130120.80	213170.94	4.3+7	TW
1209.270(7)	82694.5	1209.269(3)	0.001	$5p^2\,^3P_2$	$5s6f\ ^3F'_3$	134567.92	217262.5	4.1+9	TW
1210.195(7)	82631.3	1210.185(3)	0.010	$5p^2\,^1D_2$	$4d^9 5s^2 5p\ ^3P'_2$	128205.82	210837.8	1.3+9	TW
1210.516(10)	82609.4	1210.511(3)	0.005	$5s5p\ ^3P'_2$	$5s5d\ ^3D_3$	59228.50	141838.23	2.1+10	TW
1212.428(16)	82479.1	1212.417(4)	0.011	$5p^2\,^3P_0$	$5p6s\ ^3P'_1$	127309.52	209789.42	1.3+9	TW
1212.43(3)	82479.1	1212.450(4)	-0.02	$5p^2\,^3P_1$	$5s8p\ ^3P'_2$	130120.80	212598.4	4.9+8	TW
1214.604(7)	82331.4	1214.604(7)		$5p^2\,^3P_1$	$5s8p\ ^3P'_0$	130120.80	212452.16	1.7+8	TW

I_{obs} [a] (A. U)	Char.[b]	λ_{obs} [c] Å	σ_{obs} cm^{-1}	λ_{Ritz} [d] Å	$\Delta\lambda_{O-Ritz}$ [e] Å	Classification		E_{low} cm^{-1}	E_{upp} cm^{-1}	gA[f] S^{-1}	Lin. Ref[h]
90000		1215.096(10)	82298.0	1215.096(3)	0.000	5s5p $^3P^*_2$	5s5d $^3D_2$	59228.50	141526.53	3.8+9	TW
80000		1216.766(7)	82185.1	1216.760(3)	0.006	5p^2 $^3P_2$	5p5d $^3P^*_1$	134567.92	216753.37	2.0+9	TW
80000		1218.133(10)	82092.8	1218.130(3)	0.003	5s5p $^3P^*_2$	5s5d $^3D_1$	59228.50	141321.54	2.4+8	TW
100000		1220.231(7)	81951.7	1220.227(3)	0.004	5p^2 $^3P_2$	5s6f $^1F^*_3$	134567.92	216519.87	1.2+10	TW
74000		1221.147(7)	81890.2	1221.143(3)	0.004	5p^2 $^3P_1$	5p5d $^3D^*_1$	130120.80	212011.3	2.6+9	TW
31000		1222.033(19)	81830.9	1222.033(8)	0.000	5s5d $^3D_1$	4d^{9}5s^{2}5p $^3P^*_0$	141321.54	223152.4	1.2+8	Wu*
170000		1224.621(7)	81657.9	1224.621(7)		5s5d $^1D_2$	5s10f $^1F^*_3$	154115.63	235773.54	1.6+10	TW
90000		1225.743(7)	81583.2	1225.7365(25)	0.006	5p^2 $^1D_2$	5p6s $^3P^*_1$	128205.82	209789.42	1.9+9	TW
120000		1230.155(7)	81290.6	1230.150(3)	0.005	5p^2 $^3P_2$	5p6s $^3P^*_2$	134567.92	215858.8	9.5+9	TW
120000		1231.351(7)	81211.6	1231.355(3)	-0.004	5p^2 $^3P_2$	5p5d $^3D^*_3$	134567.92	215779.28	1.0+10	TW
33000		1237.577(19)	80803.1	1237.585(12)	-0.008	5s6s $^1S_0$	4d^{9}5s^{2}5p $^1P^*_1$	143591.94	224394.5	9.9+7	Wu*
59000		1238.928(19)	80714.9	1238.896(4)	0.032	5p^2 $^3P_1$	4d^{9}5s^{2}5p $^3P^*_2$	130120.80	210837.8	6.2+7	Wu*
120000		1241.831(7)	80526.3	1241.822(3)	0.009	5p^2 $^1D_2$	5p5d $^1D^*_2$	128205.82	208732.65	5.6+9	TW
59000		1242.148(7)	80505.7	1242.145(4)	0.003	5p^2 $^1D_2$	5p5d $^3F^*_3$	128205.82	208711.7	3.1+8	TW
120000		1243.615(10)	80410.7	1243.617(3)	-0.002	5s5p $^3P^*_2$	5s6s $^3S_1$	59228.50	139639.13	3.6+9	TW
90000		1244.538(19)	80351.1	1244.542(19)	-0.004	5s5d $^3D_2$	5s9p $^3P^*_1$	141526.53	221877.4	1.7+8	TW
51000		1246.286(19)	80238.4	1246.286(19)		5s5d $^3D_3$	5s9p $^3P^*_2$	141838.23	222076.64	2.1+8	Wu*
140000		1251.387(20)	79911.3	1251.379(7)	0.008	5s^2 $^1S_0$	5s5p $^1P^*_1$	0.0	79911.87	9.3+9	TW
80000		1252.585(7)	79834.9	1252.585(7)		5s5d $^1D_2$	5s9f $^1F^*_3$	154115.63	233950.5	1.9+9 [CF]	TW
100000		1255.199(7)	79668.6	1255.199(3)	0.000	5p^2 $^3P_1$	5p6s $^3P^*_1$	130120.80	209789.42	9.0+8	TW
65000		1256.510(7)	79585.5	1256.514(3)	-0.004	5p^2 $^3P_2$	5p5d $^3D^*_2$	134567.92	214153.21	2.4+9	TW
130000		1257.574(7)	79518.2	1257.575(5)	-0.001	5p^2 $^3P_1$	5p6s $^3P^*_0$	130120.80	209638.9	1.8+9	TW
140000		1259.887(10)	79372.2	1259.899(3)	-0.012	5s5p $^3P^*_1$	5p^2 $^3P_2$	55196.47	134567.92	3.7+9	TW
51000		1267.700(19)	78883.0	1267.699(19)	0.001	5s6s $^1S_0$	5s9p $^1P^*_1$	143591.94	222475.0	3.1+8	Wu*
160000		1272.074(7)	78611.8	1272.073(3)	0.001	5p^2 $^3P_1$	5p5d $^1D^*_2$	130120.80	208732.65	3.4+9	TW
110000		1272.210(7)	78603.4	1272.216(4)	-0.006	5p^2 $^3P_2$	5s8p $^1P^*_1$	134567.92	213170.94	3.5+8	TW
63000		1275.459(19)	78403.1	1275.416(8)	0.043	5s5d $^3D_2$	4d^{9}5s^{2}5p $^3F^*_2$	141526.53	219932.3	2.6+8	Wu*
170000	bl(Sn)	1276.295(14)	78351.8	1276.294(3)	0.001	5p^2 $^1D_2$	5p5d $^3F^*_2$	128205.82	206557.65	5.6+9	TW
71000		1281.550(7)	78030.5	1281.550(4)	0.000	5p^2 $^3P_2$	5s8p $^3P^*_2$	134567.92	212598.4	1.2+8 [CF]	TW
90000		1282.342(7)	77982.3	1282.343(3)	-0.001	5s6s $^3S_1$	5p5d $^3P^*_2$	139639.13	217621.38	1.1+9	TW

I_{obs}[a] (A. U)	Char.[b]	λ_{obs}[c] Å	σ_{obs} cm^{-1}	λ_{Ritz}[d] Å	$\Delta\lambda_{O-Ritz}$[e] Å	Classification		E_{low} cm^{-1}	E_{upp} cm^{-1}	gA[f] S^{-1}	Lin. Ref[h]
28000		1285.064(7)	77817.1	1285.059(5)	0.005	5s6p ^{3}P°$_0$	5p6p ^{3}S$_1$	159940.47	237757.9	1.0+9	TW
70000		1285.494(7)	77791.1	1285.496(4)	-0.002	5s5d ^{3}D$_1$	4d^{9}5s^{2}5p ^{3}P°$_1$	141321.54	219112.5	1.1+9	TW
69000		1287.155(7)	77690.7	1287.157(3)	-0.002	5p$^{2\,3}$P$_2$	5s8p ^{3}P°$_1$	134567.92	212258.5	6.4+8	TW
90000		1288.893(7)	77586.0	1288.893(4)	0.000	5s5d ^{3}D$_2$	4d^{9}5s^{2}5p ^{3}P°$_1$	141526.53	219112.5	1.1+9	TW
56000	bl(Sn)	1289.627(7)	77541.8	1289.625(5)	0.002	5s6p ^{3}P°$_1$	5p6p ^{3}S$_1$	160215.95	237757.9	1.6+9	TW
110000		1290.589(7)	77484.0	1290.590(4)	-0.001	5s6s ^{3}S$_1$	5p6s ^{1}P°$_1$	139639.13	217123.1	2.9+9	TW
63000		1291.277(7)	77442.7	1291.266(3)	0.011	5p$^{2\,3}$P$_2$	5p5d ^{3}D°$_1$	134567.92	212011.3	8.8+7 [CF]	TW
35000		1299.288(19)	76965.2	1299.288(19)		5s5d ^{1}D$_2$	5p5d ^{1}F°$_3$	154115.63	231080.86	3.8+9 [CF]	Wu*
190000		1305.955(10)	76572.3	1305.945(5)	0.010	5s5p ^{3}P°$_0$	5p$^{2\,3}$P$_1$	53547.9	130120.80	3.0+9	TW
23000		1308.291(19)	76435.6	1308.270(4)	0.021	5p$^{2\,3}$P$_1$	5p5d ^{3}F°$_2$	130120.80	206557.65	3.5+7	Wu*
110000		1310.625(7)	76299.5	1310.619(3)	0.006	5s5d ^{3}D$_1$	5p5d ^{3}P°$_2$	141321.54	217621.38	7.9+8	TW
130000		1311.135(7)	76269.8	1311.134(4)	0.001	5p$^{2\,3}$P$_2$	4d^{9}5s^{2}5p ^{3}P°$_2$	134567.92	210837.8	4.9+8	TW
110000		1311.332(10)	76258.3	1311.323(7)	0.009	5s5d ^{3}D$_1$	5p5d ^{3}P°$_0$	141321.54	217580.4	1.4+9	TW
110000		1311.349(7)	76257.4	1311.352(6)	-0.003	5s6p ^{3}P°$_1$	5s12d ^{3}D$_2$	160215.95	236473.1	1.1+7 [CF]	TW
210000		1312.003(7)	76219.3	1311.997(4)	0.006	5s6s ^{3}S$_1$	5p6s ^{3}P°$_2$	139639.13	215858.8	5.0+9	TW
200000		1314.151(7)	76094.8	1314.149(3)	0.002	5s5d ^{3}D$_2$	5p5d ^{3}P°$_2$	141526.53	217621.38	3.4+9	TW
110000		1315.615(7)	76010.1	1315.609(6)	0.006	5s6p ^{3}P°$_1$	5p6p ^{3}P$_2$	160215.95	236226.4	2.9+9	TW
39000	h	1319.246(10)	75800.9	1319.234(4)	0.012	5s5d ^{3}D$_1$	5p6s ^{1}P°$_1$	141321.54	217123.1	2.3+9	TW
140000		1319.561(7)	75782.8	1319.555(4)	0.006	5s5d ^{3}D$_3$	5p5d ^{3}P°$_2$	141838.23	217621.38	1.6+9	TW
120000		1320.384(7)	75735.5	1320.377(4)	0.007	5s5d ^{3}D$_2$	5s6f ^{3}F°$_3$	141526.53	217262.5	2.1+9	TW
72000	*	1321.843(10)	75651.9	1321.843(9)	0.000	5s5d ^{3}D$_1$	5s6f ^{3}F°$_2$	141321.54	216973.5	6.0+8	TW
72000	*	1321.843(10)	75651.9	1321.844(10)	-0.001	5p$^{2\,1}$S$_0$	4d^{9}5s^{2}5p ^{3}D°$_1$	154203.39	229855.3	1.5+8	TW
63000	bl(Sn)	1322.811(7)	75596.6	1322.811(4)	0.000	5s5d ^{3}D$_2$	5p6s ^{1}P°$_1$	141526.53	217123.1	1.5+9	TW
140000		1325.702(7)	75431.7	1325.700(4)	0.002	5s5d ^{3}D$_1$	5p5d ^{3}P°$_1$	141321.54	216753.37	1.9+9	TW
72000		1325.829(7)	75424.5	1325.833(4)	-0.004	5s5d ^{3}D$_3$	5s6f ^{3}F°$_3$	141838.23	217262.5	5.4+8	TW
80000		1326.856(7)	75366.1	1326.856(7)		5s6p ^{3}P°$_2$	5s12d ^{3}D$_3$	161439.23	236805.36	1.5+9	TW
260000		1327.337(10)	75338.8	1327.326(4)	0.011	5s5p ^{3}P°$_2$	5p$^{2\,3}$P$_2$	59228.50	134567.92	9.3+9	TW
200000	*	1329.325(7)	75226.1	1329.328(7)	-0.003	5s5d ^{3}D$_3$	5s6f ^{3}F°$_4$	141838.23	217064.2	2.6+9	TW
	*, m		75224.4	1329.313(4)		5s5d ^{3}D$_2$	5p5d ^{3}P°$_1$	141526.53	216753.37	2.9+8 [CF]	TW
190000		1329.414(7)	75221.1	1329.407(3)	0.007	5p$^{2\,3}$P$_2$	5p6s ^{3}P°$_1$	134567.92	209789.42	6.3+8	TW

I_{obs}[a] (A. U).	Char.[b]	λ_{obs}[c] Å	σ_{obs} cm^{-1}	λ_{Ritz}[d] Å	$\Delta\lambda_{O-Ritz}$[e] Å	Classification		E_{low} cm^{-1}	E_{upp} cm^{-1}	gA^f S^{-1}	Lin. Ref[h]
210000		1331.731(7)	75090.2	1331.721(4)	0.010	$5p^2\ ^1D_2$	$5s5f\ ^1F^o_3$	128205.82	203296.65	1.4+9	TW
47000	*	1332.739(10)	75033.4	1332.752(5)	-0.013	$5s6p\ ^1P^o_1$	$5p6p\ ^3S_1$	162725.20	237757.9	9.3+8	TW
47000	*	1332.739(10)	75033.4	1332.731(6)	0.008	$5s6p\ ^3P^o_2$	$5s12d\ ^3D_2$	161439.23	236473.1	3.5+8	TW
110000		1333.452(7)	74993.3	1333.452(3)	0.000	$5s5d\ ^3D_2$	$5s6f\ ^1F^o_3$	141526.53	216519.87	5.6+8	TW
240000		1334.696(10)	74923.4	1334.680(4)	0.016	$5s5p\ ^3P^o_1$	$5p^2\ ^3P_1$	55196.47	130120.80	2.1+9	TW
170000		1335.172(7)	74896.7	1335.170(5)	0.002	$5s6p\ ^3P^o_0$	$5p6p\ ^3P_1$	159940.47	234837.3	1.7+9	TW
230000	bl(Sn II)	1337.103(14)	74788.6	1337.128(7)	-0.025	$5s6p\ ^3P^o_2$	$5p6p\ ^3P_2$	161439.23	236226.4	1.1+9	TW
180000		1339.015(7)	74681.8	1339.017(4)	-0.002	$5s5d\ ^3D_3$	$5s6f\ ^1F^o_3$	141838.23	216519.87	3.2+9	TW
76000		1341.596(7)	74538.1	1341.611(4)	-0.015	$5s5d\ ^3D_1$	$5p6s\ ^3P^o_2$	141321.54	215858.8	6.2+8	TW
80000		1342.036(7)	74513.6	1342.028(3)	0.008	$5s6s\ ^3S_1$	$5p5d\ ^3D^o_2$	139639.13	214153.21	1.2+9	TW
18000	bl(Sn)	1342.702(14)	74476.7	1342.733(7)	-0.031	$5s5d\ ^1D_2$	$5s10p\ ^1P^o_1$	154115.63	228590.6	1.3+9[CF]	TW
48000		1344.325(7)	74386.8	1344.317(6)	0.008	$5p^2\ ^1S_0$	$5s10p\ ^1P^o_1$	154203.39	228590.6	2.1+9	TW
130000		1345.315(7)	74332.0	1345.311(4)	0.004	$5s5d\ ^3D_2$	$5p6s\ ^3P^o_2$	141526.53	215858.8	1.3+9	TW
300000		1346.045(7)	74291.7	1346.049(4)	-0.004	$5s5p\ ^1P^o_1$	$5p^2\ ^1S_0$	79911.87	154203.39	3.5+9	TW
150000		1346.367(7)	74274.0	1346.366(3)	0.001	$5p^2\ ^1D_2$	$5s5f\ ^3F^o_3$	128205.82	202479.83	1.9+8	TW
190000		1346.747(7)	74253.0	1346.751(4)	-0.004	$5s5d\ ^3D_2$	$5p5d\ ^3D^o_3$	141526.53	215779.28	1.3+9	TW
340000		1347.635(14)	74204.1	1347.641(3)	-0.006	$5s5p\ ^1P^o_1$	$5s5d\ ^1D_2$	79911.87	154115.63	2.3+10	TW
230000	*	1348.747(14)	74142.9	1348.731(5)	0.016	$5p^2\ ^3P_2$	$5p5d\ ^3F^o_3$	134567.92	208711.7	9.2+8	TW
230000	*	1348.747(14)	74142.9	1348.747(20)		$5s6p\ ^3P^o_2$	$5p6p\ ^3D_3$	161439.23	235582.1	8.5+9	TW
120000		1350.166(7)	74065.0	1350.166(7)		$5s5d\ ^1D_2$	$5s8f\ ^1F^o_3$	154115.63	228180.6	4.2+9	TW
240000	bl(Sn)?	1352.432(7)	73940.9	1352.429(4)	0.003	$5s5d\ ^3D_3$	$5p5d\ ^3D^o_3$	141838.23	215779.28	2.8+9	TW
130000		1354.380(7)	73834.5	1354.387(4)	-0.007	$5p^2\ ^1D_2$	$5s5f\ ^3F^o_2$	128205.82	202039.97	3.3+8	TW
220000	*, bl(Sn)?	1359.967(14)	73531.2	1359.956(4)	0.011	$5s6s\ ^3S_1$	$5s8p\ ^1P^o_1$	139639.13	213170.94	4.5+8	TW
220000	*, bl(Sn)?	1359.967(14)	73531.2	1359.968(5)	-0.001	$5s6s\ ^1S_0$	$5p6s\ ^1P^o_1$	143591.94	217123.1	3.6+9	TW
250000	h, bl(Sn)	1360.856(10)	73483.2	1360.856(10)		$5s5d\ ^1D_2$	$4d^95s^25p\ ^1F^o_3$	154115.63	227598.8	5.6+9	TW
110000		1361.808(7)	73431.8	1361.808(5)	0.000	$5s5d\ ^1D_2$	$5p5d\ ^1P^o_1$	154115.63	227547.4	3.0+9	TW
80000		1362.450(7)	73397.2	1362.434(5)	0.016	$5s6p\ ^3P^o_2$	$5p6p\ ^3P_1$	161439.23	234837.3	6.7+8	TW
220000		1363.437(7)	73344.1	1363.438(5)	-0.001	$5p^2\ ^1S_0$	$5p5d\ ^1P^o_1$	154203.39	227547.4	6.6+9	TW
80000		1366.836(7)	73161.7	1366.840(4)	-0.004	$5s6s\ ^1S_0$	$5p5d\ ^3P^o_1$	143591.94	216753.37	2.3+8	TW
280000		1369.688(10)	73009.3	1369.687(3)	0.001	$5s5p\ ^3P^o_1$	$5p^2\ ^1D_2$	55196.47	128205.82	4.8+8	TW

I_{obs} [a] (A. U)	Char.[b]	λ_{obs} [c] Å	σ_{obs} cm^{-1}	λ_{Ritz} [d] Å	$\Delta\lambda_{O-Ritz}$ [e] Å	Classification		E_{low} cm^{-1}	E_{upp} cm^{-1}	gA^f S^{-1}	Lin. Ref[h]
120000	h, bl(Sn II)	1370.651(14)	72958.0	1370.628(5)	0.023	$5s6s\ ^3S_1$	$5s8p\ ^3P^*_2$	139639.13	212598.4	6.6+7	TW
27000	h	1371.051(7)	72936.7	1371.051(7)		$5s6p\ ^3P^*_2$	$5s11d\ ^3D_3$	161439.23	234376.0	5.9+8	TW
130000		1373.029(7)	72831.7	1373.029(3)	0.000	$5s5d\ ^3D_1$	$5p5d\ ^3D^*_2$	141321.54	214153.21	8.5+8	TW
120000		1376.903(7)	72626.8	1376.904(3)	-0.001	$5s5d\ ^3D_2$	$5p5d\ ^3D^*_2$	141526.53	214153.21	2.0+8 [CF]	TW
150000		1377.038(7)	72619.6	1377.043(4)	-0.005	$5s6s\ ^3S_1$	$5s8p\ ^3P^*_1$	139639.13	212258.5	2.5+8	TW
210000		1382.837(7)	72315.1	1382.839(3)	-0.002	$5s5d\ ^3D_3$	$5p5d\ ^3D^*_2$	141838.23	214153.21	3.3+9	TW
330000		1386.714(7)	72112.9	1386.730(5)	-0.016	$5s6p\ ^1P^*_1$	$5p6p\ ^3P_1$	162725.20	234837.3	9.7+8	TW
330000		1386.717(10)	72112.8	1386.711(5)	0.006	$5s5p\ ^3P^*_1$	$5p^2\ ^3P_0$	55196.47	127309.52	2.5+9	TW
16000		1389.088(7)	71989.7	1389.087(4)	0.001	$5p^2\ ^3P_2$	$5p5d\ ^3F^*_2$	134567.92	206557.65	1.4+8 [CF]	TW
59000		1390.454(19)	71919.0	1390.450(4)	0.004	$5p^2\ ^3P_1$	$5s5f\ ^3F^*_2$	130120.80	202039.97	2.4+7	Wu*
57000		1391.805(7)	71849.1	1391.800(4)	0.005	$5s5d\ ^3D_1$	$5s8p\ ^1P^*_1$	141321.54	213170.94	1.4+6 [CF]	TW
100000		1395.783(7)	71644.4	1395.782(4)	0.001	$5s5d\ ^3D_2$	$5s8p\ ^1P^*_1$	141526.53	213170.94	5.4+7	TW
130000		1398.719(7)	71494.0	1398.719(7)		$5s5d\ ^3D_2$	$4d^95s^25p\ ^3F^*_3$	141526.53	213020.5	4.5+8	TW
35000	h_s*	1402.976(10)	71277.1	1402.980(4)	-0.004	$5s5d\ ^3D_1$	$5s8p\ ^3P^*_2$	141321.54	212598.4	9.0+7	TW
35000	h_s*	1402.976(10)	71277.1	1402.976(10)		$5s6p\ ^3P^*_1$	$5p6p\ ^3P_0$	160215.95	231493.0	1.1+9	TW
400000		1410.592(10)	70892.2	1410.590(4)	0.002	$5s5p\ ^3P^*_2$	$5p^2\ ^3P_1$	59228.50	130120.80	3.0+9	TW
90000		1413.218(7)	70760.5	1413.224(4)	-0.006	$5s5d\ ^3D_3$	$5s8p\ ^3P^*_2$	141838.23	212598.4	9.3+7 [CF]	TW
	m		70733.2	1429.157(8)		$5s6p\ ^3P^*_1$	$5p6p\ ^3D_2$	160215.95	230187.27	1.1+9	TW
34000	h	1413.767(10)	70733.0	1413.788(4)	-0.021	$5s5d\ ^3D_2$	$5s8p\ ^3P^*_1$	141526.53	212258.5	1.1+9	TW
120000		1414.625(7)	70690.1	1414.632(4)	-0.007	$5s5d\ ^3D_1$	$5p5d\ ^3D^*_1$	141321.54	212011.3	7.5+8	TW
180000		1418.743(7)	70484.9	1418.746(4)	-0.003	$5s5d\ ^3D_2$	$5p5d\ ^3D^*_1$	141526.53	212011.3	1.2+9	TW
35000		1423.317(7)	70258.4	1423.317(7)		$5s6p\ ^3P^*_2$	$5s10d\ ^3D_2$	161439.23	231697.65	1.1+9	TW
90000		1424.691(19)	70190.7	1424.682(15)	0.009	$5p^2\ ^1S_0$	$4d^95s^25p\ ^1P^*_1$	154203.39	224394.5	2.4+8	Wu*
310000		1425.509(7)	70150.4	1425.511(4)	-0.002	$5s6s\ ^3S_1$	$5p6s\ ^3P^*_1$	139639.13	209789.42	2.2+9	TW
230000		1428.578(7)	69999.7	1428.576(6)	0.002	$5s6s\ ^3S_1$	$5p6s\ ^3P^*_0$	139639.13	209638.9	1.1+9	TW
370000		1435.480(7)	69663.1	1435.473(6)	0.007	$5s5d\ ^1D_2$	$5s7f\ ^1F^*_3$	154115.63	223779.1	5.2+9	TW
610000		1436.929(10)	69592.9	1436.931(10)	-0.002	$5s5d\ ^3D_3$	$5p5d\ ^3F^*_4$	141838.23	211431.0	1.5+10	TW
220000		1438.507(7)	69516.5	1438.512(4)	-0.005	$5s5d\ ^3D_1$	$4d^95s^25p\ ^3P^*_2$	141321.54	210837.8	3.3+8	TW
100000	bl(Sn)	1442.759(7)	69311.6	1442.767(4)	-0.008	$5s5d\ ^3D_2$	$4d^95s^25p\ ^3P^*_2$	141526.53	210837.8	9.5+7	TW
130000		1449.011(7)	69012.6	1449.016(5)	-0.005	$5s6p\ ^3P^*_2$	$5p6p\ ^1P_1$	161439.23	230451.6	1.6+9	TW

I_{obs} [a] (A. U)	Char.[b]	λ_{obs} [c] Å	σ_{obs} cm^{-1}	λ_{Ritz} [d] Å	$\Delta\lambda_{O-Ritz}$ [e] Å	Classification		E_{low} cm^{-1}	E_{upp} cm^{-1}	gA^f S^{-1}	Lin. Ref[h]
480000		1449.742(10)	68977.8	1449.752(4)	-0.010	$5s5p\ ^3P'_2$	$5p^2\ ^1D_2$	59228.50	128205.82	1.0+9	TW
50000	h	1454.587(7)	68748.0	1454.587(7)		$5s6p\ ^3P'_2$	$5p6p\ ^3D_2$	161439.23	230187.27	2.0+9	TW
200000		1454.999(19)	68728.6	1454.996(4)	0.003	$5p^2\ ^3P_2$	$5s5f\ ^1F'_3$	134567.92	203296.65	5.8+7 [CF]	Wu
300000		1456.326(7)	68665.9	1456.313(5)	0.013	$5s6s\ ^1S_0$	$5s8p\ ^3P'_1$	143591.94	212258.5	6.1+7	TW
150000		1463.316(7)	68337.9	1463.320(7)	-0.004	$5s5d\ ^1D_2$	$4d^95s^25p\ ^3D'_3$	154115.63	222453.4	1.6+9	TW
51000	bl(Sn)?	1473.859(7)	67849.1	1473.875(4)	-0.016	$5p^2\ ^1D_2$	$5s7p\ ^1P'_1$	128205.82	196054.2	3.7+8	TW
22000		1476.534(7)	67726.2	1476.529(5)	0.005	$5s6p\ ^1P'_1$	$5p6p\ ^1P_1$	162725.20	230451.6	1.7+9	TW
18000		1476.969(7)	67706.2	1476.969(5)	0.000	$5s6p\ ^3P'_0$	$5p6p\ ^3D_1$	159940.47	227646.69	9.2+8	TW
11000		1482.997(7)	67431.0	1483.003(5)	-0.006	$5s6p\ ^3P'_1$	$5p6p\ ^3D_1$	160215.95	227646.69	1.5+9	TW
42000		1483.434(7)	67411.2	1483.435(4)	-0.001	$5s5d\ ^3D_1$	$5p5d\ ^1D'_2$	141321.54	208732.65	1.7+9	TW
32000		1487.956(7)	67206.3	1487.960(4)	-0.004	$5s5d\ ^3D_2$	$5p5d\ ^1D'_2$	141526.53	208732.65	8.7+8	TW
380000	bl(Sn IV)	1488.407(16)	67185.9	1488.424(6)	-0.017	$5s5d\ ^3D_2$	$5p5d\ ^3F'_3$	141526.53	208711.7	7.9+9	TW
20000		1488.773(7)	67169.4	1488.771(6)	0.002	$5p^2\ ^1D_2$	$5s7p\ ^3P'_1$	128205.82	195375.3	1.2+8	TW
40000		1494.891(7)	66894.5	1494.893(4)	-0.002	$5s5d\ ^3D_3$	$5p5d\ ^1D'_2$	141838.23	208732.65	1.1+9	TW
47000		1495.360(7)	66873.5	1495.361(5)	-0.001	$5s5d\ ^3D_3$	$5p5d\ ^3F'_3$	141838.23	208711.7	2.5+9	TW
36000		1510.621(7)	66197.9	1510.632(4)	-0.011	$5s6s\ ^1S_0$	$5p6s\ ^3P'_1$	143591.94	209789.42	9.0+8	TW
49000	bl(Sn IV)	1532.894(7)	65236.1	1532.893(4)	0.001	$5s5d\ ^3D_1$	$5p5d\ ^3F'_2$	141321.54	206557.65	2.9+9	TW
27000		1537.719(7)	65031.4	1537.725(4)	-0.006	$5s5d\ ^3D_2$	$5p5d\ ^3F'_2$	141526.53	206557.65	7.6+8	TW
13000		1540.328(7)	64921.2	1540.322(5)	0.006	$5s6p\ ^1P'_1$	$5p6p\ ^3D_1$	162725.20	227646.69	6.0+8	TW
46000		1570.348(12)	63680.2	1570.350(5)	-0.002	$5s5p\ ^1P'_1$	$5s6s\ ^1S_0$	79911.87	143591.94	1.3+9	TW
2600		1596.495(19)	62637.2	1596.482(6)	0.013	$5s5d\ ^1D_2$	$5p5d\ ^3P'_1$	154115.63	216753.37	1.1+8	Wu
26000		1602.457(8)	62404.2	1602.455(5)	0.002	$5s5d\ ^1D_2$	$5s6f\ ^1F'_3$	154115.63	216519.87	9.6+8	TW
19000		1621.708(8)	61663.4	1621.701(5)	0.007	$5s5d\ ^1D_2$	$5p5d\ ^3D'_3$	154115.63	215779.28	1.3+9	TW
46000		1623.009(8)	61614.0	1622.990(3)	0.019	$5s5p\ ^1P'_1$	$5s5d\ ^3D_2$	79911.87	141526.53	2.1+7	TW
5300		1626.400(8)	61485.5	1626.379(5)	0.021	$5p^2\ ^3P_2$	$5s7p\ ^1P'_1$	134567.92	196054.2	2.5+7	TW
18000	bl(Sn II)	1628.422(16)	61409.1	1628.408(4)	0.014	$5s5p\ ^1P'_1$	$5s5d\ ^3D_1$	79911.87	141321.54	1.4+7	TW
16000		1635.999(8)	61124.7	1635.995(8)	0.004	$5s5d\ ^3D_3$	$5s5f\ ^3F'_4$	141838.23	202963.1	1.9+8 [CF]	TW
21000		1640.613(8)	60952.8	1640.600(4)	0.013	$5s5d\ ^3D_2$	$5s5f\ ^3F'_3$	141526.53	202479.83	5.3+8 [CF]	TW
23000		1646.955(8)	60718.1	1646.946(5)	0.009	$5s5d\ ^3D_1$	$5s5f\ ^3F'_2$	141321.54	202039.97	9.3+8	TW
10000		1649.035(8)	60641.5	1649.033(4)	0.002	$5s5d\ ^3D_3$	$5s5f\ ^3F'_3$	141838.23	202479.83	1.7+8	TW

I_{obs} [a] (A. U)	Char.[b]	λ_{obs} [c] Å	σ_{obs} cm^{-1}	λ_{Ritz} [d] Å	$\Delta\lambda_{O-Ritz}$ [e] Å	Classification		E_{low} cm^{-1}	E_{upp} cm^{-1}	gA [f] S^{-1}	Lin, Ref [h]
13000		1652.523(8)	60513.5	1652.525(5)	-0.002	5s5d $^1D_2$	5s5f $^3F'_2$	141526.53	202039.97	2.7+8	TW
13000		1674.287(8)	59726.9	1674.277(4)	0.010	5s5p $^1P'_1$	5s6s $^3S_1$	79911.87	139639.13	8.3+6	TW
10000		1674.620(8)	59715.0	1674.620(8)	0.000	5s6p $^3P'_1$	5s8d $^3D_2$	160215.95	219931.0	1.1+8	TW
800		1686.520(19)	59293.7	1686.516(12)	0.004	5s6p $^3P'_1$	5s9s $^3S_1$	160215.95	219509.8	8.8+7	Wu
1900		1707.952(19)	58549.7	1707.952(16)	0.000	5s6p $^3P'_2$	5s8d $^3D_3$	161439.23	219988.9	2.3+8	Wu
2200		1722.033(19)	58070.9	1722.043(13)	-0.010	5s6p $^3P'_2$	5s9s $^3S_1$	161439.23	219509.8	1.5+8	Wu
5300	h	1741.195(8)	57431.8	1741.190(8)	0.005	5s6p $^1P'_1$	5s8d $^1D_2$	162725.20	220157.2	8.5+7 CF	TW
3900		1796.179(8)	55673.74	1796.177(5)	0.002	5s5d $^1D_2$	5p6s $^3P'_1$	154115.63	209789.42	2.3+8 CF	TW
10000		1811.724(20)	55196.0	1811.710(14)	0.014	5s^2 $^1S_0$	5s5p $^3P'_1$	0.0	55196.47	2.9+7	TW
3200		1829.640(8)	54655.56	1829.624(4)	0.016	5s5p $^1P'_1$	5p^2 $^3P_2$	79911.87	134567.92	5.3+6 CF	TW
64000	m, bl(Sn II)		54592.4	1831.634(9)		5s5d $^1D_2$	5p5d $^3F'_3$	154115.63	208711.7	1.7+8	TW
800		1833.951(19)	54527.1	1833.931(6)	0.020	5s5d $^3D_2$	5s7p $^1P'_1$	141526.53	196054.2	1.2+7	Wu*
660		1906.137(19)	52462.1	1906.132(8)	0.005	5s6s $^1S_0$	5s7p $^1P'_1$	143591.94	196054.2	6.4+7	Wu*
230		1906.882(19)	52441.6	1906.868(7)	0.014	5s5d $^1D_2$	5p5d $^3F'_2$	154115.63	206557.65	4.9+7 CF	Wu*
490		1931.125(19)	51783.3	1931.122(11)	0.003	5s6s $^1S_0$	5s7p $^3P'_1$	143591.94	195375.3	1.7+7	Wu
4700		1941.847(8)	51497.36	1941.861(5)	-0.014	5p^2 $^1D_2$	5s4f $^1F'_3$	128205.82	179702.8	4.2+9	TW
3500		1955.511(8)	51137.53	1955.508(5)	0.003	5p^2 $^1D_2$	5s4f $^3F'_3$	128205.82	179343.43	2.0+8	TW
1400		1991.663(8)	50209.30	1991.678(6)	-0.015	5s5p $^1P'_1$	5p^2 $^3P_1$	79911.87	130120.80	6.1+6	TW
2500		2032.646(8)	49181.14	2032.651(7)	-0.005	5s5d $^1D_2$	5s5f $^1F'_3$	154115.63	203296.65	6.6+8	TW
130		2038.340(19)	49043.8	2038.345(13)	-0.005	5s6p $^3P'_1$	5s7d $^1D_2$	160215.95	209259.6	2.2+7 CF	Wu
510		2052.091(19)	48715.2	2052.110(11)	-0.019	5s6p $^3P'_0$	5s7d $^3D_1$	159940.47	208655.2	1.6+8	Wu
800		2061.767(19)	48486.6	2061.777(11)	-0.010	5s6p $^3P'_1$	5s7d $^3D_2$	160215.95	208702.3	3.5+8	Wu
310		2063.776(19)	48439.4	2063.782(10)	-0.006	5s6p $^3P'_1$	5s7d $^3D_1$	160215.95	208655.2	1.0+8	Wu
680		2066.975(8)	48364.43	2066.985(6)	-0.010	5s5d $^1D_2$	5s5f $^3F'_3$	154115.63	202479.83	1.1+8	TW
800	bl(Sn I)	2068.564(19)	48327.3	2068.565(13)	-0.001	5s6p $^3P'_1$	5s8s $^1S_0$	160215.95	208543.2	1.7+7	Wu
2000		2069.985(10)	48294.11	2069.992(5)	-0.007	5s5p $^1P'_1$	5p^2 $^1D_2$	79911.87	128205.82	2.0+8 CF	TW
210		2081.790(19)	48020.3	2081.789(11)	0.001	5s6p $^3P'_0$	5s8s $^3S_1$	159940.47	207960.78	5.8+7	Wu
490		2093.803(19)	47744.8	2093.802(10)	0.001	5s6p $^3P'_1$	5s8s $^3S_1$	160215.95	207960.78	1.6+8	Wu
800		2109.129(19)	47397.9	2109.141(11)	-0.012	5s5p $^1P'_1$	5p^2 $^3P_0$	79911.87	127309.52	8.9+6 CF	Wu
800		2111.723(19)	47339.7	2111.733(17)	-0.010	5s6p $^3P'_2$	5s7d $^3D_3$	161439.23	208778.7	6.4+8	Wu

I_{obs}[a] (A. U)	Char.[b]	λ_{obs}[c] Å	σ_{obs} cm^{-1}	λ_{Ritz}[d] Å	$\Delta\lambda_{O-Ritz}$[e] Å	Classification		E_{low} cm^{-1}	E_{upp} cm^{-1}	gA[f] S^{-1}	Lin. Ref[h]
430		2115.136(19)	47263.3	2115.147(12)	-0.011	5s6p $^3P'_2$	5s7d $^3D_2$	161439.23	208702.3	1.1+8	Wu
68		2117.277(19)	47215.5	2117.257(11)	0.020	5s6p $^3P'_2$	5s7d $^3D_1$	161439.23	208655.2	6.9+6	Wu
630		2148.283(19)	46534.2	2148.272(14)	0.011	5s6p $^1P'_1$	5s7d $^1D_2$	162725.20	209259.6	3.7+8	Wu
610		2148.847(19)	46521.9	2148.865(11)	-0.018	5s6p $^3P'_2$	5s8s $^3S_1$	161439.23	207960.78	2.6+8	Wu
390		2155.263(19)	46383.5	2155.279(16)	-0.016	5s4f $^3F'_2$	5s7g $^3G_3$	179306.57	225689.7	4.0+8	Wu
150		2156.179(19)	46363.8	2156.179(19)		5s4f $^3F'_3$	5s7g $^1G_4$	179343.43	225707.2	1.4+8 CF	Wu
320	*, m		46346.2	2156.993(18)		5s4f $^3F'_3$	5s7g $^3G_3$	179343.43	225689.7	3.0+7	Wu
320	*	2156.998(19)	46346.2	2156.998(13)	0.000	5s4f $^3F'_3$	5s7g $^3G_4$	179343.43	225689.6	3.9+8	Wu
420	*	2160.714(19)	46266.5	2160.719(19)	-0.005	5s4f $^3F'_4$	5s7g $^3G_5$	179441.24	225707.6	7.0+8	Wu
420	*, m	2160.714(19)	46266.5	2160.738(23)		5s4f $^3F'_4$	5s7g $^1G_4$	179441.24	225707.2	1.7+7	Wu
59	*	2161.58(3)	46247.9	2161.555(18)	0.03	5s4f $^3F'_4$	5s7g $^3G_3$	179441.24	225689.7		Wu
59	*	2161.58(3)	46247.9	2161.560(16)	0.02	5s4f $^3F'_4$	5s7g $^3G_4$	179441.24	225689.6	1.4+7	Wu
350		2173.851(19)	45986.9	2173.856(13)	-0.005	5s4f $^1F'_3$	5s7g $^3G_4$	179702.8	225689.6	1.4+8	Wu
150		2174.329(19)	45976.8	2174.314(12)	0.015	5s6p $^1P'_1$	5s7d $^3D_2$	162725.20	208702.3	1.1+7 CF	Wu
58		2176.564(19)	45929.6	2176.544(11)	0.020	5s6p $^1P'_1$	5s7d $^3D_1$	162725.20	208655.2	9.4+6	Wu
380		2181.871(19)	45817.9	2181.865(14)	0.006	5s6p $^1P'_1$	5s8s $^1S_0$	162725.20	208543.2	1.5+8	Wu
72		2209.963(19)	45235.5	2209.960(11)	0.003	5s6p $^1P'_1$	5s8s $^3S_1$	162725.20	207960.78	1.2+7	Wu
520	bl(Sn IV)?	2214.839(19)	45135.9	2214.891(8)	-0.052	5p^2 $^3P_2$	5s4f $^1F'_3$	134567.92	179702.8	5.9+8	Wu
250		2232.653(19)	44775.9	2232.670(8)	-0.017	5p^2 $^3P_2$	5s4f $^3F'_3$	134567.92	179343.43	1.7+7	Wu
120		2383.730(19)	41938.3	2383.713(10)	0.017	5s5d $^1D_2$	5s7p $^1P'_1$	154115.63	196054.2	3.0+7 CF	Wu*
100		2388.685(19)	41851.3	2388.712(13)	-0.027	5p^2 $^1S_0$	5s7p $^1P'_1$	154203.39	196054.2	1.1+7	Wu*
27000		2562.522(20)	39012.4	2562.522(20)		5s4f $^3F'_2$	5s6g $^3G_3$	179306.57	218318.93	9.2+8	Wu
11000		2564.951(20)	38975.4	2564.921(15)	0.030	5s4f $^3F'_3$	5s6g $^3G_4$	179343.43	218319.3	8.9+8	Wu
16000	*	2570.20(3)	38895.8	2570.20(3)	-0.01	5s4f $^3F'_4$	5s6g $^3G_5$	179441.24	218337.0	1.6+9	Wu
16000	*	2570.20(3)	38895.8	2570.20(3)		5s4f $^3F'_4$	5s6g $^1G_4$	179441.24	218337.1	3.9+7	Wu
	m		38637.3	2587.60(3)		5s4f $^1F'_3$	5s6g $^1G_4$	179702.8	218337.1	9.3+8	Wu
14000		2588.767(20)	38616.9	2588.792(15)	-0.025	5s4f $^1F'_3$	5s6g $^3G_4$	179702.8	218319.3	3.4+8	Wu
14000		2618.704(22)	38175.4	2618.647(10)	0.057	5s5d $^3D_2$	5s4f $^1F'_3$	141526.53	179702.8	2.1+8	Wu
15000		2631.833(22)	37985.0	2631.831(13)	0.002	5s5d $^3D_1$	5s4f $^3F'_2$	141321.54	179306.57	2.5+9	Wu
6600		2640.202(22)	37864.6	2640.205(11)	-0.003	5s5d $^3D_3$	5s4f $^1F'_3$	141838.23	179702.8	2.7+7	Wu

I_{obs}[a] (A. U)	Char.[b]	λ_{obs}[c] Å	σ_{obs} cm^{-1}	λ_{Ritz}[d] Å	$\Delta\lambda_{O-Ritz}$[e] Å	Classification		E_{low} cm^{-1}	E_{upp} cm^{-1}	gA[f] S^{-1}	Lin. Ref[h]
14000	bl(Sn II)	2643.563(21)	37816.5	2643.533(10)	0.030	5s5d $^3D_2$	5s4f $^3F^*_3$	141526.53	179343.43	3.6+9	Wu
11000		2646.101(21)	37780.2	2646.112(13)	-0.011	5s5d $^3D_2$	5s4f $^3F^*_2$	141526.53	179306.57	4.5+8	Wu
12000		2658.592(21)	37602.7	2658.571(18)	0.021	5s5d $^3D_3$	5s4f $^3F^*_4$	141838.23	179441.24	5.5+9	Wu
10000		2665.508(21)	37505.1	2665.504(11)	0.004	5s5d $^3D_3$	5s4f $^3F^*_3$	141838.23	179343.43	4.2+8	Wu
6800		2668.123(21)	37468.4	2668.126(13)	-0.003	5s5d $^3D_3$	5s4f $^3F^*_2$	141838.23	179306.57	1.2+7	Wu
7600		2896.12(3)	34518.8	2896.075(17)	0.05	5p^2 $^1D_2$	5s6p $^1P^*_1$	128205.82	162725.20	3.9+8	Wu
9000		3123.07(17)	32010.5	3123.106(23)	-0.04	5p^2 $^1D_2$	5s6p $^3P^*_1$	128205.82	160215.95	2.9+7	Wu
38000		3382.22(20)	29557.9	3382.34(4)	-0.12	5s4f $^1F^*_3$	5s7d $^1D_2$	179702.8	209259.6	3.6+7	Wu*
45000		3392.00(20)	29472.7	3391.90(5)	0.10	5s6p $^3P^*_1$	5s6d $^1D_2$	160215.95	189689.5	1.2+8	Wu
17000		3408.16(20)	29332.9	3407.63(6)	0.53	5s4f $^3F^*_4$	5s7d $^3D_3$	179441.24	208778.7	2.3+7	Wu
13000		3416.34(20)	29262.7	3416.28(6)	0.06	5s6d $^3D_2$	5s6f $^3F^*_3$	187999.3	217262.5	1.8+8	Wu*
7000		3455.71(20)	28929.3	3455.43(7)	0.28	5s6d $^3D_3$	5s6f $^3F^*_4$	188132.5	217064.2	2.0+8	Wu*
10000		3550.46(21)	28157.3	3550.47(3)	0.00	5p^2 $^3P_2$	5s6p $^1P^*_1$	134567.92	162725.20	5.1+7	Wu
	:			3573.14(6)		5s6p $^3P^*_0$	5s6d $^3D_1$	159940.47	187919.1	6.6+8	TW
5700		3598.43(22)	27782.0	3598.25(6)	0.18	5s6p $^3P^*_1$	5s6d $^3D_2$	160215.95	187999.3	1.4+9	Wu
5400		3608.92(22)	27701.2	3608.67(6)	0.25	5s6p $^3P^*_1$	5s6d $^3D_1$	160215.95	187919.1	4.4+8	Wu
1400		3707.68(23)	26963.4	3707.55(6)	0.13	5s6p $^1P^*_1$	5s6d $^1D_2$	162725.20	189689.5	1.5+9	Wu
3500		3729.83(24)	26803.3	3729.82(19)	0.01	5s4f $^1F^*_2$	5s5g $^3G_3$	179306.57	206109.7	2.5+9	Wu
3600	*	3735.0(3)	26766.5	3734.98(17)	0.0	5s4f $^3F^*_3$	5s5g $^3G_3$	179343.43	206109.7	2.1+8	Wu
3600	*	3735.0(3)	26766.5	3735.04(17)	-0.1	5s4f $^3F^*_3$	5s5g $^1G_4$	179343.43	206109.3	2.4+9	Wu
3300		3739.91(24)	26731.0	3739.78(6)	0.13	5s6p $^3P^*_0$	5s7s $^3S_1$	159940.47	186672.4	1.4+8	Wu
3400		3745.33(24)	26692.3	3745.20(8)	0.13	5s6p $^3P^*_2$	5s6d $^3D_3$	161439.23	188132.5	2.4+9	Wu
3400		3746.5(3)	26684.2	3746.5(3)	0.0	5s4f $^3F^*_4$	5s5g $^3G_5$	179441.24	206125.3	4.3+9	Wu
3400		3746.5(3)	26684.2	3746.50(18)	0.0	5s4f $^3F^*_4$	5s5g $^3G_4$	179441.24	206125.2	1.1+8	Wu
2900		3763.96(24)	26560.2	3763.98(7)	-0.02	5s6p $^3P^*_2$	5s6d $^3D_2$	161439.23	187999.3	4.2+8	Wu
2500		3778.88(24)	26455.3	3778.72(6)	0.16	5s6p $^3P^*_1$	5s7s $^3S_1$	160215.95	186672.4	3.6+8	Wu
2600		3783.63(24)	26422.2	3783.59(18)	0.03	5s4f $^1F^*_3$	5s5g $^3G_4$	179702.8	206125.2	2.5+9	Wu
2500		3785.94(24)	26406.0	3785.89(20)	0.06	5s4f $^1F^*_3$	5s5g $^1G_4$	179702.8	206109.3	1.0+9	Wu
1400		3906.9(3)	25588.5	3907.10(3)	-0.2	5s5d $^1D_2$	5s4f $^1F^*_3$	154115.63	179702.8	7.7+8	Wu*
1000	bl(Sn IV)	3956.0(3)	25270.9	3956.20(11)	-0.2	5s6p $^1P^*_1$	5s7s $^1S_0$	162725.20	187994.8	3.3+8	Wu*

I_{obs} [a] (A. U)	Char.[b]	λ_{obs} [c] Å	σ_{obs} cm^{-1}	λ_{Ritz} [d] Å	$\Delta\lambda_{O-Ritz}$ [e] Å	Classification		E_{low} cm^{-1}	E_{upp} cm^{-1}	gA^f S^{-1}	Lin. Ref[h]
1000		3962.1(3)	25232.0	3961.92(7)	0.2	5s6p $^3P^*_2$	5s7s $^3S_1$	161439.23	186672.4	5.7+8	Wu
900		3968.3(3)	25192.9	3968.09(7)	0.2	5s6p $^1P^*_1$	5s6d $^3D_1$	162725.20	187919.1	3.0+7	Wu*
	m		24550.6	4071.22(7)		5s7p $^3P^*_1$	5s8d $^3D_2$	195375.3	219931.0	1.2+8	Wu*
520		4089.4(3)	24446.3	4089.44(25)	0.0	5s7p $^3P^*_1$	5s9s $^1S_0$	195375.3	219821.6	1.5+7	Wu*
330		4291.1(3)	23297.4	4290.91(12)	0.2	5s6d $^3D_3$	5p5d $^3F^*_4$	188132.5	211431.0	2.1+8	Wu*
500		4330.3(3)	23086.7	4330.40(4)	-0.1	5s6s $^3S_1$	5s6p $^1P^*_1$	139639.13	162725.20	4.4+7	Wu
310		4395.9(3)	22742.2	4395.43(10)	0.4	5s5f $^3F^*_4$	5s7g $^3G_5$	202963.1	225707.6	5.8+8	Wu*
2700		4585.9(4)	21799.8	4585.85(6)	0.1	5s6s $^3S_1$	5s6p $^3P^*_2$	139639.13	161439.23	7.7+8	Wu
2100		4670.7(4)	21404.0	4670.79(5)	-0.1	5s5d $^3D_1$	5s6p $^1P^*_1$	141321.54	162725.20	7.7+6	Wu
3600		4715.8(4)	21199.2	4715.96(5)	-0.1	5s5d $^3D_2$	5s6p $^1P^*_1$	141526.53	162725.20	2.1+7	Wu
1400		4826.8(4)	20712.1	4826.68(12)	0.1	5s6d $^3D_2$	5p5d $^3F^*_3$	187999.3	208711.7	2.9+8	Wu*
8000		4858.5(4)	20576.7	4858.48(6)	0.0	5s6s $^3S_1$	5s6p $^3P^*_1$	139639.13	160215.95	3.6+8	Wu
9000		4924.3(4)	20301.6	4924.41(7)	-0.1	5s6s $^3S_1$	5s6p $^3P^*_0$	139639.13	159940.47	1.2+8	Wu
1300		5020.5(4)	19912.8	5020.52(6)	0.0	5s5d $^3D_2$	5s6p $^3P^*_2$	141526.53	161439.23	7.5+7	Wu
1300		5100.4(4)	19600.8	5100.36(7)	0.1	5s5d $^3D_3$	5s6p $^3P^*_2$	141838.23	161439.23	4.0+8	Wu
7200		5225.0(5)	19133.3	5225.05(7)	0.0	5s6s $^1S_0$	5s6p $^1P^*_1$	143591.94	162725.20	2.7+8	Wu
2000		5291.2(5)	18894.0	5291.10(7)	0.1	5s5d $^3D_1$	5s6p $^3P^*_1$	141321.54	160215.95	5.9+7	Wu
2000		5349.2(5)	18689.3	5349.13(7)	0.0	5s5d $^3D_2$	5s6p $^3P^*_1$	141526.53	160215.95	1.7+8	Wu
15000		5363.6(5)	18638.9	5363.73(13)	-0.1	5s6d $^3D_1$	5p5d $^3F^*_2$	187919.1	206557.65	2.5+8	Wu*
16000		5369.4(5)	18618.7	5369.38(8)	0.1	5s5d $^3D_1$	5s6p $^3P^*_0$	141321.54	159940.47	8.2+7	Wu
8000		6013.3(6)	16625.3	6013.73(10)	-0.5	5s6s $^1S_0$	5s6p $^3P^*_1$	143591.94	160215.95	1.6+7	Wu
18000		6503.5(7)	15372.1	6502.73(23)	0.8	5s5f $^3F^*_4$	5s6g $^3G_5$	202963.1	218337.0	9.3+8	Wu*
3400		6533.1(7)	15302.5	6535.27(21)	-2.2	5s6d $^3D_2$	5s5f $^1F^*_3$	187999.3	203296.65	8.9+7	Wu*
10000		6593.6(7)	15162.1	6592.68(24)	0.9	5s6d $^3D_3$	5s5f $^1F^*_3$	188132.5	203296.65	6.8+6	Wu*
16000		6740.6(8)	14831.4	6741.0(3)	-0.4	5s6d $^3D_3$	5s5f $^3F^*_4$	188132.5	202963.1	1.2+9	Wu
20000		6903.7(8)	14481.0	6903.92(22)	-0.2	5s6d $^3D_2$	5s5f $^3F^*_3$	187999.3	202479.83	6.5+8	Wu
27000		7079.3(9)	14121.9	7079.76(23)	-0.5	5s6d $^3D_1$	5s5f $^3F^*_2$	187919.1	202039.97	3.8+8	Wu
23000		7200.5(9)	13884.1	7200.40(21)	0.1	5s7p $^3P^*_1$	5s7d $^1D_2$	195375.3	209259.6	1.2+8	Wu
16000		7347.2(9)	13607.0	7347.05(24)	0.1	5s6d $^1D_2$	5s5f $^1F^*_3$	189689.5	203296.65	7.4+8	Wu
3800		7502.7(10)	13324.8	7501.50(22)	1.2	5s7p $^3P^*_1$	5s7d $^3D_2$	195375.3	208702.3	3.3+8	Wu*

I_{obs}[a] (A. U)	Char.[b]	λ_{obs}[c] Å	σ_{obs} cm^{-1}	λ_{Ritz}[d] Å	$\Delta\lambda_{O-Ritz}$[e] Å	Classification		E_{low} cm^{-1}	E_{upp} cm^{-1}	gA[f] S^{-1}	Lin. Ref[h]
3600		7572.2(10)	13202.6	7570.58(20)	1.6	5s7p $^1P^*_1$	5s7d $^1D_2$	196054.2	209259.6	3.9+8	Wu
4700		7740.1(10)	12916.1	7740.7(7)	-0.6	5s7p $^3P^*_2$	5s7d $^3D_3$	195863.5	208778.7	6.8+8	Wu
11000		7894.9(11)	12662.9	7894.9(11)		5s7p $^3P^*_0$	5s8s $^3S_1$	195297.9	207960.78	4.3+7	Wu
9000		7903.2(11)	12649.6	7904.15(21)	-0.9	5s7p $^1P^*_1$	5s7d $^1D_2$	196054.2	208702.3	6.7+7	Wu*
8000		8006.7(11)	12486.2	8004.84(23)	1.8	5s7p $^1P^*_1$	5s8s $^1S_0$	196054.2	208543.2	7.8+7	Wu*
7100		8264.7(12)	12096.3	8264.0(8)	0.6	5s7p $^3P^*_2$	5s8s $^3S_1$	195863.5	207960.78	1.8+8	Wu

[a] Observed relative intensities, in terms of total energy flux under the line profile, are reduced to a common arbitrary scale corresponding to a plasma in local thermodynamic equilibrium with an effective excitation temperature of 9.0 eV. These conditions correspond to exposure 1 of the experiment of Wu [6].

[b] Character of observed line: bl—blended by a close line (the blending spectrum is indicated in parentheses); h—hazy line; H—very hazy line; s—asymmetric line extending towards shorter wavelengths; *—intensity shared by two or more transitions; m—masked by a stronger neighboring line (no wavelength measured); : —the wavelength was not measured (the value in λobs is a rounded Ritz wavelength); 2x—the given wavelengths are from 2nd order of wavelengths appeared in spectrum.

[c] Observed and Ritz wavelengths are given in standard air for wavenumbers σ between 5000 cm−1 and 50 000 cm−1 and in vacuum outside of this range. The uncertainty (standard deviation) in the last digit is given in parentheses.

[d] Ritz wavelengths and their uncertainties were determined in the least-squares level optimization procedure LOPT[34].

[e] Difference between observed and Ritz wavelength. If this column is blank, and λobs is not blank, this line alone determines one of the levels involved in the assigned transition.

[f] In the weighted (g=2Jn+1, statistical weight of upper level) transition probability values, the number after the '+' symbol means the power of 10. CF: the given TP values are too unreliable when cancellation factor |CF|<0.10 in Cowan code [33].

[g] References to observed wavelengths: Wu–lines classified by Wu [6] ; Wu*—line measured by Wu [6] with our new or revised classification; TW—this work.

Table 4.2. Optimized energy levels of Sn III.

Configuration	Term	J	Energy [a] cm^{-1}	Unc. [b] cm^{-1}	Leading percentages [c]							ΔE_{p-c} [d] cm^{-1}	No. of lines [e]
$5s^2$	^1S	0	0.0	0.4	97	2	$5p^2$	^1S				0	15
5s5p	$^3P^o$	0	53547.9	0.3	100							-186	8
5s5p	$^3P^o$	1	55196.46	0.18	99							-43	20
5s5p	$^3P^o$	2	59228.50	0.20	100							229	17
5s5p	$^1P^o$	1	79911.87	0.12	97							0	19
$5p^2$	^3P	0	127309.52	0.24	96	4	$5p^2$	^1S				27	6
$5p^2$	^1D	2	128205.82		57	30	5s5d	^1D	12	$5p^2$	^3P	4	30
$5p^2$	^3P	1	130120.80	0.15	99							-49	18
$5p^2$	^3P	2	134567.92	0.12	87	7	5s5d	^1D	5	$5p^2$	^1D	25	27
5s6s	^3S	1	139639.13	0.16	99							0	17
5s5d	^3D	1	141321.54	0.13	99							-4	24
5s5d	^3D	2	141526.53	0.11	99							0	29
5s5d	^3D	3	141838.23	0.13	99							5	18
5s6s	^1S	0	143591.94	0.18	98							0	12
5s5d	^1D	2	154115.63	0.13	61	34	$5p^2$	^1D				-4	16
$5p^2$	^1S	0	154203.39	0.23	92	4	$5p^2$	^3P				-2	7
5s6p	$^3P^o$	0	159940.47	0.3	99							10	8
5s6p	$^3P^o$	1	160215.95	0.23	91	8	5s6p	$^1P^o$				-11	21
5s6p	$^3P^o$	2	161439.23	0.25	99							4	16
5s6p	$^1P^o$	1	162725.20	0.20	89	8	5s6p	$^3P^o$				9	20
5s4f	$^3F^o$	2	179306.58	0.20	96	4	5p5d	$^3F^o$				1	5
5s4f	$^3F^o$	3	179343.43	0.14	92	5	4f5s	$^1F^o$				-20	8
5s4f	$^3F^o$	4	179441.24	0.3	97	3	5p5d	$^3F^o$				-24	8

Configuration	Term	J	Energy [a] cm^{-1}		Unc.[b] cm^{-1}	Leading percentages [c]							ΔE_{∞} [d] cm^{-1}	No. of lines [e]
5s4f	$^1F^o$	3	179702.80		0.14	92	5	4f5s	$^3F^o$				44	10
5s7s	^3S	1	186672.4		0.4	100							0	7
5s6d	^3D	1	187919.1		0.4	100							7	7
5s7s	^1S	0	187994.8	R	0.7	99							0	2
5s6d	^3D	2	187999.3		0.5	99							1	8
5s6d	^3D	3	188132.5		0.5	100							-8	6
5s6d	^1D	2	189689.5		0.4	96							1	5
5s7p	$^3P^o$	0	195297.9	N	1.7	99							2	1
5s7p	$^3P^o$	1	195375.3	N	0.3	73	26	5s7p	$^1P^o$				22	6
5s7p	$^3P^o$	2	195863.5	N	1.2	99							-99	2
5s7p	$^1P^o$	1	196054.20	N	0.17	70	26	5s7p	$^3P^o$				87	10
5s5f	$^3F^o$	2	202039.97	N	0.20	64	30	5p5d	$^3F^o$				42	5
5s5f	$^3F^o$	3	202479.83	N	0.16	74	17	5p5d	$^3F^o$	5	5s5f	$^1F^o$	-14	5
5s5f	$^3F^o$	4	202963.1	N	0.3	89	9	5p5d	$^3F^o$				9	4
5s5f	$^1F^o$	3	203296.65	N	0.20	90	6	5s5f	$^3F^o$				-18	6
5s5g	^1G	4	206109.2		1.4	50	49	5s5g	^3G				2	4
5s5g	^3G	3	206109.9		1.4	99							3	4
5s5g	^3G	4	206125.2		1.4	50	49	5s5g	^1G				-2	4
5s5g	^3G	5	206125.5	R	2.4	100							-4	3
5p5d	$^3F^o$	2	206557.65		0.19	30	37	5p5d	$^1D^o$	28	5s5f	$^3F^o$	51	7
5s8s	^3S	1	207960.78		0.3	100							-3	8
5s8s	^1S	0	208543.2	N	0.3	100							-1	4
5s7d	^3D	1	208655.2		0.3	100							1	6
5s7d	^3D	2	208702.3		0.3	99							0	7
5p5d	$^3F^o$	3	208711.7	N	0.25	66	20	5s5f	$^3F^o$				-66	5

Configuration	Term	J	Energy [a] cm^{-1}		Unc. [b] cm^{-1}	Leading percentages [c]							ΔE_{o-c} [d] cm^{-1}	No. of lines [e]
5p5d	$^1D^o$	2	208732.65	R	0.18	36	24	5p5d	$^3F^o$	10	5p5d	$^3P^o$	-90	5
5s7d	^3D	3	208778.7		0.4	100							-4	4
5s7d	^1D	2	209259.6	C	0.3	98							3	6
5p6s	$^3P^o$	0	209638.9	N	0.3	96	2	5s8p	$^3P^o$				182	2
5p6s	$^3P^o$	1	209789.42	N	0.17	62	19	5p6s	$^1P^o$	14	5s8p	$^1P^o$	-90	7
$4d^95s^25p$ (2D)	$^3P^o$	2	210837.8	N	0.2	73	11	5p5d	$^1D^o$	8	$4d^95s^25p$	$^3D^o$	312	5
5p5d	$^3F^o$	4	211431.0	N	0.5	76	10	5s5f	$^3F^o$	7	5s6f	$^3F^o$	-3	2
5p5d	$^3D^o$	1	212011.30	N	0.21	45	38	5s8p	$^3P^o$	12	5p6s	$^3P^o$	-42	5
5s8p	$^3P^o$	1	212258.5	N	0.2	36	28	5p5d	$^3D^o$	15	5p5d	$^3P^o$	-106	7
5s8p	$^3P^o$	0	212452.16	N	0.50	96	2	5p5d	$^3P^o$				116	1
5s8p	$^3P^o$	2	212598.4	N	0.22	90	4	5p5d	$^3P^o$				41	6
$4d^95s^25p$ (2D)	$^3F^o$	3	213020.5	N	0.4	52	34	$4d^95s^25p$	$^1F^o$	8	$4d^95s^25p$	$^3D^o$	-167	1
5s8p	$^1P^o$	1	213170.94	N	0.22	44	22	5s8p	$^3P^o$	18	5s8p	$^1P^o$	17	6
5p5d	$^3D^o$	2	214153.21	R	0.18	33	26	5p5d	$^3P^o$	19	5p6s	$^3P^o$	93	7
5p5d	$^3D^o$	3	215779.28	N	0.19	39	42	5s6f	$^3F^o$	9	5s6f	$^3F^o$	-185	5
5p6s	$^3P^o$	2	215858.8	R	0.21	66	28	5p5d	$^3D^o$				312	5
5s6f	$^1F^o$	3	216519.87	R	0.20	50	38	5p5d	$^3D^o$	8	5s6f	$^3F^o$	8	5
5p5d	$^3P^o$	1	216753.37	N	0.21	37	32	5p5d	$^3P^o$	19	5p5d	$^3D^o$	-132	7
5s6f	$^3F^o$	2	216973.5	N	0.5	92	3	5p5d	$^3F^o$				26	2
5s6f	$^3F^o$	4	217064.2	N	0.4	70	19	$4d^95s^25p$	$^3F^o$	11	5p5d	$^3F^o$	68	2
5p6s	$^1P^o$	1	217123.1	N	0.24	43	14	$4d^95s^25p$	$^3P^o$	12	5s8p	$^1P^o$	-681	6
5s6f	$^3F^o$	3	217262.5	N	0.24	79	14	5p5d	$^3D^o$	5	5p5d	$^3F^o$	17	5
5p5d	$^3P^o$	0	217580.4	N	0.4	89	5	$4d^95s^25p$	$^3P^o$				-128	2
5p5d	$^3P^o$	2	217621.38		0.20	50	24	5p5d	$^3D^o$	12	5p6s	$^3P^o$	-85	7
$4d^95s^25p$	$^3F^o$	4	[218072]			76	23	5s6f	$^3F^o$					

Configuration	Term	J	Energy [a] cm^{-1}		Unc.[b] cm^{-1}	Leading percentages [c]							ΔE_{o-c} [d] cm^{-1}	No. of lines [e]
5s6g	^{3}G	3	218318.94	N	0.4	99							2	1
5s6g	^{3}G	4	218319.3	N	0.24	51	48	5s6g	^{1}G				2	2
5s6g	^{3}G	5	218337.0	N	0.5	100							-3	2
5s6g	^{1}G	4	218337.1	N	0.5	52	48	5s6g	^{3}G				-1	1
5s6h	^{3}H	4, 5	[218546]		Polar									
5s6h	^{1,3}H	5, 6	[218547]		Polar									
4d^{9}5s^{2}5p (2D)	^{3}P°	1	219112.5	N	0.23	42	28	4d^{9}5s^{2}5p	^{3}P°	6	5p6s	^{1}P°	431	6
5s9s	^{3}S	1	219509.8	C	0.5	100							-25	5
5s9s	^{1}S	0	219821.6	N	1.5	100							25	2
5s8d	^{3}D	1	[219918]		LSF	99								
5s8d	^{3}D	2	219931.0	N	0.4	99							-30	2
4d^{9}5s^{2}5p (2D)	^{3}F°	2	219932.3	N	0.5	67	12	4d^{9}5s^{2}5p	^{3}D°	5	4d^{9}5s^{2}5p	^{3}P°	133	2
5s8d	^{3}D	3	219988.9	N	0.6	100							-28	2
5s8d	^{1}D	2	220157.2	N	0.3	97							-5	2
5s9p	^{3}P°	0	[221702]		LSF	92	8	4d^{9}5s^{2}5p	^{3}P°					
5s9p	^{3}P°	1	221877.4	N	1.2	92	2	5s9p	^{1}P°				-49	2
5s9p	^{3}P°	2	222076.64	N	1.2	96							25	1
4d^{9}5s^{2}5p (2D)	^{3}D°	3	222453.4	N	0.3	60	25	4d^{9}5s^{2}5p	^{1}F°	7	5s7f	^{1}F°	-236	2
5s9p	^{1}P°	1	222475.0	N	1.2	75	9	4d^{9}5s^{2}5p	^{1}P°	6	5p6s	^{1}P°	115	2
4d^{9}5s^{2}5p (2D)	^{1}D°	2	222930.8	N	1.5	60	16	4d^{9}5s^{2}5p	^{3}F°	14	4d^{9}5s^{2}5p	^{3}D°	47	1
4d^{9}5s^{2}5p (2D)	^{3}P°	0	223152.4	N	0.6	87	7	5s9p	^{3}P°	5	5p5d	^{3}P°	-186	2
5s7f	^{1}F°	3	223779.1	N	0.3	72	11	5p5d	^{1}F°	9	4d^{9}5s^{2}5p	^{3}D°	17	3
4d^{9}5s^{2}5p (2D)	^{1}P°	1	224394.5	N	0.8	71	9	5s9p	^{1}P°	7	4d^{9}5s^{2}5p	^{3}D°	-38	3
5s7f	^{3}F°	3	[224721]		LSF	97								
5s7f	^{3}F°	4	[224814]		LSF	99								

Configuration	Term	J	Energy [a] cm^{-1}		Unc. [b] cm^{-1}	Leading percentages [c]						ΔE_{o-c} [d] cm^{-1}	No. of lines [e]
5s7f	$^3F^o$	2	[224823]		LSF	97	2	$4d^95s^25p$	$^3F^o$				
5s7g	^3G	4	225689.6	N	0.3	53	47	5s7g	^1G			2	3
5s7g	^3G	3	225689.7	N	0.4	99						2	2
5s7g	^1G	4	225707.2	N	0.4	53	47	5s7g	^3G			-2	1
5s7g	^3G	5	225707.6	N	0.5	99						-2	2
5s9d	^3D	1	[226473]		LSF	56	20	5s10s	^3S	17	5p6p ^3D		
5s10s	^3S	1	[226492]		Ritz	80	14	5s9d	^3D				
5s10s	^1S	0	[226647]		Ritz	99							
5s9d	^3D	2	[226723]		LSF	71	25	5s9d	^1D				
5s9d	^1D	2	[226795]		LSF	72	27	5s9d	^3D				
5s9d	^3D	3	[226806]		LSF	99							
5p5d	$^1P^o$	1	227547.4	N	0.3	64	26	5s10p	$^1P^o$			107	2
$4d^95s^25p$ (2D)	$^1F^o$	3	227598.8	N	0.6	21	21	5s8f	$^1F^o$	16	$4d^95s^25p$ $^1F^o$	27	1
5p6p	^3D	1	227646.69	N	0.3	39	29	5s9d	^3D	29	5p6p ^3P	87	3
5s8f	$^1F^o$	3	228180.6	N	0.4	41	17	$4d^95s^25p$	$^1F^o$	16	$4d^95s^25p$ $^3F^o$	-20	1
5s10p	$^1P^o$	1	228590.6	N	0.4	65	16	5p5d	$^1P^o$	5	5p6s $^1P^o$	-32	2
$4d^95s^25p$ (2D)	$^3D^o$	1	229855.3	N	0.6	78	11	$4d^95s^25p$	$^3P^o$	5	$4d^95s^25p$ $^1P^o$	138	2
5p6p	^3D	2	230187.27	N	0.4	55	15	5s10d	^3D	11	5s10d ^1D	-197	1
5p6p	^1P	1	230451.6	N	0.3	29	29	5p6p	^3P	20	5p6p ^3D	-25	3
5s8g	^3G	3, 4	[230467]		Polar								
5s8g	$^{1,3}G$	4, 5	[230487]		Polar								
5s9f	$^1F^o$	3	231080.86	N	1.1	33	31	5p5d	$^1F^o$	16	5s9f $^1F^o$	11	1
5p6p	^3P	0	231493.0	N	0.6	82	12	$5s1^1S$	^1S	5	5p6p ^1S	37	1
5s10d	^3D	2	231697.65	N	0.4	47	26	5s10d	^1D	22	5p6p ^3D	77	1
5s10f	$^1F^o$	3	233950.5	N	0.5	79	8	5p5d	$^1F^o$	7	5s10f $^1F^o$	-2	1

Configuration	Term	J	Energy [a] cm^{-1}		Unc.[b] cm^{-1}	Leading percentages [c]							ΔE_o- cm
5s1^{1}D	^{3}D	3	234376.0	N	0.4	88	10	5p6p	^{3}D				-23
5p6p	^{3}P	1	234837.3	N	0.3	38	29	5s1^{1}D	^{3}D	20	5p6p	^{1}P	69
5p6p	^{3}D	3	235582.1	N	1.1	75	11	5s1^{1}D	^{3}D	9	5s12d	^{3}D	-10
5p5d	^{1}F°	3	235773.54	N	0.5	87	4	5p5d	^{1}F°				0
5p6p	^{3}P	2	236226.4	N	0.4	37	33	5s12d	^{1}D	8	5p6p	^{3}D	97
5s12d	^{3}D	2	236473.1	N	0.4	35	34	5s12d	^{1}D	26	5s12d	^{3}D	-21
5s12d	^{3}D	3	236805.36	N	0.5	91	8	5p6p	^{3}D				13
5p6p	^{3}S	1	237757.9	N	0.3	80	11	5p6p	^{3}P	6	5p6p	^{1}P	29
Sn IV 5s $^2S_{1/2}$	**Limit**		246059	R	9								

[a] Symbols next to the energy value have the following meaning: C – previous tentative identification has been confirmed here; N – new id previous value and/or interpretation has been revised here. Values in [ ] are unobserved energy level found from the series extrapolation by a squares fitting with Cowan's codes [33]

[b] Uncertainties resulting from the level optimization procedure are given on the level of one standard deviation. They correspond to unce separations from $5p^2\ ^2D_2$. To determine uncertainties of excitation energies from the ground level, the given values should be combined in qu uncertainty of the ground level, 0.4 cm^{-1}.

[c] The first percentage value refers to the configuration and term given in the first two columns of the table. The second/third percentage v configuration and term given next to it. The percentage compositions were determined in this work by a parametric least-squares fitting with Co

[d] Differences between observed energies and those calculated in the parametric least squares fitting.

[e] Number of observed lines determining the level in the optimization procedure LOPT[34].

Table 4.3. LSF parameters (cm^{-1}) for Sn III.

Configuration	Parameter	LSF	Group [a]	STD	HFR	LSF/HFR
Even Parity						
$5s^2$	E_{av}	4812.4		83	0	
$5p^2$	E_{av}	137144.4		41	127326.7	1.0771
	$F^2(5p,5p)$	33354.3		181	40171.6	0.8303
	$\zeta(5p)$	3739.1		47	3235.8	1.1555
5s6s	E_{av}	141413.1		59	132243.4	1.0693
	$G^0(5s,6s)$	2270.5		53	2988.2	0.7598
5s7s	E_{av}	187036.9		59	178276.7	1.0491
	$G^0(5s,7s)$	711.9		52	969.2	0.7345
5s8s	E_{av}	208121.4	2	38	199142.5	1.0451
	$G^0(5s,8s)$	312.5		49	451.2	0.6926
5s9s	E_{av}	219608	2	40	210503	1.0432
	$G^0(5s,9s)$	144.8	1	1	250.1	0.5790
5s10s	E_{av}	226533.9	2	41	217393.6	1.0420
	$G^0(5s,10s)$	89	1	0	153.8	0.5787
5s11s	E_{av}	231056.5	2	42	221888.1	1.0413
	$G^0(5s,11s)$	58.8	1	0	101.6	0.5787
5s12s	E_{av}	234166.8	2	43	224983.3	1.0408
	$G^0(5s,12s)$	41	1	0	70.8	0.5791
5s13s	E_{av}	236398.8	2	43	227210.9	1.0404
	$G^0(5s,13s)$	29.7	1	0	51.3	0.5789
5s14s	E_{av}	238053.8	2	43	228863.9	1.0401
	$G^0(5s,14s)$	22.3	1	0	38.5	0.5792
5s15s	E_{av}	239316.7	2	44	230120.2	1.0400
	$G^0(5s,15s)$	17.1	1	0	29.5	0.5797
5s16s	E_{av}	240301.4	2	44	231102.7	1.0398
	$G^0(5s,16s)$	13.4	1	0	23.2	0.5776
5s17s	E_{av}	241084.9	2	44	231883.9	1.0397
	$G^0(5s,17s)$	10.7	1	0	18.5	0.5784
5s18s	E_{av}	241717.6	2	44	232523.3	1.0395
	$G^0(5s,18s)$	8.7	1	0	15.1	0.5762
5s19s	E_{av}	242237	2	44	233036.7	1.0395
	$G^0(5s,19s)$	7.2	1	0	12.4	0.5807
5s20s	E_{av}	242667.1	2	44	233461.8	1.0394
	$G^0(5s,20s)$	6	1	0	10.4	0.5769
5s5d	E_{av}	143645.7		45	133516.8	1.0759
	$\zeta(5d)$	205.5	3	38	143.7	1.4301
	$G^2(5s,5d)$	10635.6		321	14215.4	0.7482
5s6d	E_{av}	188477.2		38	179524.4	1.0499
	$\zeta(6d)$	87.2	3	16	61	1.4295
	$G^2(5s,6d)$	3034.9		222	4191.4	0.7241
5s7d	E_{av}	208957.1		37	199895.4	1.0453
	$\zeta(7d)$	45.5	3	8	31.8	1.4308
	$G^2(5s,7d)$	1420.8	4	194	1920	0.7400
5s8d	E_{av}	220129.8	5	34	210974.3	1.0434
	$\zeta(8d)$	26.7	3	5	18.7	1.4278
	$G^2(5s,8d)$	784.2	4	107	1059.9	0.7399
5s9d	E_{av}	226903.6	5	35	217702.9	1.0423
	$\zeta(9d)$	11.9		fixed	11.9	1.0000
	$G^2(5s,9d)$	482.4	4	66	651.9	0.7400
5s10d	E_{av}	231330.7	5	35	222101.6	1.0416
	$\zeta(10d)$	8.1		fixed	8.1	1.0000
	$G^2(5s,10d)$	319	4	44	431.1	0.7400
5s11d	E_{av}	234558.8		85	225136.9	1.0419
	$\zeta(11d)$	5.7		fixed	5.7	1.0000

Configuration	Parameter	LSF	Group [a]	STD	HFR	LSF/HFR
	$G^2(5s,11d)$	222.3	4	30	300.5	0.7398
5s12d	E_{av}	236581.8	5	36	227325.2	1.0407
	$\zeta(12d)$	4.2		fixed	4.2	1.0000
	$G^2(5s,12d)$	161.4	4	22	218.1	0.7400
5s13d	E_{av}	238213.7	5	36	228949.9	1.0405
	$\zeta(13d)$	3.1		fixed	3.1	1.0000
	$G^2(5s,13d)$	120.9	4	17	163.4	0.7399
5s14d	E_{av}	239455.3	5	37	230187.4	1.0403
	$\zeta(14d)$	2.4		fixed	2.4	1.0000
	$G^2(5s,14d)$	92.9	4	13	125.6	0.7397
5s15d	E_{av}	240426.7	5	37	231155.7	1.0401
	$\zeta(15d)$	1.9		fixed	1.9	1.0000
	$G^2(5s,15d)$	73	4	10	98.7	0.7396
5s16d	E_{av}	241199.4	5	37	231927.3	1.0400
	$\zeta(16d)$	1.5		fixed	1.5	1.0000
	$G^2(5s,16d)$	58.5	4	8	79.1	0.7396
5s17d	E_{av}	241831.5	5	37	232558.4	1.0399
	$\zeta(17d)$	1.2		fixed	1.2	1.0000
	$G^2(5s,17d)$	47.5	4	6	64.2	0.7399
5s18d	E_{av}	242340.1	5	37	233065.9	1.0398
	$\zeta(18d)$	1		fixed	1	1.0000
	$G^2(5s,18d)$	39.1	4	5	52.9	0.7391
5s19d	E_{av}	242760.5	5	37	233486.3	1.0397
	$\zeta(19d)$	0.9		fixed	0.9	1.0000
	$G^2(5s,19d)$	32.6	4	4	44.1	0.7392
5s20d	E_{av}	243118.3	5	37	233844	1.0397
	$\zeta(20d)$	0.7		fixed	0.7	1.0000
	$G^2(5s,20d)$	27.5	4	4	37.2	0.7393
5s5g	E_{av}	206336		37	196829.3	1.0483
	$\zeta(5g)$	0.3		fixed	0.3	1.0000
	$G^4(5s,5g)$	149.6		fixed	176	0.8500
5s6g	E_{av}	218488.6		37	209077.6	1.0450
	$\zeta(6g)$	0.2		fixed	0.2	1.0000
	$G^4(5s,6g)$	135.7		fixed	159.6	0.8503
5s7g	E_{av}	225819.7	6	37	216464.9	1.0432
	$\zeta(7g)$	0.1		fixed	0.1	1.0000
	$G^4(5s,7g)$	103.6		fixed	121.9	0.8499
5s8g	E_{av}	230572.8	6	38	221256	1.0421
	$\zeta(8g)$	0.1		fixed	0.1	1.0000
5s9g	E_{av}	233826.8	6	39	224536	1.0414
5s10g [b]	E_{av}	236154.1	6	39	226880.3	1.0409
5s11g [b]	E_{av}	237870.5	6	39	228608.7	1.0405
5s12g [b]	E_{av}	239181.3	6	39	229927.4	1.0403
5s13g [b]	E_{av}	240199.3	6	40	230951.4	1.0400
5s14g [b]	E_{av}	241011.4	6	40	231767.5	1.0399
5s15g [b]	E_{av}	241657.9	6	40	232417	1.0398
5s16g [b]	E_{av}	242188	6	40	232948.1	1.0397
5s17g [b]	E_{av}	242636.8	6	40	233397.9	1.0396
5p6p	E_{av}	234769.2		40	222980.3	1.0529
	$\zeta(5p)$	4221.7	7	59	3732.7	1.1310
	$\zeta(6p)$	1051.5	7	15	929.7	1.1310
	$F^2(5p,6p)$	11636		386	13232.7	0.8793
	$G^0(5p,6p)$	2809.7	8	79	3233.5	0.8689
	$G^2(5p,6p)$	3459.6	8	97	3981.4	0.8689
4f5p [b]	E_{av}	250001.3		fixed	240871.3	1.0379
$6s^2$ [b]	E_{av}	295566.1		fixed	293566.1	1.0068
$6p^2$ [b]	E_{av}	340413.3		fixed	336413.3	1.0119

Configuration		Parameter	LSF	Group [a]	STD	HFR	LSF/HFR
$5d^{2}$ [b]		E_{av}	288467.7		fixed	285467.7	1.0105
$4f^{2}$ [b]		E_{av}	369312.1		fixed	367312.1	1.0054
$4d^{9}5s5p^{2}$ [b]		E_{av}	284041		fixed	284041	1.0000
R^{k} parameters [c]							
$5s^2$	$5p^2$	RD^1(5s,5s,5p,5p)	39391.4	9	183	52729.1	0.7471
$5s^2$	5s6s	RD^0(5s,5s,5s,6s)	2175.5	9	10	2912.1	0.7471
$5s^2$	5s7s	RD^0(5s,5s,5s,7s)	1111.1	9	5	1487.4	0.7470
$5s^2$	5s8s	RD^0(5s,5s,5s,8s)	723	9	3	967.8	0.7471
$5s^2$	5s9s	RD^0(5s,5s,5s,9s)	524.7	9	2	702.4	0.7470
$5s^2$	5p6p	RD^1(5s,5s,5p,6p)	10718.4	9	50	14347.6	0.7471
$5p^2$	5s6s	RD^1(5p,5p,5s,6s)	-1347.7	9	-6	-1804	0.7471
$5p^2$	5s7s	RD^1(5p,5p,5s,7s)	-1118.2	9	-5	-1496.8	0.7471
$5p^2$	5s8s	RD^1(5p,5p,5s,8s)	-868.4	9	-4	-1162.5	0.7470
$5p^2$	5s9s	RD^1(5p,5p,5s,9s)	-687.1	9	-3	-919.8	0.7471
$5p^2$	5s5d	RD^1(5p,5p,5s,5d)	26800.5	9	125	35875	0.7471
$5p^2$	5s6d	RD^1(5p,5p,5s,6d)	12924.9	9	60	17301.3	0.7471
$5p^2$	5s7d	RD^1(5p,5p,5s,7d)	8311.7	9	39	11126	0.7471
$5p^2$	5s8d	RD^1(5p,5p,5s,8d)	6009.3	9	28	8044	0.7471
$5p^2$	5p6p	RD^0(5p,5p,5p,6p)	1141.3	9	5	1527.8	0.7471
		RD^2(5p,5p,5p,6p)	5129.1	9	24	6865.8	0.7471
5s6s	5s7s	RD^0(5s,6s,5s,7s)	668.6	9	3	895	0.7470
		RE^0(5s,6s,5s,7s)	1337.3	9	6	1790.1	0.7470
5s6s	5s8s	RD^0(5s,6s,5s,8s)	451.6	9	2	604.5	0.7471
		RE^0(5s,6s,5s,8s)	903.2	9	4	1209	0.7471
5s6s	5s9s	RD^0(5s,6s,5s,9s)	333.9	9	2	447	0.7470
		RE^0(5s,6s,5s,9s)	667.9	9	3	894	0.7471
5s6s	5p6p	RD^1(5s,6s,5p,6p)	15212.5	9	71	20363.4	0.7471
		RE^1(5s,6s,5p,6p)	1877.2	9	9	2512.8	0.7471
		RE^0(5s,7s,5s,8s)	524	9	2	701.4	0.7471
		RE^0(5s,7s,5s,9s)	389.1	9	2	520.9	0.7470
5s7s	5p6p	RD^1(5s,7s,5p,6p)	2388	9	11	3196.5	0.7471
		RE^1(5s,7s,5p,6p)	859.6	9	4	1150.6	0.7471
		RE^0(5s,8s,5s,9s)	266.5	9	1	356.7	0.7470
5s8s	5p6p	RD^1(5s,8s,5p,6p)	1202.8	9	6	1610	0.7471
		RE^1(5s,8s,5p,6p)	516.9	9	2	691.9	0.7471
5s9s	5p6p	RD^1(5s,9s,5p,6p)	758.7	9	4	1015.6	0.7470
		RE^1(5s,9s,5p,6p)	356.4	9	2	477.1	0.7470
5s5d	5s6d	RD^0(5s,5d,5s,6d)	597.3	9	3	799.5	0.7471
		RE^2(5s,5d,5s,6d)	5949.2	9	28	7963.6	0.7471
5s5d	5s7d	RD^0(5s,5d,5s,7d)	395.6	9	2	529.5	0.7471
		RE^2(5s,5d,5s,7d)	3932.6	9	18	5264.1	0.7471
5s5d	5s8d	RD^0(5s,5d,5s,8d)	289.9	9	1	388.1	0.7469
		RE^2(5s,5d,5s,8d)	2879.6	9	13	3854.6	0.7471
5s5d	5p6p	RD^1(5s,5d,5p,6p)	-4431.2	9	-21	-5931.6	0.7471
		RE^1(5s,5d,5p,6p)	5777	9	27	7733	0.7471
		RE^2(5s,6d,5s,7d)	2243.7	9	10	3003.4	0.7471
		RE^2(5s,6d,5s,8d)	1659.5	9	8	2221.4	0.7471
5s6d	5p6p	RD^1(5s,6d,5p,6p)	7233.9	9	34	9683.3	0.7471
		RE^1(5s,6d,5p,6p)	3520.8	9	16	4712.9	0.7471
		RE^2(5s,7d,5s,8d)	1131.3	9	5	1514.4	0.7470
5s7d	5p6p	RD^1(5s,7d,5p,6p)	5023.9	9	23	6725	0.7471
		RE^1(5s,7d,5p,6p)	2433	9	11	3256.8	0.7471
5s8d	5p6p	RD^1(5s,8d,5p,6p)	3742	9	17	5009	0.7471
		RE^1(5s,8d,5p,6p)	1820.9	9	8	2437.5	0.7470
5s10d	5p6p	RD^1(5s,10d,5p,6p)	2380.7	9	11	3186.7	0.7471
		RE^1(5s,10d,5p,6p)	1167.4	9	5	1562.6	0.7471
5s11d	5p6p	RD^1(5s,11d,5p,6p)	1985	9	9	2657.1	0.7471

Configuration	Parameter	LSF	Group [a]	STD	HFR	LSF/HFR
	RE^1(5s,11d,5p,6p)	975.7	9	5	1306.1	0.7470
5s12d 5p6p	RD^1(5s,12d,5p,6p)	1689.2	9	8	2261.1	0.7471
	RE^1(5s,12d,5p,6p)	831.8	9	4	1113.5	0.7470
Odd Parity						
5s5p	E_{av}	64247.9		166	55404.2	1.1596
	ζ(5p)	3529.4	1	89	3240	1.0893
	G^1(5s,5p)	38594.3		589	49388.9	0.7814
5s6p	E_{av}	161881.4	3	112	152807.3	1.0594
	ζ(6p)	1007.8	1	26	925.2	1.0893
	G^1(5s,6p)	3694.4		422	5568.4	0.6635
5s7p	E_{av}	196110.1		108	187197.5	1.0476
	ζ(7p)	445.4	1	11	408.9	1.0893
	G^1(5s,7p)	1232	2	494	1969.8	0.6254
5s8p	E_{av}	212749.5		130	203863.8	1.0436
	ζ(8p)	240	1	6	220.3	1.0894
	G^1(5s,8p)	602.4	2	242	963.2	0.6254
5s9p	E_{av}	221955.3		132	213308.9	1.0405
	ζ(9p)	144.4	1	4	132.6	1.0890
	G^1(5s,9p)	344	2	138	550	0.6255
5s10p	E_{av}	227941.5		360	219197.3	1.0399
	ζ(10p)	93.7	1	2	86	1.0895
	G^1(5s,10p)	216.3	2	87	345.9	0.6253
5s11p	E_{av}	232175.8	3	160	223117.1	1.0406
	ζ(11p)	64.3	1	2	59	1.0898
	G^1(5s,11p)	145.2	2	58	232.2	0.6253
5s12p	E_{av}	234929.3	3	162	225858.5	1.0402
	ζ(12p)	46	1	1	42.2	1.0901
	G^1(5s,12p)	102.4	2	41	163.8	0.6252
5s13p	E_{av}	236928	3	163	227850.1	1.0398
	ζ(13p)	34	1	1	31.2	1.0897
	G^1(5s,13p)	75.1	2	30	120	0.6258
5s14p	E_{av}	238433.5	3	165	229350.6	1.0396
	ζ(14p)	25.8	1	1	23.7	1.0886
	G^1(5s,14p)	56.7	2	23	90.6	0.6258
5s15p [b]	E_{av}	239585.2	3	165	230500.2	1.0394
5s16p [b]	E_{av}	240492.4	3	166	231405.4	1.0393
5s17p [b]	E_{av}	241208.9	3	166	232120.8	1.0392
5s18p [b]	E_{av}	241800.8	3	167	232712.7	1.0391
4f.5s	E_{av}	180615.4		180	170833	1.0573
	ζ(4f)	1.6		fixed	1.6	1.0000
	G^3(4f,5s)	3692.8	4	832	5763.2	0.6408
5s5f	E_{av}	204079.7		189	194942.6	1.0469
	ζ(5f)	1.1		fixed	1.1	1.0000
	G^3(5s,5f)	2159.9	4	487	3370.9	0.6408
5s6f	E_{av}	216942.8		139	207894.6	1.0435
	ζ(6f)	0.8		fixed	0.8	1.0000
	G^3(5s,6f)	1292.8	4	291	2017.6	0.6408
5s7f	E_{av}	224751.5		303	215677.5	1.0421
	ζ(7f)	0.5		fixed	0.5	1.0000
	G^3(5s,7f)	818.5	4	184	1277.4	0.6408
5s8f	E_{av}	229094.8		405	220708.2	1.0380
	ζ(8f)	0.4		fixed	0.4	1.0000
	G^3(5s,8f)	546.8	4	123	853.3	0.6408
5s9f	E_{av}	233435.6		265	224142	1.0415
	ζ(9f)	0.3		fixed	0.3	1.0000
	G^3(5s,9f)	382	4	86	596.1	0.6408
5s10f	E_{av}	235473.1	5	224	226587.6	1.0392

Configuration		Parameter	LSF	Group [a]	STD	HFR	LSF/HFR
		$\zeta(10f)$	0.2		fixed	0.2	1.0000
		$G^3(5s,10f)$	277	4	62	432.2	0.6409
$5s11f$ [b]		E_{av}	237222.4	5	226	228386	1.0387
$5s12f$ [b]		E_{av}	238568.2	5	227	229754.5	1.0384
$5s13f$ [b]		E_{av}	239614.9	5	228	230814.8	1.0381
$5s14f$ [b]		E_{av}	240447.6	5	229	231657	1.0380
$5s15f$ [b]		E_{av}	241112.1	5	229	232325.8	1.0378
$5s16f$ [b]		E_{av}	241657	5	230	232874.9	1.0377
$5s17f$ [b]		E_{av}	242116.7	5	230	233336.9	1.0376
5s6h		E_{av}	218550		fixed	209325.2	1.0441
		$\zeta(6h)$	0.1		fixed	0.1	1.0000
		$G^5(5s,6h)$	3.4		fixed	4	0.8500
$5s7h$ [b]		E_{av}	225850		fixed	216611.1	1.0427
$5s8h$ [b]		E_{av}	230590		fixed	221350.1	1.0417
$5s9h$ [b]		E_{av}	233838		fixed	224600.2	1.0411
$5s10h$ [b]		E_{av}	236162		fixed	226924.3	1.0407
5p5d		E_{av}	215080.9		139	201904.6	1.0653
		$\zeta(5p)$	3801.8	1	96	3490.1	1.0893
		$\zeta(5d)$	207.2		118	156.6	1.3231
		$F^2(5p,5d)$	23865.4		952	27540.6	0.8666
		$G^1(5p,5d)$	24449.7		539	27806.2	0.8793
		$G^3(5p,5d)$	15450.3	6	1009	17488.6	0.8835
5p6s		E_{av}	214160.1		148	202901.5	1.0555
		$\zeta(5p)$	3941	1	100	3617.9	1.0893
		$G^1(5p,6s)$	4152		fixed	4884.7	0.8500
$4d^95s^25p$		E_{av}	221012.2		88	217030.5	1.0184
		$\zeta(4d)$	3445.8		92	3258.4	1.0575
		$\zeta(5p)$	4163.3	1	105	3822	1.0893
		$F^2(4d,5p)$	23388.1		646	26320.6	0.8886
		$G^1(4d,5p)$	5827.5		274	8026.1	0.7261
		$G^3(4d,5p)$	6413.5	6	419	7259.6	0.8835
$5p6d$ [b]		E_{av}	259163.4		fixed	250163.4	1.0360
$5p7s$ [b]		E_{av}	258066.8		fixed	249566.8	1.0341
$4d^95s^26p$ [b]		E_{av}	329354.8		fixed	327354.8	1.0061
$4f5d$ [b]		E_{av}	332255		fixed	324755	1.0231
$4d^95s^24f$ [b]		E_{av}	347778		fixed	346778	1.0029
R^k parameters [c]							
5s5p	5s6p	$RD^0(5s,5p,5s,6p)$	1805.6	7	99	2534.6	0.7124
		$RE^1(5s,5p,5s,6p)$	10563.1	7	578	14827.9	0.7124
5s5p	5s7p	$RD^0(5s,5p,5s,7p)$	993.5	7	54	1394.6	0.7124
		$RE^1(5s,5p,5s,7p)$	5773.8	7	316	8104.9	0.7124
5s5p	5s8p	$RD^0(5s,5p,5s,8p)$	667.3	7	37	936.7	0.7124
		$RE^1(5s,5p,5s,8p)$	3866.4	7	212	5427.5	0.7124
5s5p	5p5d	$RD^1(5s,5p,5p,5d)$	26848	7	1469	37687.8	0.7124
		$RE^2(5s,5p,5p,5d)$	18388.2	7	1006	25812.4	0.7124
5s5p	5p6s	$RD^1(5s,5p,5p,6s)$	-521.1	7	-29	-731.5	0.7124
		$RE^0(5s,5p,5p,6s)$	-7.5	7	0	-10.5	0.7143
5s5p	$4d^95s^25p$	$RD^2(4d,4d,4d,5s)$	-8416	7	-461	-11813.9	0.7124
		$RD^2(4d,5p,5s,5p)$	-12594.2	7	-689	-17679	0.7124
		$RE^1(4d,5p,5s,5p)$	-11922.2	7	-653	-16735.8	0.7124
5s6p	5s7p	$RD^0(5s,6p,5s,7p)$	414.2	7	23	581.4	0.7125
		$RE^1(5s,6p,5s,7p)$	2483.8	7	136	3486.6	0.7124
5s6p	5s8p	$RD^0(5s,6p,5s,8p)$	286.7	7	16	402.5	0.7123
		$RE^1(5s,6p,5s,8p)$	1719.2	7	94	2413.4	0.7124
5s6p	5s9p	$RD^0(5s,6p,5s,9p)$	215.2	7	12	302.1	0.7123
		$RE^1(5s,6p,5s,9p)$	1290	7	71	1810.9	0.7124
5s6p	5p5d	$RD^1(5s,6p,5p,5d)$	-3135.3	7	-172	-4401.1	0.7124

Configuration		Parameter	LSF	Group [a]	STD	HFR	LSF/HFR
		RE^2(5s,6p,5p,5d)	2852	7	156	4003.5	0.7124
5s6p	5p6s	RD^1(5s,6p,5p,6s)	14480.1	7	793	20326.4	0.7124
		RE^0(5s,6p,5p,6s)	2476.1	7	136	3475.9	0.7124
5s6p	$4d^9 5s^2 5p$	RD^2(4d,6p,5s,5p)	-3944.2	7	-216	-5536.6	0.7124
		RE^1(4d,6p,5s,5p)	-3709.4	7	-203	-5207	0.7124
		RE^1(5s,7p,5s,8p)	1040.6	7	57	1460.8	0.7124
		RE^1(5s,7p,5s,9p)	784.4	7	43	1101.1	0.7124
		RE^1(5s,7p,5s,10p)	620.7	7	34	871.2	0.7124
5s7p	5p5d	RD^1(5s,7p,5p,5d)	-1711.5	7	-94	-2402.5	0.7124
		RE^2(5s,7p,5p,5d)	1177.3	7	64	1652.6	0.7124
5s7p	5p6s	RD^1(5s,7p,5p,6s)	7044.9	7	386	9889.3	0.7124
		RE^0(5s,7p,5p,6s)	1450.6	7	79	2036.3	0.7124
5s7p	$4d^9 5s^2 5p$	RD^2(4d,7p,5s,5p)	-2220	7	-122	-3116.2	0.7124
		RE^1(4d,7p,5s,5p)	-2082	7	-114	-2922.6	0.7124
		RE^1(5s,8p,5s,9p)	550.7	7	30	773	0.7124
		RE^1(5s,8p,5s,10p)	436.2	7	24	612.4	0.7123
5s8p	5p5d	RD^1(5s,8p,5p,5d)	-1205	7	-66	-1691.5	0.7124
		RE^2(5s,8p,5p,5d)	666.3	7	36	935.2	0.7124
5s8p	5p6s	RD^1(5s,8p,5p,6s)	4603.4	7	252	6462	0.7124
		RE^0(5s,8p,5p,6s)	1003.1	7	55	1408.1	0.7124
5s8p	$4d^9 5s^2 5p$	RD^2(4d,8p,5s,5p)	-1505.9	7	-82	-2113.9	0.7124
		RE^1(4d,8p,5s,5p)	-1410.9	7	-77	-1980.5	0.7124
5s9p	5p5d	RD^1(5s,9p,5p,5d)	-918.5	7	-50	-1289.4	0.7124
		RE^2(5s,9p,5p,5d)	439.9	7	24	617.5	0.7124
5s9p	5p6s	RD^1(5s,9p,5p,6s)	3360.5	7	184	4717.3	0.7124
		RE^0(5s,9p,5p,6s)	752.5	7	41	1056.4	0.7123
5s9p	$4d^9 5s^2 5p$	RD^2(4d,9p,5s,5p)	-1117.5	7	-61	-1568.6	0.7124
		RE^1(4d,9p,5s,5p)	-1046.5	7	-57	-1469	0.7124
4f.5s	5s5f	RD3(4f,5s,5s,5f)	3305.2	7	181	4639.6	0.7124
		RE^0(4f,5s,5s,5f)	236.2	7	13	331.6	0.7123
4f.5s	5s6f	RD3(4f,5s,5s,6f)	2526.4	7	138	3546.4	0.7124
		RE^0(4f,5s,5s,6f)	180.7	7	10	253.6	0.7125
4f.5s	5p5d	RD^2(4f,5s,5p,5d)	-9233.8	7	-505	-12961.9	0.7124
		RE^1(4f,5s,5p,5d)	-18747.9	7	-1026	-26317.2	0.7124
4f.5s	$4d^9 5s^2 5p$	RD^2(4d,4f,5s,5p)	5345.3	7	293	7503.5	0.7124
		RE^3(4d,4f,5s,5p)	3408.1	7	187	4784.1	0.7124
		RE^3(5s,5f,5s,6f)	1969.1	7	108	2764.1	0.7124
5s5f	5p5d	RD^1(5s,5f,5p,5d)	-10378.7	7	-568	-14569	0.7124
		RE^2(5s,5f,5p,5d)	-6523.5	7	-357	-9157.4	0.7124
5s5f	$4d^9 5s^2 5p$	RD^2(4d,5f,5s,5p)	4192.6	7	229	5885.4	0.7124
		RE^3(4d,5f,5s,5p)	2805.6	7	154	3938.4	0.7124
5s6f	5p5d	RD^1(5s,6f,5p,5d)	-6823.2	7	-373	-9578	0.7124
		RE^2(5s,6f,5p,5d)	-4804.3	7	-263	-6744	0.7124
5s6f	$4d^9 5s^2 5p$	RD^2(4d,6f,5s,5p)	3272.1	7	179	4593.2	0.7124
		RE^3(4d,6f,5s,5p)	2243.6	7	123	3149.4	0.7124
5p5d	5p6s	RD^2(5p,5d,5p,6s)	-7843.8	7	-429	-11010.8	0.7124
		RE^1(5p,5d,5p,6s)	-2947.6	7	-161	-4137.6	0.7124
5p5d	$4d^9 5s^2 5p$	RD^2(4d,5d,5s,5s)	-6473	7	-354	-9086.5	0.7124

[a] Parameters in each numbered group were linked together with their ratio fixed at the Hartree-Fock level.

[b] These highly excited configurations are unknown experimentally. They were included in the calculations in order to account for their interaction with other configurations studied in this work. Except for the average energies E_{av} given here, all other parameters of these configurations were fixed at the 85 % of the Hartree-Fock values (F^k, G^k), 80% for R^k or 100 % of the Hartree-Fock values (ζ).

[c] Other R^k parameters of both even and odd configurations were fixed at 80 % of the Hartree-Fock value.

CHAPTER 5

The spectrum of trebly ionized tin: Sn IV

The ground state of Ag-like tin is [Kr] $4d^{10}5s\ ^2S_{1/2}$. The outer electronic excitation gives rise to [Kr] $4d^{10}n\ell$ configurations with doublet structure, while core electronic excitation makes a three electron system that produces both doublet and quartet terms from the configurations like $4d^95s$ (4f+5p), $4d^95s^2$ and $4d^95p^2$. The existing spectral data, energy levels and wavelengths, on this spectrum are based on the Shenstone's unpublished analysis which is given in *Atomic Energy Levels* (AEL) compilation by Moore [1] and also listed in ASD of NIST [2]. This was, principally, the extension of previous analyses by Carroll [3], Rao [4], Rao *et al* [5] and Lang [6, 7]. Altogether, the AEL [1] contains the energy level values of $4d^{10}n\ell$ configurations ($n\ell$= 6s, 7s, 6p, 5d, 6d, 4f, 5g) and $4d^95s^2$, and a few levels (with question mark) of $4d^95s5p$ configuration. Although, some spectral lines of Sn IV, without any state identifications were already reported by many others [8-10]. In 1967, Wu [11] analyzed this spectrum again and added a few more configurations like 8s, np (n=7, 8), 5f, ng (n=5-7, nh (n=6-8) and 19 levels of $4d^95s5p$. Kaufman *et al* [12] studied the resonance transitions between $4d^{10}5s\ ^2S_{1/2}$ and $4d^95s5p$ (J=1/2, 3/2) configurations. The same transitions were complementarily studied by Dunne and O'Sullivan [13] using laser produced plasma (LPP) source. When dual laser-produced plasma (DLP) method successfully applied to spectroscopic investigations, the 4d photoabsorption spectra of Sn IV, autoionizing transitions of $4d^{10}5\ell(\ell$=s, p) $\rightarrow$ $4d^95\ell$ (np + nf) array, were firstly studied by Lysaght *et al* [14]. Recently, Ryabtsev *et al* [15, 16] has taken the high resolution vacuum spark spectra of tin in 200-650Å range. They improved energy level values of $4d^95s5p$ and established levels of highly excited $4d^{10}$ns (n= 8–10), $4d^{10}7d$ and $4d^95p^2$ configurations. Other than the wavelengths and energy levels, the transition probabilities (gA) and lifetimes of the excited states also have been experimentally determined firstly by Anderson *et al* [17] followed by Kernahan *et al* [18] and Pennington *et al* [19]. The theoretical aspects of Sn IV are also significant.

Several authors reported data on transition parameters like oscillator strength (OS) and transition probabilities etc [20-24].

We investigated this spectrum on the basis of high-resolution spectra of tin taken by us in VUV region, the measurements of tin spectra by Dr. Ryabtsev in 200–650 Å at Troitsk, Moscow and the available online spectral line list of tin by Wu [11] to cover the higher wavelength region.

5.1. The level structure of Sn IV

The Ground configuration of Sn IV is [Kr] $4d^{10}5s$ with $^2S_{1/2}$ level.

Configuration [a]	Parent Term	Term [b]	J
$4d^{10}.ns$	(^1S)	^2S	1/2
$4d^{10}.np$	(^1S)	$^2P^\circ$	1/2, 3/2
$4d^{10}.nd$	(^1S)	^2D	3/2, 5/2
$4d^{10}.nf$	(^1S)	$^2F^\circ$	5/2, 7/2
$4d^{10}.ng$	(^1S)	^2G	7/2, 9/2
$4d^{10}.nh$	(^1S)	$^2H^\circ$	7/2, 9/2
$4d^9.5s^2$	(^1S)	^2D	5/2, 3/2
$4d^9.5s.5p$	(^3D)	$^4F^\circ$	9/2, 7/2, 5/2, 3/2
		$^4D^\circ$	7/2, 5/2, 3/2, 1/2
		$^4P^\circ$	5/2, 3/2, 1/2
		$^2F^\circ$	7/2, 5/2
		$^2D^\circ$	5/2, 3/2
		$^2P^\circ$	3/2, 1/2
	(^1D)	$^2F^\circ$	7/2, 5/2
		$^2D^\circ$	5/2, 3/2
		$^2P^\circ$	3/2, 1/2
$4d^9.5p^2$	(^3P)	^4F	9/2, 7/2, 5/2, 3/2
		^4D	7/2, 5/2, 3/2, 1/2
		^4P	5/2, 3/2, 1/2
		^2F	7/2, 5/2
		^2D	5/2, 3/2
		^2P	3/2, 1/2
	(^1D)	^2G	9/2, 7/2
		^2F	7/2, 5/2
		^2D	5/2, 3/2
		^2P	3/2, 1/2
		^2S	1/2
	(^1S)	^2D	5/2, 3/2

[a] To the given configurations, the Kernel structure '[Kr]' must be added before each of it for the completeness of electronic structure. The principal quantum number, $n \geq 5$ for all ℓ except for f sub-shell ($n \geq 4$).

[b] The strict ordering of levels are governed by Hund's rule for the fine structures.

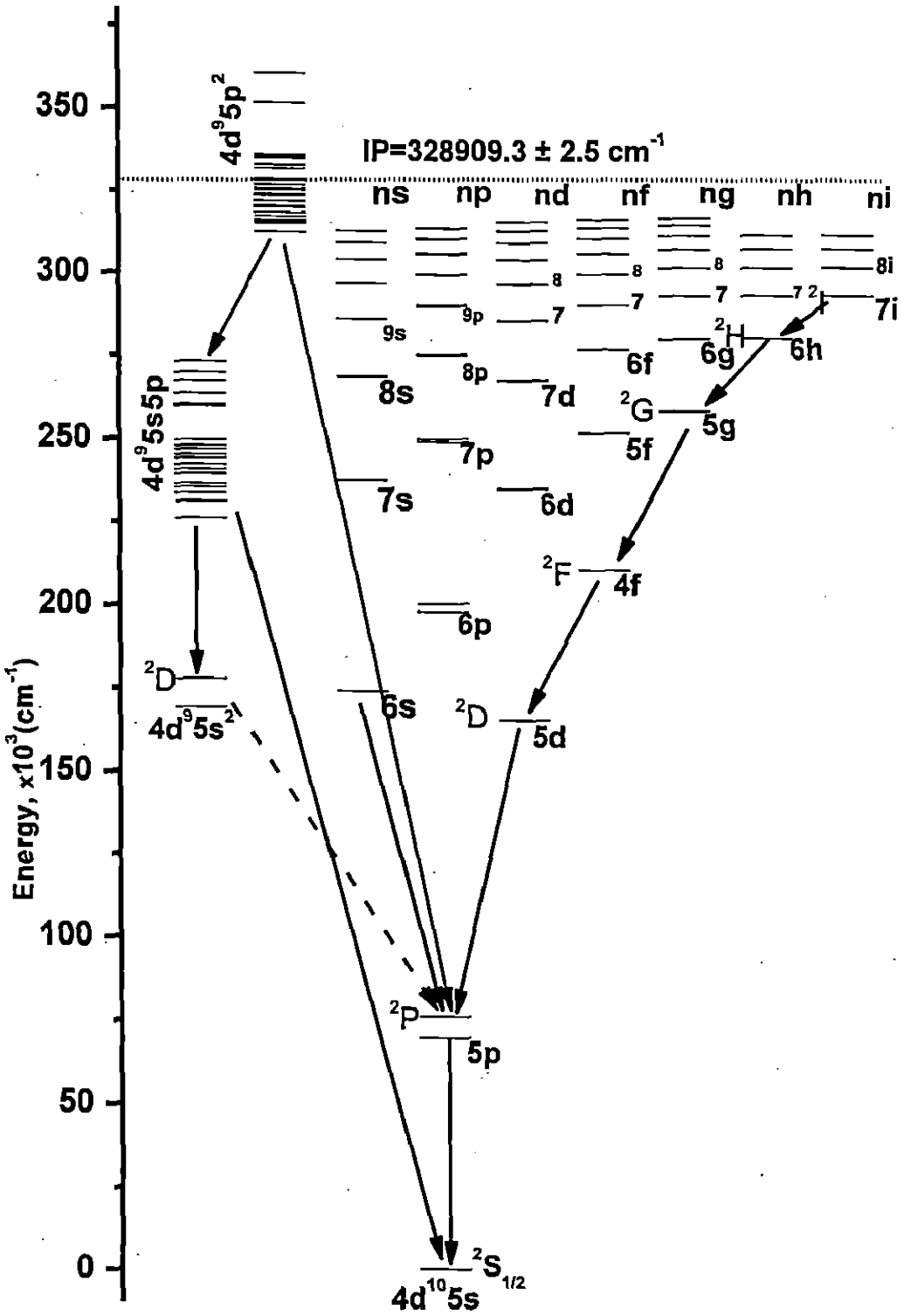

Figure 5.1. Energy level diagram of Sn IV

5.2. Results and discussion

Figure 5.1 shows the energy level structure of Sn II. The list of observed lines in this spectrum is given in table 5.1. The observed energy levels and their LS compositions obtained with least squared fitting (LSF) procedure are collected in table 5.2. and the table 5.3 contains the least squares fitted parameters of Sn IV.

5.2.1. Theoretical calculations

The theoretical predictions of Sn IV spectrum was carried out within the framework of a quasi-relativistic Hartree-Fock method with superposition of configurations implemented in Cowan's code [25]. The initial calculations were carried out with optimized scaling of Slater parameters, E_{av} and ζ_{nl} to 100% of HF value, 85% for F^k, and G^k and R^k parameters were fixed at 80% HF values, respectively. The even configurations set comprised of $4d^{10}n\ell$ (n=5-15, ℓ=s, d, g), $4d^{10}ni$ (n=7-10), $4d^95s^2$, $4d^95p^2$, $4d^95s$ (5d + 6s) and $4d^85s5p^2$ configurations, while the configurations such as $4d^{10}np$ (n=5-15), $4d^{10}nf$ (n=4-15), $4d^{10}nh$ (n=6-10), $4d^95s$ (4f+5p+6p) and $4d^85s^25p$ were included in odd parity suite. There were a total of 74 configurations included in our calculations that made it very extensive out of all existing analyses. In our least squares parametric fitting the even parity system converged to a standard deviation of 256 cm^{-1}, while the odd levels were fitted within 179 cm^{-1}. The TP values re-calculated with the fitted parameters, are given in table 5.1.

5.2.2. Analysis of the spectrum

The initial approach of the analysis was indentifying ionization character of Sn IV's previously known lines and then segregating, accordingly, the unclassified lines belonging to it. The various transition arrays and configurations studied for this spectrum are discussed in the following sub-sections.

5.2.2.1. The $4d^{10}5s - [4d^{10}np + 4d^95s5p]$ transition array

The principal transition in Ag-like Sn is $4d^{10}5p\ ^2P_{1/2,\ 3/2}$ to ground level, was firstly reported by Carroll [3] and later, in AEL [1] and Wu [11]. We observed these two resonance lines at 1314.547 and 1437.528Å. The levels of $4d^{10}6p$ are known in AEL [1], we confirmed them with improved wavelengths. Wu [11] reported the levels

of $4d^{10}np$ (n=7, 8) configurations, however none are verified as their prominent transitions were not seen. We established these two configurations at the $4d^{10}7p\ ^2P$ levels are found at 248843.8 and 249644.3 cm^{-1} with good number of supporting transitions. The levels of $4d^{10}8p$ are established at 274747.9 and 275119.8 cm^{-1}, respectively for J=1/2 and J=3/2.

Another strong excitation array connected directly to the ground level is $4d^9 5s$ (4f+5p), however, only latter is non-autoionizing configuration and number of its transitions are limited by J-selection rule. Although, some levels J≥3/2 were known in AEL [1] and almost all levels through Wu's [11] analysis, the ambiguous depictions of those were revealed when the theoretical atomic spectra was emerged, through it the picture of perturbations were more understood and accounted for. Kaufman *et al* [12] studied these ΔJ-allowed transitions of $4d^9 5s5p$ configuration in Ag-like sequence with support of Hartree-Fock calculations and reported ten levels out of eleven J=1/2, 3/2 transitions in Sn IV. In 1992, laser produced plasma spectrum of tin taken by Dunne and O'Sullivan [13] also demonstrated some of the same transitions. Recently, the high resolution spectra taken by Ryabtsev *et al* [15] revised and improved wavelengths of these transitions. However, we verified the ionization character of all the reported lines except that at 403.777 and 407.904Å for $^4D_{3/2}$ and $^4D_{1/2}$, respectively. The ionization character of second line was already mentioned as Sn V in [15]. At our spectra, on lower track the first line appeared very weak and the other is missing in contrary to prediction of two strong lines; the first somewhat weaker than the other. We observed these two lines at 403.091 and 407.462Å, in accordance with the prediction and this led to the revision of $^4D_{1/2}$ and $^4D_{3/2}$ levels now at 245424.1 and 248083 cm^{-1} respectively. Dunne and O'Sullivan [13] reported a line at 403.12Å which further confirmed our new $^4D_{3/2}$ level. The transition to high-lying $^2D_{3/2}$ could not be seen as it was weakly predicted ($gA<10^8\ sec^{-1}$). However, this level as well as the other with J≥5/2 is strongly connected to both $4d^{10}5d$ and $4d^9 5s^2$ configurations, and hence they are established from these two configurations (see the section 5.2.2.3).

5.2.2.2. The $4d^{10}5p - [4d^{10}\{ns\ (n\geq 6) + nd\ (n\geq 5)\} + 4d^9 5s^2]$ transition array

Once the low-lying excited configuration ($4d^{10}5p$) is established, the excitations to higher energetic configurations become more feasible. This fascinates

to have the transition from levels of $4d^{10}$ {ns (n≥6) + nd (n≥5)} and $4d^95s^2$ configurations. The AEL [1] and Wu [11] had reported the level values of $4d^{10}ns$ (n=6-8), $4d^{10}nd$ (n=5, 6) and ^2D of $4d^95s^2$ configurations. We confirm all of them, including the doubtful $^2D_{3/2}$ level of $4d^95s^2$ at 177885.57 cm^{-1}, with our most accurate measured wavelengths. It should be mentioned here that ^2D levels of both $4d^{10}5d$ and $4d^95s^2$ configurations are interacting with each other, as a result $4d^{10}5p \rightarrow 4d^95s^2$ transitions are observed. The further extension of the ns and nd series was done by Ryabtsev *et al* [15] from $4d^{10}5p$ levels and we confirm their reported values of ^2S series in $4d^{10}ns$ (n= 8–10). However, only $^2D_{5/2}$ of $4d^{10}7d$ is verified, but its $^2D_{3/2}$ is revised at 267215.7 cm^{-1}. Many additional transitions to $4d^{10}np$ (n=6, 7) configurations are found from our and Wu's [11] measurements. This further substantiates the observed level of the spectrum.

5.2.2.3. The $4d^{10}nf$ and $4d^95s5p$ configurations

The level values of $4d^{10}4f$ configuration were already listed in AEL [1] and Wu's [11] analysis as 210257.7 and 210318.2 cm^{-1} for J=7/2 and 5/2, respectively. These give strong transitions in ultraviolet (UV) region (~2200Å), already classified as the lines of Sn IV by [8, 9]. We confirmed the reported level values of ^2F of $4d^{10}4f$. However, we noticed the inconsistency in reported *J-inversion* of ^2F level with our least squares fitted energies of them (as $^2F_{5/2}$ indicated as the lower one, see table 5.2). This was also partially validated by the configuration interaction between ^2F levels and high-lying $4d^95s5p$ configuration, and it was observed that only $^2F_{5/2}$ is slightly perturbed and J=7/2 remains unaffected. However, due to absence of transitions accordingly (from both $4d^{10}5d$ and $4d^95s^2$ configurations) in Wu's [11] linelist, we are persevering the assignment as existing in the literature [1, 2]. In contrary to $4d^{10}4f$ configuration, $4d^{10}5f$ has considerable interaction with terms of $4d^95s5p$ and hence the terms are inverted as it has also been observed in Cd II [26] and In III [27].

The levels of $4d^95s5p$ that are excited directly from the ground $4d^{10}5s$ was discussed in above section (see section 5.2.2.1) and the remaining levels are mostly J≥5/2. It must be pointed that other than the inter-configuration interaction for $4d^95s5p$, the levels are largely subjected to spin-orbit interaction and due to which their LS components are exceedingly admixed with each other. We have established

five high-lying levels (three J=5/2 and one each for J=3/2 and 7/2) of $4d^9 5s5p$ on the basis of their strong transitions from ^2D of $4d^9 5d$ and $4d^9 5s^2$ configurations (see table 5.1). Therefore, fifteen out of 23 levels are being established from the lower configurations and the remaining eight levels could be established when $4d^9 5s5p$ – $4d^9 5p^2$ transition array is studied.

5.2.2.4. The $4d^{10}$ (ng + nh + ni) series and autoionized levels of $4d^9 5p^2$ configuration

Only 5g ^2G levels were listed in AEL [1], however Wu [11] extended the series upto 7g and used them for the determination of ionization potential (IP) of Sn IV. The transitions for $^2F_{7/2,\ 5/2}$ 4f →5g $^2G_{7/2,\ 9/2}$ were observed from Wu's [11] lines list at 2081.569 and 2084.186Å, respectively. The 6g and 7g transitions were present on our plates and they are confirmed in this work. No fine-structure spitting was observed for any of observed ^2G $4d^{10}$ng series. Since the excitation condition of Wu's electrodeless discharge source (ED) was better than our triggered spark source, hence this data motivated us to extend the analysis towards high-ng (n≥8), nh and ni series. These terms were predicted precisely using the extrapolations from the core-polarization formula (see section 5.2.5). Since ionization limit was already determined by using $4d^{10}$ng (5-7) ^2G series then extrapolating it to locate the positions of the other $4d^{10}n\ell$ (n=5-10, ℓ=4-6) terms. We established successfully the levels of $4d^{10}$ng (n=8, 9), $4d^{10}$nh (n=6-9) and $^2I_{11/2,\ 13/2}$ of $4d^{10}$ni (7-8) using Wu's [11] linelist.

The first attempt to study the low-lying autoionizing configuration $4d^9 5p^2$ of Sn IV was made by Ryabtsev *et al* [15, 16] from the ^2P levels of excited $4d^{10}5p$ configuration. The features of autoionizing lines, extra-ordinarily width of lines, could be an inducement for them to study it in the sequence from In III–Te VI and that could also be helpful for the identification of lines within the theoretical predictions. Out of 28 levels of $4d^9 5p^2$, twenty one levels having J=1/2, 3/2 and 5/2, are connected to $4d^{10}5p$ configuration. Ryabtsev *et al* [16] could observe only ten of them. These levels were also connected from $4d^9 5s5p$ configuration and are lying in 800-1900Å range. However, due to weak excitations of these lines on our plates, we could not see them with clear ionization characters and hence $4d^9 5s5p$ → $4d^9 5p^2$ array is yet to be completed. We retained observed transitions of Ryabtsev *et al* [16] just for the sake of completeness of spectral information on this ion.

5.2.3. Optimization of the energy levels

The transition wavelengths observed for this spectrum were used to derive the energy level values, for this purpose a least-squares level optimization code LOPT [28] was used. The lines observed from the Wu's [11] measurements were used after removing the systematic shifts and assigning the uncertainties (see chapter 3). Only three lines were observed from higher-order spectra, having the uncertainty 0.004Å.

The optimization of levels values have been made with the help of 139 observed lines for this spectrum, out which more than 50 lines are newly identified. Some lines are supplemented from the line list of Ryabtsev [29]. Hence a total of 66 levels observed for this ion, out of which 25 are newly observed in this work and results are given in table 5.2.

5.2.4. Intensities of observed lines

The excitation temperature for Sn IV ions in Wu's exposure is found to larger than our triggered source. The Wu's exposure 1 shows the maximum effective temperature 11.1 eV, i.e. the good excitation conditions for three-time ionized tin ion.

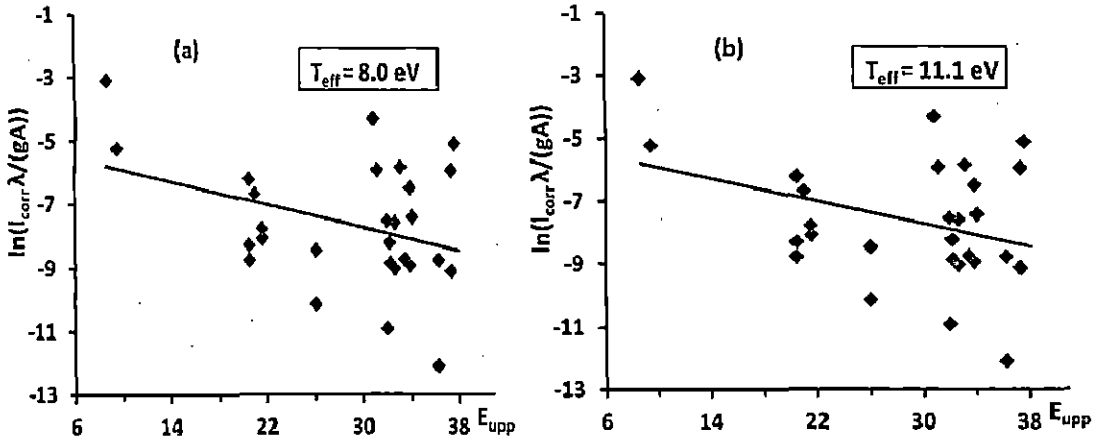

Figure 5.2. Boltzmann plots (a, b) for the triggered spark source and those for Wu's [11] ED discharge lamp. The upper level energies E_{upp} in the Boltzmann plots are given in eV. The effective temperatures given in boxes, for excitation of Sn IV ions, are derived from the negative slope of the Boltzmann plots.

The triggered vacuum spark source gave the spectrum of Sn IV ions at 8.0 eV temperature. The other exposures of Wu showed the temperatures as 10.2, 10.4 and 10.7 eV, respectively for exposure 2–4. The logarithm correction functions obtained from Sn II and Sn III were used for the corrections of the original observed intensities

of lines. The Boltzmann plots obtained for Wu's exposure 1 and those of our triggered spark light source is given in figure 5.2. By this method, reliable values of intensities of observed lines of Sn IV are given and those are given in table 5.1. Many line of Sn IV are either masked or blended, in such case either their intensities are not observed or unreliable due to the contribution of the other intra or inter ionic lines.

5.2.5. Ionization potential

The value of ionization limit of Sn IV given in AEL [1] at 328550 cm^{-1}, was derived by Ritz series extrapolation of $4d^{10}ns$ (n=6, 7). The observation of $4d^{10}ng$ (n=5-7) series by Wu [11] alternately found the limit at 328842.6 cm^{-1} (core-polarization approach). Recently, Ryabtsev *et al* [15] made the improvement in the value of ionization potential of Sn IV, at 328910 ± 5 cm^{-1}, with extended $4d^{10}ns$ (n=7-10) series observed by them. For us multiple number of series, such as ^2S $4d^{10}$ ns (n=6-11), $4d^{10}ng$ (n=5-9), $4d^{10}nh$ (n=6-9) and $4d^{10}ni$ (n=7-8), are known now. This helped us to calculate the limit more accurately applying different approximations (Ritz quantum defect and core-polarization method), with the aid of RITZPL and POLAR codes [30]. The IP obtained from $^2S_{1/2}$ $4d^{10}ns$ (n=7-10) found to be at 328904.5±2.9 cm^{-1}. However the non-penetrating sub-shells are known more accurately now, thus the limit obtained from $4d^{10}n\ell$ {$n\ell$= (5-9)g, (6-9)h, (7, 8)i} is found at 328909.3±2.5 cm^{-1} or 40.77955(31) eV. We adapt this value as the series limit of Sn IV.

References:

[1] Moore C E 1958 *Atomic Energy Levels, National Bureau of Standards Circular 467* vol. III (Washington, DC: US Govt. Printing Office)

[2] Kramida A, Ralchenko Yu., Reader J and NIST ASD Team 2012 *NIST Atomic Spectra Database, v.5.0*, National Institute of Standards and Technology, Gaithersburg, MD, USA. Available from: http://physics.nist.gov/ASD

[3] Carroll J A 1926 *Philos. Trans. R. Soc. London, Ser. A* **225** 357

[4] Rao K R 1927 *Proc. Phys. Soc.* **39** 408

[5] Rao K R, Narayan A L and Rao A S 1928 *Indian J. Phys.* **2** 477

[6] Lang R J 1927 *Proc. Natl. Acad. Sci. Amer.* **13** 341

[7] Lang R J 1929 *Proc. Natl. Acad. Sci. Amer.* **15** 414

[8] Kimura M and Nakamura 1924 *Jap. J. Phys.* **3** 197

[9] Kimura M 1924 *Jap. J. Phys.* **3** 217

[10] Gibbs R C, Vieweg A M and Gartlein C W 1929 Phys. Rev. **34** 406

[11] Wu C M 1967 *The Atomic Spark Spectra of Tin, Sn III, Sn IV, Sn V* Master thesis University of British Columbia, Canada

[12] Kaufman V, Sugar J, van Kleef Th A M and Joshi Y N 1985 *J. Opt. Soc. Am. B* **2** (3) 426

[13] Dunne P and O'Sullivan G 1992 *J. Phys. B: At. Mol. Opt. Phys.* **25** L593

[14] Lysaght M A *et al* 2005 *J. Phys. B: At. Mol. Opt. Phys.* **38** 4247

[15] Ryabtsev A N, Churilov S S and Kononov É Ya 2006 *Opt. and Spectrosc.* **100** 652

[16] Ryabtsev A N, Churilov S S and Kononov É Ya 2007 *Opt. and Spectrosc.* **102** 354

[17] Andersen T, Kirkegård Nielsen A and Sørensen G 1972 *Phys. Scr.* **6** 122

[18] Kernahan J A, Pinnington E H, Ansbacher W and Bahr J L 1985 *Nucl. Instrum. Methods Phys. Res. B* **9** 616

[19] Pinnington E H, Kernahan J A and Ansbacher W 1987 *Can. J. Phys.* **65** 7

[20] Migdalek J and Baylis W E 1979 *J. Quant. Spectrosc. Radiat. Transfer* **22** 133

[21] Cheng K T and Kim Y K 1979 *J. Opt. Soc. Am.* **69** 125

[22] Safronova U I, Savukov I M, Safronova M S and Johnson W R 2003 *Phys. Rev. A* **68** 062505

[23] Ivanova E P 2009 *Opt. and Spectrosc.***107** 1

[24] Ivanova E P 2011 *At. Data Nucl. Data Tables* **97** 1

[25] Cowan R D 1981 *The Theory of Atomic Structure and Spectra* (Berkeley, CA: University of California Press) and Cowan code package for Windows by A. Kramida, available from http://das101.isan.troitsk.ru/COWAN

[26] Shenstone A G and Pittenger J T 1949 *J. Opt. Soc. Am.* **39** 219

[27] Bhatia K S 1978 *J. Phys. B: At. Mol. Phys.* **11** 2421

[28] Kramida A E 2011 *Comput. Phys. Commun.* **182** 419

[29] Ryabtsev A N 2013 *The spectral data of tin ions*, private communication

[30] Sansonetti C J 2005 *Computer programs RITZPL and POLAR*, private communication

lines in Sn IV.

λ_{obs}[c](Å)	σ_{obs} (cm^{-1})	λ_{Ritz}[d](Å)	$\delta\lambda_{obs-Ritz}$[e] (Å)	Classification[f]		E_{low}(cm^{-1})	E_{upp}(cm^{-1})	gA[g](s^{-1})	Lin. Ref.[h]
373.836(12)	267497	373.8480(11)	-0.012	$5s\ ^2S_{1/2}$	$d^9 5s(^3D)5p\ ^2P^*_{1/2}$	0.0	267488.4	1.1+10	TW
380.349(6)	262916	380.349(3)	0.000	$5p\ ^2P^*_{1/2}$	$d^9 5p^2(^3P)\ ^2P_{1/2}$	69563.7	332480.0	8.9+9	Ry
384.804(6)	259873	384.8008(9)	0.003	$5s\ ^2S_{1/2}$	$d^9 5s(^3D)5p\ ^2P^*_{3/2}$	0.0	259874.7	3.1+10	TW
386.518(11)	258720	386.518(11)	0.000	$5p\ ^2P^*_{3/2}$	$d^9 5p^2(^3P)\ ^2P_{3/2}$	76071.65	334792	1.7+10	Ry
386.560(11)	258692	386.560(11)	0.000	$5p\ ^2P^*_{1/2}$	$d^9 5p^2(^1D)\ ^2D_{3/2}$	69563.7	328256	4.5+10	Ry
386.650(11)	258632	386.650(11)	0.000	$5p\ ^2P^*_{3/2}$	$d^9 5p^2(^1D)\ ^2F_{5/2}$	76071.65	334703.5	2.6+10	Ry
389.140(5)	256977	389.146(3)	-0.006	$5p\ ^2P^*_{1/2}$	$d^9 5p^2(^3P)\ ^2F_{3/2}$	69563.7	326536.7	1.3+8[CF]	Ry
389.724(6)	256592	389.724(6)	0.000	$5p\ ^2P^*_{3/2}$	$d^9 5p^2(^3P)\ ^4P_{3/2}$	76071.65	332663.5	2.3+10	Ry
390.003(3)	256408.3	390.003(3)	0.000	$5p\ ^2P^*_{3/2}$	$d^9 5p^2(^3P)\ ^2P_{1/2}$	76071.65	332480.0	9.2+9	Ry
391.19(3)	255630	391.19(3)	0.00	$5p\ ^2P^*_{1/2}$	$d^9 5p^2(^3P)\ ^4F_{3/2}$	69563.7	325194	8.5+9	Ry
391.33(3)	255539	391.33(3)	0.00	$5p\ ^2P^*_{3/2}$	$d^9 5p^2(^3P)\ ^2D_{5/2}$	76071.65	331610	4.9+10	Ry
396.952(3)	251919.6	396.952(3)	0.000	$5p\ ^2P^*_{3/2}$	$d^9 5p^2(^3P)\ ^4F_{5/2}$	76071.65	327991.3	1.2+9	Ry
399.263(5)	250461	399.257(4)	0.006	$5p\ ^2P^*_{3/2}$	$d^9 5p^2(^3P)\ ^2F_{3/2}$	76071.65	326536.7	1.2+8[F]	Ry
400.572(12)	249643	400.5699(9)	0.002	$5s\ ^2S_{1/2}$	$7p\ ^2P^*_{3/2}$	0.0	249644.3	1.1+9	TW
		401.8585(10)		$5s\ ^2S_{1/2}$	$7p\ ^2P^*_{1/2}$	0.0	248843.8	2.4+7[CF]	TW
403.091(6)	248083	403.091(6)	0.000	$5s\ ^2S_{1/2}$	$d^9 5s(^3D)5p\ ^4D^*_{3/2}$	0.0	248083	2.3+9	TW
406.281(9)	246135	406.268(3)	0.013	$5p\ ^2P^*_{1/2}$	$d^9 5p^2(^1D)\ ^2S_{1/2}$	69563.7	315706.6	1.0+10	Ry
407.462(6)	245422	407.4579(10)	0.004	$5s\ ^2S_{1/2}$	$d^9 5s(^3D)5p\ ^4D^*_{1/2}$	0.0	245424.1	5.8+9	TW
409.087(6)	244447	409.0766(15)	0.010	$5s\ ^2S_{1/2}$	$d^9 5s(^1D)5p\ ^2P^*_{3/2}$	0.0	244453.0	3.1+10	TW
409.520(6)	244188	409.520(6)	0.000	$5s\ ^2S_{1/2}$	$d^9 5s(^1D)5p\ ^2P^*_{1/2}$	0.0	244188.3	1.6+10	TW
415.157(6)	240873	415.1505(9)	0.006	$5s\ ^2S_{1/2}$	$d^9 5s(^1D)5p\ ^2D^*_{3/2}$	0.0	240876.5	7.8+8	TW
416.800(3)	239923.2	416.800(3)	0.000	$5p\ ^2P^*_{3/2}$	$d^9 5p^2(^3P)\ ^2D_{3/2}$	76071.65	315994.9	2.5+9[CF]	Ry
417.300(3)	239635.8	417.301(3)	-0.001	$5p\ ^2P^*_{3/2}$	$d^9 5p^2(^1D)\ ^2S_{1/2}$	76071.65	315706.6	1.4+9[CF]	Ry
422.444(6)	236718	422.4491(15)	-0.005	$5s\ ^2S_{1/2}$	$d^9 5s(^3D)5p\ ^4P^*_{1/2}$	0.0	236714.9	1.6+9	TW
424.153(6)	235764	424.153(6)	0.000	$5s\ ^2S_{1/2}$	$d^9 5s(^3D)5p\ 4F^*_{3/2}$	0.0	235764	1.5+8	TW
432.094(6)	231431	432.0862(13)	0.008	$5s\ ^2S_{1/2}$	$d^9 5s(^3D)5p\ ^4P^*_{3/2}$	0.0	231435.3	1.9+9	TW
438.698(12)	227947	438.693(4)	0.005	$5p\ ^2P^*_{3/2}$	$11s\ ^2S_{1/2}$	76071.65	304021.3	2.7+8	Ry*
439.989(6)	227278	439.9850(13)	0.004	$5p\ ^2P^*_{1/2}$	$10s\ ^2S_{1/2}$	69563.7	296844.2	2.1+8	Ry

I_{obs} [a] (A.U)	Char. [b]	λ_{obs} [c] (Å)	σ_{obs} (cm^{-1})	λ_{Ritz} [d] (Å)	$\delta\lambda_{obs-Ritz}$ [e] (Å)	Classification [f]		E_{low} (cm^{-1})	E_{upp} (cm^{-1})	gA [g] (s^{-1})	Lin. Ref [h]
6000		452.953(6)	220773	452.9549(13)	-0.002	$5p\ ^2P'_{3/2}$	$10s\ ^2S_{1/2}$	76071.65	296844.2	3.8+8	Ry
	m(Sn)	461.999(6)	216451	462.0047(14)	-0.006	$5p\ ^2P'_{1/2}$	$9s\ ^2S_{1/2}$	69563.7	286011.7	3.2+8	Ry
7000		476.330(6)	209938	476.3265(14)	0.004	$5p\ ^2P'_{3/2}$	$9s\ ^2S_{1/2}$	76071.65	286011.7	5.8+8	Ry
28000	bl(O II)	499.925(6)	200030.0	499.9243(10)	0.001	$5s\ ^2S_{1/2}$	$6p\ ^2P'_{3/2}$	0.0	200030.30	4.2+8	TW
5100		502.561(6)	198980.8	502.5641(18)	-0.003	$5p\ ^2P'_{1/2}$	$8s\ ^2S_{1/2}$	69563.7	268543.3	5.3+8	TW
24000		505.435(6)	197849.4	505.4324(12)	0.003	$5s\ ^2S_{1/2}$	$6p\ ^2P'_{1/2}$	0.0	197850.4	1.9+8	TW
4400		505.935(6)	197653.8	505.9395(13)	-0.004	$5p\ ^2P'_{1/2}$	$7d\ ^2D_{3/2}$	69563.7	267215.8	5.0+8	TW
7000		519.556(6)	192472.0	519.5570(18)	-0.001	$5p\ ^2P'_{3/2}$	$8s\ ^2S_{1/2}$	76071.65	268543.3	9.5+8	TW
4100		522.675(6)	191323.5	522.6748(11)	0.000	$5p\ ^2P'_{3/2}$	$7d\ ^2D_{5/2}$	76071.65	267395.2	8.6+8	TW
19000	2x	595.051(4)	168052.8	595.0507(15)	0.000	$5p\ ^2P'_{1/2}$	$7s\ ^2S_{1/2}$	69563.7	237616.6	1.0+9	TW
9000		605.209(6)	165232.2	605.2085(16)	0.000	$5p\ ^2P'_{1/2}$	$6d\ ^2D_{3/2}$	69563.7	234796.0	1.7+9	TW
9000	2x	619.025(4)	161544.4	619.0228(13)	0.002	$5p\ ^2P'_{3/2}$	$7s\ ^2S_{1/2}$	76071.65	237616.6	1.8+9	TW
9000	2x	628.712(4)	159055.3	628.7127(15)	-0.001	$5p\ ^2P'_{3/2}$	$6d\ ^2D_{5/2}$	76071.65	235126.82	2.8+9	TW
4500		630.020(6)	158725.1	630.0231(14)	-0.003	$5p\ ^2P'_{3/2}$	$6d\ ^2D_{3/2}$	76071.65	234796.0	3.1+8	TW
2000		911.476(19)	109712.2	911.495(4)	-0.019	$5d\ ^2D_{5/2}$	$8p\ ^2P'_{3/2}$	165409.92	275119.8	3.0+8	Wu*
900		913.709(19)	109444.0	913.709(19)	0.000	$5d\ ^2D_{3/2}$	$8p\ ^2P'_{1/2}$	165303.90	274747.9	1.7+8	Wu*
3500		926.571(19)	107924.8	926.565(6)	0.006	$5d\ ^2D_{3/2}$	$d^95s(^3D)5p\ ^2D'_{3/2}$	165303.90	273229.4	2.0+8	TW
12000		956.256(6)	104574.5	956.254(4)	0.002	$5p\ ^2P'_{1/2}$	$6s\ ^2S_{1/2}$	69563.7	174138.4	2.6+9	TW
3200		957.609(12)	104426.8	957.591(6)	0.018	$5d\ ^2D_{5/2}$	$d^95s(^3D)5p\ ^2F'_{5/2}$	165409.92	269838.6	$4.1+8^{CF}$	TW
5300		961.619(19)	103991.3	961.622(18)	-0.003	$6p\ ^2P'_{3/2}$	$11s\ ^2S_{1/2}$	200030.30	304021.3	1.1+8	Wu*
1700	m			978.622(7)		$5d\ ^2D_{3/2}$	$d^95s(^3D)5p\ ^2P'_{1/2}$	165303.90	267488.4	1.7+8	TW
5300	H, bl(Sn)	982.154(12)	101817.0	982.184(4)	-0.030	$5p\ ^2P'_{3/2}$	$d^95s^2\ ^2D_{3/2}$	76071.65	177885.57	$8.0+6^{CF}$	TW
300	m			993.973(6)		$d^95s^2\ ^2D_{5/2}$	$d^95s(^3D)5p\ ^2F'_{5/2}$	169232.20	269838.6	$2.0+9^{CF}$	TW
9000		1017.230(6)	98306.2	1017.233(4)	-0.003	$5d\ ^2D_{5/2}$	$d^95s(^3D)5p\ ^2D'_{5/2}$	165409.92	263715.8	3.2+9	TW
17000		1019.717(6)	98066.4	1019.714(4)	0.003	$5p\ ^2P'_{3/2}$	$6s\ ^2S_{1/2}$	76071.65	174138.4	4.2+9	TW
	m			1028.444(6)		$d^95s^2\ ^2D_{3/2}$	$8p\ ^2P'_{3/2}$	177885.57	275119.8	1.3+8	Wu*
	m			1032.393(25)		$d^95s^2\ ^2D_{3/2}$	$8p\ ^2P'_{1/2}$	177885.57	274747.9	1.2+8	Wu*
10000	bl(Sn)	1032.90(3)	96815	1032.90(3)	0.00	$4f\ ^2F'_{5/2}$	$9g\ ^2G_{7/2,9/2}$	210317.62	307132.5	9.4+8	Wu*
10000	bl(Sn)	1032.90(3)	96815	1032.910(6)	-0.01	$6p\ ^2P'_{3/2}$	$10s\ ^2S_{1/2}$	200030.30	296844.2	1.7+8	Wu*

I_{obs} [a] (A.U)	Char. [b]	λ_{obs} [c] (Å)	σ_{obs} (cm^{-1})	λ_{Ritz} [d] (Å)	$\delta\lambda_{obs-Ritz}$ [e] (Å)	Classification [f]		E_{low} (cm^{-1})	E_{upp} (cm^{-1})	gA [g] (s^{-1})	Lin. Ref [h]
21000		1044.494(6)	95740.1	1044.493(4)	0.001	$5p\ ^2P^*_{1/2}$	$5d\ ^2D_{3/2}$	69563.7	165303.90	1.5+10	TW
15000		1048.835(7)	95343.9	1048.836(7)	-0.001	$d^9 5s^2\ ^2D_{5/2}$	$d^9 5s(^3D)5p\ ^2D^*_{3/2}$	177885.57	273229.4	1.7+10	TW
15000		1052.771(7)	94987.4	1052.773(5)	-0.002	$5d\ ^2D_{5/2}$	$d^9 5s(^3D)5p\ ^2F^*_{7/2}$	165409.92	260397.2	3.4+9	TW
18000		1058.383(7)	94483.8	1058.385(4)	-0.002	$d^9 5s^2\ ^2D_{5/2}$	$d^9 5s(^3D)5p\ ^2D^*_{5/2}$	169232.20	263715.8	2.0+10	TW
11000		1058.595(7)	94464.8	1058.596(5)	-0.001	$5d\ ^2D_{5/2}$	$d^9 5s(^3D)5p\ ^2P^*_{3/2}$	165409.92	259874.7	2.7+9	TW
25000		1073.416(7)	93160.5	1073.416(4)	0.000	$5p\ ^2P^*_{3/2}$	$d^9 5s^2\ ^2D_{5/2}$	76071.65	169232.20	2.5+9	TW
23000		1087.507(7)	91953.4	1087.512(6)	-0.005	$d^9 5s^2\ ^2D_{3/2}$	$d^9 5s(^3D)5p\ ^2F^*_{5/2}$	177885.57	269838.6	2.1+10	TW
25000		1096.915(7)	91164.8	1096.912(5)	0.003	$d^9 5s^2\ ^2D_{5/2}$	$d^9 5s(^3D)5p\ ^2F^*_{7/2}$	169232.20	260397.2	2.6+10	TW
	m(Sn IV)			1097.977(8)		$4f\ ^2F^*_{7/2}$	$8g\ ^2G_{7/2,9/2}$	210257.03	301333.6	1.8+9	Wu*
33000		1098.705(19)	91016.2	1098.708(8)	-0.003	$4f\ ^2F^*_{5/2}$	$8g\ ^2G_{7/2,9/2}$	210317.62	301333.6	1.4+9	Wu*
23000		1103.235(10)	90642.5	1103.235(5)	0.000	$d^9 5s^2\ ^2D_{5/2}$	$d^9 5s(^3D)5p\ ^2P^*_{3/2}$	169232.20	259874.7	1.2+10	TW
7000		1116.037(7)	89602.8	1116.036(7)	0.001	$d^9 5s^2\ ^2D_{3/2}$	$d^9 5s(^3D)5p\ ^2P^*_{1/2}$	177885.57	267488.4	7.2+9	TW
40000		1119.339(7)	89338.4	1119.341(4)	-0.002	$5p\ ^2P^*_{3/2}$	$5d\ ^2D_{5/2}$	76071.65	165409.92	2.0+10	TW
39000		1120.672(7)	89232.2	1120.671(4)	0.001	$5p\ ^2P^*_{3/2}$	$5d\ ^2D_{3/2}$	76071.65	165303.90	2.5+9	TW
240	m			1134.285(8)		$6p\ ^2P^*_{1/2}$	$9s\ ^2S_{1/2}$	197850.4	286011.7	1.4+8	TW
1700	m(Sn)			1160.329(7)		$5d\ ^2D_{5/2}$	$5f\ ^2F^*_{7/2}$	165409.92	251592.4	8.4+7[CF]	TW
4000	bl(Sn II)	1163.043(8)	85981.3	1163.042(8)	0.001	$6p\ ^2P^*_{3/2}$	$9s\ ^2S_{1/2}$	200030.30	286011.7	2.6+8	TW
9000		1165.097(8)	85829.8	1165.091(6)	0.006	$d^9 5s^2\ ^2D_{3/2}$	$d^9 5s(^3D)5p\ ^2D^*_{5/2}$	177885.57	263715.8	1.7+9[CF]	TW
36000		1185.675(14)	84340.1	1185.671(6)	0.004	$5d\ ^2D_{3/2}$	$7p\ ^2P^*_{3/2}$	165303.90	249644.3	4.1+7	TW
3800		1187.179(14)	84233.3	1187.164(6)	0.015	$5d\ ^2D_{5/2}$	$7p\ ^2P^*_{3/2}$	165409.92	249644.3	1.9+8	TW
11000		1197.028(8)	83540.2	1197.033(7)	-0.005	$5d\ ^2D_{3/2}$	$7p\ ^2P^*_{1/2}$	165303.90	248843.8	2.1+8	TW
80000	bl(Sn III)	1210.195(21)	82631.3	1210.234(6)	-0.039	$4f\ ^2F^*_{7/2}$	$7g\ ^2G_{7/2,9/2}$	210257.03	292885.66	3.0+9	TW
60000		1211.131(8)	82567.5	1211.122(6)	0.009	$4f\ ^2F^*_{5/2}$	$7g\ ^2G_{7/2,9/2}$	210317.62	292885.66	2.3+9	Wu
26000	bl(Sn V)	1214.190(14)	82359.4	1214.179(7)	0.011	$d^9 5s^2\ ^2D_{5/2}$	$5f\ ^2F^*_{7/2}$	169232.20	251592.4	1.9+9	TW
9000		1219.674(10)	81989.1	1219.674(7)	0.000	$d^9 5s^2\ ^2D_{3/2}$	$d^9 5s(^3D)5p\ ^2P^*_{3/2}$	177885.57	259874.7	2.0+8[CF]	TW
70000	bl(Sn III)	1243.615(14)	80410.7	1243.594(7)	0.021	$d^9 5s^2\ ^2D_{5/2}$	$7p\ ^2P^*_{3/2}$	169232.20	249644.3	3.4+8	TW
25000		1244.086(7)	80380.3	1244.086(7)	0.000	$d^9 5s^2\ ^2D_{5/2}$	$d^9 5s(^1D)5p\ ^2D^*_{5/2}$	169232.20	249612.5	1.1+8[CF]	TW
200000		1314.547(7)	76071.8	1314.550(6)	-0.003	$5s\ ^2S_{1/2}$	$5p\ ^2P^*_{3/2}$	0.0	76071.65	5.4+9	TW
120000	bl(Sn III)	1329.414(14)	75221.1	1329.420(14)	-0.006	$d^9 5s^2\ ^2D_{5/2}$	$d^9 5s(^1D)5p\ ^2P^*_{3/2}$	169232.20	244453.0	2.2+8[CF]	TW

I_{obs} [a] (A.U)	Char. [b]	λ_{obs} [c] (Å)	σ_{obs} (cm^{-1})	λ_{Ritz} [d] (Å)	$\delta\lambda_{obs-Ritz}$ [e] (Å)	Classification [f]		E_{low} (cm^{-1})	E_{upp} (cm^{-1})	gA [g] (s^{-1})	Lin. Ref [h]
70000		1338.596(19)	74705.1	1338.591(10)	0.005	$6s\ ^2S_{1/2}$	$7p\ ^2P^*_{1/2}$	174138.4	248843.8	1.6+6	Wu*
39000	bl(Sn II)	1393.510(20)	71761.2	1393.559(10)	-0.049	$d^95s^2\ ^2D_{3/2}$	$7p\ ^2P^*_{3/2}$	177885.57	249644.3	5.5+6[CF]	TW
60000	bl(Sn III)	1395.783(7)	71644.4	1395.784(6)	-0.001	$d^95s^2\ ^2D_{5/2}$	$d^95s(^1D)5p\ ^2D^*_{3/2}$	169232.20	240876.5	8.4+7[CF]	TW
14000	m(Sn III)			1414.569(13)		$6p\ ^2P^*_{1/2}$	$8s\ ^2S_{1/2}$	197850.4	268543.3	2.6+8	TW
90000		1436.657(7)	69606.0	1436.652(6)	0.005	$4f\ ^2F^*_{7/2}$	$6g\ ^2G_{7/2,9/2}$	210257.03	279863.3	5.6+9	TW
420000		1437.528(14)	69563.9	1437.531(9)	-0.003	$5s\ ^2S_{1/2}$	$5p\ ^2P^*_{1/2}$	0.0	69563.7	2.1+9	TW
23000	m(Sn IV)	1437.879(14)	69546.9	1437.904(7)	-0.025	$4f\ ^2F^*_{5/2}$	$6g\ ^2G_{7/2,9/2}$	210317.62	279863.3	4.3+9	TW
53000		1441.645(7)	69365.2	1441.641(6)	0.004	$6p\ ^2P^*_{1/2}$	$7d\ ^2D_{3/2}$	197850.4	267215.8	6.0+8	TW
48000		1459.576(14)	68513.0	1459.577(13)	-0.001	$6p\ ^2P^*_{3/2}$	$8s\ ^2S_{1/2}$	200030.30	268543.3	4.7+8	TW
9000		1480.635(7)	67538.6	1480.636(7)	-0.001	$d^95s^2\ ^2D_{3/2}$	$d^95s(^3D)5p\ ^4D^*_{1/2}$	177885.57	245424.1	2.1+7[CF]	TW
10000		1484.453(7)	67364.9	1484.453(7)	0.000	$6p\ ^2P^*_{3/2}$	$7d\ ^2D_{5/2}$	200030.30	267395.2	9.8+8	TW
9000	bl(Sn III)	1488.407(16)	67185.9	1488.416(8)	-0.009	$6p\ ^2P^*_{3/2}$	$7d\ ^2D_{3/2}$	200030.30	267215.8	1.1+8	TW
7000			66562.5	1502.236(20)		$d^95s^2\ ^2D_{3/2}$	$d^95s(^1D)5p\ ^2P^*_{3/2}$	177885.57	244453.0	1.3+7[CF]	TW
9000		1514.618(19)	66023.2	1514.569(13)	0.049	$5d\ ^4D_{5/2}$	$d^95s(^3D)5p\ ^4P^*_{3/2}$	165409.92	231435.3	1.0+7	Wu*
10000	bl(Sn II)	1587.532(19)	62990.9	1587.530(12)	0.002	$d^95s^2\ ^2D_{3/2}$	$d^95s(^1D)5p\ ^2D^*_{3/2}$	177885.57	240876.5	3.2+7[CF]	Wu*
21000		1607.587(19)	62205.0	1607.637(14)	-0.050	$d^95s^2\ ^2D_{5/2}$	$d^95s(^3D)5p\ ^4P^*_{3/2}$	169232.20	231435.3	5.4+7	Wu*
1800		1699.836(19)	58829.2	1699.832(19)	0.004	$d^95s^2\ ^2D_{3/2}$	$d^95s(^3D)5p\ ^4P^*_{1/2}$	177885.57	236714.9	1.0+7[CF]	Wu*
	m			1800.50(8)		$5f\ ^2F^*_{7/2}$	$9g\ ^2G_{7/2,9/2}$	251592.4	307132.5	7.2+8	Wu*
	m			1804.11(8)		$5f\ ^2F^*_{5/2}$	$9g\ ^2G_{7/2,9/2}$	251703.5	307132.5	6.2+8	TW
	m			2009.756(25)		$5f\ ^2F^*_{7/2}$	$8g\ ^2G_{7/2,9/2}$	251592.4	301333.6	1.1+9	TW
410		2014.258(19)	49630.0	2014.256(18)	0.002	$5f\ ^2F^*_{5/2}$	$8g\ ^2G_{7/2,9/2}$	251703.5	301333.6	9.0+8	Wu
	m			2043.21(5)		$5g\ ^2G_{7/2,9/2}$	$9h\ ^2H^*_{9/2,11/2}$	258282.57	307209.5	3.6+8	Wu*
1000		2081.569(19)	48025.4	2081.562(14)	0.007	$4f\ ^2F^*_{7/2}$	$5g\ ^2G_{7/2,9/2}$	210257.03	258282.57	1.3+10	Wu
900		2084.186(19)	47965.1	2084.192(14)	-0.006	$4f\ ^2F^*_{5/2}$	$5g\ ^2G_{7/2,9/2}$	210317.62	258282.57	1.0+10	Wu
150		2117.977(19)	47199.9	2117.978(18)	-0.001	$7p\ ^2P^*_{3/2}$	$10s\ ^2S_{1/2}$	249644.3	296844.2	1.0+8	Wu*
540		2220.853(19)	45013.7	2220.854(13)	-0.001	$5d\ ^2D_{3/2}$	$4f\ ^2F^*_{5/2}$	165303.90	210317.62	5.4+9	Wu
330		2226.095(19)	44907.7	2226.097(12)	-0.002	$5d\ ^2D_{5/2}$	$4f\ ^2F^*_{5/2}$	165409.92	210317.62	3.4+8	Wu
520		2229.096(19)	44847.3	2229.105(13)	-0.009	$5d\ ^2D_{5/2}$	$4f\ ^2F^*_{7/2}$	165409.92	210257.03	6.8+9	Wu
110		2316.454(19)	43156.2	2316.451(19)	0.003	$5g\ ^2G_{7/2,9/2}$	$8h\ ^2H^*_{9/2,11/2}$	258282.57	301438.8	6.3+8	Wu*

I_{obs} [a] (A.U)	Char. [b]	λ_{obs} [c] (Å)	σ_{obs} (cm^{-1})	λ_{Ritz} [d] (Å)	$\delta\lambda_{obs-Ritz}$ [e] (Å)	Classification [f]		E_{low} (cm^{-1})	E_{upp} (cm^{-1})	gA [g] (s^{-1})	Lin. Ref. [h]
27		2420.957(19)	41293.4	2420.967(18)	-0.010	$5f\ ^2F^o_{7/2}$	$7g\ ^2G_{7/2,9/2}$	251592.4	292885.66	1.7+9	Wu*
29		2427.501(19)	41182.1	2427.499(18)	0.002	$5f\ ^2F^o_{5/2}$	$7g\ ^2G_{7/2,9/2}$	251703.5	292885.66	1.4+9	Wu*
80		2433.211(19)	41085.5	2433.215(14)	-0.004	$d^9 5s^2\ ^2D_{5/2}$	$4f\ ^2F^o_{5/2}$	169232.20	210317.62	3.3+7	Wu
130		2436.824(19)	41024.6	2436.809(14)	0.015	$d^9 5s^2\ ^2D_{5/2}$	$4f\ ^2F^o_{7/2}$	169232.20	210257.03	6.8+8	Wu
430		2499.689(19)	39992.9	2499.685(19)	0.004	$6d\ ^2D_{5/2}$	$8p\ ^2P^o_{3/2}$	235126.82	275119.8	1.2+8	Wu
1600		2513.909(19)	39766.7	2513.942(16)	-0.033	$6p\ ^2P^o_{1/2}$	$7s\ ^2S_{1/2}$	197850.4	237616.6	6.0+8	Wu
700		2659.777(21)	37586.0	2659.753(17)	0.024	$6p\ ^2P^o_{3/2}$	$7s\ ^2S_{1/2}$	200030.30	237616.6	1.0+9	Wu
700		2705.909(22)	36945.2	2705.880(18)	0.029	$6p\ ^2P^o_{1/2}$	$6d\ ^2D_{3/2}$	197850.4	234796.0	2.8+9	Wu
600				2748.90(5)		$7p\ ^2P^o_{3/2}$	$9s\ ^2S_{1/2}$	249644.3	286011.7	1.7+8	Wu*
540		2848.437(24)	35096.7	2848.448(22)	-0.011	$6p\ ^2P^o_{3/2}$	$6d\ ^2D_{5/2}$	200030.30	235126.82	4.2+9	Wu
370		2875.54(3)	34765.9	2875.554(20)	-0.02	$6p\ ^2P^o_{3/2}$	$6d\ ^2D_{3/2}$	200030.30	234796.0	4.6+8	Wu
380	m			2876.21(15)		$5g\ ^2G_{7/2,9/2}$	$7h\ ^2H^o_{9/2,11/2}$	258282.57	293040.3	1.4+9	Wu*
400		2878.82(3)	34726.3	2878.809(19)	0.01	$5d\ ^2D_{3/2}$	$6p\ ^2P^o_{3/2}$	165303.90	200030.30	1.5+8	Wu
500		2887.61(3)	34620.6	2887.625(19)	-0.02	$5d\ ^2D_{5/2}$	$6p\ ^2P^o_{3/2}$	165409.92	200030.30	1.1+9	Wu
800		3071.64(16)	32546.4	3071.63(3)	0.01	$5d\ ^2D_{3/2}$	$6p\ ^2P^o_{1/2}$	165303.90	197850.4	6.0+8	Wu
1200		3246.13(18)	30797.0	3246.02(3)	0.11	$d^9 5s^2\ ^2D_{5/2}$	$6p\ ^2P^o_{3/2}$	169232.20	200030.30	1.6+8	Wu
1300		3536.15(21)	28271.3	3536.20(7)	-0.05	$5f\ ^2F^o_{7/2}$	$6g\ ^2G_{7/2,9/2}$	251592.4	279863.3	2.6+9	Wu*
800	bl(Sn III)	3550.46(21)	28157.3	3550.15(7)	0.31	$5f\ ^2F^o_{5/2}$	$6g\ ^2G_{7/2,9/2}$	251703.5	279863.3	2.1+9	Wu*
180	m	3655.85(23)	27345.7	3655.77(17)	0.07	$6g\ ^2G_{7/2,9/2}$	$9h\ ^2H^o_{9/2,11/2}$	279863.3	307209.5	3.9+8	Wu*
140		3861.3(3)	25890.6	3861.12(7)	0.2	$6s\ ^2S_{1/2}$	$6p\ ^2P^o_{3/2}$	174138.4	200030.30	9.2+8	Wu
90		3956.0(3)	25270.9	3956.08(8)	-0.1	$6d\ ^2D_{5/2}$	$d^9 5s(^3D)5p\ ^2F^o_{7/2}$	235126.82	260397.2	1.9+8	Wu*
56		4019.7(3)	24870.7	4019.81(6)	-0.1	$4f\ ^2F^o_{7/2}$	$6d\ ^2D_{5/2}$	210257.03	235126.82	4.5+8	Wu
51		4029.7(3)	24808.7	4029.62(6)	0.1	$4f\ ^2F^o_{5/2}$	$6d\ ^2D_{5/2}$	210317.62	235126.82	2.2+7	Wu
54		4084.1(3)	24478.1	4084.08(6)	0.0	$4f\ ^2F^o_{5/2}$	$6d\ ^2D_{3/2}$	210317.62	234796.0	3.0+8	Wu
45		4216.2(3)	23711.1	4216.09(9)	0.2	$6s\ ^2S_{1/2}$	$6p\ ^2P^o_{1/2}$	174138.4	197850.4	3.5+8	Wu
180		4588.4(4)	21787.8	4588.4(4)	0.0	$5g\ ^2G_{7/2,9/2}$	$6h\ ^2H^o_{9/2,11/2}$	258282.57	280070.4	4.2+9	Wu*
120		4633.5(4)	21575.8	4633.59(11)	-0.1	$6g\ ^2G_{7/2,9/2}$	$8h\ ^2H^o_{9/2,11/2}$	279863.3	301438.8	6.7+8	Wu*
130		4673.2(4)	21392.4	4673.2(4)	0.0	$6h\ ^2H^o_{9/2,11/2}$	$8i\ ^2I_{11/2,13/2}$	280070.4	301462.8	7.4+8	Wu*
600			19692.9	5074.86(20)		$7p\ ^2P^o_{1/2}$	$8s\ ^2S_{1/2}$	248843.8	268543.3	2.0+8	Wu*

I_{obs} [a](A.U)	Char.[b]	λ_{obs} [c](Å)	σ_{obs} (cm^{-1})	λ_{Ritz} [d](Å)	$\delta\lambda_{obs-Ritz}$ [e] (Å)	Classification [f]		E_{low}(cm^{-1})	E_{upp}(cm^{-1})	gA [g] (s^{-1})	Lin. Ref [h]
700	bl(Sn III)	5291.2(10)	18894	5289.81(21)	1.4	$7p\ ^2P'_{3/2}$	$8s\ ^2S_{1/2}$	249644.3	268543.3	3.4+8	Wu*
300		5441.4(5)	18372.5	5441.55(17)	-0.2	$7p\ ^2P'_{1/2}$	$7d\ ^2D_{3/2}$	248843.8	267215.8	7.8+8	Wu*
400	bl(Sn I)	5631.9(5)	17751.0	5631.95(17)	0.0	$7p\ ^2P'_{3/2}$	$7d\ ^2D_{5/2}$	249644.3	267395.2	1.2+9	Wu*
900		5914.3(6)	16903.6	5912.90(19)	1.4	$6d\ ^2D_{3/2}$	$5f\ ^2F'_{5/2}$	234796.0	251703.5	9.4+8	Wu*
800		6069.3(6)	16471.9	6071.59(20)	-2.3	$6d\ ^2D_{5/2}$	$5f\ ^2F'_{7/2}$	235126.82	251592.4	1.2+9	Wu*
300	m(Sn)			6326.24(23)		$5f\ ^2F'_{7/2}$	$7d\ ^2D_{5/2}$	251592.4	267395.2	3.5+8	Wu*
900		6733.8(8)	14846.4	6732.92(22)	0.9	$6d\ ^2D_{3/2}$	$7p\ ^2P'_{3/2}$	234796.0	249644.3	4.5+7	Wu*
270		6886.4(8)	14517.5	6886.35(24)	0.0	$6d\ ^2D_{5/2}$	$7p\ ^2P'_{3/2}$	235126.82	249644.3	3.8+8	Wu*
290		6979.1(8)	14324.5	6979.4(6)	-0.3	$7g\ ^2G_{7/2,9/2}$	$9h\ ^2H'_{9/2,11/2}$	292885.66	307209.5	3.2+8	Wu*
480	bl(Sn I)	7117.2(9)	14046.6	7116.6(3)	0.6	$6d\ ^2D_{3/2}$	$7p\ ^2P'_{1/2}$	234796.0	248843.8	1.8+8	Wu*
700		7586.9(10)	13177.0	7586.9(10)	0.0	$6g\ ^2G_{7/2,9/2}$	$7h\ ^2H'_{9/2,11/2}$	279863.3	293040.3	1.3+9	Wu*
600		7697.6(10)	12987.4	7697.6(10)	0.0	$6h\ ^2H'_{9/2,11/2}$	$7i\ ^2I_{11/2,13/2}$	280070.4	293057.83	2.4+9	Wu*
220		8310.5(12)	12029.7	8311.9(3)	-1.4	$7s\ ^2S_{1/2}$	$7p\ ^2P'_{3/2}$	237616.6	249644.3	2.5+8	Wu*

[a] Observed relative intensities, in terms of total energy flux under the line profile, are reduced to a common arbitrary scale corresponding to a plasma in local thermodynamic equilibrium with an effective excitation temperature of 11.1 eV. These conditions correspond to exposure 1 of the experiment of Wu [11] (see section 5.3.4).

[b] Character of observed line: bl – blended by a close line (the blending spectrum is indicated in parentheses); e – the given intensity from original work Ryabtsev et al [15, 16] and they have been excluded from the given LTE model; h – hazy line; H – very hazy line; * – intensity shared by two or more transitions; m – masked by a stronger neighboring line (no wavelength measured); : – the wavelength was not measured (the value in λ_{obs} is a rounded Ritz wavelength)

[c] Observed and Ritz wavelengths are given in standard air for wavenumbers σ between 5000 cm^{-1} and 50000 cm^{-1} and in vacuum outside of this range. The uncertainty (standard deviation) in the last digit is given in parentheses.

[d] Ritz wavelengths and their uncertainties were determined in the least-squares level optimization procedure (see section 5.3.3).

[e] Difference between observed and Ritz wavelength. If this column is blank, and λ_{obs} is not blank, this line alone determines one of the levels involved in the assigned transition. An "x" after the value indicates that this line was excluded from the level optimization.

[f] The completely filled shell $4d^{10}$ omitted for each $4d^{10}n[$ configurations, $d^9 5s^2$ and $d^9 5s(^M T)5p$ stands for $4d^9 5s^2$ and $4d^9 5s5p$ configurations.
In the transition probability values, the number after the "+" symbol means the power of 10.

[g] Markings to the cancellation effects involved for the computed gA values: the given gA values are too unreliable when their |CF|< 0.1

[h] References to observed wavelengths: TW – This work; Ry – Ryabtsev et al [15, 16]; Ry* – lines measured by Ryabtsev [29] with our revised or new identification; Wu – Wu 67 [11]; Wu* – line measured by Wu [11] with our new or revised classification

Table 5.2. Optimized energy levels of Sn IV.

Configuration	Term	J	Energy [a] cm^{-1}		Unc. [b] cm^{-1}	Leading percentages [c]	ΔE_{o-c} [d] cm^{-1}	No. of lines [e]
$4d^{10}5s$	^2S	1/2	0.0		0.4	99	0	12
$4d^{10}5p$	$^2P^o$	1/2	69563.7		0.4	100	-32	12
$4d^{10}5p$	$^2P^o$	3/2	76071.65		0.3	100	33	17
$4d^{10}5d$	^2D	3/2	165303.90		0.23	99	44	8
$4d^{10}5d$	^2D	5/2	165409.92		0.23	87 13 $4d^95s^2$ ^2D	-51	11
$4d^95s^2$	^2D	5/2	169232.2		0.3	84 13 $4d^{10}5d$ ^2D	8	12
$4d^{10}6s$	^2S	1/2	174138.4		0.4	100	0	5
$4d^95s^2$	^2D	3/2	177885.57	C	0.40	96 2 $4d^95p^2(1S)$ ^2D	0	10
$4d^{10}6p$	$^2P^o$	1/2	197850.4		0.3	100	32	6
$4d^{10}6p$	$^2P^o$	3/2	200030.3			100	-33	14
$4d^{10}4f$	$^2F^o$	7/2	210257.03	I?	0.30	100	-48	6
$4d^{10}4f$	$^2F^o$	5/2	210317.62	I?	0.30	99	48	9
$4d^95s(^3D)5p$	$^4P^o$	5/2	[226278]			89 9 $4d^95s(^3D)5p$ $^4D^o$		
$4d^95s(^3D)5p$	$^4F^o$	7/2	[230978]			72 13 $4d^95s(^3D)5p$ $^4D^o$ 9 $4d^95s(^3D)5p$ $^2F^o$		
$4d^95s(^3D)5p$	$^4F^o$	5/2	[231228]			55 25 $4d^95s(^1D)5p$ $^2F^o$ 10 $4d^95s(^3D)5p$ $^2F^o$		
$4d^95s(^3D)5p$	$^4P^o$	3/2	231435.3			71 14 $4d^95s(^3D)5p$ $^4D^o$ 9 $4d^95s(^1D)5p$ $^2P^o$	20	3
$4d^95s(^3D)5p$	$^4F^o$	4.5	[233919]			100		
$4d^{10}6d$	^2D	3/2	234796.00		0.24	100	0	8
$4d^{10}6d$	^2D	5/2	235126.82		0.30	100	0	8
$4d^95s(^3D)5p$	$^4F^o$	3/2	235764		3	82 9 $4d^95s(^3D)5p$ $^4P^o$	-317	1
$4d^95s(^3D)5p$	$^4P^o$	1/2	236714.9		0.8	81 9 $4d^95s(^1D)5p$ $^2P^o$ 9 $4d^95s(^3D)5p$ $^4D^o$	-30	2
$4d^{10}7s$	^2S	1/2	237616.60		0.24	100	0	5

Configuration	Term	J	Energy [a] cm^{-1}		Unc. [b] cm^{-1}	Leading percentages [c]							ΔE_{o-c} [d] cm^{-1}	No. of lines [e]
$4d^9 5s(^3D)5p$	$^4D^\circ$	5/2	[239418]			39	32	$4d^9 5s(^1D)5p$	$^2F^\circ$	8	$4d^9 5s(^3D)5p$	$^2F^\circ$		
$4d^9 5s(^3D)5p$	$^4D^\circ$	7/2	[239661]			80	12	$4d^9 5s(^1D)5p$	$^2F^\circ$					
$4d^9 5s(^1D)5p$	$^2D^\circ$	3/2	240876.5		0.4	42	17	$4d^9 5s(^3D)5p$	$^2D^\circ$	13	$4d^9 5s(^3D)5p$	$^4D^\circ$	195	3
$4d^9 5s(^3D)5p$	$^4F^\circ$	5/2	[242328]			33	19	$4d^9 5s(^1D)5p$	$^2F^\circ$	18	$4d^9 5s(^1D)5p$	$^2D^\circ$		
$4d^9 5s(^1D)5p$	$^2P^\circ$	1/2	244188.3		4	59	16	$4d^9 5s(^3D)5p$	$^4P^\circ$	13	$4d^9 5s(^3D)5p$	$^2P^\circ$	-188	1
$4d^9 5s(^1D)5p$	$^2P^\circ$	3/2	244453.0		0.8	68	17	$4d^9 5s(^3D)5p$	$^4D^\circ$	10	$4d^9 5s(^3D)5p$	$^2P^\circ$	64	2
$4d^9 5s(^3D)5p$	$^4D^\circ$	1/2	245424.1	N	0.5	78	11	$4d^9 5s(^1D)5p$	$^2P^\circ$	8	$4d^9 5s(^3D)5p$	$^2P^\circ$	117	2
$4d^9 5s(^1D)5p$	$^2F^\circ$	7/2	[246996]			44	24	$4d^9 5s(^3D)5p$	$^2F^\circ$	23	$4d^9 5s(^3D)5p$	$^4F^\circ$		
$4d^9 5s(^3D)5p$	$^4D^\circ$	3/2	248083	N	4	51	23	$4d^9 5s(^1D)5p$	$^2D^\circ$	11	$4d^9 5s(^3D)5p$	$^2D^\circ$	197	1
$4d^{10}7p$	$^2P^\circ$	1/2	248843.8	N	0.5	99							77	4
$4d^9 5s(^1D)5p$	$^2D^\circ$	5/2	249612.5	N	0.5	37	33	$4d^9 5s(^3D)5p$	$^4D^\circ$	22	$4d^9 5s(^3D)5p$	$^2D^\circ$	-66	1
$4d^{10}7p$	$^2P^\circ$	3/2	249644.3	N	0.4	98							-82	11
$4d^{10}5f$	$^2F^\circ$	7/2	251592.4	N	0.5	94	6	$4d^9 5s(^3D)5p$	$^2F^\circ$				42	4
$4d^{10}5f$	$^2F^\circ$	5/2	251703.5	N	0.5	98	2	$4d^9 5s(^3D)5p$	$^2F^\circ$				-52	4
$4d^{10}5g$	^2G	7/2,9/2	258282.57		0.4	100							2	3
$4d^9 5s(^3D)5p$	$^2P^\circ$	3/2	259874.7	N	0.5	85	8	$4d^9 5s(^1D)5p$	$^2P^\circ$				112	4
$4d^9 5s(^3D)5p$	$^2F^\circ$	7/2	260397.2	N	0.5	57	36	$4d^9 5s(^1D)5p$	$^2F^\circ$	5	$4d^{10}5f$	$^2F^\circ$	234	3
$4d^9 5s(^3D)5p$	$^2D^\circ$	5/2	263715.8	N	0.4	47	24	$4d^9 5s(^3D)5p$	$^2F^\circ$	23	$4d^9 5s(^1D)5p$	$^2D^\circ$	-337	3
$4d^{10}7d$	^2D	3/2	267215.8	R	0.4	100							-1	4
$4d^{10}7d$	^2D	5/2	267395.2		0.3	100							-2	3
$4d^9 5s(^3D)5p$	$^2P^\circ$	1/2	267488.4	N	0.7	76	20	$4d^9 5s(^1D)5p$	$^2P^\circ$				-95	2
$4d^{10}8s$	^2S	1/2	268543.3		0.6	100							0	4
$4d^9 5s(^3D)5p$	$^2F^\circ$	5/2	269838.6	N	0.7	51	17	$4d^9 5s(^1D)5p$	$^2F^\circ$	14	$4d^9 5s(^3D)5p$	$^2D^\circ$	316	2
$4d^9 5s(^3D)5p$	$^2D^\circ$	3/2	273229.4	N	0.7	66	29	$4d^9 5s(^1D)5p$	$^2D^\circ$				-204	2

Configuration	Term	J	Energy [a] cm^{-1}		Unc. [b] cm^{-1}	Leading percentages [c]	ΔE_{o-c} [d] cm^{-1}	No. of lines [e]
$4d^{10}8p$	$^2P^o$	1/2	274747.9	N	2.3	99	94	1
$4d^{10}8p$	$^2P^o$	3/2	275119.8	N	0.4	99	-88	2
$4d^{10}6f$	$^2F^o$	7/2	[276661]			99		
$4d^{10}6f$	$^2F^o$	5/2	[276735]			98		
$4d^{10}6g$	^2G	7/2,9/2	279863.3		0.4	100	0	6
$4d^{10}6h$	^2H	9/2,11/2	280070.4	N	1.8	100	-1	1
$4d^{10}8d$	^2D	3/2	[285257]			100		
$4d^{10}8d$	^2D	5/2	[285367]			100		
$4d^{10}9s$	^2S	1/2	286011.7		0.6	100	0	3
$4d^{10}9p$	$^2P^o$	1/2	[289574]			100		
$4d^{10}9p$	$^2P^o$	3/2	[289937]			100		
$4d^{10}7g$	^2G	7/2,9/2	292885.66		0.5	100	1	5
$4d^{10}7h$	^2H	9/2,11/2	293040.3	N	1.7	100	-1	1
$4d^{10}7i$	^2I	11/2,13/2	293057.83	N	2.4	100	-0.8	1
$4d^{10}10s$	^2S	1/2	296844.2		0.6	100	0	4
$4d^{10}8g$	^2G	7/2,9/2	301333.6	N	0.7	100	1	2
$4d^{10}8h$	^2H	9/2,11/2	301438.8	N	0.5	100	0	2
$4d^{10}8i$	^2I	11/2,13/2	301462.8	N	2.4	100	-0.8	1
$4d^{10}8k$	^2K	13/2,15/2	[301469.8]	Polar				
$4d^{10}11s$	^2S	1/2	304021.3	N	2	100	1	2
$4d^{10}9g$	^2G	7/2,9/2	307132.5	N	3	100	0	1
$4d^{10}9h$	^2H	9/2,11/2	307209.5	N	1.3	100	0	2
$4d^{10}9i$	^2I	11/2,13/2	[307223]	Polar				
$4d^{10}9k$	^2K	13/2,15/2	[307228]	Polar				

Configuration	Term	J	Energy [a] cm^{-1}	Unc. [b] cm^{-1}	Leading percentages [c]							ΔE_{o-c} [d] cm^{-1}	No. of lines [e]
$4d^{10}12s$	^2S	1/2	[309036]	Ritz	100								
$4d^{10}10g$	^2G	7/2,9/2	[311275]	Polar									
$4d^{10}10h$	$^2H^e$	9/2,11/2	[311331]	Polar									
$4d^{10}10i$	^2I	11/2,13/2	[311344]	Polar									
$4d^{10}10k$	^2K	13/2,15/2	[311348]	Polar									
$4d^95p^2(^3P)$	^4D	5/2	[312431]		42	21	$4d^{10}12d$	^2D	9	$4d^95p^2(^3P)$	4F		
$4d^{10}13s$	^2S	1/2	[312673]	Ritz	100								
$4d^{10}11g$	^2G	7/2,9/2	[314341]	Polar	100								
$4d^95p^2(^3P)$	^4D	7/2	[315006]		79	12	$4d^95p^2(^3P)$	4F	5	$4d^95p^2(^1D)$	^2F		
$4d^95p^2(^1D)$	^2G	9/2	[315519]		63	20	$4d^95s(^3D)5d$	^2G	12	$4d^95p^2(^3P)$	4F		
$4d^95p^2(^1D)$	^2S	1/2	315706.6	1.7	47	19	$4d^95p^2(^1D)$	^2P	9	$4d^95s(^3D)5d$	^2S	-284	2
$4d^95p^2(^3P)$	^2D	3/2	315994.9	1.8	42	13	$4d^95s(^3D)5d$	^2P	11	$4d^95p^2(^3P)$	^2P	248	1
$4d^{10}12g$	^2G	7/2,9/2	[316671]	Polar	100								
$4d^95p^2(^3P)$	^4D	3/2	[317190]		54	13	$4d^{10}14D$	^2D	9	$4d^95p^2(^1D)$	^2P		
$4d^95p^2(^1D)$	^2D	5/2	[318234]		37	14	$4d^95p^2(^3P)$	^2F	12	$4d^95s(^3D)5d$	^2D		
$4d^{10}13g$	^2G	7/2,9/2	[318485]	Polar	100								
$4d^{10}14g$	^2G	7/2,9/2	[319923]	Polar	98								
$4d^95p^2(^1D)$	^2F	7/2	[319946]		29	24	$4d^95p^2(^3P)$	4F	14	$4d^95p^2(^3P)$	^2F		
$4d^95p^2(^3P)$	^2F	5/2	[320204]		43	22	$4d^95p^2(^3P)$	^4P	17	$4d^95p^2(^3P)$	4F		
$4d^{10}15g$	^2G	7/2	[321083]	Polar	100								
$4d^95p^2(^3P)$	^4D	1/2	[321764]		88	6	$4d^95p^2(^1D)$	^2S					
$4d^95p^2(^3P)$	4F	7/2	[323479]		34	32	$4d^95p^2(^1D)$	^2G	13	$4d^95p^2(^3P)$	^4D		
$4d^95p^2(^1D)$	^2P	1/2	[323850]		42	16	$4d^95s(^3D)5d$	^2P	12	$4d^95p^2(^1D)$	^2S		
$4d^95p^2(^3P)$	4F	9/2	[325114]		87	7	$4d^95p^2(^1D)$	^2G	5	$4d^95s(^3D)5d$	^2G		

Configuration	Term	J	Energy [a] cm^{-1}		Unc. [b] cm^{-1}	Leading percentages [c]							ΔE_{o-c} [d] cm^{-1}	No. of lines [e]
$4d^9 5p^2(^3P)$	4F	3/2	325194		17	57	23	$4d^9 5p^2(^3P)$	^2D	9	$4d^9 5p^2(^1D)$	^2D	-115	1
$4d^9 5p^2(^3P)$	^2F	3/2	326536.7		2.3	27	23	$4d^9 5p^2(^3P)$	4F	23	$4d^9 5p^2(^1D)$	^2D	-274	2
$4d^9 5p^2(^3P)$	^4P	5/2	[326744]			54	22	$4d^9 5p^2(^3P)$	^4D	9	$4d^9 5p^2(^1D)$	^2F		
$4d^9 5p^2(^3P)$	4F	5/2	327991.3		1.9	42	22	$4d^9 5p^2(^1D)$	^2F	18	$4d^9 5p^2(^3P)$	^2F	346	1
$4d^9 5p^2(^1D)$	^2D	3/2	328256		7	50	14	$4d^9 5p^2(^1D)$	^2D	11	$4d^9 5p^2(^3P)$	^2P	29	1
Sn V $4d^{10}\,^1S_0$	**Limit**		**328909.3**	R	2.5									
$4d^9 5p^2(^3P)$	^2D	5/2	331610		17	39	13	$4d^9 5p^2(^1D)$	^2F	13	$4d^9 5p^2(^1D)$	^2D	231	1
$4d^9 5p^2(^3P)$	^2P	1/2	332480		1.8	78	5	$4d^9 5p^2(^3P)$	^4P				-172	2
$4d^9 5p^2(^3P)$	^4P	3/2	332663.5		4	27	23	$4d^9 5p^2(^3P)$	^2P	12	$4d^9 5s(^3D)5d$	^2P	469	1
$4d^9 5p^2(^1D)$	^2F	5/2	334703.5		7	38	13	$4d^9 5p^2(^3P)$	^4D	12	$4d^9 5p^2(^3P)$	^2F	45	1
$4d^9 5p^2(^3P)$	^2P	3/2	334792		7	48	35	$4d^9 5p^2(^3P)$	^4P	7	$4d^9 5p^2(^3P)$	^2D	-441	1

[a] Symbols next to the energy value have the following meaning: C – previous tentative identification has been confirmed here; N – new identification; I? represents the questionable inversion (see the text) ; R – previous value and/or interpretation has been revised here. Values in [ ] are unobserved energy level found from the series extrapolation by a parametric least-squares fitting with Cowan's codes [25] or extrapolation of series using Polar/Ritz code with determined IP.

[b] Uncertainties resulting from the level optimization procedure are given on the level of one standard deviation. They correspond to uncertainties of level separations from $4d^{10}6p\ ^2P^*_{3/2}$. To determine uncertainties of excitation energies from the ground level, the given values should be combined in quadrature with the uncertainty of the ground level, 0.4 cm^{-1}.

[c] The first percentage value refers to the configuration and term given in the first two columns of the table. The second/third percentage value refers to the configuration and term given next to it. The percentage compositions were determined in this work by a parametric least-squares fitting with Cowan's codes [25].

[d] Differences between observed energies and those calculated in the parametric least squares fitting.

[e] Number of observed lines determining the level in the optimization procedure LOPT[28].

Table 5.3. Least squares fitted energy parameters (cm^{-1}) for Sn IV.

Configuration	Parameter	LSF	Group [a]	STD	HFR	LSF/HFR
Even Parity						
$4d^{10}5s$	E_{av}	1905.8	258		0	
$4d^{10}6s$	E_{av}	174232.8	257		169921	1.0254
$4d^{10}7s$	E_{av}	237675.9	257		232675.8	1.0215
$4d^{10}8s$	E_{av}	268584.2	257		263250.1	1.0203
$4d^{10}9s$	E_{av}	286041.4	257		280543.2	1.0196
$4d^{10}10s$	E_{av}	296866.5	257		291287.2	1.0192
$4d^{10}11s$	E_{av}	304037.6	257	1	298426.6	1.0188
$4d^{10}12s$	E_{av}	309050.3	261	1	303408.1	1.0186
$4d^{10}13s$	E_{av}	312685	264	1	307018.1	1.0185
$4d^{10}14s$	E_{av}	315320.8	fixed		309728.8	1.0181
$4d^{10}15s$	E_{av}	317494.5	268	1	311805.5	1.0183
$4d^{10}5d$	E_{av}	165998.7	198		160701.3	1.0330
	$\zeta(5d)$	227.6	fixed		227.6	1.0000
$4d^{10}6d$	E_{av}	235082.3	184		229874.2	1.0227
	$\zeta(6d)$	131.4	128	3	101.1	1.2997
$4d^{10}7d$	E_{av}	267379.7	182	2	261970.1	1.0207
	$\zeta(7d)$	70.6	69	3	54.3	1.3002
$4d^{10}8d$	E_{av}	285361.4	195	2	279841.7	1.0197
	$\zeta(8d)$	42.4	41	3	32.6	1.3006
$4d^{10}9d$	E_{av}	296432.1	202	2	290857.4	1.0192
	$\zeta(9d)$	27.4	27	3	21.1	1.2986
$4d^{10}10d$	E_{av}	303745.1	207	2	298142.9	1.0188
	$\zeta(10d)$	18.7	18	3	14.4	1.2986
$4d^{10}11d$	E_{av}	308823.3	211	2	303207.3	1.0185
	$\zeta(11d)$	13.4	13	3	10.3	1.3010
$4d^{10}12d$	E_{av}	312495.9	213	2	306873.1	1.0183
	$\zeta(12d)$	9.9	10	3	7.6	1.3026
$4d^{10}13d$	E_{av}	315247.9	215	2	309621.8	1.0182
	$\zeta(13d)$	7.4	7	3	5.7	1.2983
$4d^{10}14d$	E_{av}	317350.3	216	2	311722.5	1.0181
	$\zeta(14d)$	5.8	6	3	4.5	1.2889
$4d^{10}15d$	E_{av}	318999.9	218	2	313371.2	1.0180
	$\zeta(15d)$	4.5	4	3	3.5	1.2857
$4d^{10}5g$	E_{av}	258290.2	181		252464.5	1.0231
	$\zeta(5g)$	0.6	fixed		0.6	1.0000
$4d^{10}6g$	E_{av}	279870.7	181		274072.7	1.0212
	$\zeta(6g)$	0.3	fixed		0.3	1.0000
$4d^{10}7g$	E_{av}	292891.9	181		287122.8	1.0201
	$\zeta(7g)$	0.2	fixed		0.2	1.0000
$4d^{10}8g$	E_{av}	301338.7	181		295589.4	1.0195
	$\zeta(8g)$	0.1	fixed		0.1	1.0000

Configuration	Parameter	LSF	Group [a]	STD	HFR	LSF/HFR
$4d^{10}9g$	E_{av}	307136.7	181	4	301392.3	1.0191
	$\zeta(9g)$	0.1	fixed		0.1	1.0000
$4d^{10}10g$	E_{av}	311280.1	184	4	305541.8	1.0188
	$\zeta(10g)$	0.1	fixed		0.1	1.0000
$4d^{10}11g$ [c]	E_{av}	314344.9	186	4	308606.4	1.0186
$4d^{10}12g$ [c]	E_{av}	316675	187	4	310937.8	1.0185
$4d^{10}13g$ [c]	E_{av}	318487.9	188	4	312755.4	1.0183
$4d^{10}14g$ [c]	E_{av}	319925.9	189	4	314190.3	1.0183
$4d^{10}15g$ [c]	E_{av}	321085.7	190	4	315345.2	1.0182
$4d^{10}7i$	E_{av}	293057.8	185		287335.3	1.019916
$4d^{10}8i$	E_{av}	301462.5	185	5	295735.6	1.019365
$4d^{10}9i$	E_{av}	307223.4	185	5	301496.6	1.018995
$4d^{10}10i$	E_{av}	311344.2	185	5	305615.2	1.018746
$4d^{9}5s^{2}$	E_{av}	177462.5	213		177240.7	1.0013
	$\zeta(4d)$	3618.5	162		3280.6	1.1030
$4d^{9}5p^{2}$	E_{av}	330554.4	133		326636.1	1.0120
	$F^{2}(5p,5p)$	38930.3	fixed		44746.2	0.8700
	$\alpha(5p)$	0.1			0	
	$\zeta(4d)$	3502	125		3307.6	1.0588
	$\zeta(5p)$	5374.7	179		4352.5	1.2349
	$F^{2}(4d,5p)$	21892.9	899		28614.2	0.7651
	$G^{1}(4d,5p)$	8681	312	6	8708.4	0.9969
	$G^{3}(4d,5p)$	7947.4	285	6	7972.5	0.9969
$4d^{9}5s5d$ [c]	E_{av}	343604.1	fixed		343604.1	1.0000
$4d^{9}5s6s$ [c]	E_{av}	353187.5	fixed		353187.5	1.0000
$4d^{8}5s5p^{2}$ [c]	E_{av}	525025.4	fixed		525025.4	1.0000
Odd parity						
$4d^{10}5p$	E_{av}	74894.3	150		71660.4	1.0451
	$\zeta(5p)$	4315.5	177	1	3825.1	1.1282
$4d^{10}6p$	E_{av}	199552.7	144		194965.8	1.0235
	$\zeta(6p)$	1504.8	62	1	1333.8	1.1282
$4d^{10}7p$	E_{av}	249594.1	97	2	244417.1	1.0212
	$\zeta(7p)$	714.5	29	1	633.3	1.1282
$4d^{10}8p$	E_{av}	274989.9	107	2	269723.5	1.0195
	$\zeta(8p)$	398.4	16	1	353.1	1.1283
$4d^{10}9p$	E_{av}	289825.6	113	2	284488.3	1.0188
	$\zeta(9p)$	245	10	1	217.2	1.1280
$4d^{10}10p$	E_{av}	299241.8	117	2	293869.3	1.0183
	$\zeta(10p)$	161.4	7	1	143.1	1.1279
$4d^{10}11p$	E_{av}	305596.2	119	2	300205.1	1.0180
	$\zeta(11p)$	112	5	1	99.3	1.1279
$4d^{10}12p$	E_{av}	310089.6	121	2	304689.6	1.0177
	$\zeta(12p)$	80.9	3	1	71.7	1.1283

Configuration	Parameter	LSF	Group [a]	STD	HFR	LSF/HFR
$4d^{10}13p$ [c]	E_{av}	313378.8	122	2	307974.1	1.0176
$4d^{10}14p$ [c]	E_{av}	315862	123	2	310454.8	1.0174
$4d^{10}15p$ [c]	E_{av}	317787.5	124	2	312378.9	1.0173
$4d^{10}4f$ [c]	E_{av}	210514.1	143		205049.2	1.0267
	$\zeta(4f)$	6	fixed		6	1.0000
$4d^{10}5f$	E_{av}	251877.1	149		247211.9	1.0189
	$\zeta(5f)$	5	fixed		5	1.0000
$4d^{10}6f$	E_{av}	276557.9	fixed	3	270579.9	1.0221
	$\zeta(6f)$	3.5	fixed		3.5	1.0000
$4d^{10}7f$ [c]	E_{av}	290030	fixed	3	284752.5	1.0185
$4d^{10}8f$ [c]	E_{av}	299358.7	fixed	3	293930.7	1.0185
$4d^{10}9f$ [c]	E_{av}	305699.8	fixed	3	300196.8	1.0183
$4d^{10}10f$ [c]	E_{av}	310194.3	fixed	3	304654.3	1.0182
$4d^{10}11f$ [c]	E_{av}	313483.5	fixed	3	307930.5	1.0180
$4d^{10}12f$ [c]	E_{av}	315983	fixed	3	310414.7	1.0179
$4d^{10}13f$ [c]	E_{av}	317913	fixed	3	312338.8	1.0179
$4d^{10}14f$ [c]	E_{av}	319429	fixed	3	313853.8	1.0178
$4d^{10}15f$ [c]	E_{av}	320649.1	fixed	3	315073.1	1.0177
$4d^{10}6h$	E_{av}	280070.9	143		274346	1.0209
	$\zeta(6h)$	0.3	fixed		0.3	1.0000
$4d^{10}7h$	E_{av}	293040.8	143		287293	1.0200
	$\zeta(7h)$	0.2	fixed		0.2	1.0000
$4d^{10}8h$	E_{av}	301439.3	143		295701.5	1.0194
	$\zeta(8h)$	0.1	fixed		0.1	1.0000
$4d^{10}9h$ [c]	E_{av}	307209.9	143	4	301470.8	1.0190
$4d^{10}10h$ [c]	E_{av}	311334.7	144	4	305596.9	1.0188
$4d^{9}5s5p$	E_{av}	245448.9	68		243146.3	1.0095
	$\zeta(4d)$	3646.3	66		3293.4	1.1072
	$\zeta(5p)$	4729.7	168		4380.8	1.0796
	$F^2(4d,5p)$	24205.6	522		28671.6	0.8442
	$G^2(4d,5s)$	12814.6	fixed		14238.4	0.9000
	$G^1(4d,5p)$	8574.9	284	5	8787.4	0.9758
	$G^3(4d,5p)$	7843.4	260	5	8037.8	0.9758
	$G^1(5s,5p)$	39189.4	182		54846	0.7145
$4d^{9}5s6p$ [c]	E_{av}	379911.9	fixed		379911.9	1.0000
$4d^{9}5s4f$ [c]	E_{av}	389040.6	fixed		389040.6	1.0000
$4d^{8}5s^{2}5p$ [c]	E_{av}	447627.2	fixed		447627.2	1.0000

[a] Parameters in each numbered group were linked together with their ratio fixed at the Hartree-Fock level.

[b] These highly excited configurations are unknown experimentally. They were included in the calculations in order to account for their interaction with other configurations studied in this work. Except for the average energies E_{av} and $\zeta(4d)$ given here, all other parameters of these configurations were fixed at the 85 % of the Hartree-Fock values (F^k, G^k) and 80% R^k) or 100 % of the Hartree-Fock values (ζ).

CHAPTER 6

The spectrum of quadruply ionized tin: Sn V

The four time ionized tin (Sn V) is fifth member of Pd I isoelectronic sequence. It has got the [Kr] $4d^{10}$ as lowest configuration with $^1S_0$ as ground state. The Pd-I sequence has special attraction as some lasing short-wave radiations were observed in Xe IX [1]. The structural study of this ion was initiated by Gibbs and White [2, 3] and followed by Kruger and Shoupp [4]. Several lines of Sn V ionization state were reported by Gibbs *et al* [5] on their ionization separation experiments. The extension and revision of the earlier works, was carried out by Shenstone. His analysis on the $4d^9n\ell$ ($n\ell$ =5s, 5p, 5d, 6s) configurations was compiled in AEL [6] and also listed in ASD of NIST [7] that contains 23 energy levels (four of $4d^95s$, eleven of $4d^95p$, seven of $4d^95d$ and one of $4d^96s$) including three doubtful and four with ambiguous J values. Wu's [8] work also includes the analysis of Sn V. As it is noticed in prior ions of Sn, a number of reported energy level values of Wu [8] were incorrect despite their primary data, i.e. wavelength or wavenumber, being right. Joshi and van Kleef [9, 10] improved the accuracy of resonance lines given by Gibbs and White [2] and hence, suggested that AEL [6] levels must be corrected by + 426.2 cm^{-1}. In 1981, van Kleef and Joshi [11] further extended the analysis to include the $4d^95d$, $4d^85s^2$ and $4d^96s$ configurations.

The ground excitations to $4d^9(np+n'f)$ were reported first time by Churilov *et al* [12], they reported J=1 levels of $4d^9$ {np (n=5-7) + n'f (n'=4-9)}. Recently, Ryabtsev *et al* [13] studied this spectrum extensively using their recorded spectrum in the 200-650Å wavelength region. They reported the level energies of $4d^97s$, $4d^96p$, $4d^96d$ and $4d^85s5p$ configurations along with their corresponding transition wavelengths and transition probabilities. It should be mentioned that wavelengths given in [13] are most reliable and less affected to systematic errors (due to the poor quality of instrumental resolution and/or known reference lines for the calibration). Further, no experimental data are available for transition parameters like TP, OS, and

etimes of levels etc. for this spectrum, however, some theoretical works are ported by others [14-17].

A complete analysis for this spectrum is highly desirable as the improved avelengths of tin now available with us (our normal incidence spectral data, yabtsev supplementary linelist and Wu's lines for λ>2000Å).

1. Level structure of Sn V

Configuration [a]	Parent Term	Term [b]	J
$4d^{10}$	(^{1}S)	^{1}S	0
$4d^8.5s^2$	(^{3}F)	^{3}F	4, 3, 2
	(^{3}P)	^{3}P	2, 1, 0
	(^{1}G)	^{1}G	4
	(^{1}D)	^{1}D	2
	(^{1}S)	^{1}S	0
$4d^9$.ns	(^{2}D)	^{3}D	3, 2, 1
		^{1}D	2
$4d^9$.np	(^{2}D)	^{3}F°	4, 3, 2
		^{3}D°	3, 2, 1
		^{3}P°	2, 1, 0
		^{1}F°	3
		^{1}D°	2
		^{1}P°	1
$4d^9$.nd	(^{2}D)	^{3}G	5, 4, 3
		^{3}F	4, 3, 2
		^{3}D	3, 2, 1
		^{3}P	2, 1, 0
		^{3}S	1
		^{1}G	4
		^{1}F	3
		^{1}D	2
		^{1}P	1
		^{1}S	0
$4d^9$.nf	(^{2}D)	^{3}H°	6, 5, 4
		^{3}G°	5, 4, 3
		^{3}F°	4, 3, 2
		^{3}D°	3, 2, 1
		^{3}P°	2, 1, 0
		^{1}H°	5
		^{1}G°	4
		^{1}F°	3
		^{1}D°	2
		^{1}P°	1
$4d^8.5s.5p$	(^{4}F)	^{5}G°	6, 5, 4, 3, 2
		^{5}F°	5, 4, 3, 2, 1
		^{5}D°	4, 3, 2, 1, 0

Configuration [a]	Parent Term	Term [b]	J
		$^3G^\circ$	5, 4, 3
		$^3F^\circ$	4, 3, 2
		$^3D^\circ$	3, 2, 1
	(^4P)	$^5D^\circ$	4, 3, 2, 1, 0
		$^5P^\circ$	3, 2, 1
		$^5S^\circ$	2
		$^3D^\circ$	3, 2, 1
		$^3P^\circ$	2, 1, 0
		$^3S^\circ$	1
	(^2G)	$^3H^\circ$	6, 5, 4
		$^3G^\circ$	5, 4, 3
		$^3F^\circ$	4, 3, 2
		$^1H^\circ$	5
		$^1G^\circ$	4
		$^1F^\circ$	3
	(^2F)	$^3G^\circ$	5, 4, 3
		$^3F^\circ$	4, 3, 2
		$^3D^\circ$	3, 2, 1
		$^1G^\circ$	4
		$^1F^\circ$	3
		$^1D^\circ$	2
	(^2D)	$^3F^\circ$	4, 3, 2
		$^3D^\circ$	3, 2, 1
		$^3P^\circ$	2, 1, 0
		$^1F^\circ$	3
		$^1D^\circ$	2
		$^1P^\circ$	1
	(^2P)	$^3D^\circ$	3, 2, 1
		$^3P^\circ$	2, 1, 0
		$^3S^\circ$	1
		$^1D^\circ$	2
		$^1P^\circ$	1
		$^1S^\circ$	0
	(^2S)	$^3P^\circ$	2, 1, 0
		$^1P^\circ$	1

[a] To the given configurations, the Kernel structure '[Kr]' must be added before each of it for the completeness of electronic structure. The principal quantum number, $n \geq 5$ for all ℓ except for f sub-shell ($n \geq 4$).

[b] The strict ordering of levels are governed by Hund's rule for the fine structures.

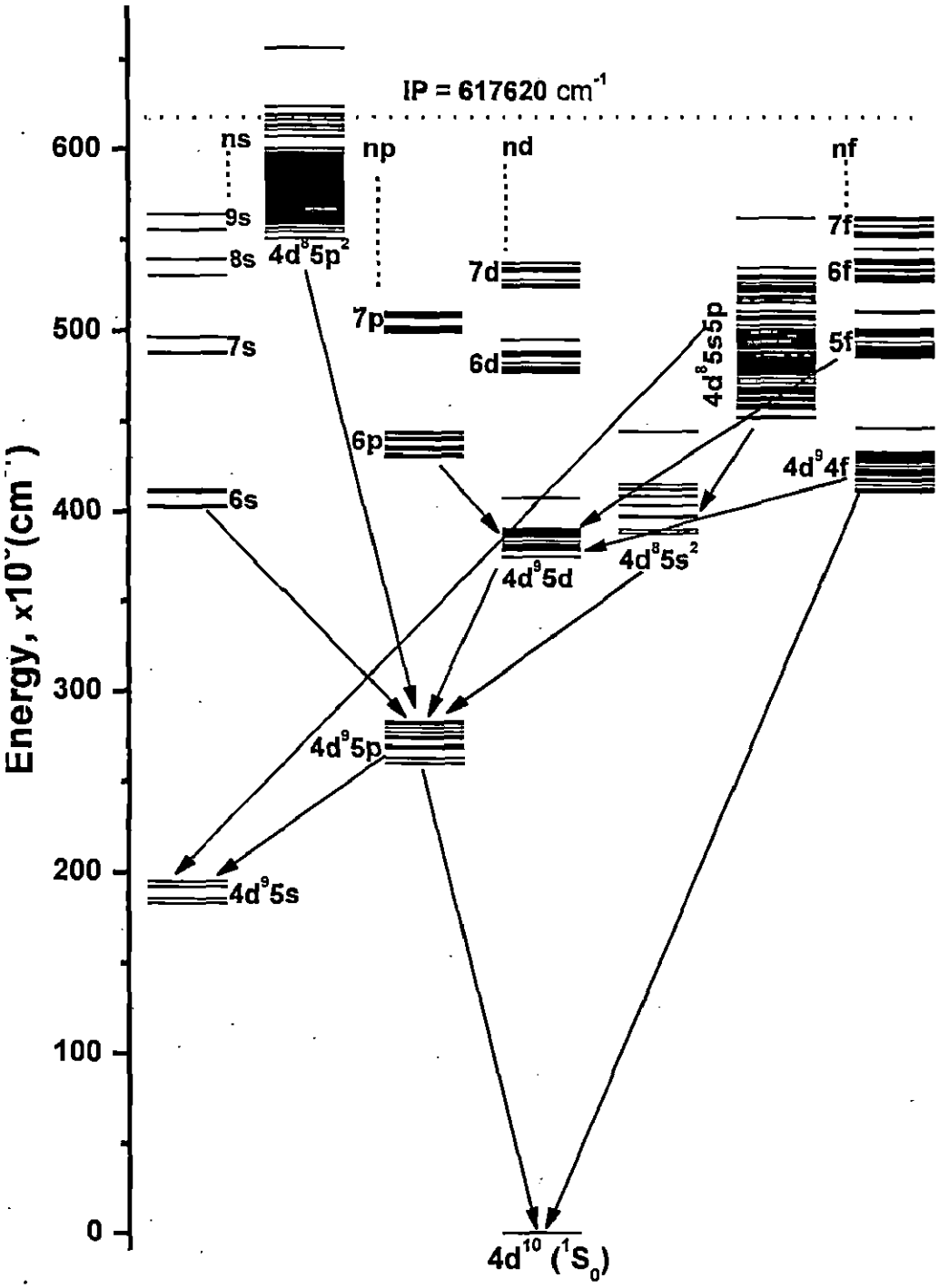

Figure 6.1. Energy level diagram of Sn V

6.2. Results and discussion

Figure 6.1 describes the energy level diagram of Sn V, some of the prominent transition arrays are indicated in it. Table 6.1 contains the list of observed lines of this spectrum. The optimized energy values are tabulated in table 6.2 along with their uncertainty and LS components. The least-squared fitted parametric values are given table 6.3.

6.2.1. Theoretical calculations

The energy levels, transition wavelengths and transition rates were predicted using Cowan code [18]. In initial calculations, the Slater parameters were scaled as E_{av} and ζ_{nl} to full HF value, 85% of HF values for F^k, and 80% for G^k and R^k integrals. The even configurations set contains the $4d^{10}$, $4d^9ns$ (n=5-10), $4d^9nd$ (n=5-9), $4d^9ng$ (n=5, 6), $4d^85\ell^2$ (ℓ=s, p, d), $4d^85s5d$ and $4p^54d^{10}$ (5p+4f). And the $4d^9np$ (n=5-9), $4d^9nf$ (n=4-8), $4d^85s$ (5p+6p), $4d^85s4f$ and $4p^54d^{10}$ (5s+5d) configurations were incorporated in odd parity matrix. The observed levels of both the parity were adjusted within the least squares fitting procedure of Cowan code [18]. The even parity levels were fitted within 145 cm^{-1} and odd system was converged to a standard deviation of 140cm^{-1}. Using these fitted parameters, the initially obtained transition parameters like transition rates (gA) and oscillator strengths (gf) were re-calculated and assembled in table 6.1 for classified lines.

6.2.2. Analysis of the spectrum

The ionization state of Sn V lines were analyzed before their transition assignments. Most of its lines were showing the polar effect at second or third track of the spectrum taken by us. This helped us to carry out the analysis.

6.2.2.1. The $4d^{10}\,{}^1S_0 - 4d^9(np+n'f)$ transition array

The ΔJ allowed transitions of $4d^{10}\,{}^1S_0 - 4d^95p$ reported by Gibbs and White [1], were later refined through the accurate measurements by Joshi and van Kleef [9]. They showed that energy levels given in AEL [6] were shifted up by ~ 415 cm-^{1}. However, the same transitions were further measured at higher orders by Srivastava *et al* [10] who suggested a correction of +426.2 cm^{-1}. Therefore, this correction must be applied to the level values in AEL [6] or ASD NIST [7] (here onward they would be called

'*derived AEL energy*'). The extension of this array, to np (≥6) and n'f (n≥4) series, was made by Churilov *et al* [11]. Only $4d^9 5p$ transitions are falling in our normal incidence wavelength region and we confirmed them by the ionization character. The remaining lines are in grazing incidence region (supplement from the linelist of Ryabtsev [19]). We have confirmed them with the predictions from Cowan code programs [18], considering parameter's ratio and gA values, with observed intensities.

6.2.2.2. The levels of $4d^9 n\ell$ (n≥5, ℓ=s, p, d) and $4d^8 5s^2$ configurations

As we discussed in earlier section, the remaining nine levels of $4d^9 5p$ are J-forbidden to the ground $4d^{10}\ ^1S_0$, thus they can be studied through $4d^9 5s - 4d^9 5p$ and/or $4d^9 5p - 4d^9 5d$ transition arrays. It should be mentioned that levels of $4d^9 5s$ are highly metastable to the ground $4d^{10}\ ^1S_0$, i.e. they lie below the excited energies of $4d^9 5p$ configuration, other than some of the J-forbidden levels of the first excited $4d^9 5p$ configuration. This was an advantageous state to observe the strong transitions between $4d^9 5s$ and $4d^9 5p$ in the wavelength range 1000– 1540Å. Due to our improved wavelengths and comprehensive optimization of levels of this spectrum, the newly found energy level values of $4d^9 5s$ configuration are further shifted by an average of -9.04 cm^{-1} from the *derived AEL energies*.

As a consequence of the study of above transition array (5s→5p), all the twelve levels of $4d^9 5p$ were also established. All the newly obtained energy levels are ~419.76 cm^{-1} higher than the AEL [7] values. Once the levels $4d^9 5p$ were established completely, their further excitations to $4d^9 nd$ and $4d^9 ns$ (n≥6) configurations were undertaken. All the $4d^9 5d$ and $4d^9 6s$ configurations energy levels reported earlier by van Kleef and Joshi [11] are confirmed with best optimized energy values except $^1G_4$ of $4d^9 5d$ for which we found a new value at 387991.4 cm^{-1}. The missing $4d^9 5d\ ^1S_0$ level is now established at 407703.1 cm^{-1} (see table 6.2). The next transition array $4d^9 5p - 4d^9(6d+7s)$, already studied by Ryabtsev *et al* [13], thoroughly checked in the present work and were found satisfactory.

Due to the strong configuration interactions present between the $4d^9 5d$ and $4d^8 5s^2$ configurations, some strong transitions were predicted from $4d^8 5s^2$ to $4d^9 5p$. This array was previously studied by van Kleef and Joshi [11]. We could confirm only a few transitions reported by them as our source excitation conditions were

different from their sliding spark. We improved the wavelengths of twelve transitions out of 30 lines reported in [11].

Next, the higher excitations from $4d^9 5s$ configuration were considered. This resulted in establishment of the $4d^9 6p$ levels which were earlier reported by Ryabtsev *et al* [13]. These transitions falling in 388-425Å region, were confirmed again from the Ryabtsev's linelist. However, this configuration is also strongly connected to the $4d^9 5d$ configuration; those are lying in our wavelength range 1500–2300Å. We have observed fourteen new lines, in 1650-2010Å range, that are associated to the $4d^9 5d \rightarrow 4d^9 6p$ array. This identification helped us to improve the level values of both $4d^9 5d$ and $4d^9 6p$ configurations.

6.2.2.3. The $4d^9 5s - 4d^8 5s5p$ transition array

The excitation of one more 4d electron, from the lowest excited $4d^9 5s$ configuration generates the $4d^8 5s5p$ configuration. This array was already studied by Ryabtsev *et al* [13]. We have verified all their reported transitions from their supplied linelist and found them satisfactory based on the character of Sn V lines and predicted gA-values from Cowan's code [18]. Additionally, the observed levels adjusted nicely to the least-squares fitting of Cowan code [18]. The level designations were retained as reported in [13] (See table 6.2).

6.2.3. Optimization of the energy levels

The comprehensive optimization of the observed energy levels for this spectrum were required as there were various wavelengths observed (previous or new) by us and others [9, 10–12]. The optimization was made with a least-squares level optimization LOPT [20] program, after the measured lines were absolved from systematic errors and uncertainties were assessed.

A total of more than 430 observed lines (188 lines from our measurements, 217 lines from Ryabtsev linelist and remaining from ref [8, 11,12]) were now used for the optimization which makes it become extensive, and that enabled to achieve the 143 optimized levels (see table 6.1, 7.2). Some masked lines were also observed, however they are excluded from the optimization. The $4d^9 5s\ ^1D_2$ level has maximum number of accurately measured lines and hence, this level was treated as a base for determining the uncertainty of all other observed levels. In this procedure the ground

uncertainty obtained at 2 cm^{-1}, and for obtaining the uncertainty of excitation energy of any level with respect to the ground, the quadrature inclusion of error of both the given and ground level must be done.

It was noticed that the optimized level values of both $4d^9 5d$ and $4d^9 6s$ levels were deviated by an average value of -8.9 cm^{-1} from the previously reported one's by van Kleef and Joshi [11]. With the help of improved optimization, the wavelengths of forbidden multipole transition is now predicted and given table 6.1. The metastability such levels ($4d^9 5s$) can be exploited for variety of applications that involved in short-wave range.

6.2.4. Ionization potential

The recent value of ionization limit of Sn V to the ground $4d^9\ ^2D_{5/2}$ of Sn VI, was given by Churilov *et al* [11] at 621300cm^{-1}, was obtained using the perturbed series of $4d^9(np + n'f)$. Fortunately, the unperturbed series $^3D_1$ and $^3D_3$ of $4d^9ns$ (n=5-7) are available now, and hence the IP can be derived using Ritz-method that implemented in RITZPL code [21]. In series limit calculations, the separate convergences[1] of $^3D_1$ and $^3D_3$ of $4d^9ns$ series is well known as the $^3D_1$ will converge to $^2D_{3/2}$ $4d^9$ of Sn VI and the $^3D_3$ to ground state ($^2D_{5/2}$) of Sn VI. We obtained IP using $^3D_1$ of $4d^9ns$ (n=5-7) at 617619.5cm^{-1}, after subtracting the ground ^2D interval (8698.5 cm^{-1}) of Sn VI. The converged values of the series limit from $^3D_3$ $4d^9ns$ (n=5-7) was found at 617605.0 cm^{-1}. It has been noticed that two values obtained were differed by ~14 cm^{-1}, this is somewhat larger than the expected, and could be due to slightly perturbed $^3D_3$ (by 1%) of $4d^97s$ configuration (see table 6.2). Thus, we adapt the series limit at 6176120 cm^{-1} within an accuracy 14 cm^{-1} or 76.5751(17) eV.

[1] The convergence is easily elucidated in jj-notation of $^3D_1$ as $(3/2, 1/2)_1$ and $(5/2, 1/2)_3$ for $^3D_3$, accordingly their convergence to Sn^{5+} $4d^9\ ^2D_{3/2}$ and $^2D_{5/2}$, respectively.

References:

[1] Lemoff B E, Yin G Y, Gordon C L, Barty C P J and Harris S E 1996 *J. Opt. Soc. Am. B* **13** 180

[2] Gibbs R C and White H E 1928 *Proc. Natl. Acad. Sci. Amer.* **14** 345

[3] Gibbs R C and White H E 1928 *Proc. Natl. Acad. Sci. Amer.* **14** 559

[4] Kruger P G and Shoupp W E 1934 *Phys. Rev.* **46** 124

[5] Gibbs R C, Vieweg A M and Gartlein C W 1929 Phys. Rev. **34** 406

[6] Moore C E 1958 *Atomic Energy Levels, National Bureau of Standards Circular 467* vol. III (Washington, DC: US Govt. Printing Office)

[7] Kramida A, Ralchenko Yu., Reader J and NIST ASD Team 2012 *NIST Atomic Spectra Database, v.5.0*, National Institute of Standards and Technology, Gaithersburg, MD, USA. Available from: http://physics.nist.gov/ASD

[8] Wu C M 1967 *The Atomic Spark Spectra of Tin, Sn III, Sn IV, Sn V* Master thesis University of British Columbia, Canada

[9] Joshi Y N and van Kleef Th A M 1977 *Can. J. Phys.* **55** 714

[10] Srivastava R P, Joshi Y N and van Kleef Th A M 1977 *Can. J. Phys.* **55** 1936

[11] van Kleef Th A M and Joshi Y N 1981 *Phys. Scr.* **24** 557

[12] Churilov S S, Joshi Y N and Ryabtsev A N 1994 *J. Phys. B: At. Mol. Opt. Phys.* **27** 5485

[13] Ryabtsev A N, Churilov S S and Kononov E Ya 2005 *Phys. Scr.* **72** 377

[14] Younger S M 1980 *Phys. Rev. A* **22** 2682

[15] Loginov A V and Tuchkin V I 1999 *Opt. Spectrosc.* **86** 148

[16] Ivanova E P 2003 Opt. Spectrosc. **94** 151

[17] Safronova U I, Cowan T E and Johnson W R 2005 *Can. J. Phys.* **83** 813

[18] Cowan R D 1981 *The Theory of Atomic Structure and Spectra* (Berkeley, CA: University of California Press) and Cowan code package for Windows by A. Kramida, available from http://das101.isan.troitsk.ru/COWAN

[19] Ryabtsev A N 2013 *The spectral data of tin ions*, private communication

[20] Kramida A E 2011 *Comput. Phys. Commun.* **182** 419

[21] Sansonetti C J 2005 *Computer programs RITZP*, private communication

s in Sn V.

	σ_{obs} (cm^{-1})	λ_{Ritz} [d] (Å)	$\delta\lambda_{obs-Ritz}$ [e] (Å)	Classification		E_{low}(cm^{-1})	E_{upp}(cm^{-1})	gA^{f}(s-1)	Lin. Ref[g]
(5)	583669	171.330(5)	0.000	$4d^{10}\,^1S_0$	$4d^9 9f\,^3D_1$	0	583669		Ch
(5)	572833	174.571(5)	0.000	$4d^{10}\,^1S_0$	$4d^9 8f\,^3D_1$	0	572833	7.6E+10	Ch
(5)	565496	176.836(5)	0.000	$4d^{10}\,^1S_0$	$4d^9 7f\,^1P_1$	0	565496	4.5E+10 [CF]	Ch
(5)	557740	179.295(5)	0.000	$4d^{10}\,^1S_0$	$4d^9 7f\,^3D_1$	0	557740	6.7E+10	Ch
(5)	543987	183.828(5)	0.000	$4d^{10}\,^1S_0$	$4d^9 6f\,^1P_1$	0	543987	1.4E+11	Ch
(5)	533755	187.352(5)	0.000	$4d^{10}\,^1S_0$	$4d^9 6f\,^3D_1$	0	533755	3.3E+10	Ch
(5)	510853	195.7541(13)	-0.003	$4d^{10}\,^1S_0$	$4d^9 5f\,^1P_1$	0	510845	1.2E+11	Ch
(5)	508994	196.4662(10)	0.000	$4d^{10}\,^1S_0$	$4d^9 7p\,^3D_1$	0	508993.5		Ch
(5)	507588	197.0117(11)	-0.002	$4d^{10}\,^1S_0$	$4d^9 7p\,^1P_1$	0	507584	1.6E+9 [CF]	Ch
(3)	493403	202.6741(10)	0.000	$4d^{10}\,^1S_0$	$4d^9 5f\,^3D_1$	0	493403.0	1.9E+10	Ry*
(3)	488451	204.7303(11)	-0.001	$4d^{10}\,^1S_0$	$4d^8 5s(^2P)5p\,^3D_1$	0	488447.5	4.7E+8	Ry
(3)	485347	206.0381(11)	0.000	$4d^{10}\,^1S_0$	$4d^8 5s(^2D)5p\,^3Db_1$	0	485347.2	1.1E+8	Ry
(3)	446335	224.047(3)	0.000	$4d^{10}\,^1S_0$	$4d^9 4f\,^1P_1$	0	446335	3.6E+11	Ry*
(3)	443410	225.5224(18)	0.003	$4d^{10}\,^1S_0$	$4d^9 6p\,^3D_1$	0	443415	2.8E+9	Ry*
(3)	439800	227.3719(15)	0.004	$4d^{10}\,^1S_0$	$4d^9 6p\,^1P_1$	0	439808	4.2E+9 [CF]	Ry*
(3)	423366	236.202(3)	0.000	$4d^{10}\,^1S_0$	$4d^9 4f\,^3D_1$	0	423366	9.5E+9	Ry*
(3)	412342	242.517(3)	0.000	$4d^{10}\,^1S_0$	$4d^9 4f\,^3P_1$	0	412342	7.7E+8	Ry*
(3)	333016	300.2881(21)	-0.002	$4d^9 5s\,^3D_3$	$4d^8 5s(^4P)5p\,^3P_2$	182996.46	516010	2.6E+10	Ry
(6)	330071	302.966(3)	-0.001	$4d^9 5s\,^3D_2$	$4d^8 5s(^4P)5p\,^3P_1$	185475.22	515545	1.3E+10	Ry
(3)	324389	308.2696(22)	0.002	$4d^9 5s\,^3D_1$	$4d^8 5s(^4P)5p\,^3P_2$	191618.62	516010	7.3E+9	Ry
(3)	323925	308.712(3)	0.001	$4d^9 5s\,^3D_1$	$4d^8 5s(^4P)5p\,^3P_1$	191618.62	515545	1.5E+10	Ry
(3)	323517	309.1015(17)	0.001	$4d^9 5s\,^3D_2$	$4d^9 7p\,^3D_1$	185475.22	508993.5		Ry
(3)	322111	310.4541(21)	-0.002	$4d^9 5s\,^3D_2$	$4d^9 7p\,^1P_1$	185475.22	507584	2.4E+9	Ry
(3)	317375	315.0848(17)	0.000	$4d^9 5s\,^3D_1$	$4d^9 7p\,^3D_1$	191618.62	508993.5		Ry
(3)	316388	316.067(3)	0.001	$4d^9 5s\,^3D_3$	$4d^8 5s(^4F)5p\,^3D_3$	182996.46	499385		Ry
(3)	316199	316.257(3)	0.000	$4d^9 5s\,^1D_2$	$4d^9 5f\,^1P_1$	194646.26	510845	5.0E+8 [CF]	Ry
(3)	315964	316.4904(21)	0.002	$4d^9 5s\,^3D_1$	$4d^9 7p\,^1P_1$	191618.62	507584	2.2E+7 [CF]	Ry
(3)	315809	316.6516(19)	-0.005	$4d^9 5s\,^3D_3$	$4d^9 5f\,^3F_3$	182996.46	498801	2.1E+9	Ry
(3)	315373	317.0803(17)	0.005	$4d^9 5s\,^3D_3$	$4d^8 5s(^2G)5p\,^3G_3$	182996.46	498374	1.2E+10	Ry

I_{obs} [a] (A.U)	Char.[b]	λ_{obs} [c] (Å)	σ_{obs} (cm^{-1})	λ_{Ritz} [d] (Å)	$\delta\lambda_{obs-Ritz}$ [e] (Å)	Classification		E_{low}(cm^{-1})	E_{upp}(cm^{-1})	gA^{f}(s-1)	Lin. Ref[g]
90		318.118(3)	314349	318.1195(18)	-0.002	$4d^9 5s\ ^1D_2$	$4d^9 7p\ ^3D_1$	194646.26	508993.5		Ry
720	m(Sn VI)	318.561(6)	313912	318.563(3)	-0.002	$4d^9 5s\ ^3D_2$	$4d^8 5s(^4F)5p\ ^3D_3$	185475.22	499385		Ry
60		319.117(3)	313365	319.1178(17)	-0.001	$4d^9 5s\ ^3D_3$	$4d^8 5s(^2P)5p\ ^1D_2$	182996.46	496360.4	6.8E+8	Ry
50		319.141(6)	313341	319.1566(20)	-0.016	$4d^9 5s\ ^3D_2$	$4d^9 5f\ ^3F_3$	185475.22	498801	3.4E+8 [CF]	Ry
60		319.594(3)	312897	319.5922(17)	0.002	$4d^9 5s\ ^3D_2$	$4d^8 5s(^2G)5p\ ^3G_3$	185475.22	498374	1.1E+9 [CF]	Ry
110		320.216(3)	312289	320.2185(21)	-0.002	$4d^9 5s\ ^3D_2$	$4d^8 5s(^2D)5p\ ^3P_1$	185475.22	497762	3.6E+8 [CF]	Ry
260		320.672(3)	311845	320.6760(17)	-0.004	$4d^9 5s\ ^3D_3$	$4d^8 5s(^4P)5p\ ^3D_3$	182996.46	494837.7	1.0E+9 [CF]	Ry
640	m(O III)	320.983(6)	311543	320.983(6)	0.000	$4d^9 5s\ ^3D_3$	$4d^8 5s(^2D)5p\ ^3F_4$	182996.46	494539	5.8E+9	Ry
200		322.227(3)	310340	322.2316(19)	-0.005	$4d^9 5s\ ^3D_2$	$4d^8 5s(^2P)5p\ ^3S_1$	185475.22	495811	1.8E+9 [CF]	Ry
460		322.417(3)	310157	322.4210(16)	-0.004	$4d^9 5s\ ^3D_3$	$4d^8 5s(^4P)5p\ ^5S2$	182996.46	493150	8.0E+9	Ry
620		323.246(3)	309362	323.2454(17)	0.001	$4d^9 5s\ ^3D_2$	$4d^8 5s(^4P)5p\ ^3D_3$	185475.22	494837.7	3.4E+9 [CF]	Ry
530		323.867(3)	308769	323.8714(16)	-0.004	$4d^9 5s\ ^3D_3$	$4d^8 5s(^2G)5p\ ^3Fa_2$	182996.46	491761.0	1.3E+10	Ry
70		324.745(3)	307934	324.7515(16)	-0.006	$4d^9 5s\ ^3D_2$	$4d^9 5f\ ^3D_1$	185475.22	493403.0	6.6E+7 [CF]	Ry
330	bl	325.019(8)	307674	325.0185(17)	0.000	$4d^9 5s\ ^3D_2$	$4d^8 5s(^4P)5p\ ^5S2$	185475.22	493150	1.5E+8 [CF]	Ry
330	bl	325.019(8)	307674	325.0210(20)	-0.002	$4d^9 5s\ ^3D_3$	$4d^8 5s(^2P)5p\ ^3D_3$	182996.46	490668.9	9.9E+8 [CF]	Ry
330	m(Sn VI)	326.491(6)	306287	326.4925(16)	-0.001	$4d^9 5s\ ^3D_2$	$4d^8 5s(^2G)5p\ ^3Fa_2$	185475.22	491761.0	7.4E+9 [CF]	Ry
390		327.461(3)	305380	327.4665(17)	-0.005	$4d^9 5s\ ^3D_2$	$4d^8 5s(^2P)5p\ ^1P_1$	185475.22	490850	8.1E+9	Ry
480		327.659(3)	305195	327.6608(20)	-0.002	$4d^9 5s\ ^3D_2$	$4d^8 5s(^2P)5p\ ^3D_3$	185475.22	490668.9	1.4E+10	Ry
310		328.076(3)	304807	328.0781(17)	-0.002	$4d^9 5s\ ^3D_3$	$4d^9 5f\ ^3P_2$	182996.46	487801.9	2.7E+9	Ry
280		328.146(3)	304742	328.1467(18)	-0.001	$4d^9 5s\ ^3D_1$	$4d^8 5s(^2P)5p\ ^1D_2$	191618.62	496360.4	1.8E+9	Ry
390		328.635(3)	304289	328.6363(17)	-0.001	$4d^9 5s\ ^3D_3$	$4d^8 5s(^2D)5p\ ^3D_3$	182996.46	487284.2	7.6E+9	Ry
360	m(O VI)	328.746(6)	304186	328.7393(20)	0.007	$4d^9 5s\ ^3D_1$	$4d^8 5s(^2P)5p\ ^3S_1$	191618.62	495811	2.0E+9	Ry
140		328.787(3)	304148	328.7800(21)	0.007	$4d^9 5s\ ^1D_2$	$4d^9 5f\ ^3F_3$	194646.26	498801	1.8E+9	Ry
90		329.236(3)	303733	329.2422(18)	-0.006	$4d^9 5s\ ^1D_2$	$4d^8 5s(^2G)5p\ ^3G_3$	194646.26	498374	3.2E+9	Ry
560		329.909(3)	303114	329.9070(22)	0.002	$4d^9 5s\ ^1D_2$	$4d^8 5s(^2D)5p\ ^3P_1$	194646.26	497762	2.2E+10	Ry
740	bl	330.064(8)	302972	330.0632(19)	0.001	$4d^9 5s\ ^3D_2$	$4d^8 5s(^2P)5p\ ^3D_1$	185475.22	488447.5	5.3E+9	Ry
740	bl	330.064(8)	302972	330.0647(19)	-0.001	$4d^9 5s\ ^3D_3$	$4d^8 5s(^2P)5p\ ^3D_2$	182996.46	485967.4	1.1E+10	Ry
630		330.113(3)	302927	330.1136(21)	-0.001	$4d^9 5s\ ^3D_1$	$4d^8 5s(^2G)5p\ ^3Fb_2$	191618.62	494544.6	2.3E+10	Ry
160		330.153(3)	302890	330.1538(17)	-0.001	$4d^9 5s\ ^3D_3$	$4d^8 5s(^2G)5p\ ^3F_3$	182996.46	485885.6	3.9E+9	Ry
80		330.469(3)	302600	330.4711(21)	-0.002	$4d^9 5s\ ^1D_2$	$4d^8 5s(^2D)5p\ ^3P_2$	185475.22	488073.5	1.1E+9 [CF]	Ry
90		330.770(3)	302325	330.7680(17)	0.002	$4d^9 5s\ ^1D_2$	$4d^9 5f\ ^3P_2$	185475.22	487801.9	3.2E+8 [CF]	Ry

I_{obs}[a] (A.U)	Char.[b]	λ_{obs}[c] (Å)	σ_{obs} (cm^{-1})	λ_{Ritz}[d] (Å)	$\delta\lambda_{obs-Ritz}$[e] (Å)	Classification		E_{low}(cm^{-1})	E_{upp}(cm^{-1})	gA^f(s-1)	Lin. Ref[g]
630		331.217(3)	301917	331.2179(17)	-0.001	$4d^95s\ ^3D_3$	$4d^85s(^2D)5p\ ^3D_2$	182996.46	484912.5	2.2E+10	Ry
330		331.336(3)	301808	331.3354(17)	0.001	$4d^95s\ ^3D_2$	$4d^85s(^2D)5p\ ^3D_3$	185475.22	487284.2	3.9E+9 CF	Ry
150		331.362(3)	301785	331.3624(17)	0.000	$4d^95s\ ^3D_1$	$4d^95f\ ^3D_1$	191618.62	493403.0	8.9E+7 CF	Ry
70		331.441(3)	301713	331.4396(18)	0.001	$4d^95s\ ^1D_2$	$4d^85s(^2P)5p\ ^1D_2$	194646.26	496360.4	1.1E+9 CF	Ry
1000		331.519(3)	301642	331.519(3)	0.000	$4d^95s\ ^3D_3$	$4d^85s(^2G)5p\ ^3F_4$	182996.46	484638	7.5E+10	Ry
340		331.639(3)	301533	331.6404(17)	-0.001	$4d^95s\ ^3D_1$	$4d^85s(^4P)5p\ ^5S2$	191618.62	493150	5.9E+9	Ry
450		332.048(3)	301161	332.0442(21)	0.004	$4d^95s\ ^1D_2$	$4d^85s(^2P)5p\ ^3S_1$	194646.26	495811	1.2E+10	Ry
300		332.257(3)	300972	332.257(3)	0.000	$4d^95s\ ^3D_1$	$4d^85s(^2D)5p\ ^3P_0$	191618.62	492590.5	6.3E+9	Ry
770		332.377(3)	300863	332.377(3)	0.000	$4d^95s\ ^3D_3$	$4d^85s(^4P)5p\ ^5D_4$	182996.46	483860	4.9E+9	Ry
730		332.725(3)	300549	332.7206(17)	0.004	$4d^95s\ ^3D_3$	$4d^85s(^4P)5p\ ^5D_2$	182996.46	483548.9	1.8E+10	Ry
700		332.757(3)	300520	332.757(3)	0.000	$4d^95s\ ^3D_3$	$4d^85s(^2G)5p\ ^3H_4$	182996.46	483516	9.7E+9	Ry
760		332.881(3)	300408	332.8780(17)	0.003	$4d^95s\ ^3D_2$	$4d^85s(^2G)5p\ ^3F_3$	185475.22	485885.6	2.2E+10	Ry
180		333.124(3)	300189	333.1208(18)	0.003	$4d^95s\ ^1D_2$	$4d^85s(^4P)5p\ ^3D_3$	194646.26	494837.7	2.1E+9 CF	Ry
260		333.176(3)	300142	333.1752(17)	0.001	$4d^95s\ ^3D_1$	$4d^85s(^2G)5p\ ^3Fa_2$	191618.62	491761.0	5.9E+9	Ry
170		333.447(3)	299898	333.4463(21)	0.001	$4d^95s\ ^1D_2$	$4d^85s(^2G)5p\ ^3Fb_2$	194646.26	494544.6	3.2E+9	Ry
390		333.476(3)	299872	333.4756(20)	0.000	$4d^95s\ ^3D_2$	$4d^85s(^2D)5p\ ^3Db_1$	185475.22	485347.2	8.0E+9	Ry
630		334.191(3)	299230	334.1895(18)	0.001	$4d^95s\ ^3D_1$	$4d^85s(^2P)5p\ ^1P_1$	191618.62	490850	2.3E+10	Ry
40		334.727(3)	298751	334.7205(17)	0.007	$4d^95s\ ^1D_2$	$4d^95f\ ^3D_1$	194646.26	493403.0	3.6E+8	Ry
60		335.009(3)	298499	335.0042(18)	0.005	$4d^95s\ ^1D_2$	$4d^85s(^4P)5p\ ^3S_1$	194646.26	493150	8.5E+8 CF	Ry
170		335.973(3)	297643	335.9739(17)	-0.001	$4d^95s\ ^3D_3$	$4d^85s(^4P)5p\ ^5P_3$	182996.46	480638.6	1.1E+10	Ry
420		336.154(3)	297483	336.1535(17)	0.000	$4d^95s\ ^3D_3$	$4d^85s(^2F)5p\ ^3F_2$	182996.46	480479.6	3.7E+9	Ry
610		336.245(3)	297402	336.2397(17)	0.005	$4d^95s\ ^3D_2$	$4d^85s(^4P)5p\ ^5D_1$	185475.22	482882.1	8.2E+9	Ry
710		336.443(3)	297227	336.4404(20)	0.003	$4d^95s\ ^3D_3$	$4d^85s(^4P)5p\ ^5D_3$	182996.46	480225.9	7.2E+9	Ry
720		336.574(3)	297111	336.5703(17)	0.004	$4d^95s\ ^1D_2$	$4d^85s(^2G)5p\ ^3Fa_2$	194646.26	491761.0	3.1E+10	Ry
120		336.897(3)	296827	336.8944(20)	0.003	$4d^95s\ ^3D_1$	$4d^85s(^2P)5p\ ^3D_1$	191618.62	488447.5	1.4E+9 CF	Ry
550		337.183(3)	296575	337.1801(17)	0.003	$4d^95s\ ^3D_2$	$4d^85s(^2F)5p\ ^3D_1$	185475.22	482052.6	1.2E+10	Ry
230		337.609(3)	296201	337.6055(18)	0.004	$4d^95s\ ^1D_2$	$4d^85s(^2P)5p\ ^1P_1$	194646.26	490850	7.0E+9	Ry
140		337.629(3)	296183	337.6288(18)	0.000	$4d^95s\ ^3D_1$	$4d^95f\ ^3P_2$	191618.62	487801.9	1.2E+9	Ry
240		337.814(3)	296021	337.8120(21)	0.002	$4d^95s\ ^1D_2$	$4d^85s(^2P)5p\ ^3D_3$	194646.26	490668.9	8.3E+9	Ry
350		338.423(3)	295488	338.4200(16)	0.003	$4d^95s\ ^3D_3$	$4d^85s(^2D)5p\ ^3F_2$	182996.46	478487.3	5.6E+9	Ry
280		338.797(3)	295162	338.7954(17)	0.002	$4d^95s\ ^3D_2$	$4d^85s(^4P)5p\ ^5P_3$	185475.22	480638.6	6.2E+9	Ry

I_{obs} [a] (A.U)	Char.[b]	λ_{obs} [c] (Å)	σ_{obs} (cm^{-1})	λ_{Ritz} [d] (Å)	$\delta\lambda_{obs-Ritz}$ [e] (Å)	Classification		E_{low} (cm^{-1})	E_{upp} (cm^{-1})	gA^f (s^{-1})	Lin. Ref [g]
90		338.979(3)	295004	338.9780(17)	0.001	$4d^95s\ ^3D_2$	$4d^85s(^2F)5p\ ^3F_2$	185475.22	480479.6		Ry
770		339.090(3)	294907	339.090(3)	0.000	$4d^95s\ ^3D_3$	$4d^85s(^2F)5p\ ^1G_4$	182996.46	477903	1.0E+10	Ry
110		339.267(3)	294753	339.2698(20)	-0.003	$4d^95s\ ^3D_2$	$4d^85s(^4P)5p\ ^5D_3$	185475.22	480225.9	2.6E+8 [CF]	Ry
420		339.735(3)	294347	339.7330(20)	0.002	$4d^95s\ ^3D_1$	$4d^85s(^2P)5p\ ^3D_2$	191618.62	485967.4	1.1E+10	Ry
50		340.364(3)	293803	340.3662(20)	-0.002	$4d^95s\ ^1D_2$	$4d^85s(^2P)5p\ ^3D_1$	194646.26	488447.5	5.8E+8 [CF]	Ry
310		340.450(3)	293729	340.4504(21)	0.000	$4d^95s\ ^3D_1$	$4d^85s(^2D)5p\ ^3Db_1$	191618.62	485347.2	6.1E+9	Ry
500		340.802(3)	293426	340.8000(22)	0.002	$4d^95s\ ^1D_2$	$4d^85s(^2D)5p\ ^3P_2$	194646.26	488073.5	7.1E+9	Ry
50		340.958(3)	293291	340.9549(18)	0.003	$4d^95s\ ^3D_1$	$4d^85s(^2D)5p\ ^3D_2$	191618.62	484912.5	3.7E+8 [CF]	Ry
880		341.088(3)	293179	341.0858(21)	0.002	$4d^95s\ ^3D_3$	$4d^85s(^2F)5p\ ^1F_3$	182996.46	476177.8	3.3E+10	Ry
790		341.283(3)	293012	341.2829(17)	0.000	$4d^95s\ ^3D_2$	$4d^85s(^2D)5p\ ^3F_2$	185475.22	478487.3	2.8E+10	Ry
840		341.512(3)	292815	341.512(3)	0.000	$4d^95s\ ^3D_3$	$4d^85s(^2F)5p\ ^3F_4$	182996.46	475812	1.5E+10	Ry
560		341.720(3)	292637	341.7192(18)	0.001	$4d^95s\ ^1D_2$	$4d^85s(^2D)5p\ ^3D_3$	194646.26	487284.2	8.8E+9	Ry
320		342.547(3)	291931	342.5475(18)	-0.001	$4d^95s\ ^3D_1$	$4d^85s(^4P)5p\ ^5D_2$	191618.62	483548.9	5.3E+9	Ry
850		342.854(3)	291669	342.8548(24)	-0.001	$4d^95s\ ^3D_2$	$4d^85s(^2F)5p\ ^1D_2$	185475.22	477143.9	3.3E+10	Ry
250		343.262(3)	291323	343.2638(21)	-0.002	$4d^95s\ ^1D_2$	$4d^85s(^2P)5p\ ^3D_2$	194646.26	485967.4	7.8E+9	Ry
100		343.330(3)	291265	343.3317(18)	-0.002	$4d^95s\ ^3D_1$	$4d^85s(^4P)5p\ ^5D_1$	191618.62	482882.1	4.6E+8 [CF]	Ry
550		343.358(3)	291241	343.3602(18)	-0.002	$4d^95s\ ^1D_2$	$4d^85s(^2G)5p\ ^3F_3$	194646.26	485885.6	1.3E+10	Ry
140		343.681(3)	290967	343.681(3)	0.000	$4d^95s\ ^3D_1$	$4d^85s(^4P)5p\ ^5D_0$	191618.62	482586	8.9E+8	Ry
550		343.992(3)	290704	343.9942(21)	-0.002	$4d^95s\ ^3D_2$	$4d^85s(^2F)5p\ ^1F_3$	185475.22	476177.8	8.6E+9	Ry
90		344.226(3)	290507	344.226(3)	0.000	$4d^95s\ ^3D_2$	$4d^85s(^4F)5p\ ^5F_1$	185475.22	475981.8	4.7E+8 [CF]	Ry
130		344.247(3)	290489	344.2471(21)	0.000	$4d^95s\ ^3D_3$	$4d^85s(^2F)5p\ ^1G_3$	182996.46	473485.5	1.2E+9	Ry
440		344.309(3)	290437	344.3123(18)	-0.003	$4d^95s\ ^3D_1$	$4d^85s(^2F)5p\ ^3D_1$	191618.62	482052.6	6.9E+9	Ry
600		344.509(3)	290268	344.5113(18)	-0.002	$4d^95s\ ^1D_2$	$4d^85s(^2D)5p\ ^3D_2$	194646.26	484912.5	1.4E+10	Ry
200		346.134(3)	288905	346.1374(18)	-0.003	$4d^95s\ ^1D_2$	$4d^85s(^4P)5p\ ^5D_2$	194646.26	483548.9	2.5E+9	Ry
350		346.159(3)	288885	346.1639(20)	-0.005	$4d^95s\ ^3D_3$	$4d^85s(^2F)5p\ ^3D_2$	182996.46	471877	2.3E+9	Ry
860		346.213(3)	288840	346.2145(21)	-0.002	$4d^95s\ ^3D_3$	$4d^85s(^2F)5p\ ^3D_3$	182996.46	471834.7	2.0E+10	Ry
70		346.935(3)	288238.4	346.9381(18)	-0.003	$4d^95s\ ^1D_2$	$4d^85s(^4P)5p\ ^5D_1$	194646.26	482882.1	4.4E+8 [CF]	Ry
400		347.210(3)	288010.1	347.2098(21)	0.000	$4d^95s\ ^3D_2$	$4d^85s(^2F)5p\ ^3G_3$	185475.22	473485.5	2.2E+9	Ry
80		347.940(3)	287405.9	347.9394(18)	0.001	$4d^95s\ ^1D_2$	$4d^85s(^2F)5p\ ^3D_1$	194646.26	482052.6	8.8E+8 [CF]	Ry
230		348.588(3)	286871.6	348.5916(17)	-0.004	$4d^95s\ ^3D_1$	$4d^85s(^2D)5p\ ^3F_2$	191618.62	478487.3	2.4E+9	Ry
730		349.162(3)	286400.0	349.1598(20)	0.002	$4d^95s\ ^3D_2$	$4d^85s(^2F)5p\ ^3D_2$	185475.22	471877	1.1E+10	Ry

I_{obs} [a] (A.U)	Char.[b]	λ_{obs} [c] (Å)	σ_{obs} (cm^{-1})	λ_{Ritz} [d] (Å)	$\delta\lambda_{obs-Ritz}$ [e] (Å)	Classification		E_{low}(cm^{-1})	E_{upp}(cm^{-1})	gA^{f}(s-1)	Lin. Ref[g]
100		349.213(3)	286358.2	349.2114(21)	0.002	$4d^9 5s\ ^3D_2$	$4d^8 5s(^2F)5p\ ^3D_3$	185475.22	471834.7	1.6E+9 CF	Ry
70		349.659(3)	285992.9	349.6597(18)	-0.001	$4d^9 5s\ ^1D_2$	$4d^8 5s(^4P)5p\ ^5P_3$	194646.26	480638.6	5.3E+8 CF	Ry
230		349.798(3)	285879.3	349.7968(24)	0.001	$4d^9 5s\ ^3D_3$	$4d^8 5s(^4F)5p\ ^5F_3$	182996.46	468876.7	6.2E+8 CF	Ry
630		349.853(3)	285834.3	349.8542(18)	-0.001	$4d^9 5s\ ^1D_2$	$4d^8 5s(^2F)5p\ ^3F_2$	194646.26	480479.6	1.2E+10	Ry
530		350.166(6)	285579	350.1650(21)	0.001	$4d^9 5s\ ^1D_2$	$4d^8 5s(^4P)5p\ ^5D_3$	194646.26	480225.9	7.9E+9	Ry
160		350.237(6)	285521	350.232(3)	0.005	$4d^9 5s\ ^3D_1$	$4d^8 5s(^2F)5p\ ^1D_2$	191618.62	477143.9	3.4E+9	Ry
770		351.101(6)	284818	351.101(3)	0.000	$4d^9 5s\ ^3D_3$	$4d^8 5s(^2F)5p\ ^3F_3$	182996.46	467815	1.6E+10	Ry
470		351.664(6)	284362	351.663(3)	0.001	$4d^9 5s\ ^3D_1$	$4d^8 5s(^4F)5p\ ^5F_1$	191618.62	475981.8	4.6E+9	Ry
180		351.950(6)	284131	351.950(6)	0.000	$4d^9 5s\ ^3D_3$	$4d^8 5s(^4F)5p\ ^5F_4$	182996.46	467128	4.8E+8	Ry
160		352.312(6)	283839	352.3099(18)	0.002	$4d^9 5s\ ^1D_2$	$4d^8 5s(^2D)5p\ ^3F_2$	194646.26	478487.3	2.9E+9 CF	Ry
190		352.641(6)	283575	352.645(4)	-0.004	$4d^9 5s\ ^3D_3$	$4d^8 5s(^4P)5p\ ^5P_2$	182996.46	466568	7.1E+8 CF	Ry
330		352.855(6)	283403	352.8563(25)	-0.001	$4d^9 5s\ ^3D_2$	$4d^8 5s(^4F)5p\ ^5F_3$	185475.22	468876.7	2.0E+9	Ry
510		353.983(6)	282499	353.985(3)	-0.002	$4d^9 5s\ ^1D_2$	$4d^8 5s(^2F)5p\ ^1D_2$	194646.26	477143.9	9.4E+9	Ry
670		354.177(6)	282345	354.183(3)	-0.006	$4d^9 5s\ ^3D_2$	$4d^8 5s(^2F)5p\ ^3F_3$	185475.22	467815	9.3E+9	Ry
58		355.136(6)	281582	355.1323(25)	0.004	$4d^{10}\ ^1S_0$	$4d^9 5p\ ^3D_1$	0	281585.18	1.2E+10	TW
150		356.825(6)	280249	356.8136(21)	0.011	$4d^9 5s\ ^3D_1$	$4d^8 5s(^2F)5p\ ^3D_2$	191618.62	471877	2.2E+9 CF	Ry
72		361.002(6)	277007	361.004(3)	-0.002	$4d^{10}\ ^1S_0$	$4d^9 5p\ ^1P_1$	0	277005.34	4.7E+10	TW
140		362.945(6)	275524	362.945(6)	0.000	$4d^9 5s\ ^3D_1$	$4d^8 5s(^2D)5p\ ^3Da_1$	191618.62	467142.5	1.1E+9 CF	Ry
50		364.654(6)	274233	364.657(3)	-0.003	$4d^9 5s\ ^1D_2$	$4d^8 5s(^4F)5p\ ^5F_3$	194646.26	468876.7	2.2E+8 CF	Ry
40		366.078(6)	273166	366.074(4)	0.004	$4d^9 5s\ ^1D_2$	$4d^8 5s(^2F)5p\ ^3F_3$	194646.26	467815	7.3E+7 CF	Ry
70		367.757(6)	271919	367.753(4)	0.004	$4d^9 5s\ ^1D_2$	$4d^8 5s(^4P)5p\ ^5P_2$	194646.26	466568	5.0E+8 CF	Ry
82		372.552(6)	268419	372.560(3)	-0.008	$4d^{10}\ ^1S_0$	$4d^9 5p\ ^3P_1$	0	268413.14	7.8E+8	TW
130		388.248(6)	257567	388.2458(9)	0.002	$4d^9 5s\ ^3D_2$	$4d^9 6p\ ^1F_3$	185475.22	443044.0	1.8E+8 CF	Ry
130		393.176(6)	254339	393.186(4)	-0.010	$4d^9 5s\ ^3D_2$	$4d^9 6p\ ^1P_1$	185475.22	439808	1.0E+8 CF	Ry
700		395.720(12)	252704	395.7353(7)	-0.015	$4d^9 5s\ ^3D_3$	$4d^9 6p\ ^3D_3$	182996.46	435690.62	1.6E+9	Ry
360		395.962(6)	252549	395.964(6)	-0.002	$4d^9 5s\ ^3D_1$	$4d^9 6p\ ^3D_2$	191618.62	444167	6.0E+8	Ry
580		397.143(6)	251798	397.146(5)	-0.003	$4d^9 5s\ ^3D_1$	$4d^9 6p\ ^3D_1$	191618.62	443415	1.0E+9	Ry
810		398.525(6)	250925	398.5266(8)	-0.002	$4d^9 5s\ ^3D_3$	$4d^9 6p\ ^3F_4$	182996.46	433920.71	3.4E+9	Ry
480		399.645(6)	250222	399.6557(7)	-0.011	$4d^9 5s\ ^3D_2$	$4d^9 6p\ ^3D_3$	185475.22	435690.62	6.8E+8	Ry
820		400.557(6)	249652	400.5514(5)	0.006	$4d^9 5s\ ^3D_2$	$4d^9 6p\ ^1D_2$	185475.22	435131.1	1.7E+9	Ry

I_{obs} [a] (A.U)	Char.[b]	λ_{obs} [c] (Å)	σ_{obs} (cm^{-1})	λ_{Ritz} [d] (Å)	$\delta\lambda_{obs-Ritz}$ [e] (Å)	Classification		E_{low} (cm^{-1})	E_{upp} (cm^{-1})	gA^f(s-1)	Lin. Ref [g]
790	bl	400.776(17)	249516	400.768(6)	0.008	$4d^9 5s\ ^1D_2$	$4d^9 6p\ ^3D_2$	194646.26	444167	1.1E+9	Ry
790	bl	400.776(17)	249516	400.776(17)	0.000	$4d^9 5s\ ^3D_1$	$4d^9 6p\ ^3P_0$	191618.62	441134.6	4.9E+8	Ry
710		402.038(6)	248733	402.0461(9)	-0.008	$4d^9 5s\ ^3D_2$	$4d^9 6p\ ^3P_1$	185475.22	434202.9	1.1E+9	Ry
680		402.276(6)	248586	402.2870(4)	-0.011	$4d^9 5s\ ^3D_3$	$4d^9 6p\ ^3F_3$	182996.46	431575.20	6.3E+8	Ry
780		402.599(12)	248386	402.5802(10)	0.019	$4d^9 5s\ ^1D_2$	$4d^9 6p\ ^1F_3$	194646.26	443044.0	2.7E+9	Ry
720		402.664(6)	248346	402.667(4)	-0.003	$4d^9 5s\ ^3D_1$	$4d^9 6p\ ^3F_2$	191618.62	439963	1.2E+9	Ry
590		404.201(6)	247402	404.1869(5)	0.014	$4d^9 5s\ ^3D_3$	$4d^9 6p\ ^3P_2$	182996.46	430406.74	2.2E+9	Ry
80		404.404(6)	247277	404.409(4)	-0.005	$4d^9 5s\ ^3D_3$	$4d^9 4f\ ^3F_3$	182996.46	430271	2.6E+7 [CF]	Ry
810		406.328(6)	246107	406.3389(4)	-0.011	$4d^9 5s\ ^3D_2$	$4d^9 6p\ ^3F_3$	185475.22	431575.20	1.8E+9	Ry
620		407.640(6)	245314	407.636(4)	0.004	$4d^9 5s\ ^1D_2$	$4d^9 6p\ ^3F_2$	194646.26	439963	6.0E+8	Ry
630		407.897(6)	245160	407.894(4)	0.003	$4d^9 5s\ ^1D_2$	$4d^9 6p\ ^1P_1$	194646.26	439808	9.4E+8	Ry
220		408.507(6)	244794	408.504(4)	0.003	$4d^9 5s\ ^3D_2$	$4d^9 4f\ ^3F_3$	185475.22	430271	8.4E+7 [CF]	Ry
190		414.856(6)	241047	414.8614(7)	-0.005	$4d^9 5s\ ^1D_2$	$4d^9 6p\ ^3D_3$	194646.26	435690.62	1.9E+8	Ry
60		415.827(6)	240485	415.8266(6)	0.000	$4d^9 5s\ ^1D_2$	$4d^9 6p\ ^1D_2$	194646.26	435131.1	8.8E+7 [CF]	Ry
290		422.082(6)	236921	422.0675(4)	0.015	$4d^9 5s\ ^1D_2$	$4d^9 6p\ ^3F_3$	194646.26	431575.20	1.9E+8 [CF]	Ry
330		424.168(6)	235756	424.1593(4)	0.009	$4d^9 5s\ ^1D_2$	$4d^9 6p\ ^3P_2$	194646.26	430406.74	3.6E+7 [CF]	Ry
50		437.176(6)	228741	437.165(3)	0.011	$4d^9 5p\ ^3P_2$	$4d^9 6d\ ^3F_3$	259788.94	488535.6	2.1E+8 [CF]	Ry
260		438.698(6)	227947	438.691(3)	0.007	$4d^9 5p\ ^3P_1$	$4d^9 7s\ ^3D_2$	268413.14	496363.9	1.2E+9	Ry
530		439.249(6)	227661	439.249(3)	0.000	$4d^9 5p\ ^3P_2$	$4d^9 7s\ ^3D_3$	259788.94	487450.1	4.5E+9	Ry
150		440.819(6)	226850	440.818(3)	0.001	$4d^9 5p\ ^3F_2$	$4d^9 7s\ ^3D_2$	269512.91	496363.9	1.3E+9	Ry
280		441.245(6)	226631	441.253(3)	-0.008	$4d^9 5p\ ^3F_2$	$4d^9 7s\ ^3D_1$	269512.91	496140.3	2.5E+9	Ry
220		443.768(6)	225343	443.7742(22)	-0.006	$4d^9 5p\ ^3F_3$	$4d^9 6d\ ^3D_2$	262734.7	488074.5	2.2E+9	Ry
420		444.570(6)	224936	444.5735(22)	-0.003	$4d^9 5p\ ^3F_3$	$4d^9 7s\ ^1D_2$	262734.7	487669.4	2.4E+9	Ry
280		444.996(6)	224721	445.007(3)	-0.011	$4d^9 5p\ ^3F_3$	$4d^9 7s\ ^3D_3$	262734.7	487450.1	1.9E+9	Ry
100		449.664(6)	222388	449.664(3)	0.000	$4d^9 5p\ ^1D_2$	$4d^9 7s\ ^3D_1$	273752.04	496140.3	7.5E+8	Ry
190		455.244(6)	219662	455.2462(24)	-0.002	$4d^9 5p\ ^3P_1$	$4d^9 6d\ ^3D_2$	268413.14	488074.5	1.8E+9	Ry
200		455.884(6)	219354	455.875(3)	0.009	$4d^9 5p\ ^1P_1$	$4d^9 7s\ ^3D_2$	277005.34	496363.9	1.4E+9	Ry
170		455.922(6)	219336	455.936(3)	-0.014	$4d^9 5p\ ^3P_2$	$4d^9 6d\ ^3D_3$	259788.94	479118	1.4E+9	Ry
110		456.086(6)	219257	456.0873(23)	-0.001	$4d^9 5p\ ^3P_1$	$4d^9 7s\ ^1D_2$	268413.14	487669.4	1.1E+8 [CF]	Ry
230	bl	457.097(17)	218772	457.1026(11)	-0.006	$4d^9 5p\ ^3P_2$	$4d^9 6d\ ^3P_2$	259788.94	478558.2	1.9E+9	Ry

I_{obs}[a] (A.U)	Char.[b]	λ_{obs}[c] (Å)	σ_{obs} (cm^{-1})	λ_{Ritz}[d] (Å)	$\delta\lambda_{obs-Ritz}$[e] (Å)	Classification	E_{low}(cm^{-1})	E_{upp}(cm^{-1})	gA^f(s-1)	Lin. Ref[g]
230	bl	457.097(17)	218772	457.114(3)	-0.017	$4d^95p\ ^3F_2$ $4d^96d\ ^3F_2$	269512.91	488276.6	8.7E+8	Ry
70		457.532(6)	218564	457.5369(24)	-0.005	$4d^95p\ ^3F_2$ $4d^96d\ ^3D_2$	269512.91	488074.5	3.0E+8	Ry
760		458.091(6)	218297	458.077(3)	0.014	$4d^95p\ ^3F_4$ $4d^97s\ ^3D_3$	269146.4	487450.1	7.8E+9	Ry
160		458.379(6)	218160	458.3865(23)	-0.008	$4d^95p\ ^3F_2$ $4d^97s\ ^1D_2$	269512.91	487669.4	6.8E+8	Ry
40		458.651(6)	218031	458.650(4)	0.001	$4d^95p\ ^3P_1$ $4d^96d\ ^3P_1$	268413.14	486444.4	3.8E+8[CF]	Ry
45		458.998(6)	217866	458.998(6)	0.000	$4d^95p\ ^1P_1$ $4d^96d\ ^1S_0$	277005.34	494871	1.5E+9	Ry*
220		459.952(6)	217414	459.953(4)	-0.001	$4d^95p\ ^3F_2$ $4d^96d\ ^3G_3$	269512.91	486926.3	2.8E+9	Ry
120		460.675(6)	217073	460.6768(10)	-0.002	$4d^95p\ ^3P_2$ $4d^96d\ ^3S_1$	259788.94	476860.86	1.0E+9	Ry
90		461.089(12)	216878	461.111(3)	-0.022	$4d^95p\ ^3F_3$ $4d^96d\ ^1F_3$	262734.7	479602.2	9.3E+8	Ry
500		461.447(6)	216710	461.463(3)	-0.016	$4d^95p\ ^1F_3$ $4d^97s\ ^3D_2$	279661.63	496363.9	5.7E+9	Ry
100		462.136(6)	216387	462.143(3)	-0.007	$4d^95p\ ^3F_3$ $4d^96d\ ^3D_3$	262734.7	479118	8.1E+8	Ry
60		463.327(6)	215830	463.3416(11)	-0.015	$4d^95p\ ^3F_3$ $4d^96d\ ^3P_2$	262734.7	478558.2	2.0E+8	Ry
360		463.857(6)	215584	463.8512(11)	0.006	$4d^95p\ ^3F_3$ $4d^96d\ ^3G_4$	262734.7	478321.10	4.6E+9	Ry
320		466.088(6)	214552	466.081(3)	0.007	$4d^95p\ ^3D_1$ $4d^97s\ ^3D_1$	281585.18	496140.3	1.9E+9	Ry
160		466.147(6)	214525	466.147(3)	0.000	$4d^95p\ ^1D_2$ $4d^96d\ ^3F_2$	273752.04	488276.6	1.4E+8[CF]	Ry
190		466.582(6)	214325	466.5867(25)	-0.005	$4d^95p\ ^1D_2$ $4d^96d\ ^3D_2$	273752.04	488074.5	1.8E+9	Ry
330	u	467.465(17)	213920	467.465(17)	0.000	$4d^95p\ ^3P_1$ $4d^96d\ ^3P_0$	268413.14	482333	5.0E+8	Ry*
330		467.465(8)	213920	467.4702(24)	-0.005	$4d^95p\ ^1D_2$ $4d^97s\ ^1D_2$	273752.04	487669.4	1.4E+9	Ry
60		467.851(6)	213743	467.854(3)	-0.003	$4d^95p\ ^3D_3$ $4d^96d\ ^3F_3$	274793.85	488535.6	2.1E+8[CF]	Ry
30	H		213515	468.802(4)		$4d^95p\ ^3P_0$ $4d^96d\ ^3D_1$	274056.4	487366	6.7E+8	Ry
380	m(O II)	468.758(12)	213330	468.760(3)	-0.002	$4d^95p\ ^3D_2$ $4d^97s\ ^3D_2$	283035.3	496363.9	2.7E+9	Ry
110		468.860(17)	213283	468.854(6)	0.006	$4d^95p\ ^3D_1$ $4d^96d\ ^1S_0$	281585.18	494871	3.1E+8	Ry*
110		468.860(17)	213283	468.866(3)	-0.006	$4d^95p\ ^3D_3$ $4d^96d\ ^3D_2$	274793.85	488074.5	6.5E+8	Ry
160		469.101(6)	213174	469.100(4)	0.001	$4d^95p\ ^1D_2$ $4d^96d\ ^3G_3$	273752.04	486926.3	9.5E+8	Ry
180		469.252(6)	213105	469.252(3)	0.000	$4d^95p\ ^3D_2$ $4d^97s\ ^3D_1$	283035.3	496140.3	1.3E+9	Ry
220		469.759(6)	212875	469.7580(24)	0.001	$4d^95p\ ^3D_3$ $4d^97s\ ^1D_2$	274793.85	487669.4	1.1E+9	Ry
460		470.240(6)	212657	470.242(3)	-0.002	$4d^95p\ ^3D_3$ $4d^97s\ ^3D_3$	274793.85	487450.1	3.4E+9	Ry
70		473.164(6)	211343	473.1796(11)	-0.016	$4d^95p\ ^3P_1$ $4d^96d\ ^1D_2$	268413.14	479749.4	5.6E+8	Ry
40		473.320(6)	211274	473.325(3)	-0.005	$4d^95p\ ^1P_1$ $4d^96d\ ^3F_2$	277005.34	488276.6	6.9E+8	Ry
30		473.776(6)	211070	473.778(3)	-0.002	$4d^95p\ ^1P_1$ $4d^96d\ ^3D_2$	277005.34	488074.5	1.8E+8[CF]	Ry

I_{obs} [a] (A.U)	Char. [b]	λ_{obs} [c] (Å)	σ_{obs} (cm^{-1})	λ_{Ritz} [d] (Å)	$\delta\lambda_{obs-Ritz}$ [e] (Å)	Classification		E_{low} (cm^{-1})	E_{upp} (cm^{-1})	gA^{f} (s-1)	Lin. Ref [g]
130		474.476(6)	210759	474.4929(15)	-0.017	$4d^9 5p\ ^3F_4$	$4d^9 6d\ ^3F_4$	269146.4	479897.7	1.6E+9	Ry
120		474.694(6)	210662	474.6894(25)	0.005	$4d^9 5p\ ^1P_1$	$4d^9 7s\ ^1D_2$	277005.34	487669.4	5.6E+8	Ry
60		475.362(6)	210366	475.374(4)	-0.012	$4d^9 5p\ ^1P_1$	$4d^9 6d\ ^3D_1$	277005.34	487366	4.2E+8	Ry
50		475.657(6)	210236	475.6548(11)	0.002	$4d^9 5p\ ^3F_2$	$4d^9 6d\ ^1D_2$	269512.91	479749.4	3.2E+8	Ry
60		475.727(6)	210205	475.725(4)	0.002	$4d^9 5p\ ^3P_1$	$4d^9 6d\ ^1P_1$	268413.14	478618.7	5.3E+8	Ry
60		475.988(6)	210089	475.988(3)	0.000	$4d^9 5p\ ^3F_2$	$4d^9 6d\ ^1F_3$	269512.91	479602.2	6.9E+8	Ry
350		477.604(6)	209378	477.604(6)	0.000	$4d^9 5p\ ^3F_4$	$4d^9 6d\ ^3G_5$	269146.4	478525	6.2E+9	Ry
40		478.101(12)	209161	478.0693(13)	0.032	$4d^9 5p\ ^3F_4$	$4d^9 6d\ ^3G_4$	269146.4	478321.10	3.2E+8	Ry
50		478.754(6)	208876	478.758(3)	-0.004	$4d^9 5p\ ^1F_3$	$4d^9 6d\ ^3F_3$	279661.63	488535.6	8.2E+8	Ry
170		479.359(6)	208612	479.352(4)	0.007	$4d^9 5p\ ^1F_3$	$4d^9 6d\ ^3F_2$	279661.63	488276.6	6.1E+7 [CF]	Ry
380	m(O III)	480.950(12)	207922	480.950(12)	0.000	$4d^9 5p\ ^1F_3$	$4d^9 6d\ ^1G_4$	279661.63	487583.4	4.60E+09	Ry
120		485.246(6)	206081	485.239(3)	0.007	$4d^9 5p\ ^3D_1$	$4d^9 7s\ ^1D_2$	281585.18	487669.4	1.0E+9	Ry
140		485.792(6)	205849	485.790(3)	0.002	$4d^9 5p\ ^1D_2$	$4d^9 6d\ ^1F_3$	273752.04	479602.2	1.8E+9	Ry
40		485.964(6)	205777	485.954(4)	0.010	$4d^9 5p\ ^3D_1$	$4d^9 6d\ ^3D_1$	281585.18	487366	1.6E+8 [CF]	Ry
140		486.615(6)	205501	486.617(3)	-0.002	$4d^9 5p\ ^3D_2$	$4d^9 6d\ ^3F_3$	283035.3	488535.6	2.5E+9	Ry
210		487.553(6)	205106	487.5579(15)	-0.005	$4d^9 5p\ ^3D_3$	$4d^9 6d\ ^3F_4$	274793.85	479897.7	3.1E+9	Ry
60		487.730(6)	205031	487.712(3)	0.018	$4d^9 5p\ ^3D_2$	$4d^9 6d\ ^3D_2$	283035.3	488074.5	5.8E+8 [CF]	Ry
40		488.139(6)	204860	488.140(5)	-0.001	$4d^9 5p\ ^3D_1$	$4d^9 6d\ ^3P_1$	281585.18	486444.4	2.8E+8	Ry
50		488.265(6)	204807	488.261(3)	0.004	$4d^9 5p\ ^3D_3$	$4d^9 6d\ ^1F_3$	274793.85	479602.2	3.8E+8	Ry
80		489.435(6)	204317	489.418(4)	0.017	$4d^9 5p\ ^3D_3$	$4d^9 6d\ ^3D_3$	274793.85	479118	1.2E+9	Ry
40		490.780(6)	203757.3	490.7630(12)	0.017	$4d^9 5p\ ^3D_3$	$4d^9 6d\ ^3P_2$	274793.85	478558.2	4.0E+8	Ry
40		493.239(6)	202741.5	493.2327(12)	0.006	$4d^9 5p\ ^1P_1$	$4d^9 6d\ ^1D_2$	277005.34	479749.4	1.7E+8 [CF]	Ry
40		495.997(6)	201614.1	495.999(4)	-0.002	$4d^9 5p\ ^1P_1$	$4d^9 6d\ ^1P_1$	277005.34	478618.7	2.9E+8 [CF]	Ry
16		654.543(5)	152778.4	654.5395(24)	0.003	$4d^9 5p\ ^3P_2$	$4d^8 5s^2\ ^1D_2$	259788.94	412568.1		VJ
10		659.256(6)	151686.1	659.2577(17)	-0.002	$4d^9 5p\ ^3P_2$	$4d^9 6s\ ^3D_2$	259788.94	411474.7	2.1E+8 [CF]	TW
17		661.725(6)	151120.2	661.7356(20)	-0.011	$4d^9 5p\ ^3P_2$	$4d^9 6s\ ^3D_1$	259788.94	410906.7	3.0E+7 [CF]	TW
40		672.326(5)	148737.4	672.3141(17)	0.012	$4d^9 5p\ ^3F_3$	$4d^9 6s\ ^3D_2$	262734.7	411474.7	3.5E+7 [CF]	VJ
4		672.643(10)	148667.3	672.645(3)	-0.002	$4d^9 5p\ ^3P_2$	$4d^8 5s^2\ ^3P_1$	259788.94	408455.7		VJ
78		695.815(6)	143716.4	695.8208(24)	-0.006	$4d^9 5p\ ^3P_2$	$4d^8 5s^2\ ^3P_2$	259788.94	403504.1		TW
4		698.309(6)	143203.1	698.3106(19)	-0.002	$4d^9 5p\ ^3P_2$	$4d^9 6s\ ^1D_2$	259788.94	402991.7	1.2E+8 [CF]	TW
82		698.993(6)	143062.9	698.9998(19)	-0.007	$4d^9 5p\ ^3P_1$	$4d^9 6s\ ^3D_2$	268413.14	411474.7	2.7E+9	TW

I_{obs} [a] (A.U)	Char.[b]	λ_{obs} [c] (Å)	σ_{obs} (cm^{-1})	λ_{Ritz} [d] (Å)	$\delta\lambda_{obs-Ritz}$ [e] (Å)	Classification	E_{low}(cm^{-1})	E_{upp}(cm^{-1})	gA^f(s-1)	Lin. Ref[g]
48		701.794(6)	142492.0	701.7861(22)	0.008	$4d^95p\ ^3P_1$ $4d^96s\ ^3D_1$	268413.14	410906.7	2.0E+8 [CF]	TW
88		702.002(6)	142449.7	702.0098(21)	-0.008	$4d^95p\ ^3P_2$ $4d^96s\ ^3D_3$	259788.94	402237.1	1.1E+10	TW
68		704.408(6)	141963.2	704.4149(19)	-0.007	$4d^95p\ ^3F_2$ $4d^96s\ ^3D_2$	269512.91	411474.7	2.9E+9	TW
86		707.241(6)	141394.5	707.2446(22)	-0.004	$4d^95p\ ^3F_2$ $4d^96s\ ^3D_1$	269512.91	410906.7	6.0E+9	TW
7		710.393(5)	140767.2	710.3817(24)	0.011	$4d^95p\ ^3F_3$ $4d^85s^2\ ^3P_2$	262734.7	403504.1		VJ
19		712.682(10)	140315.0	712.682(10)	0.000	$4d^95p\ ^3P_1$ $4d^85s^2\ ^3P_0$	268413.14	408728.2		VJ
63		712.963(6)	140259.7	712.9769(19)	-0.014	$4d^95p\ ^3F_3$ $4d^96s\ ^1D_2$	262734.7	402991.7	1.1E+10	TW
15		714.067(5)	140042.9	714.069(3)	-0.002	$4d^95p\ ^3P_1$ $4d^85s^2\ ^3P_1$	268413.14	408455.7		VJ
5		714.575(5)	139943.3	714.581(4)	-0.006	$4d^95p\ ^3D_3$ $4d^85s^2\ ^1G_4$	274793.85	414735.9		VJ
80		716.824(6)	139504.3	716.8335(21)	-0.010	$4d^95p\ ^3F_3$ $4d^96s\ ^3D_3$	262734.7	402237.1	4.9E+9	TW
38		720.379(5)	138815.8	720.378(3)	0.001	$4d^95p\ ^1D_2$ $4d^85s^2\ ^1D_2$	273752.04	412568.1		VJ
68		726.090(6)	137724.0	726.0969(20)	-0.007	$4d^95p\ ^1D_2$ $4d^96s\ ^3D_2$	273752.04	411474.7	1.0E+9 [CF]	TW
74		729.101(6)	137155.2	729.1039(24)	-0.003	$4d^95p\ ^1D_2$ $4d^96s\ ^3D_1$	273752.04	410906.7	1.8E+9	TW
76		730.725(17)	136850	730.7235(23)	0.001	$4d^95p\ ^3P_2$ $4d^85s^2\ ^3F_3$	259788.94	396639.6		TW
76		730.725(17)	136850	730.725(3)	0.000	$4d^95p\ ^3P_0$ $4d^96s\ ^3D_1$	274056.4	410906.7	2.0E+9	TW
62		731.623(6)	136682.4	731.6314(21)	-0.008	$4d^95p\ ^3D_3$ $4d^96s\ ^3D_2$	274793.85	411474.7	5.2E+8 [CF]	TW
41		740.240(5)	135091.3	740.242(3)	-0.002	$4d^95p\ ^3P_1$ $4d^85s^2\ ^3P_2$	268413.14	403504.1		VJ
72		740.339(5)	135073.3	740.333(4)	0.006	$4d^95p\ ^1F_3$ $4d^85s^2\ ^1G_4$	279661.63	414735.9		VI
84		743.055(6)	134579.5	743.0604(21)	-0.005	$4d^95p\ ^3P_1$ $4d^96s\ ^1D_2$	268413.14	402991.7	3.5E+9	TW
82		743.664(6)	134469.3	743.6638(21)	0.000	$4d^95p\ ^1P_1$ $4d^96s\ ^3D_2$	277005.34	411474.7	3.5E+9	TW
62		746.813(6)	133902.3	746.818(3)	-0.005	$4d^95p\ ^1P_1$ $4d^96s\ ^3D_1$	277005.34	410906.7	1.1E+9	TW
88		749.186(6)	133478.2	749.1827(21)	0.003	$4d^95p\ ^3F_2$ $4d^96s\ ^1D_2$	269512.91	402991.7	2.4E+9	TW
78		751.367(6)	133090.8	751.367(3)	0.000	$4d^95p\ ^3F_4$ $4d^96s\ ^3D_3$	269146.4	402237.1	1.8E+10	TW
42		752.409(5)	132906.4	752.409(3)	0.000	$4d^95p\ ^1F_3$ $4d^85s^2\ ^1D_2$	279661.63	412568.1		VJ
64		758.653(5)	131812.6	758.6501(22)	0.003	$4d^95p\ ^1F_3$ $4d^96s\ ^3D_2$	279661.63	411474.7	1.3E+10	VJ
35		760.745(5)	131450.1	760.743(4)	0.002	$4d^95p\ ^1P_1$ $4d^85s^2\ ^3P_1$	277005.34	408455.7		VJ
40		763.442(10)	130985.7	763.458(3)	-0.016	$4d^95p\ ^3D_1$ $4d^85s^2\ ^1D_2$	281585.18	412568.1		VJ
74		764.163(6)	130862.1	764.1687(22)	-0.006	$4d^95p\ ^3P_2$ $4d^95d\ ^3F_3$	259788.94	390650.1	3.5E+8 [CF]	TW
82		765.146(6)	130694.0	765.142(4)	0.004	$4d^95p\ ^1P_1$ $4d^95d\ ^1S_0$	277005.34	407700.0	6.6E+9	TW
72		769.749(6)	129912.5	769.7485(19)	0.000	$4d^95p\ ^3P_2$ $4d^95d\ ^3D_2$	259788.94	389701.5	1.2E+8 [CF]	TW

Int. (A.U)	λ_{obs} (Å)	σ (cm^{-1})	λ_{Ritz} (Å)	O-C (Å)	Classification		E_{low} (cm^{-1})	E_{upp} (cm^{-1})	gA (s^{-1})	Ref[a]
58	769.886(6)	129889.4	769.8851(23)	0.001	$4d^9 5p\ ^3D_1$	$4d^9 6s\ ^3D_2$	281585.18	411474.7	2.6E+8[CF]	TW
68	773.273(6)	129320.4	773.267(3)	0.006	$4d^9 5p\ ^3D_1$	$4d^9 6s\ ^3D_1$	281585.18	410906.7	4.3E+9	TW
82	773.759(6)	129239.2	773.7563(22)	0.003	$4d^9 5p\ ^1D_2$	$4d^9 6s\ ^1D_2$	273752.04	402991.7	7.3E+9	TW
6	776.941(10)	128709.9	776.939(3)	0.002	$4d^9 5p\ ^3D_3$	$4d^8 5s^2\ ^3P_2$	274793.85	403504.1		VJ
40	778.304(6)	128484.5	778.3006(25)	0.003	$4d^9 5p\ ^1D_2$	$4d^9 6s\ ^3D_3$	273752.04	402237.1	5.4E+7[CF]	TW
74	778.584(6)	128438.3	778.5773(23)	0.007	$4d^9 5p\ ^3D_2$	$4d^9 6s\ ^3D_2$	283035.3	411474.7	6.3E+9	TW
80	780.040(6)	128198.6	780.0443(23)	-0.004	$4d^9 5p\ ^3D_3$	$4d^9 6s\ ^1D_2$	274793.85	402991.7	3.6E+9	TW
65	781.694(5)	127927.3	781.692(3)	0.002	$4d^9 5p\ ^3F_2$	$4d^8 5s^2\ ^3F_2$	269512.91	397440.5	2.4E+8	VJ
18	781.771(6)	127914.7	781.7667(22)	0.004	$4d^9 5p\ ^3F_3$	$4d^9 5d\ ^3F_3$	262734.7	390650.1	1.2E+8[CF]	TW
70	782.042(6)	127870.4	782.036(3)	0.006	$4d^9 5p\ ^3D_2$	$4d^9 6s\ ^3D_1$	283035.3	410906.7	2.8E+9	TW
60		127649.5	783.368(3)		$4d^9 5p\ ^3P_2$	$4d^9 5d\ ^3G_3$	259788.94	387442.9	6.7E+7[CF]	TW
54	784.325(6)	127498.2	784.3180(19)	0.007	$4d^9 5p\ ^3F_3$	$4d^9 5d\ ^3F_2$	262734.7	390234.0	1.9E+7[CF]	TW
13	784.363(5)	127492.0	784.356(3)	0.007	$4d^9 5p\ ^3F_4$	$4d^8 5s^2\ ^3F_3$	269146.4	396639.6	1.7E+7[CF]	VJ
80	784.648(6)	127445.7	784.663(3)	-0.015	$4d^9 5p\ ^3D_3$	$4d^9 6s\ ^3D_3$	274793.85	402237.1	8.3E+9	TW
88	786.484(6)	127148.2	786.494(3)	-0.010	$4d^9 5p\ ^3F_3$	$4d^8 5s^2\ ^3F_4$	262734.7	389881.2	1.0E+7[CF]	TW
78	787.605(6)	126967.2	787.6075(19)	-0.002	$4d^9 5p\ ^3F_3$	$4d^9 5d\ ^3D_2$	262734.7	389701.5		TW
38	792.925(6)	126115.3	792.928(4)	-0.003	$4d^9 5p\ ^3D_1$	$4d^9 5d\ ^1S_0$	281585.18	407700.0	1.3E+9	TW
70	793.737(6)	125986.3	793.7367(24)	0.000	$4d^9 5p\ ^1P_1$	$4d^9 6s\ ^1D_2$	277005.34	402991.7	1.3E+9	TW
66	801.876(6)	124707.6	801.872(3)	0.004	$4d^9 5p\ ^3F_3$	$4d^9 5d\ ^3G_3$	262734.7	387442.9	3.2E+8[CF]	TW
70	807.476(6)	123842.7	807.477(3)	-0.001	$4d^9 5p\ ^1F_3$	$4d^8 5s^2\ ^3P_2$	279661.63	403504.1		TW
5	810.841(6)	123328.7	810.8323(25)	0.009	$4d^9 5p\ ^1F_3$	$4d^9 6s\ ^1D_2$	279661.63	402991.7	8.2E+7[CF]	TW
44	813.749(6)	122888.0	813.752(3)	-0.003	$4d^9 5p\ ^1D_2$	$4d^8 5s^2\ ^3F_3$	273752.04	396639.6	9.6E+7[CF]	TW
68	815.832(6)	122574.3	815.824(3)	0.008	$4d^9 5p\ ^1F_3$	$4d^9 6s\ ^3D_3$	279661.63	402237.1	3.8E+8[CF]	TW
76	819.359(6)	122046.6	819.3492(18)	0.010	$4d^9 5p\ ^3P_2$	$4d^9 5d\ ^1D_2$	259788.94	381837.02	8.0E+8[CF]	TW
30	820.712(6)	121845.4	820.710(3)	0.002	$4d^9 5p\ ^3D_3$	$4d^8 5s^2\ ^3F_3$	274793.85	396639.6	7.9E+7[CF]	TW
74	820.887(6)	121819.4	820.8775(21)	0.010	$4d^9 5p\ ^3P_1$	$4d^9 5d\ ^3F_2$	268413.14	390234.0	8.6E+8	TW
72	823.685(6)	121405.6	823.679(3)	0.006	$4d^9 5p\ ^3D_1$	$4d^9 6s\ ^1D_2$	281585.18	402991.7	7.4E+8	TW
86	824.476(6)	121289.2	824.4814(21)	-0.005	$4d^9 5p\ ^3P_1$	$4d^9 5d\ ^3D_2$	268413.14	389701.5	3.9E+9	TW
66	825.520(6)	121135.8	825.5103(25)	0.010	$4d^9 5p\ ^3F_2$	$4d^9 5d\ ^3F_3$	269512.91	390650.1	3.1E+8[CF]	TW
88	827.156(6)	120896.2	827.1581(18)	-0.002	$4d^9 5p\ ^3P_2$	$4d^9 5d\ ^3D_3$	259788.94	380684.81	1.5E+10	TW

I_{obs} [a] (A.U)	Char.[b]	λ_{obs} [c] (Å)	σ_{obs} (cm^{-1})	λ_{Ritz} [d] (Å)	$\delta\lambda_{obs-Ritz}$ [e] (Å)	Classification	E_{low} (cm^{-1})	E_{upp} (cm^{-1})	gA^{r} (s-1)	Lin. Ref [f]
84		828.268(6)	120733.9	828.262(4)	0.006	$4d^95p\ ^3F_4$ — $4d^85s^2\ ^3F_4$	269146.4	389881.2	1.4E+9	TW
86		828.348(6)	120722.2	828.3557(21)	-0.008	$4d^95p\ ^3F_2$ — $4d^95d\ ^3F_2$	269512.91	390234.0	1.0E+10	TW
5		830.075(10)	120471.0	830.090(3)	-0.015	$4d^95p\ ^3D_2$ — $4d^85s^2\ ^3P_2$	283035.3	403504.1		VJ
44		830.322(5)	120435.2	830.322(4)	0.000	$4d^95p\ ^1P_1$ — $4d^85s^2\ ^3F_2$	277005.34	397440.5	3.0E+7 [CF]	VJ
10		832.025(5)	120188.7	832.0257(21)	-0.001	$4d^95p\ ^3F_2$ — $4d^95d\ ^3D_2$	269512.91	389701.5		VJ
82		833.473(6)	119979.9	833.4621(23)	0.011	$4d^95p\ ^3P_1$ — $4d^95d\ ^3D_1$	268413.14	388394.6	2.0E+9	TW
88		835.572(6)	119678.5	835.5653(23)	0.007	$4d^95p\ ^3P_2$ — $4d^95d\ ^1P_1$	259788.94	379468.4	3.7E+9	TW
78		837.300(6)	119431.5	837.2937(19)	0.006	$4d^95p\ ^3P_2$ — $4d^95d\ ^3P_2$	259788.94	379221.34	2.3E+10	TW
54		838.928(6)	119199.7	838.914(3)	0.014	$4d^95p\ ^3D_2$ — $4d^96s\ ^3D_3$	283035.3	402237.1	1.3E+8 [CF]	TW
80		839.618(6)	119101.8	839.6142(17)	0.004	$4d^95p\ ^3F_3$ — $4d^95d\ ^1D_2$	262734.7	381837.02	2.2E+9	TW
84		839.717(6)	119087.7	839.7115(17)	0.005	$4d^95p\ ^3F_3$ — $4d^95d\ ^1F_3$	262734.7	381823.22	9.3E+9	TW
40		840.978(6)	118909.2	840.977(3)	0.001	$4d^95p\ ^3F_3$ — $4d^95d\ ^3F_4$	262734.7	381644.0	2.8E+8 [CF]	TW
76		841.176(6)	118881.2	841.1724(23)	0.004	$4d^95p\ ^3F_2$ — $4d^95d\ ^3D_1$	269512.91	388394.6	1.5E+9	TW
86		847.818(6)	117949.8	847.8161(17)	0.002	$4d^95p\ ^3F_3$ — $4d^95d\ ^3D_3$	262734.7	380684.81	1.1E+10	TW
99		847.965(16)	117929.4	847.961(3)	0.004	$4d^95p\ ^3F_2$ — $4d^95d\ ^3G_3$	269512.91	387442.9	2.8E+10	TW
86		848.525(6)	117851.6	848.5222(24)	0.003	$4d^95p\ ^3P_1$ — $4d^95d\ ^3P_1$	268413.14	386265.1	3.7E+9	TW
76		854.865(6)	116977.5	854.862(3)	0.003	$4d^95p\ ^1F_3$ — $4d^85s^2\ ^3F_3$	279661.63	396639.6	4.5E+8	TW
15		855.454(5)	116897.0	855.446(3)	0.008	$4d^95p\ ^1D_2$ — $4d^95d\ ^3F_3$	273752.04	390650.1	1.1E+8 [CF]	VJ
3		856.511(6)	116752.7	856.5150(23)	-0.004	$4d^95p\ ^3F_2$ — $4d^95d\ ^3P_1$	269512.91	386265.1	2.1E+8 [CF]	TW
94		858.455(5)	116488.3	858.4675(17)	-0.013	$4d^95p\ ^3F_3$ — $4d^95d\ ^3P_2$	262734.7	379221.34	2.9E+9	VJ
94		858.497(5)	116482.6	858.5020(22)	-0.005	$4d^95p\ ^1D_2$ — $4d^95d\ ^3F_2$	273752.04	390234.0	2.6E+9	VJ
82		862.429(17)	115951.6	862.4260(22)	0.003	$4d^95p\ ^3F_3$ — $4d^95d\ ^3G_4$	262734.7	378686.68	5.4E+10	TW
97		862.429(17)	115951.6	862.4447(23)	-0.016	$4d^95p\ ^1D_2$ — $4d^95d\ ^3D_2$	273752.04	389701.5	2.2E+8 [CF]	TW
80		863.132(17)	115857.1	863.139(3)	-0.007	$4d^95p\ ^1D_3$ — $4d^95d\ ^3F_3$	274793.85	390650.1	7.8E+8 [CF]	TW
80		863.132(17)	115857.1	863.146(4)	-0.014	$4d^95p\ ^3D_1$ — $4d^85s^2\ ^3F_2$	281585.18	397440.5	3.8E+8	TW
60		866.255(6)	115439.4	866.2497(23)	0.005	$4d^95p\ ^3D_3$ — $4d^95d\ ^3F_2$	274793.85	390234.0	8.7E+7 [CF]	TW
82		868.912(6)	115086.5	868.905(4)	0.007	$4d^95p\ ^3D_3$ — $4d^85s^2\ ^3F_4$	274793.85	389881.2	6.4E+8 [CF]	TW
90		869.643(6)	114989.7	869.646(4)	-0.003	$4d^95p\ ^3P_1$ — $4d^95d\ ^3P_0$	268413.14	383402.5	6.1E+9	TW
56		870.263(6)	114907.8	870.2641(23)	-0.001	$4d^95p\ ^3D_3$ — $4d^95d\ ^3D_2$	274793.85	389701.5	2.0E+8 [CF]	TW
86		871.272(6)	114774.7	871.2753(23)	-0.003	$4d^95p\ ^3P_2$ — $4d^95d\ ^3S_1$	259788.94	374563.23	1.5E+10	TW
30		872.275(6)	114642.7	872.2764(25)	-0.001	$4d^95p\ ^1D_2$ — $4d^95d\ ^3D_1$	273752.04	388394.6	1.5E+8 [CF]	TW

I_{obs}[a] (A.U)	Char.[b]	λ_{obs}[c] (Å)	σ_{obs} (cm^{-1})	λ_{Ritz}[d] (Å)	$\delta\lambda_{obs-Ritz}$[e] (Å)	Classification		E_{low} (cm^{-1})	E_{upp} (cm^{-1})	gA^f (s^{-1})	Lin. Ref[g]
88		874.597(6)	114338.4	874.598(3)	-0.001	$4d^95p\ ^3P_0$	$4d^95d\ ^3D_1$	274056.4	388394.6	6.4E+9	TW
86		879.579(12)	113690.8	879.578(3)	0.001	$4d^95p\ ^1D_2$	$4d^95d\ ^3G_3$	273752.04	387442.9	1.4E+10	TW
88		880.236(6)	113605.9	880.248(3)	-0.012	$4d^95p\ ^3D_2$	$4d^85s^2\ ^3F_3$	283035.3	396639.6	1.9E+9	TW
80		881.642(6)	113424.7	881.6486(20)	-0.007	$4d^95p\ ^3P_1$	$4d^95d\ ^1D_2$	268413.14	381837.02	6.8E+9	TW
84		883.165(6)	113229.1	883.1686(24)	-0.004	$4d^95p\ ^1P_1$	$4d^95d\ ^3F_2$	277005.34	390234.0	9.9E+9	TW
82		883.439(6)	113194.0	883.436(4)	0.003	$4d^95p\ ^3D_3$	$4d^95d\ ^1G_4$	274793.85	387988.3	2.1E+9	TW
70		887.335(6)	112697.0	887.3417(25)	-0.007	$4d^95p\ ^1P_1$	$4d^95d\ ^3D_2$	277005.34	389701.5	3.7E+8[CF]	TW
52	m		112680.1	887.494(3)		$4d^95p\ ^3F_4$	$4d^95d\ ^1F_3$	269146.4	381823.22	2.5E+7[CF]	TW
48		887.702(12)	112650.4	887.713(3)	-0.011	$4d^95p\ ^3D_3$	$4d^95d\ ^3G_3$	274793.85	387442.9	1.7E+8[CF]	TW
70		888.794(6)	112512.0	888.7857(25)	0.008	$4d^95p\ ^1D_2$	$4d^95d\ ^3P_1$	273752.04	386265.1	3.2E+8[CF]	TW
80		888.905(6)	112498.0	888.908(3)	-0.003	$4d^95p\ ^3F_4$	$4d^95d\ ^3F_4$	269146.4	381644.0	1.6E+10	TW
72		890.275(6)	112324.8	890.2808(19)	-0.006	$4d^95p\ ^3F_2$	$4d^95d\ ^1D_2$	269512.91	381837.02	3.9E+9	TW
93		890.390(6)	112310.3	890.3902(20)	0.000	$4d^95p\ ^3F_2$	$4d^95d\ ^1F_3$	269512.91	381823.22	1.1E+10	TW
72		891.187(6)	112209.9	891.196(3)	-0.009	$4d^95p\ ^3P_0$	$4d^95d\ ^3P_1$	274056.4	386265.1	3.2E+9	TW
78		896.549(6)	111538.8	896.552(3)	-0.003	$4d^95p\ ^3F_4$	$4d^95d\ ^3D_3$	269146.4	380684.81	3.4E+9	TW
76		897.750(6)	111389.6	897.753(3)	-0.003	$4d^95p\ ^1P_1$	$4d^95d\ ^3D_1$	277005.34	388394.6	5.8E+9	TW
68		899.517(6)	111170.8	899.5079(19)	0.009	$4d^95p\ ^3F_2$	$4d^95d\ ^3D_3$	269512.91	380684.81	2.3E+8[CF]	TW
82		900.452(6)	111055.3	900.453(3)	-0.001	$4d^95p\ ^3P_1$	$4d^95d\ ^1P_1$	268413.14	379468.4	5.9E+9	TW
82		900.982(6)	110990.0	900.994(3)	-0.012	$4d^95p\ ^1F_3$	$4d^95d\ ^3F_3$	279661.63	390650.1	9.9E+9	TW
40		902.469(6)	110807.1	902.4603(21)	0.009	$4d^95p\ ^3P_1$	$4d^95d\ ^3P_2$	268413.14	379221.34	1.5E+8[CF]	TW
68		904.389(6)	110571.9	904.3851(25)	0.004	$4d^95p\ ^1F_3$	$4d^95d\ ^3F_2$	279661.63	390234.0	8.4E+8	TW
76		907.266(12)	110221.3	907.280(4)	-0.014	$4d^95p\ ^1F_3$	$4d^85s^2\ ^3F_4$	279661.63	389881.2	2.1E+10	TW
91		908.216(12)	110106.0	908.235(5)	-0.019	$4d^95p\ ^3F_4$	$4d^95d\ ^3G_5$	269146.4	379250.1	6.4E+10	TW
60		908.771(6)	110038.7	908.762(3)	0.009	$4d^95p\ ^1F_3$	$4d^95d\ ^3D_2$	279661.63	389701.5	9.2E+8	TW
68		909.461(6)	109955.2	909.4589(25)	0.002	$4d^95p\ ^3F_2$	$4d^95d\ ^1P_1$	269512.91	379468.4	6.8E+8	TW
45	m		109712.4	911.5070(20)		$4d^95p\ ^3F_2$	$4d^95d\ ^3P_2$	269512.91	379221.34	1.1E+8[CF]	TW
80		912.903(6)	109540.7	912.906(3)	-0.003	$4d^95p\ ^3F_4$	$4d^95d\ ^3G_4$	269146.4	378686.68	3.2E+9	TW
72		915.238(6)	109261.2	915.250(3)	-0.012	$4d^95p\ ^1P_1$	$4d^95d\ ^3P_1$	277005.34	386265.1	3.0E+9	TW
82	m		109060.9	916.885(3)		$4d^95p\ ^3D_1$	$4d^95d\ ^3F_3$	281585.18	390650.1		TW
78		920.394(6)	108649.1	920.397(3)	-0.003	$4d^95p\ ^3D_1$	$4d^95d\ ^3F_2$	281585.18	390234.0	6.6E+9	TW
74		923.131(6)	108327.0	923.134(5)	-0.003	$4d^95p\ ^1F_3$	$4d^95d\ ^1G_4$	279661.63	387988.3	2.9E+10	TW

I_{obs} [a] (A.U)	Char.[b]	λ_{obs} [c] (Å)	σ_{obs} (cm^{-1})	λ_{Ritz} [d] (Å)	$\delta\lambda_{obs-Ritz}$ [e] (Å)	Classification	E_{low}(cm^{-1})	E_{upp}(cm^{-1})	gA^f(s-1)	Lin. Ref[g]
76		924.929(6)	108116.4	924.930(3)	-0.001	$4d^9 5p\ ^3D_1$ $4d^9 5d\ ^3D_2$	281585.18	389701.5	1.1E+10	TW
72		925.197(6)	108085.1	925.1979(19)	-0.001	$4d^9 5p\ ^1D_2$ $4d^9 5d\ ^1D_2$	273752.04	381837.02	1.2E+10	TW
72		925.317(6)	108071.1	925.3161(20)	0.001	$4d^9 5p\ ^1D_2$ $4d^9 5d\ ^1F_3$	273752.04	381823.22	1.6E+10	TW
70		927.812(6)	107780.5	927.805(4)	0.007	$4d^9 5p\ ^1F_3$ $4d^9 5d\ ^3G_3$	279661.63	387442.9	2.2E+9	TW
80		929.235(6)	107615.4	929.240(3)	-0.005	$4d^9 5p\ ^3D_2$ $4d^9 5d\ ^3F_3$	283035.3	390650.1	2.6E+10	TW
74		932.846(6)	107198.8	932.847(3)	-0.001	$4d^9 5p\ ^3D_2$ $4d^9 5d\ ^3F_2$	283035.3	390234.0	1.3E+9	TW
30		934.210(6)	107042.3	934.2025(21)	0.007	$4d^9 5p\ ^3D_3$ $4d^9 5d\ ^1D_2$	274793.85	381837.02	2.4E+8 [CF]	TW
78		934.324(6)	107029.3	934.3230(21)	0.001	$4d^9 5p\ ^3D_3$ $4d^9 5d\ ^1F_3$	274793.85	381823.22	5.1E+9	TW
20		935.166(6)	106932.9	935.1670(20)	-0.001	$4d^9 5p\ ^1D_2$ $4d^9 5d\ ^3D_3$	273752.04	380684.81		TW
74		935.887(6)	106850.5	935.890(3)	-0.003	$4d^9 5p\ ^3D_3$ $4d^9 5d\ ^3F_4$	274793.85	381644.0	3.2E+10	TW
72		936.244(6)	106809.8	936.247(3)	-0.003	$4d^9 5p\ ^3D_1$ $4d^9 5d\ ^3D_1$	281585.18	388394.6	2.4E+9	TW
77		937.509(6)	106665.6	937.504(3)	0.005	$4d^9 5p\ ^3D_2$ $4d^9 5d\ ^3D_2$	283035.3	389701.5	1.1E+10	TW
6	h	939.875(10)	106397.1	939.875(4)	0.000	$4d^9 5p\ ^1P_1$ $4d^9 5d\ ^3P_0$	277005.34	383402.5	2.7E+7 [CF]	TW
76		942.062(6)	106150.1	942.062(3)	0.000	$4d^9 5p\ ^3P_1$ $4d^9 5d\ ^3S_1$	268413.14	374563.23	1.9E+9	TW
76		944.364(6)	105891.4	944.3677(21)	-0.004	$4d^9 5p\ ^3D_3$ $4d^9 5d\ ^3D_3$	274793.85	380684.81	1.4E+10	TW
78		945.921(6)	105717.1	945.927(3)	-0.006	$4d^9 5p\ ^1D_2$ $4d^9 5d\ ^1P_1$	273752.04	379468.4	2.3E+9	TW
68		948.143(6)	105469.3	948.1432(20)	0.000	$4d^9 5p\ ^1D_2$ $4d^9 5d\ ^3P_2$	273752.04	379221.34	3.3E+8 [CF]	TW
17		948.654(6)	105412.5	948.659(3)	-0.005	$4d^9 5p\ ^3P_0$ $4d^9 5d\ ^1P_1$	274056.4	379468.4	7.0E+7 [CF]	TW
66		949.131(6)	105359.5	949.133(3)	-0.002	$4d^9 5p\ ^3D_2$ $4d^9 5d\ ^3D_1$	283035.3	388394.6	4.6E+8 [CF]	TW
66		951.924(6)	105050.4	951.925(3)	-0.001	$4d^9 5p\ ^3F_2$ $4d^9 5d\ ^3S_1$	269512.91	374563.23	2.2E+8	TW
76		953.918(6)	104830.8	953.9101(23)	0.008	$4d^9 5p\ ^1P_1$ $4d^9 5d\ ^1D_2$	277005.34	381837.02	2.4E+9	TW
71	bl(Sn II)	955.296(6)	104679.6	955.293(3)	0.003	$4d^9 5p\ ^3D_1$ $4d^9 5d\ ^3P_1$	281585.18	386265.1	4.1E+9	TW
77		957.603(6)	104427.4	957.6023(21)	0.001	$4d^9 5p\ ^3D_3$ $4d^9 5d\ ^3P_2$	274793.85	379221.34	5.9E+9	TW
74		957.778(6)	104408.3	957.785(4)	-0.007	$4d^9 5p\ ^3D_2$ $4d^9 5d\ ^3G_3$	283035.3	387442.9	1.9E+9	TW
80		962.542(12)	103891.6	962.530(3)	0.012	$4d^9 5p\ ^3D_3$ $4d^9 5d\ ^3G_4$	274793.85	378686.68	2.6E+9	TW
80		968.723(6)	103228.7	968.713(3)	0.010	$4d^9 5p\ ^3D_2$ $4d^9 5d\ ^3P_1$	283035.3	386265.1	2.4E+9	TW
80		975.967(6)	102462.5	975.961(3)	0.006	$4d^9 5p\ ^1P_1$ $4d^9 5d\ ^1P_1$	277005.34	379468.4	3.4E+9	TW
64		978.837(6)	102162.1	978.8415(23)	-0.004	$4d^9 5p\ ^1F_3$ $4d^9 5d\ ^1F_3$	279661.63	381823.22	2.2E+8 [CF]	TW
70		980.560(6)	101982.5	980.562(3)	-0.002	$4d^9 5p\ ^1F_3$ $4d^9 5d\ ^3F_4$	279661.63	381644.0	5.5E+7 [CF]	TW
72		982.153(6)	101817.1	982.151(4)	0.002	$4d^9 5p\ ^3D_1$ $4d^9 5d\ ^3P_0$	281585.18	383402.5	1.7E+8 [CF]	TW
70		989.871(6)	101023.3	989.8718(22)	-0.001	$4d^9 5p\ ^1F_3$ $4d^9 5d\ ^3D_3$	279661.63	380684.81	9.4E+8 [CF]	TW

I_{obs}[a] (A.U)	Char.[b]	λ_{obs}[c] (Å)	σ_{obs} (cm^{-1})	λ_{Ritz}[d] (Å)	$\delta\lambda_{obs-Ritz}$[e] (Å)	Classification		E_{low}(cm^{-1})	E_{upp}(cm^{-1})	gA[f](s-1)	Lin. Ref[g]
68		991.951(6)	100811.4	991.953(3)	-0.002	$4d^9 5p\ ^1D_2$	$4d^9 5d\ ^3S_1$	273752.04	374563.23	6.5E+8	TW
67		994.963(5)	100506.2	994.957(3)	0.006	$4d^9 5p\ ^3P_0$	$4d^9 5d\ ^3S_1$	274056.4	374563.23	2.2E+8 CF	VJ
60		997.486(6)	100252.0	997.4879(25)	-0.002	$4d^9 5p\ ^3D_1$	$4d^9 5d\ ^1D_2$	281585.18	381837.02	5.9E+8 CF	TW
74		999.614(6)	100038.6	999.612(3)	0.002	$4d^9 5s\ ^3D_3$	$4d^9 5p\ ^3D_2$	182996.46	283035.3	2.1E+8 CF	TW
64		1004.427(6)	99559.3	1004.4224(23)	0.005	$4d^9 5p\ ^1F_3$	$4d^9 5d\ ^3P_2$	279661.63	379221.34	3.9E+8	TW
40		1012.124(6)	98802.1	1012.1281(25)	-0.004	$4d^9 5p\ ^3D_2$	$4d^9 5d\ ^1D_2$	283035.3	381837.02	1.5E+8 CF	TW
75		1012.275(6)	98787.4	1012.270(3)	0.005	$4d^9 5p\ ^3D_2$	$4d^9 5d\ ^1F_3$	283035.3	381823.22	3.6E+7 CF	TW
78		1021.625(6)	97883.3	1021.626(3)	-0.001	$4d^9 5p\ ^3D_1$	$4d^9 5d\ ^1P_1$	281585.18	379468.4	1.1E+9	TW
25	m		97647.2	1024.071(3)		$4d^9 5p\ ^3D_2$	$4d^9 5d\ ^3D_3$	283035.3	380684.81		TW
74	bl	1025.013(17)	97559.7	1025.009(3)	0.004	$4d^9 5s\ ^3D_2$	$4d^9 5p\ ^3D_2$	185475.22	283035.3	4.8E+8 CF	TW
74	bl	1025.013(17)	97559.7	1025.032(3)	-0.019	$4d^9 5p\ ^1P_1$	$4d^9 5d\ ^3S_1$	277005.34	374563.23	1.4E+8	TW
70		1034.506(6)	96664.5	1034.499(3)	0.007	$4d^9 5s\ ^3D_3$	$4d^9 5p\ ^1F_3$	182996.46	279661.63	5.3E+8 CF	TW
62	bl(C II)	1036.990(20)	96432.9	1036.988(3)	0.002	$4d^9 5p\ ^3D_2$	$4d^9 5d\ ^1P_1$	283035.3	379468.4	3.0E+7 CF	TW
30			96185.8	1039.652(3)		$4d^9 5p\ ^3D_2$	$4d^9 5d\ ^3P_2$	283035.3	379221.34	9.7E+7 CF	TW
74		1040.480(6)	96109.5	1040.475(3)	0.005	$4d^9 5s\ ^3D_2$	$4d^9 5p\ ^3D_1$	185475.22	281585.18	7.4E+8	TW
80		1061.733(7)	94185.6	1061.724(3)	0.009	$4d^9 5s\ ^3D_2$	$4d^9 5p\ ^1F_3$	185475.22	279661.63	1.3E+9 CF	TW
64		1075.521(7)	92978.2	1075.523(3)	-0.002	$4d^9 5p\ ^3D_1$	$4d^9 5d\ ^3S_1$	281585.18	374563.23		TW
72		1089.357(7)	91797.3	1089.356(3)	0.001	$4d^9 5s\ ^3D_3$	$4d^9 5p\ ^3D_3$	182996.46	274793.85	8.8E+9	TW
76		1092.532(7)	91530.5	1092.537(3)	-0.005	$4d^9 5s\ ^3D_2$	$4d^9 5p\ ^1P_1$	185475.22	277005.34	6.3E+8	TW
78		1093.897(7)	91416.3	1093.892(3)	0.005	$4d^9 5s\ ^3D_1$	$4d^9 5p\ ^3D_2$	191618.62	283035.3	3.0E+9	TW
74		1101.857(7)	90755.9	1101.861(3)	-0.004	$4d^9 5s\ ^3D_3$	$4d^9 5p\ ^1D_2$	182996.46	273752.04	8.9E+7 CF	TW
78		1111.520(7)	89966.9	1111.524(3)	-0.004	$4d^9 5s\ ^3D_1$	$4d^9 5p\ ^3D_1$	191618.62	281585.18	4.3E+9	TW
70		1119.583(7)	89319.0	1119.587(3)	-0.004	$4d^9 5s\ ^3D_2$	$4d^9 5p\ ^3D_3$	185475.22	274793.85	3.0E+9	TW
86		1131.365(7)	88388.8	1131.362(3)	0.003	$4d^9 5s\ ^1D_2$	$4d^9 5p\ ^3D_2$	194646.26	283035.3	5.4E+9	TW
72		1132.794(7)	88277.3	1132.800(3)	-0.006	$4d^9 5s\ ^3D_2$	$4d^9 5p\ ^1D_2$	185475.22	273752.04	5.2E+9	TW
84		1150.233(7)	86938.9	1150.233(3)	0.000	$4d^9 5s\ ^1D_2$	$4d^9 5p\ ^3D_1$	194646.26	281585.18	5.2E+8	TW
74		1160.766(7)	86150.0	1160.767(4)	-0.001	$4d^9 5s\ ^3D_3$	$4d^9 5p\ ^3F_4$	182996.46	269146.4	1.5E+10	TW
78		1171.142(7)	85386.7	1171.142(4)	0.000	$4d^9 5s\ ^3D_1$	$4d^9 5p\ ^1P_1$	191618.62	277005.34	8.2E+8	TW
78		1176.261(7)	85015.1	1176.258(3)	0.003	$4d^9 5s\ ^1D_2$	$4d^9 5p\ ^1F_3$	194646.26	279661.63	9.5E+9	TW
82		1189.947(7)	84037.4	1189.942(3)	0.005	$4d^9 5s\ ^3D_2$	$4d^9 5p\ ^3F_2$	185475.22	269512.91	2.7E+9	TW
78		1205.722(7)	82937.9	1205.721(4)	0.001	$4d^9 5s\ ^3D_2$	$4d^9 5p\ ^3P_1$	185475.22	268413.14	3.5E+9	TW

I_{obs} [a] (A.U)	Char. [b]	λ_{obs} [c] (Å)	σ_{obs} (cm^{-1})	λ_{Ritz} [d] (Å)	$\delta\lambda_{obs-Ritz}$ [e] (Å)	Classification		E_{low} (cm^{-1})	E_{upp} (cm^{-1})	gA^{r} (s^{-1})	Lin. Ref [g]
78		1213.031(7)	82458.1	1213.036(5)	-0.005	$4d^9 5s\ ^3D_1$	$4d^9 5p\ ^3P_0$	191618.62	274056.4	1.5E+9	TW
78		1214.190(7)	82359.4	1214.195(3)	-0.005	$4d^9 5s\ ^1D_2$	$4d^9 5p\ ^1P_1$	194646.26	277005.34	3.1E+9	TW
78		1217.532(7)	82133.4	1217.531(4)	0.001	$4d^9 5s\ ^3D_1$	$4d^9 5p\ ^1D_2$	191618.62	273752.04	1.2E+9	TW
68		1247.702(7)	80147.3	1247.698(3)	0.004	$4d^9 5s\ ^1D_2$	$4d^9 5p\ ^3D_3$	194646.26	274793.85	9.5E+8	TW
84		1254.103(7)	79738.3	1254.103(4)	0.000	$4d^9 5s\ ^3D_3$	$4d^9 5p\ ^3F_3$	182996.46	262734.7	2.7E+9	TW
78		1264.132(7)	79105.7	1264.130(3)	0.002	$4d^9 5s\ ^1D_2$	$4d^9 5p\ ^1D_2$	194646.26	273752.04	1.5E+9	TW
82		1283.789(7)	77894.4	1283.791(4)	-0.002	$4d^9 5s\ ^3D_1$	$4d^9 5p\ ^3F_2$	191618.62	269512.91	3.1E+9	TW
72		1294.342(7)	77259.3	1294.340(4)	0.002	$4d^9 5s\ ^3D_2$	$4d^9 5p\ ^3F_3$	185475.22	262734.7	5.5E+9	TW
86		1302.204(20)	76792.9	1302.176(5)	0.028	$4d^9 5s\ ^3D_1$	$4d^9 5p\ ^3P_1$	191618.62	268413.14	1.4E+8 [CF]	TW
86		1302.204(20)	76792.9	1302.211(5)	-0.007	$4d^9 5s\ ^3D_3$	$4d^9 5p\ ^3P_2$	182996.46	259788.94	5.8E+9	TW
92		1335.705(7)	74866.8	1335.708(4)	-0.003	$4d^9 5s\ ^1D_2$	$4d^9 5p\ ^3F_2$	194646.26	269512.91	6.8E+8	TW
64		1355.622(7)	73766.9	1355.622(4)	0.000	$4d^9 5s\ ^1D_2$	$4d^9 5p\ ^3P_1$	194646.26	268413.14	5.9E+8	TW
38		1468.668(7)	68088.9	1468.678(4)	-0.010	$4d^9 5s\ ^1D_2$	$4d^9 5p\ ^3F_3$	194646.26	262734.7	1.4E+8 [CF]	TW
38		1535.091(7)	65142.7	1535.092(5)	-0.001	$4d^9 5s\ ^1D_2$	$4d^9 5p\ ^3P_2$	194646.26	259788.94	8.2E+7 [CF]	TW
8		1651.039(8)	60567.9	1651.040(7)	-0.001	$4d^9 5d\ ^3S_1$	$4d^9 6p\ ^1D_2$	374563.23	435131.1	1.7E+8	TW
5	H	1788.648(20)	55908.1	1788.596(10)	0.052	$4d^9 5d\ ^3P_2$	$4d^9 6p\ ^1D_2$	379221.34	435131.1	8.3E+7 [CF]	TW
5	h		55674.0	1796.535(12)		$4d^9 5d\ ^1P_1$	$4d^9 6p\ ^1D_2$	379468.4	435131.1	3.7E+8	TW
8	h	1810.498(16)	55233.4	1810.478(15)	0.020	$4d^9 5d\ ^3G_4$	$4d^9 6p\ ^3F_4$	378686.68	433920.71	3.2E+8	TW
71	bl(Sn)	1817.999(16)	55005.5	1817.990(12)	0.009	$4d^9 5d\ ^3D_3$	$4d^9 6p\ ^3D_3$	380684.81	435690.62	1.6E+9	TW
18		1829.133(8)	54670.71	1829.136(8)	-0.003	$4d^9 5d\ ^3G_5$	$4d^9 6p\ ^3F_4$	379250.1	433920.71	6.1E+9	TW
76	bl(Sn)	1850.242(16)	54047.0	1850.254(13)	-0.012	$4d^9 5d\ ^3F_4$	$4d^9 6p\ ^3D_3$	381644.0	435690.62	3.0E+9	TW
4	H	1875.856(20)	53309.0	1875.895(11)	-0.039	$4d^9 5d\ ^1F_3$	$4d^9 6p\ ^1D_2$	381823.22	435131.1	2.5E+9	TW
10	m(Si III)		53242.8	1878.432(18)		$4d^9 5d\ ^3D_3$	$4d^9 6p\ ^3F_4$	380684.81	433920.71	4.4E+8	TW
84		1890.765(8)	52888.65	1890.769(8)	-0.004	$4d^9 5d\ ^3G_4$	$4d^9 6p\ ^3F_3$	378686.68	431575.20	3.7E+9	TW
48		1910.083(8)	52353.75	1910.079(6)	0.004	$4d^9 5d\ ^3P_2$	$4d^9 6p\ ^3F_3$	379221.34	431575.20	2.6E+8	TW
14		1953.673(8)	51185.64	1953.682(7)	-0.009	$4d^9 5d\ ^3P_2$	$4d^9 6p\ ^3P_2$	379221.34	430406.74	1.4E+9	TW
34		1964.998(8)	50890.64	1965.008(6)	-0.010	$4d^9 5d\ ^3D_3$	$4d^9 6p\ ^3F_3$	380684.81	431575.20	5.7E+8	TW
34		2009.329(8)	49751.77	2009.321(7)	0.008	$4d^9 5d\ ^1F_3$	$4d^9 6p\ ^3F_3$	381823.22	431575.20	6.1E+8	TW
8	h	2009.881(8)	49738.11	2009.878(7)	0.003	$4d^9 5d\ ^1D_2$	$4d^9 6p\ ^3F_3$	381837.02	431575.20	1.3E+8	TW
32		2010.542(8)	49721.76	2010.535(7)	0.007	$4d^9 5d\ ^3D_3$	$4d^9 6p\ ^3P_2$	380684.81	430406.74	9.1E+8	TW
110		2075.143(19)	48174.1	2075.138(18)	0.005	$4d^9 6p\ ^3F_3$	$4d^9 6d\ ^1D_2$	431575.20	479749.4	3.2E+8	Wu [g]

I_{obs}[a] (A.U)	Char.[b]	λ_{obs}[c] (Å)	σ_{obs} (cm^{-1})	λ_{Ritz}[d] (Å)	$\delta\lambda_{obs-Ritz}$[e] (Å)	Classification		E_{low} (cm^{-1})	E_{upp} (cm^{-1})	gA[f] (s^{-1})	Lin. Ref[g]
171			46749.3	2138.551(23)		$4d^9 6p\ ^3F_3$	$4d^9 6d\ ^3G_4$	431575.20	478321.10	1.1E+10	Wu*
884	bl(Sn II)		46464.7	2151.985(22)		$4d^9 6p\ ^3P_2$	$4d^9 6d\ ^3S_1$	430406.74	476860.86	3.4E+9	Wu*
190		2174.329(19)	45976.8	2174.319(19)	0.010	$4d^9 6p\ ^3F_4$	$4d^9 6d\ ^3F_4$	433920.71	479897.7	3.3E+9	Wu*
552	m(Sn III)		44408.2	2251.53(4)		$4d^9 6p\ ^3F_4$	$4d^9 6d\ ^3G_4$	433920.71	478321.10	6.3E+8	Wu*
172		2332.049(19)	42867.6	2332.050(19)	-0.001	$4d^9 6p\ ^3D_3$	$4d^9 6d\ ^3P_2$	435690.62	478558.2	1.4E+9	Wu*
142		2343.507(19)	42658.0	2343.510(19)	-0.003	$4d^9 6p\ ^3P_1$	$4d^9 6d\ ^3S_1$	434202.9	476860.86	3.09E+08	Wu*
120		2345.014(19)	42630.6	2345.021(19)	-0.007	$4d^9 6p\ ^3D_3$	$4d^9 6d\ ^3G_4$	435690.62	478321.10	4.7E+8	Wu*
102		2395.645(19)	41729.7	2395.642(19)	0.003	$4d^9 6p\ ^1D_2$	$4d^9 6d\ ^3S_1$	435131.1	476860.86	2.1E+8	Wu*
697		2833.866(24)	35277.1	2833.867(24)	-0.001	$4d^9 6p\ ^1F_3$	$4d^9 6d\ ^3G_4$	443044.0	478321.10		Wu*
	M1			521.870(5)		$4d^{10}\ ^1S_0$	$4d^9 5s\ ^3D_1$	0	191618.62		TW

[a] Observed relative intensities, in terms visual estimates of photographic plate blackening for lines from this work (TW) and for other lines their given values from original work.

[b] Character of observed line: bl – blended by a close line (the blending spectrum is indicated in parentheses); h – hazy line; H – very hazy line; * – intensity shared by two or more transitions; m – masked by a stronger neighboring line (no wavelength measured); : – the actual wavelength is masked by lines at higher wavelength

[c] Observed and Ritz wavelengths are given in standard air for wavenumbers σ between 5000 cm^{-1} and 50000 cm^{-1} and in vacuum outside of this range. The uncertainty (standard deviation) in the last digit is given in parentheses.

[d] Ritz wavelengths and their uncertainties were determined in the least-squares level optimization procedure (see section 6.3.3).

[e] Difference between observed and Ritz wavelength. If this column is blank, and λ_{obs} is not blank, this line alone determines one of the levels involved in the assigned transition.

[f] Markings to the cancellation effects involved for the computed gA values: the given gA values are too unreliable when their |CF|< 0.1

[g] References to observed wavelengths: Ch – Churilov et al [12]; Ry – Ryabtsev et al [13]; Ry* – lines measured by Ryabtsev [19] with our revised or new identification; VJ – Van Kleef & Joshi [11] TW – This work; Wu – Wu [8]; Wu* – line measured by Wu [11] with our new or revised classification

Table 6.2. Optimized levels of Sn V.

Configuration	Term	J	Energy [a] cm^{-1}	Unc. [b] cm^{-1}	Leading percentages [c]							ΔE_{o-c} [d] cm^{-1}	No. of lines [e]
4d10	^{1}S	0	0.0	2.0	100							0	11
4d95s	^{3}D	3	182996.46	0.3	100							-56.54	38
4d95s	^{3}D	2	185475.22	0.22	70	29	4d95s	^{1}D				-2.78	50
4d95s	^{3}D	1	191618.62	0.24	100							50.62	33
4d95s	^{1}D	2	194646.26		70	29	4d95s	^{3}D				-2.74	49
4d95p	^{3}P°	2	259788.94	0.22	85	11	4d95p	^{3}D°				-87.06	22
4d95p	^{3}F°	3	262734.7	0.2	57	33	4d95p	^{1}F°	10	4d95p	^{3}D°	55.7	25
4d95p	^{3}P°	1	268413.14	0.21	88	11	4d95p	^{3}D°				-7.86	24
4d95p	^{3}F°	4	269146.4	0.3	100							-33.6	11
4d95p	^{3}F°	2	269512.91	0.2	86	9	4d95p	^{3}D°				27.91	26
4d95p	^{1}D°	2	273752.04	0.2	67	20	4d95p	^{3}D°	7	4d95p	^{3}P°	-31.96	28
4d95p	^{3}P°	0	274056.4	0.3	100							52.4	6
4d95p	^{3}D°	3	274793.85	0.21	71	28	4d95p	^{1}F°				21.85	29
4d95p	^{1}P°	1	277005.34	0.22	78	21	4d95p	^{3}D°				-4.66	26
4d95p	^{1}F°	3	279661.63	0.21	39	43	4d95p	^{3}F°	18	4d95p	^{3}D°	-16.37	23
4d95p	^{3}D°	1	281585.18	0.22	68	20	4d95p	^{1}P°	12	4d95p	^{3}P°	-24.82	23
4d95p	^{3}D°	2	283035.3	0.22	59	30	4d95p	^{1}D°	7	4d95p	^{3}F°	10.3	22
4d95d	^{3}S	1	374563.23	0.3	81	16	4d95d	^{3}P				43.23	8
4d95d	^{3}G	4	378686.68	0.3	53	45	4d95d	^{1}G				-189.32	5
4d95d	^{3}P	2	379221.34	0.22	65	32	4d95d	^{3}D				83.34	9
4d95d	^{3}G	5	379250.1	0.6	100							-126.9	2
4d95d	^{1}P	1	379468.4	0.3	50	25	4d95d	^{3}D	24	4d95d	^{3}P	-68.6	8
4d95d	^{3}D	3	380684.81	0.22	67	27	4d95d	^{3}F				65.81	10
4d95d	^{3}F	4	381644	0.4	73	14	4d95d	^{1}G	9	$4d^8$5s2	^{3}F	-189	5
4d95d	^{1}F	3	381823.22	0.23	46	19	4d95d	^{3}D	19	4d95d	^{3}G	32.22	8

Configuration	Term	J	Energy [a] cm^{-1}		Unc. [b] cm^{-1}	Leading percentages [c]							ΔE_{o-c} [d] cm^{-1}	No. of lines [e]
4d95d	^{1}D	2	381837.02		0.22	46	22	4d95d	^{3}D	16	4d95d	^{3}F	68.02	10
4d95d	^{3}P	0	383402.5		0.5	97	2	4d95d	^{1}S				92.5	3
4d95d	^{3}P	1	386265.1		0.3	45	37	4d95d	^{1}P	16	4d95d	^{3}S	20.1	7
4d95d	^{3}G	3	387442.9		0.4	76	15	4d95d	^{1}F	8	4d95d	^{3}F	-99.1	6
4d95d	^{1}G	4	387988.3	N	0.5	31	38	$4d^85s2$	^{3}F	29	4d95d	^{3}G	-159.7	2
4d95d	^{3}D	1	388394.6		0.3	74	15	4d95d	^{3}P	11	4d95d	^{1}P	121.6	7
4d95d	^{3}D	2	389701.5		0.3	43	32	4d95d	^{1}D	19	4d95d	^{3}P	145.5	10
$4d^85s2$	^{3}F	4	389881.2		0.5	49	23	4d95d	^{3}F	14	4d95d	^{3}G	176.2	4
4d95d	^{3}F	2	390234		0.3	74	20	4d95d	^{1}D				-5	9
4d95d	^{3}F	3	390650.1		0.4	42	37	4d95d	^{1}F	13	4d95d	^{3}D	-56.9	7
$4d^85s2$	^{3}F	3	396639.6		0.4	89	7	4d95d	^{3}F				34.6	6
$4d^85s2$	^{3}F	2	397440.5		0.6	46	34	$4d^85s2$	^{1}D	14	$4d^85s2$	^{3}P	291.5	3
4d96s	^{3}D	3	402237.1		0.4	100							-36.9	7
4d96s	^{1}D	2	402991.7		0.4	52	48	4d96s	^{3}D				-41.3	9
$4d^85s2$	^{3}P	2	403504.1		0.5	57	34	$4d^85s2$	^{3}F	5	$4d^85s2$	^{1}D	-214.9	6
4d95d	^{1}S	0	407700	N	0.7	92	3	4d96d	^{1}S				-9	2
$4d^85s2$	^{3}P	1	408455.7		0.6	97	2	4d85p2	^{3}P				-274.3	3
$4d^85s2$	^{3}P	0	408728.2		2	91	6	$4d^85s2$	^{1}S				454.2	1
4d96s	^{3}D	1	410906.7		0.4	100							43.7	8
4d96s	^{3}D	2	411474.7		0.4	52	48	4d96s	^{1}D				21.7	10
4d94f	^{3}P°	1	412342		5	94	4	4d94f	^{3}D°				-89	1
$4d^85s2$	^{1}D	2	412568.1		0.6	58	26	$4d^85s2$	^{3}P	14	$4d^85s2$	^{3}F	-294.9	4
$4d^85s2$	^{1}G	4	414735.9		0.7	95	2	4d85p2	^{1}G				-23.1	2
4d94f	^{3}D°	1	423366		6	93	4	4d94f	^{3}P°				185	1
4d94f	^{3}F°	3	430271		3	31	27	4d94f	^{3}G°	18	4d94f	^{3}D°	-98	2
4d96p	^{3}P°	2	430406.74		0.25	81	15	4d96p	^{3}D°				-143.26	4

Configuration	Term	J	Energy [a] cm^{-1}	Unc. [b] cm^{-1}	Leading percentages [c]							ΔE_{o-c} [d] cm^{-1}	No. of lines [e]
4d96p	^{3}F°	3	431575.2	0.21	46	36	4d96p	^{1}F°	10	4d96p	^{3}D°	137.2	9
4d96p	^{3}F°	4	433920.71	0.5	97							-12.29	4
4d96p	^{3}P°	1	434202.9	0.6	44	47	4d96p	^{1}P°	7	4d96p	^{3}D°	111.9	2
4d96p	^{1}D°	2	435131.1	0.3	49	25	4d96p	^{3}D°	13	4d96p	^{3}P°	59.1	6
4d96p	^{3}D°	3	435690.62	0.4	79	20	4d96p	^{1}F°				-74.38	7
4d96p	^{1}P°	1	439808	2.4	44	37	4d96p	^{3}P°	12	4d96p	^{3}D°	-74	3
4d96p	^{3}F°	2	439963	3	78	21	4d96p	^{1}D°				59	2
4d96p	^{3}P°	0	441134.6	11	100							-22.4	1
4d96p	^{1}F°	3	443044	0.6	41	49	4d96p	^{3}F°	10	4d96p	^{3}D°	58	3
4d96p	^{3}D°	1	443415	3	81	18	4d96p	^{3}P°				-18	2
4d96p	^{3}D°	2	444167	4	59	28	4d96p	^{1}D°	8	4d96p	^{3}F°	-103	2
4d^{8}5s2	^{1}S	0	[444365]		91	6	4d^{8}5s2	^{3}P					
4d94f	^{1}P°	1	446335	6	75	10	4d95f	^{1}P°	8	4d96p	^{1}P°	8	1
4d^{8}5s(^{4}F)5p	^{5}D°	4	[452131]		78	11	4d^{8}5s(^{4}F)5p	^{5}F°	5	4d^{8}5s(^{4}P)5p	^{5}D°		
4d^{8}5s(^{4}F)5p	^{5}D°	3	[457232]		64	14	4d^{8}5s(^{4}F)5p	^{5}F°	9	4d^{8}5s(^{4}P)5p	^{5}D°		
4d^{8}5s(^{4}F)5p	^{5}G°	5	[457744]		52	32	4d^{8}5s(^{4}F)5p	^{5}F°	9	4d^{8}5s(^{4}F)5p	^{3}G°		
4d^{8}5s(^{4}F)5p	^{5}G°	4	[459346]		50	14	4d^{8}5s(^{2}F)5p	^{3}G°	10	4d^{8}5s(^{4}F)5p	^{5}F°		
4d^{8}5s(^{4}F)5p	^{5}G°	6	[461810]		98	2	4d^{8}5s(^{2}G)5p	^{3}H°					
4d^{8}5s(^{4}F)5p	^{5}D°	2	[462179]		63	16	4d^{8}5s(^{4}P)5p	^{5}D°	9	4d^{8}5s(^{4}F)5p	^{5}F°		
4d^{8}5s(^{4}F)5p	^{5}G°	3	[462707]		68	11	4d^{8}5s(^{4}F)5p	^{5}F°					
4d^{8}5s(^{4}F)5p	^{5}G°	2	[463697]		57	11	4d^{8}5s(^{4}F)5p	^{5}F°	11	4d^{8}5s5p	^{3}F°		
4d^{8}5s(^{4}F)5p	^{5}D°	1	[465370]		61	20	4d^{8}5s(^{4}P)5p	^{5}D°	10	4d^{8}5s(^{4}F)5p	^{5}F°		
4d^{8}5s(^{4}F)5p	^{5}F°	5	[465837]		65	19	4d^{8}5s(^{4}F)5p	^{5}G°	9	4d^{8}5s(^{2}F)5p	^{3}G°		
4d^{8}5s(^{4}P)5p	^{5}P°	2	466568	3	28	23	4d^{8}5s(^{4}F)5p	^{5}G°	13	4d^{8}5s5p	^{3}D°	-171	2
4d^{8}5s(^{4}F)5p	^{5}D°	0	[466589]		60	29	4d^{8}5s(^{4}P)5p	^{5}D°	6	4d^{8}5s5p	^{3}P°		
4d^{8}5s(^{4}F)5p	^{5}F°	4	467128	5	39	22	4d^{8}5s(^{2}F)5p	^{1}G°	21	4d^{8}5s(^{2}F)5p	^{3}G°	-63	1

Configuration	Term	J	Energy [a] cm^{-1}	Unc. [b] cm^{-1}	Leading percentages [c]							ΔE_{o-c} [d] cm^{-1}	No. of lines [e]
$4d^8 5s5p$	$^5D_a^\circ$	1	467142.5	5	30	23	$4d^8 5s(^4F)5p$	$^5F^\circ$	10	$4d^8 5s(^4P)5p$	$^5P^\circ$	-106.5	1
$4d^8 5s5p$	$^3F^\circ$	3	467815	3	21	32	$4d^8 5s(^2F)5p$	$^3D^\circ$	11	$4d^8 5s(^4F)5p$	$^5D^\circ$	102	3
$4d^8 5s(^4F)5p$	$^5F^\circ$	3	468876.7	2	29	21	$4d^8 5s(^4P)5p$	$^5P^\circ$	11	$4d^8 5s(^4F)5p$	$^5G^\circ$	-63.3	3
$4d^8 5s(^4F)5p$	$^5G^\circ$	4	[469040]		34	19	$4d^8 5s(^2F)5p$	$^3F^\circ$	17	$4d^8 5s(^4F)5p$	$^5F^\circ$		
$4d^8 5s(^4F)5p$	$^5F^\circ$	2	[471474]		53	11	$4d^8 5s(^4F)5p$	$^5D^\circ$	9	$4d^8 5s(^2F)5p$	$^3F^\circ$		
$4d^8 5s(^4P)5p$	$^5P^\circ$	1	[471515]		71	16	$4d^8 5s(^4F)5p$	$^5F^\circ$					
$4d^8 5s(^2F)5p$	$^3D^\circ$	3	471834.7	1.8	20	17	$4d^8 5s(^4F)5p$	$^5F^\circ$	15	$4d^8 5s(^4P)5p$	$^5P^\circ$	11.7	2
$4d^8 5s5p$	$^3D^\circ$	2	471877	1.7	22	36	$4d^8 5s(^4P)5p$	$^5P^\circ$	9	$4d^8 5s(^4F)5p$	$^3D^\circ$	-47	3
$4d^8 5s5p$	$^3G^\circ$	3	473485.5	1.8	32	36	$4d^8 5s(^4P)5p$	$^5P^\circ$	12	$4d^8 5s(^4F)5p$	$^3G^\circ$	203.5	2
$4d^8 5s(^2F)5p$	$^3G^\circ$	5	[473750]		41	30	$4d^8 5s(^4F)5p$	$^3G^\circ$	27	$4d^8 5s(^4F)5p$	$^5G^\circ$		
$4d^8 5s(^2F)5p$	$^3F^\circ$	4	475812	3	33	23	$4d^8 5s(^4F)5p$	$^3F^\circ$	22	$4d^8 5s(^4F)5p$	$^5F^\circ$	-71	1
$4d^8 5s(^4F)5p$	$^5F^\circ$	1	475981.8	2.3	39	17	$4d^8 5s(^2F)5p$	$^3D^\circ$	10	$4d^8 5s(^4P)5p$	$^5P^\circ$	74.8	2
$4d^8 5s(^2F)5p$	$^1F^\circ$	3	476177.8	1.8	25	19	$4d^8 5s(^4F)5p$	$^5F^\circ$	14	$4d^8 5s(^2F)5p$	$^3D^\circ$	8.8	2
4d96d	^3S	1	476860.86	0.5	70	25	4d96d	^3P				7.86	3
$4d^8 5s(^2F)5p$	$^1D^\circ$	2	477143.9	2.1	27	19	$4d^8 5s5p$	$^3F^\circ$	10	$4d^8 5s(^2F)5p$	$^3F^\circ$	-197.1	3
$4d^8 5s5p$	$^1G^\circ$	4	477903	3	25	37	$4d^8 5s5p$	$^3F^\circ$	18	$4d^8 5s(^4P)5p$	$^5D^\circ$	132	1
4d96d	^3G	4	478321.1	0.5	51	47	4d96d	^1G				-66.9	4
$4d^8 5s5p$	$^3F^\circ$	2	478487.3	1.4	23	22	$4d^8 5s(^2F)5p$	$^1D^\circ$	17	$4d^8 5s(^2F)5p$	$^3D^\circ$	-82.7	4
4d96d	^3G	5	478525	3	100							-74	1
4d96d	^3P	2	478558.2	0.5	59	38	4d96d	^3D				6.2	4
4d96d	^1P	1	478618.7	1.8	52	27	4d96d	^3D	18	4d96d	^3P	-65.3	2
4d96d	^3D	3	479118	1.6	69	28	4d96d	^3F				-17	3
$4d^8 5s(^2P)5p$	$^3P^\circ$	0	[479300]		42	29	$4d^8 5s5p$	$^3P^\circ$	14	$4d^8 5s(^4P)5p$	$^3P^\circ$		
4d96d	^1F	3	479602.2	1.4	56	18	4d96d	^3F	14	4d96d	^3D	-57.8	4
4d96d	^1D	2	479749.4	0.5	55	16	4d96d	^3F	15	4d96d	^3P	48.4	4
4d96d	^3F	4	479897.7	0.6	85	12	4d96d	^1G				-32.3	3

Configuration	Term	J	Energy [a] cm^{-1}	Unc. [b] cm^{-1}	Leading percentages [c]							ΔE_{o-c} [d] cm^{-1}	No. of lines [e]
$4d^8 5s(^4P)5p$	$^5D^o$	3	480225.9	1.7	26	18	$4d^8 5s(^2F)5p$	$^1F^o$	15	$4d^8 5s5p$	$^3F^o$	-159.1	3
$4d^8 5s(^2F)5p$	$^3F^o$	2	480479.6	1.5	23	17	$4d^8 5s(^4F)5p$	$^3F^o$	14	$4d^8 5s5p$	$^3P^o$	-36.4	3
$4d^8 5s5p$	$^5P^o$	3	480638.6	1.5	15	22	$4d^8 5s5p$	$^3D^o$	10	$4d^8 5s(^2F)5p$	$^1F^o$	-89.4	3
$4d^8 5s(^2F)5p$	$^3D^o$	1	482052.6	1.5	24	23	$4d^8 5s(^2P)5p$	$^3P^o$	13	$4d^8 5s(^4P)5p$	$^5D^o$	102.6	3
4d96d	^3P	0	482333	8	90	9	4d96d	^1S				32	1
$4d^8 5s(^4P)5p$	$^5D^o$	0	482586	3	56	31	$4d^8 5s(^4F)5p$	$^5D^o$				106	1
$4d^8 5s(^4P)5p$	$^5D^o$	1	482882.1	1.5	51	24	$4d^8 5s(^4F)5p$	$^5D^o$	7	$4d^8 5s(^2P)5p$	$^3P^o$	69.1	3
$4d^8 5s(^2G)5p$	$^3H^o$	4	483516	3	62	8	$4d^8 5s(^2G)5p$	$^3F^o$	8	$4d^8 5s(^2F)5p$	$^3G^o$	199	1
$4d^8 5s(^4P)5p$	$^5D^o$	2	483548.9	1.5	45	11	$4d^8 5s(^4F)5p$	$^5D^o$	10	$4d^8 5s5p$	$^3D^o$	-71.1	3
$4d^8 5s(^4P)5p$	$^5D^o$	4	483860	3	46	17	$4d^8 5s(^2F)5p$	$^1G^o$	16	$4d^8 5s(^2G)5p$	$^3H^o$	61	1
$4d^8 5s(^2G)5p$	$^3F^o$	4	484638	3	58	15	$4d^8 5s(^2G)5p$	$^3H^o$	9	$4d^8 5s(^2F)5p$	$^1G^o$	-48	1
$4d^8 5s5p$	$^3D^o$	2	484912.5	1.5	17	17	$4d^8 5s(^2P)5p$	$^3P^o$	13	$4d^8 5s(^2F)5p$	$^1D^o$	-35.5	3
$4d^8 5s5p$	$^3D_b^o$	1	485347.2	1.8	33	17	$4d^8 5s(^2P)5p$	$^1P^o$	10	$4d^8 5s5p$	$^3P^o$	-87.8	3
$4d^8 5s5p$	$^3F^o$	3	485885.6	1.5	29	30	$4d^8 5s(^4P)5p$	$^5D^o$	16	$4d^8 5s5p$	$^3F^o$	-28.4	3
$4d^8 5s(^2P)5p$	$^3D^o$	2	485967.4	1.8	20	14	$4d^8 5s5p$	$^3P^o$	13	$4d^8 5s(^2P)5p$	$^3P^o$	19.4	3
4d96d	^3P	1	486444.4	1.9	38	32	4d96d	^1P	27	4d96d	^3S	45.4	2
4d96d	^3G	3	486926.3	2	85	11	4d96d	^1F				-24.7	2
$4d^8 5s5p$	$^3D^o$	3	487284.2	1.6	30	23	$4d^8 5s(^2F)5p$	$^1F^o$	18	$4d^8 5s(^2G)5p$	$^3F^o$	-151.8	3
4d96d	^3D	1	487366	1.8	69	18	4d96d	^3P	11	4d96d	^1P	53	2
4d97s	^3D	3	487450.1	1.5	99							-57.9	4
4d96d	^1G	4	487583.4	5	40	46	4d96d	^3G	13	4d96d	^3F	30.4	1
4d97s	^1D	2	487669.4	1.1	30	24	4d97s	^3D	19	4d96d	^3D	-29.6	7
4d95f	$^3P^o$	2	487801.9	1.6	57	18	4d95f	$^3D^o$	15	4d95f	$^1D^o$	194.9	3
$4d^8 5s5p$	$^3P^o$	2	488073.5	1.9	29	14	$4d^8 5s5p$	$^3D^o$	12	$4d^8 5s(^4P)5p$	$^5S^o$	34.5	2
4d96d	^3D	2	488074.5	1.1	22	26	4d97s	^1D	19	4d97s	^3D	74.5	7
4d96d	^3F	2	488276.6	1.5	81	12	4d96d	^1D	7	4d96d	^3D	28.6	4

Configuration	Term	J	Energy [a] cm^{-1}	Unc. [b] cm^{-1}	Leading percentages [c]							ΔE$_{o-c}$ [d] cm^{-1}	No. of lines [e]
$4d^8 5s(^2P)5p$	$^3D^\circ$	1	488447.5	1.8	45	16	$4d^8 5s(^4P)5p$	$^3D^\circ$	15	$4d^8 5s5p$	$^3P^\circ$	216.5	4
4d96d	^3F	3	488535.6	1.4	49	33	4d96d	^1F	17	4d96d	^3D	16.6	4
$4d^8 5s(^2P)5p$	$^3D^\circ$	3	490668.9	1.9	18	17	$4d^8 5s(^2G)5p$	$^3F^\circ$	14	$4d^8 5s(^4P)5p$	$^5D^\circ$	-166.1	3
$4d^8 5s(^2P)5p$	$^1P^\circ$	1	490850	1.6	29	18	$4d^8 5s5p$	$^3D^\circ$	12	$4d^8 5s(^2F)5p$	$^3D^\circ$	42	3
$4d^8 5s(^2G)5p$	$^3F_3^\circ$	2	491761	1.5	20	19	$4d^8 5s(^2P)5p$	$^3P^\circ$	10	$4d^8 5s(^2P)5p$	$^1D^\circ$	115	4
$4d^8 5s5p$	$^3P^\circ$	0	492590.5	3	37	31	$4d^8 5s(^2P)5p$	$^1S^\circ$	23	$4d^8 5s(^2P)5p$	$^3P^\circ$	118.5	1
$4d^8 5s(^4P)5p$	$^5S^\circ$	2	493150	1.6	66	12	$4d^8 5s5p$	$^3P^\circ$	9	$4d^8 5s(^2G)5p$	$^3F^\circ$	1	4
4d95f	$^3D^\circ$	1	493403	1.6	83	9	4d95f	$^3P^\circ$				158	4
$4d^8 5s5p$	$^3F^\circ$	4	494539	6	54	15	$4d^8 5s(^4P)5p$	$^5D^\circ$	11	$4d^8 5s(^2G)5p$	$^3F^\circ$	207	1
$4d^8 5s(^2G)5p$	$^3F_3^\circ$	2	494544.6	1.9	40	10	$4d^8 5s(^2P)5p$	$^3D^\circ$	10	$4d^8 5s(^4P)5p$	$^5S^\circ$	56.6	2
$4d^8 5s(^2P)5p$	$^3D^\circ$	3	494837.7	1.6	20	19	$4d^8 5s5p$	$^3F^\circ$	19	$4d^8 5s(^4P)5p$	$^3D^\circ$	185.7	3
4d96d	^1S	0	494871	3	82	10	4d96d	^3P				-10	2
$4d^8 5s(^2P)5p$	$^3S^\circ$	1	495811	1.9	30	23	$4d^8 5s(^4P)5p$	$^3S^\circ$	11	$4d^8 5s(^2P)5p$	$^1P^\circ$	-44	3
4d97s	^3D	1	496140.3	1.4	100							15.3	4
$4d^8 5s(^2P)5p$	$^1D^\circ$	2	496360.4	1.6	37	19	4d95f	$^3D^\circ$	12	4d95f	$^3P^\circ$	-387.6	3
4d97s	^3D	2	496363.9	1.4	57	43	4d97s	^1D				10.9	5
Sn VI $4d^9\ ^2D_{5/2}$	**limit**		617620 R										

[a] Symbols next to the energy value have the following meaning: N – new identification; R – previous value and/or interpretation has been revised here. Values in [ ] are unobserved energy level found from the series extrapolation by a parametric least-squares fitting with Cowan's codes [18]

[b] Uncertainties resulting from the level optimization procedure are given on the level of one standard deviation. They correspond to uncertainties of level separations from $4d^9 5s\ ^1D_2$. To determine uncertainties of excitation energies from the ground level, the given values should be combined in quadrature with the uncertainty of the ground level, 2.0 cm^{-1}.

[c] The first percentage value refers to the configuration and term given in the first two columns of the table. The second/third percentage value refers to the configuration and term given next to it. The percentage compositions were determined in this work by a parametric least-squares fitting with Cowan's codes [18]

[d] Differences between observed energies and those calculated in the parametric least squares fitting.

[e] Number of observed lines determining the level in the optimization procedure LOPT[21].

Table 6.3. Least squares fitted (LSF) parameters (cm^{-1}) for Sn V.

Configuration	Parameter	LSF	Group [a]	STD	HFR	LSF/HFR
Even Parity						
$4d^{10}$	E_{av}	2806.7	148		0	
$4d^9 5s$	E_{av}	189584	74		189245.6	1.0018
	$\zeta(4d)$	3400.8	19	1	3321.6	1.0238
	$G^2(4d,5s)$	13848.7	640		14938.4	0.9271
$4d^9 6s$	E_{av}	406194.5	74		403255.3	1.0073
	$\zeta(4d)$	3436.2	19	1	3356.2	1.0238
	$G^2(4d,6s)$	3299.4	690	2	3409.1	0.9678
$4d^9 7s$	E_{av}	491185.7	80	3	487495.3	1.0076
	$\zeta(4d)$	3443.7	19	1	3363.5	1.0238
	$G^2(4d,7s)$	1375.6	288	2	1421.3	0.9678
$4d^9 8s$	E_{av}	534084.1	87	3	529888.6	1.0079
	$\zeta(4d)$	3446.5	19	1	3366.2	1.0239
	$G^2(4d,8s)$	720.3	151	2	744.2	0.9679
$4d^9 9s$	E_{av}	558855.9	91	3	554361.9	1.0081
	$\zeta(4d)$	3447.8	19	1	3367.5	1.0238
	$G^2(4d,9s)$	427	89	2	441.2	0.9678
$4d^9 10s$	E_{av}	574485.8	94	3	569785.1	1.0082
	$\zeta(4d)$	3448.5	19	1	3368.2	1.0238
	$G^2(4d,10s)$	274.9	57	2	284	0.9680
$4d^9 5d$	E_{av}	385255.7	39		380591	1.0123
	$\zeta(4d)$	3435.6	19	1	3355.6	1.0238
	$\zeta(5d)$	408.8	42	4	346.2	1.1808
	$F^2(4d,5d)$	14217.7	331		17753.5	0.8008
	$F^4(4d,5d)$	7131.7	451		7669.2	0.9299
	$G^0(4d,5d)$	3536.3	23	5	3934.7	0.8987
	$G^2(4d,5d)$	4304.1	28	5	4789.1	0.8987
	$G^4(4d,5d)$	3509.9	23	5	3905.4	0.8987
$4d^9 6d$	E_{av}	482658.4	37	6	478942.1	1.0078
	$\zeta(4d)$	3443.5	19	1	3363.3	1.0238
	$\zeta(6d)$	184.9	19	4	156.6	1.1807
	$F^2(4d,6d)$	6047.6	321	7	6993.5	0.8647
	$F^4(4d,6d)$	3043.2	555	8	3026.5	1.0055
	$G^0(4d,6d)$	1364.1	25	9	1529.2	0.8920
	$G^2(4d,6d)$	1740.2	32	9	1950.8	0.8920
	$G^4(4d,6d)$	1453	27	9	1628.8	0.8921
$4d^9 7d$	E_{av}	528681.3	41	6	525557.3	1.0059
	$\zeta(4d)$	3446.4	19	1	3366.1	1.0239
	$\zeta(7d)$	100.5	10	4	85.1	1.1810
	$F^2(4d,7d)$	3070.7	163	7	3551.1	0.8647
	$F^4(4d,7d)$	1573.7	287	8	1565.1	1.0055
	$G^0(4d,7d)$	693	13	9	776.8	0.8921
	$G^2(4d,7d)$	902.6	17	9	1011.9	0.8920
	$G^4(4d,7d)$	761.4	14	9	853.5	0.8921

Configuration	Parameter	LSF	Group [a]	STD	HFR	LSF/HFR
$4d^9 8d$	E_{av}	554553.5	43	6	551832.6	1.0049
	$\zeta(4d)$	3447.8	19	1	3367.5	1.0238
	$\zeta(8d)$	60.7	6	4	51.4	1.1809
	$F^2(4d,8d)$	1787.2	95	7	2066.7	0.8648
	$F^4(4d,8d)$	929	170	8	923.9	1.0055
	$G^0(4d,8d)$	404	8	9	452.9	0.8920
	$G^2(4d,8d)$	532.4	10	9	596.8	0.8921
	$G^4(4d,8d)$	451.6	8	9	506.2	0.8921
$4d^9 9d$	E_{av}	570643.6	44	6	568172	1.0044
	$\zeta(4d)$	3448.4	19	1	3368.1	1.0238
	$\zeta(9d)$	39.6	4	4	33.5	1.1821
	$F^2(4d,9d)$	1135.8	60	7	1313.4	0.8648
	$F^4(4d,9d)$	596.3	109	8	593.1	1.0054
	$G^0(4d,9d)$	257.3	5	9	288.5	0.8919
	$G^2(4d,9d)$	341.3	6	9	382.6	0.8921
	$G^4(4d,9d)$	290.5	5	9	325.6	0.8922
$4d^9 5g$ [b]	E_{av}	510330	fixed		506331.5	1.0079
	$\zeta(4d)$	3449.4	19	1	3369.1	1.0238
$4d^9 6g$ [b]	E_{av}	543050	fixed		540211.6	1.0053
	$\zeta(4d)$	3449.5	19	1	3369.2	1.0238
$4d^8 5s^2$	E_{av}	407737.1	65		411642.2	0.9905
	$F^2(4d,4d)$	74025.1	785		99090.1	0.7470
	$F^4(4d,4d)$	52547.8	1598		65839.8	0.7981
	$A(4d)$	96.5	16		0	
	$\zeta(4d)$	3552.5	19	1	3469.8	1.0238
$4d^8 5p^2$ [b]	E_{av}	583350	fixed		581257.5	1.0036
	$\zeta(4d)$	3579.1	20	1	3495.7	1.0239
$4d^8 5s5d$ [b]	E_{av}	611400	fixed		607908.3	1.0057
	$\zeta(4d)$	3586.6	20	1	3503.1	1.0238
$4d^8 5d^2$ [b]	E_{av}	817800	fixed		818762.2	0.9988
	$\zeta(4d)$	3621.7	20	1	3537.4	1.0238
$4p^5 4d^{10} 5p$ [b]	E_{av}	868372.6	fixed		868372.6	1.0000
$4p^5 4d^{10} 4f$ [b]	E_{av}	1017670	fixed		1017670	1.0000
Odd parity						
$4d^9 5p$	E_{av}	273848.3	42		271595.5	1.0083
	$\zeta(4d)$	3436	20	1	3335	1.0303
	$\zeta(5p)$	5679	82		4957.2	1.1456
	$F^2(4d,5p)$	25307	360		30899.9	0.8190
	$G^1(4d,5p)$	9035.2	148	3	9484.5	0.9526
	$G^3(4d,5p)$	8355.8	137	3	8771.4	0.9526
$4d^9 6p$	E_{av}	437377.2	42		434145.8	1.0074
	$\zeta(4d)$	3460.1	21	1	3358.4	1.0303
	$\zeta(6p)$	2072.3	23	2	1847.2	1.1219
	$F^2(4d,6p)$	9200.5	380	15	10265.4	0.8963
	$G^1(4d,6p)$	2173	210	4	2606.9	0.8336
	$G^3(4d,6p)$	2189.6	211	4	2626.8	0.8336

Configuration	Parameter	LSF	Group [a]	STD	HFR	LSF/HFR
$4d^9 7p$	E_{av}	504088.4	110	14	502508.5	1.0031
	$\zeta(4d)$	3466.1	21	1	3364.2	1.0303
	$\zeta(7p)$	1015.5	11	2	905.2	1.1219
	$F^2(4d,7p)$	4214.2	174	15	4702	0.8963
	$G^1(4d,7p)$	965.4	93	4	1158.1	0.8336
	$G^3(4d,7p)$	998.3	96	4	1197.6	0.8336
$4d^9 8p$	E_{av}	538001.3	117	14	538347.6	0.9994
	$\zeta(4d)$	3468.4	21	1	3366.5	1.0303
	$\zeta(8p)$	576.6	6	2	514	1.1218
	$F^2(4d,8p)$	2300.4	95	15	2566.7	0.8962
	$G^1(4d,8p)$	523.3	50	4	627.8	0.8335
	$G^3(4d,8p)$	547.7	53	4	657.1	0.8335
$4d^9 9p$	E_{av}	559170.7	122	14	559598.3	0.9992
	$\zeta(4d)$	3469.6	21	1	3367.6	1.0303
	$\zeta(9p)$	359.5	4	2	320.4	1.1220
	$F^2(4d,9p)$	1398.4	58	15	1560.2	0.8963
	$G^1(4d,9p)$	317.6	31	4	381.1	0.8334
	$G^3(4d,9p)$	334.7	32	4	401.5	0.8336
$4d^9 4f$	E_{av}	424612.7	91		421866	1.0065
	$\zeta(4d)$	3440.3	20	1	3339.2	1.0303
	$\zeta(4f)$	25.2	fixed		25.2	1.0000
	$F^2(4d,4f)$	26803.2	548	5	29724.5	0.9017
	$F^4(4d,4f)$	14273.6	292	5	15829.3	0.9017
	$G^1(4d,4f)$	22417.3	111	6	26163.8	0.8568
	$G^3(4d,4f)$	13131.2	65	6	15325.8	0.8568
	$G^5(4d,4f)$	9040.4	45	6	10551.3	0.8568
$4d^9 5f$	E_{av}	493682.8	90	16	491175.7	1.0051
	$\zeta(4d)$	3452.1	20	1	3350.6	1.0303
	$\zeta(5f)$	19.1	fixed		19.1	1.0000
	$F^2(4d,5f)$	13763.4	281	5	15263.4	0.9017
	$F^4(4d,5f)$	7828.4	160	5	8681.6	0.9017
	$G^1(4d,5f)$	12974.5	64	6	15142.8	0.8568
	$G^3(4d,5f)$	7840.2	39	6	9150.5	0.8568
	$G^5(4d,5f)$	5461	27	6	6373.6	0.8568
$4d^9 6f$	E_{av}	533007.6	97	16	530546.1	1.0046
	$\zeta(4d)$	3460.4	21	1	3358.7	1.0303
	$\zeta(6f)$	12	fixed		12	1.0000
	$F^2(4d,6f)$	7326.3	150	5	8124.8	0.9017
	$F^4(4d,6f)$	4234.8	87	5	4696.4	0.9017
	$G^1(4d,6f)$	6992.9	35	6	8161.5	0.8568
	$G^3(4d,6f)$	4301.7	21	6	5020.6	0.8568
	$G^5(4d,6f)$	3016.9	15	6	3521.1	0.8568
$4d^9 7f$	E_{av}	556725	101	16	554317.4	1.0043
	$\zeta(4d)$	3464.8	21	1	3363	1.0303
	$\zeta(7f)$	7.7	fixed		7.7	1.0000
	$F^2(4d,7f)$	4296.8	88	5	4765.1	0.9017

Configuration	Parameter	LSF	Group [a]	STD	HFR	LSF/HFR
	F^4(4d,7f)	2499.2	51	5	2771.5	0.9017
	G^1(4d,7f)	4089	20	6	4772.4	0.8568
	G^3(4d,7f)	2543.1	13	6	2968.1	0.8568
	G^5(4d,7f)	1791.2	9	6	2090.6	0.8568
$4d^9 8f$	E_{av}	571992.2	104	16	569584.8	1.0042
	ζ(4d)	3467.1	21	1	3365.2	1.0303
	ζ(8f)	5.1	fixed		5.1	1.0000
	F^2(4d,8f)	2728.8	56	5	3026.2	0.9017
	F^4(4d,8f)	1592.1	33	5	1765.6	0.9017
	G^1(4d,8f)	2583.9	13	6	3015.8	0.8568
	G^3(4d,8f)	1618.7	8	6	1889.2	0.8568
	G^5(4d,8f)	1143.3	6	6	1334.4	0.8568
$4d^8 5s5p$	E_{av}	488916.4	42		487170.8	1.0036
	F^2(4d,4d)	80251.5	493	7	99325.6	0.8080
	F^4(4d,4d)	57538.2	961	8	66017.3	0.8716
	α(4d)	33.3	9			
	ζ(4d)	3587.5	21	1	3482.1	1.0303
	ζ(5p)	6202.7	69	2	5528.8	1.1219
	F^2(4d,5p)	29172.2	291	9	32483.3	0.8981
	G^2(4d,5s)	11935.6	303	10	15037.4	0.7937
	G^1(4d,5p)	10469.4	208	11	9789.2	1.0695
	G^3(4d,5p)	9811.8	195	11	9174.4	1.0695
	G^1(5s,5p)	53617.6	198	12	59351.6	0.9034
$4d^8 5s6p$	E_{av}	665800	fixed		664474.8	1.0020
	F^2(4d,4d)	80644.4	495	7	99812	0.8080
	F^4(4d,4d)	57856.2	966	8	66382.2	0.8716
	ζ(4d)	3611.6	21	1	3505.4	1.0303
	ζ(6p)	2144.8	24	2	1911.8	1.1219
	F^2(4d,6p)	9247.5	92	9	10297.1	0.8981
	G^2(4d,5s)	12349.4	313	10	15558.8	0.7937
	G^1(4d,6p)	2704.2	54	11	2528.5	1.0695
	G^3(4d,6p)	2752.3	55	11	2573.5	1.0695
	G^1(5s,6p)	6051.1	22	12	6698.2	0.9034
$4d^8 5s4f$ [b]	E_{av}	646050	fixed		645057.3	1.0015
$4p^5 4d^{10} 5s$ [b]	E_{av}	785277.7	fixed		785277.7	1.0000
$4p^5 4d^{10} 5d$ [b]	E_{av}	977488.1	fixed		977488.1	1.0000

[a] Parameters in each numbered group were linked together with their ratio fixed at the Hartree-Fock level.

[b] These highly excited configurations are unknown experimentally. They were included in the calculations in order to account for their interaction with other configurations studied in this work. Except for the average energies E_{av} and ζ(4d) given here, all other parameters of these configurations were fixed at the 85 % of the Hartree-Fock values (F^k, G^k) and 80% R^k) or 100 % of the Hartree-Fock values (ζ).

CONCLUSION

Comprehensive interpretations of the spectra of singly to quadruply ionized tin ions (Sn II–V) have been presented in this thesis on the basis of spectra taken by us on a 3m normal incidence spectrograph (300–2080Å), Wu's (corrected) measurements (350–9000Å) and Troitsk's measurements in 200–650Å wavelength region. The main emphasis was to provide data with high accuracies, thus, the wavelength uncertainties of each observed lines have been estimated and could be used for the optimization of the observed energy values within one level of standard deviation in each spectrum and thereafter, the corresponding Ritz wavelengths with their uncertainties have also been generated. The plasma modeling, a local thermodynamical equilibrium (LTE) for optically thin plasma state, has been applied to estimate the intensities of observed lines. The analyses have been supported by the theoretical predictions from the pseudo–relativistic Hartree-Fock method with superposition of configurations to account the configuration interactions (CI) implemented in Cowan suit programs for the atomic structure calculations. The extensive calculations, to account the effects of configuration interaction, with least squares fitted parametrization enable to lessen the disagreement between observed and theoretical results. With the help of observed spectroscopic data, the improved and revised values of ionization potentials of Sn II–V have been derived. A summary of the work carried out in each ion is briefly discussed here.

In **singly ionized tin (Sn II)**, the analysis covers the vast wavelength region 888 Å to 10740 Å. The earlier reported levels of even parity configurations, $5s^2nd$ (n=5–11), $5s^2ns$ (n=6–11), $5s^2ng$ ($n = 6$–11) and $5s5p^2$ have been confirmed with minor improvements in their level values, while the $5s^25g$ levels have been newly identified. The questions in the assignments of the $^2S_{1/2}$ and $^2P_{1/2}$ levels of the $5s5p^2$ configuration have been resolved. In odd parity, the previously reported levels of the $5s^2np$ ($n = 5$–9) and $5s^2nf$ ($n = 4$–6) configurations have been verified. Sixty-nine

levels are now known in Sn II. Among these, eight are new, and for 11 levels previous values or interpretations have been revised. All the energy level values, which are based on the identification of about 200 spectral lines, have been optimized in a least-squares fitting procedure. About 70 of these lines were measured by us either for the first time or with significant improvements. With these improved data, the ionization energy of Sn II has been determined with better accuracy. For 140 transitions out of a total 215, we gave a critically evaluated value of transition probability with an estimated uncertainty. About 40 % of these transition probabilities have an accuracy C+ ($\leq$ 18 %) or better.

The revised and extended **analysis of Sn III** includes a total 115 observed levels (out of which 50 levels are new) based on more than 350 classified lines. The previously reported level values of $5p^2$, 5sns (n=6-9), 5snd (n=5-7) and 4f5s configurations have been confirmed with improved energy values. The missing $^1S_0$ level of $5p^2$ and 5sns (n=7, 9) configurations have now been established. In 5s5g configuration, all levels have been confirmed except the reported value of $^3G_5$ level for which the value is revised. The analysis has been extended to the levels of 5s8d, 5p (5d+6s), 5snf (n=5-10), 5sng (n=6-7), 5p6p configurations and a few levels of 5snd (n=10-12) Rydberg members. These observed series have been used for the improved determination of the ionization potential.

In chapter 5, the spectroscopic interpretations of the **trebly ionized tin (Sn IV)** is given, a total of 66 levels observed for this ion, out of which 25 are newly observed in this work. The relative intensities of the lines have been provided with the support of Boltzmann LTE conditions. All the levels of previously known single electron configurations have been confirmed in this analysis. The $4d^9 5s5p$ configuration has been studied in depth by this time, and out of its 23 possible levels, 15 are known now. The optimization of levels values have been made with the help of 139 observed line for this spectrum, out of which more than 50 lines are newly identified. The outermost single electronic excitation favored us to observe the levels of $4d^{10}ng$ (8, 9), $4d^{10}nh$ (n=6-9) and $4d^{10}ni$ (7, 8) configurations. With these high-lying series, the ionization limit of the Sn IV was accurately determined, which in return used for the predictions of levels of $4d^{10}n\ell$ ($n\geq5$, ℓ= g, h, i, k) Rydberg members.

The spectrum of four times ionized tin (Sn V) has been described in next chapter 6. The analysis of this spectrum includes all the levels of $4d^9n\ell$ ($n\ell$ = 5s, 5p, 5d, 6s, 6p, 6d, 7s), $4d^85s^2$ and $4d^85s5p$ configurations. These configurations were studied before. However, the radiation data was incomplete. More than 450 lines have been used in optimization of the energy level values, out of which 194 lines are taken from our accurate measurements in the VUV region and 10 lines from the Wu's measurements. This corrected longer-wavelength data had improved accuracies of earlier reported energy values of the levels of $4d^95s$, $4d^95p$, $4d^95d$ $4d^96p$ and $4d^96d$ configurations. A total of 57 even levels and 80 levels of the odd parity configurations were observed. The calculated transition probabilities (gA) of each transition were also given. Finally, the earlier reported ionization potential of this ion has been revised.

In these analyses of tin spectra, Sn II–V, altogether 387 energy levels and 1139 spectral lines have been observed. More than 1000 lines have now been reported with the transition rates. This strengthened us to bring a comparison between the number of levels and lines available for these ions in databases, as only 162 levels, 125 lines, and 16 lines with transition rates were known in atomic data sources.

In the present study, the wavelengths used were treated as either absence of systematic shifts/errors or corrected from them if present (For example Wu's original measurements), and such shifts may be due to a variety of reasons such as low resolution instruments, less accuracy in reference lines used for calibration, method of detections and their measurement techniques etc. However, an additional shift for the lines of various ionization stages, as they would be emitted from different spatial points of the plasma produced, might have also been expected. But in the present work, such possibilities were not incorporated due to less availability of wavelengths in longer wavelengths region with interferometric technique.

As far as the relative intensities of lines are concerned, for Sn II-IV, the relative intensities of lines of each ion have been derived with the help of local thermodynamical equilibrium states for thin plasmas. This model only qualitatively expresses the relative intensities of various lines within a particular ionization stage. However, for even better estimate of them the model like collisional radiative (CR) model- which incorporate the various collisional processes and radiative process (non-local), may be applied.

The **critical evaluation** of transition probabilities has been carried out for the spectrum of Sn II only. The Singly ionized spectrum of tin was well studied from theoretical aspects; however, more data from external sources are not available for the other ions. Thus, only gA values were given without any uncertainty assessments. However, some transitions whose given gA values are too unreliable (by orders of magnitude) due to larger cancellation effects on their computed line strengths. Such type of transitions has been specially marked by CF.

Our VUV measurements contain about 7000 lines belonging to various ionization stages of tin. Only about 8% of lines have been indentified so far and used in this work. The similar figure was also noticed for Wu's measurements, only 7% lines are assigned by this work from about 3400 lines. This indicates the possibilities of future studies on other ions from Sn VI onwards. It can also be articulated that more precise measurements on both wavelengths and absolute intensities of lines are still needed for future work.

In addition to the studies on low-charged system, we have made some efforts to investigate the highly charged ion (HCI) spectra of tin. The physics of highly charged ions are different from those of low charged. Some aspects of HCI has direct special implications in astrophysics. The X-ray spectrum of highly charged tin (Sn) ions in 1–10 keV energy range using delayed beam-foil technique have been examined. The spectral excitation was carried out with passage of 165–200 MeV $^{120}Sn^{q+}$ (q=12–15) ions through 40 $\mu g/cm^2$ thick carbon foil, a 15 UD Pelletron accelerator facility at Inter University Accelerator Centre was sued for this purpose. The spectra were recorded by keeping the target at two delayed positions (2 & 6 mm away from the centre of the chamber). The detector used was a Low Energy Germanium (LEGe) which is focused at centre of chamber. The spectra contain primarily two prominent spectral peaks at 3.7 keV and 4.6 keV energies, and are presently attributed to bunch of forbidden (M2, E2) multipole transitions from Ne- and Na-like Sn ions (predictions were done with Cowan code). Our next goal is to resolve them with a Multi-channel Doppler tuned spectrometer (MCDTS) whose expected resolution is 6eV at 6 keV.

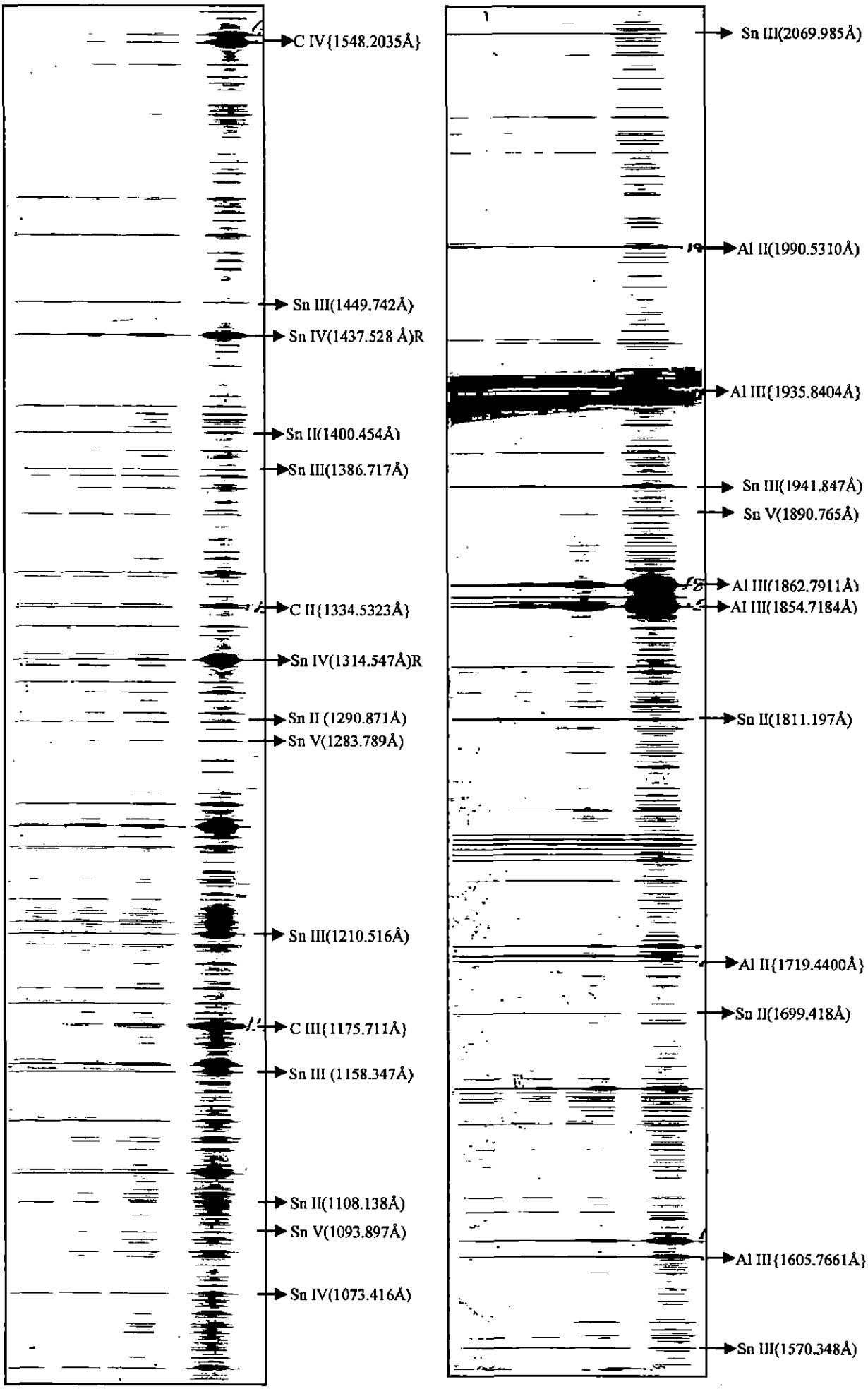
C IV{1548.2035Å}
Sn III(1449.742Å)
Sn IV(1437.528 Å)R
Sn II(1400.454Å)
Sn III(1386.717Å)
C II{1334.5323Å}
Sn IV(1314.547Å)R
Sn II (1290.871Å)
Sn V(1283.789Å)
Sn III(1210.516Å)
C III{1175.711Å}
Sn III (1158.347Å)
Sn II(1108.138Å)
Sn V(1093.897Å)
Sn IV(1073.416Å)
Sn III(2069.985Å)
Al II(1990.5310Å)
Al III{1935.8404Å}
Sn III(1941.847Å)
Sn V(1890.765Å)
Al III(1862.7911Å)
Al III(1854.7184Å)
Sn II(1811.197Å)
Al II{1719.4400Å}
Sn II(1699.418Å)
Al III{1605.7661Å}
Sn III(1570.348Å)

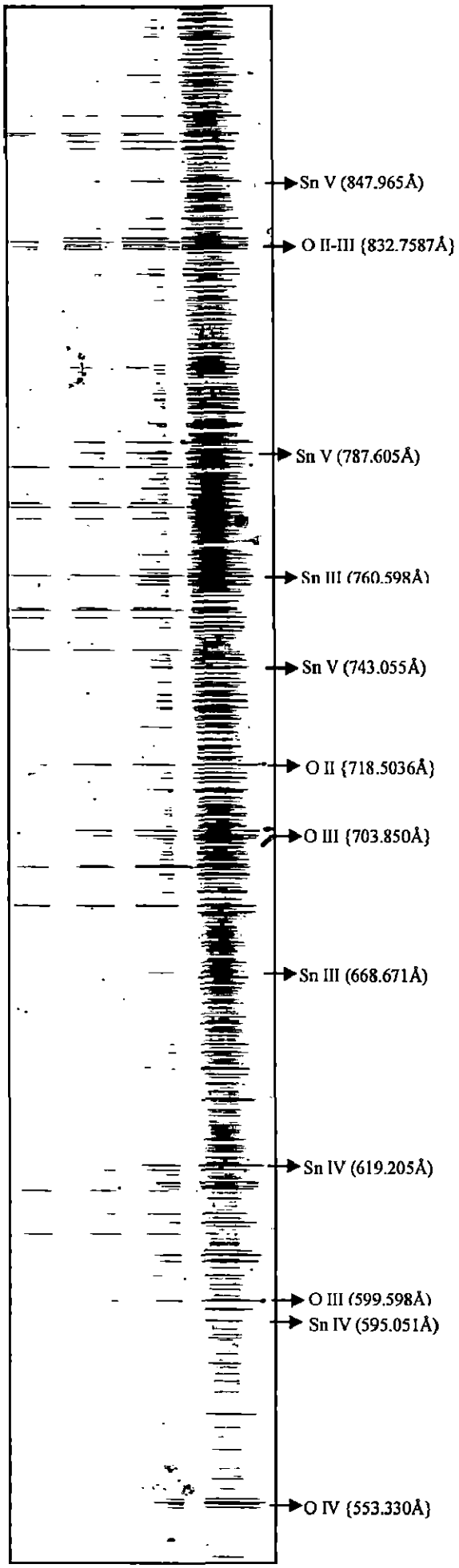
Sn V (847.965Å)
O II-III (832.7587Å)
Sn V (787.605Å)
Sn III (760.598Å)
Sn V (743.055Å)
O II (718.5036Å)
O III (703.850Å)
Sn III (668.671Å)
Sn IV (619.205Å)
O III (599.598Å)
Sn IV (595.051Å)
O IV (553.330Å)

IOP Publishing | Royal Swedish Academy of Sciences Physica Scripta

Phys. Scr. 89 (2014) 115403 (21pp) doi:10.1088/0031-8949/89/11/115403

Extended and revised analysis of singly ionized tin: Sn II

K Haris[1], A Kramida[2] and A Tauheed[1]

[1] Department of Physics, Aligarh Muslim University, Aligarh 202002, India
[2] National Institute of Standards and Technology, Gaithersburg, MD 20899, USA

E-mail: alexander.kramida@nist.gov

Received 2 December 2013, revised 21 May 2014
Accepted for publication 28 August 2014
Published 28 October 2014

Abstract

The electronic structure of singly ionized tin (Sn II) is partly a one-electron and partly a three-electron system with ground configuration $5s^25p$. The excited configurations are of the type $5s^2n\ell$ in the one-electron part, and $5s5p^2$, $5p^3$ and $5s5pn\ell$ ($n\ell = 6s$, 5d) in the three-electron system with quartet and doublet levels. The spectrum analyzed in this work was recorded on a 3 m normal incidence vacuum spectrograph of the Antigonish laboratory (Canada) in the wavelength region 300 Å–2080 Å using a triggered spark source. The existing interpretation of the one-electron level system was confirmed in this paper, while the $^2S_{1/2}$ level of the $5s5p^2$ configuration has been revised. The analysis has been extended to include new configurations $5p^3$, 5s5p5d and 5s5p6s with the aid of superposition-of-configurations Hartree–Fock calculations with relativistic corrections. The ionization potential obtained from the ng series was found to be 118 023.7(7) cm^{-1} (14.633 07(8) eV). We give a complete set of critically evaluated data on energy levels, observed wavelengths and transition probabilities of Sn II in the range 888–10 740 Å involving excitation of the $n = 5$ electrons.

Online supplementary data available from stacks.iop.org/PS/89/115403/mmedia

Keywords: singly ionized tin, energy levels, classified lines, transition probabilities, ionization energy

(Some figures may appear in colour only in the online journal)

1. Introduction

Accurate data on the spectrum of singly ionized tin are needed in different fields of scientific research and industry. Such data are useful for astrophysical observations, development of various light sources, and for plasma diagnostics in fusion power plants. The astrophysical importance of tin has increased since gas-phase tin was first detected by Hobbs *et al* [1] in the spectra acquired with the Goddard High Resolution Spectrograph on board the *Hubble Space Telescope*. They observed the absorption line of Sn II at 1400.45 Å from various interstellar sources. Later, the same line was observed in diffuse interstellar clouds by Sofia *et al* [2]. They discovered that the gas-phase abundance of Sn in the interstellar medium (ISM) appears to be supersolar, which further substantiates the slow neutron capture (s-process) enrichment believed to be a major contributor to the nucleosynthesis of elements beyond the iron peak in the ISM. In erosion probing of vessel wall tiles of future fusion power plants, such as ITER, spectroscopic data on tin may play a major diagnostic role [3].

Singly ionized tin (Sn II) is the second member of the In I isoelectronic sequence with the ground configuration $4d^{10}5s^25p$ consisting of the ground level $^2P^o_{1/2}$ and first excited level $^2P^o_{3/2}$. The currently available spectroscopic information on Sn II compiled in Moore's Atomic Energy Levels (AEL) compilation [4] and listed in the Atomic Spectra Database (ASD) [5] of the National Institute of Standards and Technology (NIST) is based on an unpublished work of Shenstone. Prior to AEL, extensive work in this spectrum was carried out by McCormick and Sawyer [6], who revised the earlier findings of Green and Loring [7], Narayan and Rao [8], and Lang [9]. Shenstone in his work quoted in AEL re-investigated this spectrum in the wavelength range of

Nuclear Instruments and Methods in Physics Research A 767 (2014) 199–205

Contents lists available at ScienceDirect

Nuclear Instruments and Methods in Physics Research A

journal homepage: www.elsevier.com/locate/nima

Photostimulated phosphor based image plate detection system for HRVUV beamline at Indus-1 synchrotron radiation source

K. Haris [a], Param Jeet Singh [b], Aparna Shastri [b,*], Sunanda K.[b], Babita K.[b], S.V.N. Bhaskara Rao [b], Shabbir Ahmad [a], A. Tauheed [a]

[a] Department of Physics, Aligarh Muslim University, Aligarh 202002, India
[b] Atomic & Molecular Physics Division, Bhabha Atomic Research Centre, Mumbai 400085, India

ARTICLE INFO

Article history:
Received 25 June 2014
Received in revised form
14 August 2014
Accepted 14 August 2014
Available online 23 August 2014

Keywords:
Image plate
Vacuum ultraviolet
Synchrotron radiation
Photostimulated phosphor
Position sensitive

ABSTRACT

A high resolution vacuum ultraviolet (HRVUV) beamline based on a 6.65 m off-plane Eagle spectrometer is in operation at the Indus-1 synchrotron radiation source, RRCAT, Indore, India. To facilitate position sensitive detection and fast spectral recording, a new BaFBr:Eu^{2+} phosphor based image plate (IP) detection system interchangeable with the existing photomultiplier (PMT) scanning system has been installed on this beamline. VUV photoabsorption studies on Xe, O_2, N_2O and SO_2 are carried out to evaluate the performance of the IP detection system. An FWHM of ~0.5 Å is achieved for the Xe atomic line at 1469.6 Å. Reproducibility of spectra is found to be within the experimental resolution. Compared to the PMT scanning system, the IP shows several advantages in terms of sensitivity, recording time and *S/N* ratio, which are highlighted in the paper. This is the first report of incorporation of an IP detection system in a VUV beamline using synchrotron radiation. Commissioning of the new detection system is expected to greatly enhance the utilization of the HRVUV beamline as a number of spectroscopic experiments which require fast recording times combined with a good signal to noise ratio are now feasible.

1. Introduction

Spectroscopy in the vacuum ultraviolet (VUV) region has always posed a challenge due to scarcity of suitable sources and detection methods. With the advent of dedicated synchrotron radiation (SR) sources, highly intense and tunable beams of VUV photons are now available which have facilitated a variety of experiments which were either impossible or very difficult to perform with traditional laboratory sources [1–3]. Detection of VUV radiation in the early years was carried out using specially prepared gelatin-free photographic glass plates like Kodak make short wavelength radiation (SWR) plates [3,4]. Due to some inherent disadvantages like fragility, aging problems, cumbersome dark room procedures for loading and developing, etc. these plates were gradually phased out and replaced by electronic detectors like photomultiplier tubes (PMTs), microchannel plates (MCPs) and charge coupled devices (CCDs). While VUV PMTs with MgF_2 windows are available for direct detection of radiation down to 1100 Å, for lower wavelengths, one has to use a scintillator. Most commonly used is a sodium salicylate film which absorbs in the VUV and emits fluorescence in the visible region, which is then detected by a visible PMT [3]. In cases where position sensitive detection or imaging is desirable, MCPs and CCDs have been used. However, besides being much more expensive, these have limited wavelength coverage and resolution as compared to photographic plates. PMTs, MCPs and CCDs are also prone to electrical noise. Typically, in high resolution spectrometers, photographic plates have been replaced with PMTs using a precision scanning mechanism along the Rowland circle to cover the wavelength region of interest. This means that for achieving high resolution and good signal to noise ratios small step sizes and long integration times have to be used. Due to these reasons, SWR plates are still in use for a number of spectroscopic applications. However, since the manufacturing of these plates has been recently discontinued, an urgent necessity is created to find alternative position sensitive detectors.

The photostimulated phosphor based image plate (IP) detector is one such alternative which is inexpensive and offers many advantages over both PMTs and traditional photographic plates. This detector consists of a film of BaFBr with trace amounts of Eu^{2+} coated on a flexible plastic substrate and works on the principle of photostimulated luminescence (PSL) [5]. Although phosphor based IPs had been in wide use in the X-ray region for crystallography and medical diagnostics for quite some time, their

* Corresponding author. Tel.: +91 22 25590343; fax: +91 22 25502652.
E-mail address: ashastri@barc.gov.in (A. Shastri).

http://dx.doi.org/10.1016/j.nima.2014.08.022
0168-9002/

Fast Ion Surface Energy Loss and Straggling in the Surface Wake Fields

T. Nandi,[1,*] K. Haris,[2] Hala,[2] Gurjeet Singh,[3] Pankaj Kumar,[1] Rajesh Kumar,[1] S. K. Saini,[1] S. A. Khan,[1] Akhil Jhingan,[1] P. Verma,[4] A. Tauheed,[2] D. Mehta,[3] and H. G. Berry[5,†]

[1]*Inter-University Accelerator Centre, JNU New Campus, New Delhi 110067, India*
[2]*Department of Physics, Aligarh Muslim University, Aligarh 202002, India*
[3]*Department of Physics, Panjab University, Chandigarh 160014, India*
[4]*Department of Physics, Kalindi College, East Patel Nagar, New Delhi 110008, India*
[5]*Department of Physics, University of Notre Dame, Notre Dame, Indiana 46556, USA*

(Received 30 November 2012; revised manuscript received 14 February 2013; published 19 April 2013)

We have measured the stopping powers and straggling of fast, highly ionized atoms passing through thin bilayer targets made up of metals and insulators. We were surprised to find that the energy losses as well as the straggling depend on the ordering of the target and have small but significantly different values on bilayer reversal. We ascribe this newly found difference in energy loss to the surface energy loss field effect due to the differing surface wake fields as the beam exits the target in the two cases. This finding is validated with experiments using several different projectiles, velocities, and bilayer targets. Both partners of the diatomic molecular ions also display similar results. A comparison of the energy loss results with those of previous theoretical predictions for the surface wake potential for fast ions in solids supports the existence of a self-wake.

DOI: 10.1103/PhysRevLett.110.163203 PACS numbers: 34.35.+a, 34.20.−b

Energy dissipation of fast charged particles through matter has been a subject of great interest for 100 years [1]. Although the energy loss mechanism in solids consists of contributions from both the bulk as well as the surfaces of a thin target foil [2], most studies consider only the bulk effects because major energy loss takes place through ionization processes in the bulk. Much smaller dissipating channels such as excitation and charge exchange processes can occur in both the bulk and at the surface. The energy loss contribution from the bulk is presumed to be much larger than that from the surface, although sometimes even the energy loss at the front surface can supersede the bulk energy loss for highly charged slow ions in very thin solid foils [3].

Besides the excitation and the charge exchange processes at the surface, three other processes can be responsible for the energy loss: the ion interaction with the surface potential barrier [4], with the image potential [5], and with the wake potential [6]. The first process is important only at the front surface. The second exists at both surfaces but its magnitude is very small for ion velocities higher than the Fermi velocity (v_f) of the electrons in the target. The third acts only at the exit surface and is significant at high velocities. For slow grazing incidence ions [7,8] it is not possible to segregate the surface effects from the bulk. For experiments conducted with ions traversing a target, the bulk energy loss will be admixed with the energy losses at the two surfaces. Segregating the contributions of the two surfaces from the bulk has not yet been possible. However, many years ago, bulk wake-field-induced Stark mixing of the sub states in H-like Kr ions [9] and recently the surface wake field intensity [10] in carbon foils have been measured. The latter showed that small surface wake field can be distinguished from the large bulk energy loss field in an atomic level lifetime measurement [10]. This experiment in fact supports the original Bohr prediction [11]. In this Letter, we search for the effect of the exit-surface wake potential through direct energy loss measurements. Our challenge has been to develop an energy loss measurement technique which can distinguish the bulk and surface energy loss contributions: we have achieved this by the simple trick of using bilayer reversible targets.

All theoretical developments [12–15] assume that the wake potential is caused by collective plasmon excitations of the electronic states of the fast beam ions formed at the exit surface of a conducting foil. Our hypothesis was that in the case of a bilayer target (one part metallic and other part insulating), the bulk wake will be formed equally in both configurations, but, the surface wake will be greater for the beam inputting on the insulator side and exiting from the metal side of the bilayer target. Thus, the differences in the wake fields for two different orientations could be large enough to become measurable: the inverse geometry with the insulator at the exit side of the target foil will not allow much collective plasmon excitation to take place. As a result, in one configuration the wake potential is present and in the other it is absent, and thus the energy loss difference between the two geometries should give a measure of both the ion energy loss and the straggling in the surface wake potential: we have identified this as the surface energy loss field (SELF) effect. The SELF is not merely important in understanding ion-matter interaction but also it finds applications in broad areas of radiation damage, including biological systems. Aluminized

IOP PUBLISHING PHYSICA SCRIPTA
Phys. Scr. 85 (2012) 055301 (13pp) doi:10.1088/0031-8949/85/05/055301

Revised and extended analysis of doubly ionized tin: Sn III

K Haris and A Tauheed

Department of Physics, Aligarh Muslim University, Aligarh 202002, India

E-mail: ahmadtauheed@rediffmail.com

Received 5 November 2011
Accepted for publication 26 March 2012
Published 2 May 2012
Online at stacks.iop.org/PhysScr/85/055301

Abstract

A spectral analysis of doubly ionized tin (Sn III) has been carried out with the help of spectra photographed on a 3 m normal incidence vacuum spectrograph of the Antigonish laboratory (Canada) using a triggered spark light source. The ground configuration of Sn III is $4d^{10}5s^2$. The outer and inner shell electron excitation involves configurations of the type $4d^{10}5sn\ell$ and $4d^95s^2(4f+5p)$, respectively. Further excitation leads to $4d^{10}5p^2$ as well as $4d^{10}5p(5d+6s)$ configurations. The levels of low excitations reported earlier are confirmed in this paper except for $5s7s\,^1S_0$. Six new configurations, 5p5d, 5p6s, 5snp (n = 7, 8) and 5snf (n = 5, 6), are added. In addition to that, the missing $^1S_0$ level in $5p^2$ and 5sns (n = 8, 9) configurations have also been found. The analysis is supported by Hartree–Fock and least-squares fitted parametric calculations with configuration interactions. On the basis of the identifications of 264 lines, 85 levels have been established in this spectrum out of which 43 are new. The ionization energy was determined to be 246 047.3 ± 25.0 cm^{-1} (30.505 98 ± 0.003 10 eV).

PACS numbers: 32.30.−r, 32.30.Jc, 32.10.−f, 32.70.Cs

(Some figures may appear in colour only in the online journal)

1. Introduction

The spectroscopic analysis of tin has very high relevance: firstly, to update the atomic database, which is informative to physicists and as well to technologists; secondly, tin plasmas sources have attracted much attention in the rapidly growing industry of extreme ultraviolet plasma lithography (EUVL). There have been several works on tin plasma EUVL [1–4]. Recent cosmic observations showed the abundance of tin in astrophysical sources [5]. The very recent demand for high-resolution spectral information on neutral and multiply ionized atoms will help astrophysicists to interpret stellar spectra. This motivated us to carry out this study.

The third spectrum of tin (Sn III) is a Cd-I-like ion with ground configuration $4d^{10}5s^2$. The excited configurations are of the type $4d^{10}5s\,n\ell$. The core excitation leads to $4d^95s^25p$ and $4d^95s^24f$ configurations. This is generally a two-electron system with singlet and triplet levels. The following is a brief survey of the literature on Sn III. The present analysis is mainly by Shenstone, which is compiled in atomic energy levels (AEL) [6], and at the NIST database[1], which has revised and extended the earlier works of Rao [7], Green and Loring [8] and Gibbs and Vieweg [9]. Shenstone added new configurations to include the 5s7d, 5sns (n = 8, 9) and a few levels of 5p5d. It should be pointed out that a master's thesis by C-M Wu [10] that is available online at the University of British Colombia's library website includes these configurations listed in AEL [6] and added a few additional configurations such as 5p6s, 5p6p, 5s7p and 5p4f. Apart from this, core excitation in Sn III was reported by Dunne *et al* [11] using the dual-laser plasma (DLP) technique. Duffy *et al* [12] have published a few transitions between $4d^{10}5s5p$ and $4d^95s5p^2$ using the same method. The radiative lifetimes of a few levels in Sn III have been experimentally measured by Andersen *et al* [13], followed by Kernahan *et al* [14] and Pinnington *et al* [15, 16] using beam-foil techniques. Besides these experimental works on Sn III, a number of papers have appeared on theoretical calculations. The most extensive, covering almost all earlier works on oscillator strengths, transition probabilities and radiative lifetimes of the excited states, were published by Colón and Alonso-Medina [17].

The analyses of two odd parity configurations 5p5d and 5p6s of the Cd-I isoelectronic sequence Sb IV–I VI [18–20] have recently been reported in our laboratory and on Xe

[1] http://physics.nist.gov/PhysRefData/ASD/levels_form.html

